Fibrin Mediated Proangiogenic and Secretory Control Gene Therapy for Compromised Wound Healing

A thesis submitted to the National University of Ireland for the

degree of Doctor of Philosophy

By

Mangesh Kulkarni

Jan 2012

Network of Excellence for Functional Biomaterials
National University of Ireland, Galway

Research Supervisor: Professor Abhay Pandit

TABLE OF CONTENTS

LIST OF FIGURES

Chapter 1

Chapter 2

Chapter 3

Appendices

LIST OF TABLES

Acknowledgements

"Om ajnana-timirandhasya jnananjana-salakaya
caksur unmilitam yena tasmai sri-gurave namah"

I would like to sincerely thank Professor Abhay Pandit for his valuable guidance, immense support, and encouragement to think independently and collaborate when necessary, and impetus to always work hard towards the right goal with right attitude of perpetual development. I thank you Professor from bottom of my heart for putting so much of your time, energy and efforts in me. I would also like to thank Science Foundation Ireland, Research Frontier Project for providing funds for this project. I would also like to thank Baxter Healthcare, Vienna for their kind sponsorship of fibrin.

I would like to thank Professor Timothy O'Brien for his ideas and providing a clinician's viewpoint to this project. I would like to thank Dr. Udo Greiser for his continual guidance from the beginning of the project. I would also like to thank all the former and current members of Network of Excellence for Functional Biomaterials. A special thanks to Dr. Ailish Breen for her excellent mentoring in the early months of the project and imparting me the critical skills required for this project. I would also like to specifically thank Dr. Oliver Carroll for his assistance in day-to-day laboratory issues and help in plasmid expansion, Anthony Sloan for his language editing, Keith Feerick for his assistance with reports and Tara Cosgrave and Vidoja Kovacevic for their phenomenal assistance in administrative matters.

Within the National Centre for Biomedical Engineering Science and Regenerative Medicine Institute, I have received wonderful support and assistance from excellent researchers and technical staff. Very special thank Dr. Aonghus O`Loughlin for his exceptional help in performing the surgeries during the seemingly insurmountable difficulties with my allergy. I would like to express my gratitude to Dr. Yolanda Garcia, Charles Mchale, Gerry Mchale, Michael Schonfeld and Dr. Xizhe Chen for their crucial help in facilitating the preclinical studies. I would like to take this opportunity to thanks all the rabbits who laid down their lives for the preclinical phase of this project. I would like to extend my gratitude to David Connolly for assistance with microscopes, Enda O'Connell for assistance with PCR, Robert Giblin for assistance with orders, Eadaoin

Timmins for assistance with SEM and Pierce Lalor for assistance with TEM. I would also like to thank Dr. Karl Mccullagh for providing eNOS plasmid and primer sequences. I would also like to thank Dr. Kaveh Mashayekhi for microarray analysis.

I would like to express my gratitude to Professor Richard O'Kennedy, all his lab members, and Dr. Marie Leberre and John Butler for their help with surface plasmon resonance studies. I would also like to thank Professor Maria Malagon and Dr. Rafael Vazquez for providing Rab18 plasmid and primer sequences. I would also like to thank Professor Edel O'Toole for her guidance in pathway analysis and keratinocytes cell culture.

Finally, to express my gratitude for those closest to me, the words fall short. I am eternally indebted to my spiritual teacher HH Radhanath Swami for giving me a sound spiritual foundation and meaning in life, based on true principles of humility compassion, love and integrity. Through his teachings and regular mentoring from many of his senior disciples such as HG Gauranga P, HG Krishnaan P, HG Amritnaam M, HG Shyamcharan P, HG Venumadhav P and many others; I could go through the thick and thins of life with a smile. I would like to sincerely thank HG Vrajendra P and HG Maharani M for being my Galway family and making me feel at home. Very special thanks to boys at the house, Inniyakumar, Aditya, HG Dmitry P and all devotees at Inis Rath, Dublin temple, Galway bhakti club and elsewhere. I am incomplete without my wife and so is my PhD. Apart from her direct practical help at the bench side in techniques such as PCR and histology; she has been incredible to support me emotionally and encourage me, even through those insane hair pulling phases. Thank you very much my love. How can I thank enough to my wonderful sister and her family! She has been my role model and impetus since childhood. Being elder to me, she not only set a perfect example of dedication and hard work but also encouraged and helped me even to this day. Even if I dedicate this PhD to her, I can't repay even a fraction of her favors. Thank you very much Tai. Last but not the least, prostrated obeisance to my mother and father for their unprecedented sacrifices, selfless love and encouragement while undergoing relentless hardships. Thank you very much Aai and Baba for being such wonderful parents.

LIST OF ABBREVIATIONS

AAV	Adeno-associated Virus
Ang-1	Angiopoietin-1
ARF1	ADP-Ribosylation Factor-1
bFGF	Basic Fibroblast Growth Factor
CD	Cluster of Differentiation
cGMP	Cyclic Gaunosine Monophosphate
DOPC	Dioleoyl Phosphatidylcholine
DOPE	Dioleoylphosphatidylethanolamine
DOTMA	N-[1-(2, 3-dioleyloxy) propyl]-n, n, n-trimethyl ammonium chloride
ECM	Extracellular Matrix
EDC/NHS	*N*-Ethyl-*N*-(3-Diethylaminopropyl)-Carbodiimide/*N*-Hydroxysuccinimide
EGF	Epidermal Growth Factor
eNOS	Endothelial NOS
Fc	Flow Cell
FGF	Fibroblast Growth Factor
FM	Fibrin Microspheres
FPA	Fibrinopeptide A
FPB	Fibrinopeptide B
GAG	Glycosaminoglycan
GALA	Glutamic Acid–Alanine–Leucine–Alanine
GAM	Gene Activated Matrix
GDNF	Glial Cell Line-Derived Neurotrophic Factor
HBO	Hyperbaric Oxygen
HIF	Hypoxia Inducible Factor
HIV-1	Human Immunodeficiency Virus Type 1
HSP47	Heat Shock Protein 47
IFN- γ	Interferon-γ
IGF	Insulin-like Growth Factor
IL	Interleukin

iNOS	Inducible NOS
IWGDF	International Working Group on Diabetic Foot
KGF-1	Keratinocyte Growth Factor-1
MMPs	Matrix Metalloproteinases
MSCs	Mesenchymal Stem Cells
NDSK	N-terminal Disulfide Knot
NF-κB	Nuclear Factor κB
NGF	Nerve Growth Factor
NHEK	Normal Human Epidermal Keratinocytes
NLS	Nuclear Localization Signal
nNOS	Neuronal NOS
NO	Nitric Oxide
NOS	Nitric Oxide Synthase
NPWT	Negative Pressure Wound Therapy
NT-3	Neurotrophin-3
OGFr	Rat Opioid Growth Factor Receptor
PDGF	Platelet Derived Growth Factor
PDMS	Polydimethylsiloxane
PEG	Polyethylene Glycol
PLA	Polylactic Acid
PLGA	Poly (Lactic-*Co*-Glycolic Acid)
PlGF	Placenta Growth Factor
PTD	Protein Transduction Domain
pVEGF	Vascular Endothelial Growth Factor Plasmid
RCGP	Royal College of General Practitioners'
RCT	Randomized Controlled Trial
RES	Reticuloendothelial System
ROS	Reactive Oxygen Species
SDF-1 α	Stromal Cell-Derived Factor-1α
SDF-1α	Stromal-Derived Growth Factor-1α
SEM	Scanning Electron Microscopy

Shh	Sonic Hedgehog
SIGN	Scottish Intercollegiate Guidelines Network
SPR	Surface Plasmon Resonance
TEM	Transmission Electron Microscopy
TGF-α	Transforming Growth Factor- α
TGF-β	Transforming Growth Factor- β
TIMP	Tissue Inhibitor of Metalloproteinases
TNF-α	Tumor Necrosis Factor-α
tPA	Tissue Plasminogen Activator
uPA	Urokinase Plasminogen Activator
USD	United States Dollars
VEGF	Vascular Endothelial Growth Factor
V_V	Volume Fraction

Abstract

Chronic or compromised healing is a major clinical problem. Particularly, in diabetes where the disease process hinders the capacity to repair the tissue damage, the patients are more susceptible to chronic ulcers, especially on the lower extremity. Despite rigorous treatment regimes, there has been modest success in reducing the rate of amputations in these patients. Hyperglycemia, the defining biochemical phenomenon of diabetes, is by far the most important predisposing factor for chronic wound healing complications. The objective of this thesis was to unleash the pathological disarray by studying the effects of hyperglycemia at molecular level on wounded keratinocytes and subsequently to develop a controlled delivery system capable of delivering therapeutic genes in an extended manner. A fibrin lipoplex system capable of simultaneous delivery of multiple genes was tested *in vitro* and *in vivo*. As a step to improve this system for controlled release and increase the capacity of the system, fibrin microspheres loaded with gene complexes were successfully developed and investigated for functional gene delivery *in vivo* using proangiogenic gene – eNOS. From the microarray data analysis on the wounded keratinocytes under hyperglycemic culture conditions, a profound differential gene regulation was revealed with a number of up- and down-regulated genes. The secretory control molecule Rab18, found to be significantly down-regulated, was chosen as target therapeutic gene considering the hypersecretory state of pro-inflammatory cytokines and proteolytic enzymes in diabetic wound healing. eNOS was chosen as other therapeutic gene, considering its proangiogenic action and reduced angiogenesis in diabetic wound healing. With eNOS gene complexes in fibrin gel and Rab18 gene complexes in fibrin microspheres embedded in fibrin gel, the Rab18-eNOS loaded fibrin-in-fibrin system was investigated in alloxan induced hyperglycemic rabbit ear ulcer model of compromised wound healing. Rab18-eNOS treated group showed significantly higher percent wound closure at day 14 post-wounding with reduced inflammatory cell infiltrate and more functional angiogenesis. Thus, fibrin mediated non-viral delivery of Rab18-eNOS is a promising therapy towards normalization of diabetic wound healing.

Chapter One

Introduction

Contents of this chapter have previously been published:

Kulkarni M., Greiser U., O'Brien T. and Pandit A. 'Liposomal Gene Delivery Mediated by Tissue-engineered Scaffolds.' *Trends Biotechnol* 2010;28(1):28-36.

1.1 Normal Wound Healing

Biological systems, in health, generally tend to maintain a state of homeostasis and any disturbance, physiological or pathological, generally triggers a host of responses from the body to restore that state. Wound healing is a classic example of complex and highly intricate response to repair or in some cases, such as early fetal skin wound healing[1 2], to completely regenerate the damaged tissue. Under physiological conditions, a normal adult skin has a considerable capacity for structural and functional repair via a highly orchestrated process tightly regulated by growth factors and cytokines and characterized by distinct but overlapping phases of wound healing, namely hemostasis, inflammation, proliferation and remodeling.

1.1.1 Inflammatory Phase

The inflammatory response is an essential part of the wound-healing process. This phase can be divided into hemostasis and inflammation. Hemostasis is generally the first response to wounding for the control of blood loss. Following damage, the vessels constrict to reduce blood flow and the platelets adhere to the exposed matrix via integrins, primarily $\alpha_2\beta_1$ and $\alpha_6\beta_1$ that allow them to bind with collagens, primarily collagen- I and IV and laminins, primarily laminin 8 respectively. These adhered platelets become activated and attract more platelets and form a platelet aggregate. Fibrin clot formed locally keeps the platelets together to prevent blood loss. While a dynamic interplay between fibrinolytic and anti-fibrinolytic substances maintains the size of clot, activated platelets degranulate to secrete various factors that play an indispensable role in wound healing. Platelet derived growth factor (PDGF) is a well-known mitogenic agent which is chemotactic for fibroblasts and smooth muscle cells and stimulates production of collagen, glycosaminoglycan, and collagenase by fibroblasts[3]. The inflammatory cells, however, are attracted by selectins.

The inflammatory response is generally a local phenomenon with four cardinal signs of inflammation at gross level; namely rubor (redness due to increased blood flow to the area), tumor (swelling due to the accumulation of fluid in the tissue), calor (heat due to increased blood flow to the area), dolor (pain due to the action of bradykinin and prostaglandins on local nerve tissue). At microscopic and biochemical level,

inflammation is a complex but well organized cellular and biochemical phenomenon. The tissue macrophages, the first line of defense, start their phagocytic actions almost immediately after inflammation begins. Soon, other local macrophages become active and start phagocytosis. The pro-inflammatory cytokines such as interleukin (IL)-1β tumor necrosis factor-α (TNF-α) and interferon-γ (IFN- γ) play a major role[4]. This initial tissue macrophage action is followed by neutrophil invasion that can be considered as the second line of defense. The vascular permeability is greatly increased[7] at this stage to direct and facilitate neutrophil invasion by a process called diapedesis[5] to the wound area. The neutrophils roll on the endothelial lining which is rendered sticky by upregulation of selectins (P-selectin and E-selectin) and adhesion molecules such as I-CAM and V-CAM[6 7]. Following adherence via integrins, neutrophils squeeze out in extravascular space through space between endothelial cells in an amoeboid fashion through interactions involving PECAM and CD99[8]. In the case of knockouts or genetic deficiency diseases of adhesion molecules or blockade of any of the steps involved, it has been shown that the neutrophils cannot migrate efficiently[9-11].

The prime role of neutrophils appears to be to kill microbes and this is usually achieved in phagolysosomes[8]. They seem to employ other mechanisms including release of antimicrobial substances such as oxidants or reactive oxygen species (ROS), cationic peptides, and proteases[4] or release of granule proteins and chromatin that form neutrophil extracellular traps (NETs) which degrade virulence factors and kill bacteria[12]. ROS not only play an important role in inflammatory phase[13] but also regulates signaling pathway and gene expression involving cell proliferation, survival and apoptosis[14-16]. Activation of plasma membrane bound NADPH oxidase causes burst release of superoxide ions (O_2^-)[13]. SODs convert superoxide enzymatically into hydrogen peroxide[17]. While these ions kill the microorganisms, too many of them can also be detrimental to host cells. Therefore, a tight regulation of ROS production and detoxification by ROS-detoxifying enzymes, exogenous and endogenous low molecular weight antioxidants and hemeoxygenases, is crucial for the normal repair process[18]. Nitric oxide (NO) also plays a beneficial role. It will be discussed in detail later (Chapter 5, section 5.1).

Acute inflammation mediated by neutrophils usually resolves in about a week's time. Around 48 hours after inflammation first starts, monocytes are recruited as the third level of defense. They rapidly mature to phagocytic macrophages and become players that are more prominent in inflammatory response. These cells are another major source of ROS. These macrophages not only phagocytize voraciously, clearing the wound of all the cell debris including fibrin and spent neutrophils but also produce numerous cytokines, growth and angiogenic factors that are believed to play important roles in the regulation of fibro-proliferation and angiogenesis[8]. Alongside the inflammatory cells, immune cells such as lymphocytes have been shown to play a distinct, regulatory role in normal wound healing[19-21] through the secretion of lymphokines. Evidence also suggests involvement of mast cells in early stages of wound healing, especially in fibroblast proliferation and in wound contraction[22].

1.1.2 Proliferative Phase

This is the second phase of wound healing, occurring 2–10 days after injury, and is characterized by cellular proliferation and migration of different cell types, mainly endothelial cells, keratinocytes and fibroblasts which undergo marked changes in gene expression (which is poorly understood) and phenotype during this phase[23]. The major events during this phase are the creation of a permeability barrier (i.e. reepithelialization), the establishment of appropriate blood supply (i.e. angiogenesis), and reinforcement of the injured dermal tissue (i.e. fibroplasia)[24].

This phase starts with migration and proliferation of keratinocytes which are at the wound edge and is followed by proliferation of dermal fibroblasts in the neighborhood of the wound which migrate into the provisional matrix and deposit large amounts of extracellular matrix[25]. Next, a huge number of new blood vessels form by process called angiogenesis leading to development of granulation tissue. The macrophages provide a continual supply of growth factors necessary to stimulate fibroplasia and angiogenesis[26]. Re-epithelialization is essential for successful wound healing[27] and continues over the granulation tissue by keratinocyte proliferation and migration to restore the barrier function of skin. PDGF, fibroblast growth factor (FGF), vascular endothelial growth factor (VEGF), transforming growth factor-β (TGF-β) and transforming growth factor-α

(TGF-α) are important players in proliferation phase, required for inducing cell migration as well as proliferation and matrix production[24 28]. Many studies suggest that NO plays an important role in wound healing[29-33]. While the highly beneficial effect of NO has been attributed to scavenging superoxide, NO also influences angiogenesis, proliferation and remodeling[30]. NO has been reported to potentiate the mitogenic activity of FGF, epidermal growth factor (EGF) and insulin-like growth factor (IGF) through cGMP-mediated mechanisms[34]. It has also been shown that NO is directly involved in collagen synthesis by fibroblasts[35 36].

Reepithelialization of wounds beginning within hours after injury[26] is the re-growth of epithelia over a denuded surface[37]. Reepithelialization requires epithelial cells at the edge of the wounded tissue to loosen their cell-cell and cell-extracellular matrix (ECM) contacts and assume a migratory phenotype[37]. A complex balance of signaling factors and surface proteins are expressed and regulated in a spatio-temporal manner that promotes keratinocyte motility and survival to activate wound re-epithelialization[38]. Of the number of factors involved, probably the most important are (FGF-7[25], EGF[39], TGF-α[39]which stimulate this phase while the role of TGF-β is controversial but nevertheless it can be considered as a negative regulator[25]. Migrating cells assemble actin-rich lamellar protrusions for crawling and upregulate the expression of proteolytic enzymes[40].

Matrix metalloproteinases (MMPs) are a family of zinc dependent endopeptidases which to degrade all components of extracellular matrix[41-44] and basement membrane proteins at neutral pH[45]. Till date, more than 25 different MMPs have been identified in vertebrates and classified as collagenases, gelatinases, stromelysins, membrane type and others depending on their structural similarity and substrate specificity[46]. They play indispensable role throughout the entire wound healing process such as scavenging the damaged proteins, degrading and remodeling ECM to facilitate migration of cells towards the center of wound[47]. Thus, involvement of multiple MMPs in wound healing has been identified[42 47-55]. In normal wound healing set up, the degradation and remodeling of ECM is highly controlled through spatiotemporally regulated induction and expression of various MMPs and their inhibitors[42 56-61] by fibroblasts, macrophages,

neutrophils and keratinocytes. The migrating epidermal cells express integrins which help them attach to extracellular proteins and move in between viable tissue and eschar, thus separating them[26]. The proliferating cells follow the migrating cells. In a very orderly fashion, the basement membrane proteins start to reappear and migrating cells start to revert to their normal phenotype to become keratinocytes[26]. Once the migration has ceased, possibly due to contact inhibition, keratinocytes reconstitute the basement membrane and resume the process of terminal differentiation to form a stratified epithelium[24].

Another crucial aspect of tissue repair in this phase is angiogenesis. Angiogenesis can be defined as sprouting of new capillary buds from existing blood vessels. It is essential for providing the oxygen and nutrients to the healing wounds[62]. It is not just the number of vessels but the functional efficiency and temporal control that heralds the angiogenesis phase. Although a number of factors such as bFGF[63 64], TGF-β1[65-67], angiotensin II[68] stimulate angiogenesis, VEGF-A[69] is by far the most important mediator. Hypoxic conditions seen in early wound stimulate expression of hypoxia inducible factors (HIFs) which in turn stimulate production of various proangiogenic factors such as VEGF[70 71]. VEGF mediates its activities via three major tyrosine kinase receptors, VEGFR-1, 2 and 3 which are located on vascular and lymph-vessel endothelial cells[72]. VEGF stimulates multiple components of the angiogenic cascade including vasodilation, basement membrane degradation, endothelial cell migration and endothelial cell proliferation[73]. One of the earliest demonstrated downstream signal targets of VEGF is endothelial nitric oxide synthase (eNOS)[74].Thus, it is believed that VEGF induces angiogenesis and regulates endothelial function via production and release of NO. NO has also been shown to mediate the angiogenic effect of platelet-activating factor and tumor necrosis factor-alpha[75], substance P[76] while NO-generating drug, sodium nitroprusside, was shown to induce endothelial cell proliferation[77]. Recently, it has been shown that VEGF stimulation of endothelial cells results in rapid and transient activation of ADP-ribosylation factor-1 (ARF1), which acts to regulate activation of PI3K, phosphorylation of Akt and eNOS as well as NO release[78]. eNOS also regulates another important proangiogenic factor called stromal cell-derived factor-1α (SDF-1 α), which is involved in cellular processes as tubulogenesis and endothelial

cell migration. Recently it has been shown that after SDF-1 α administration the activation of eNOS leads to NO production, and subsequent nitrosylation of MAPK phosphatase 7 (MKP7) and in turn activation of JNK3, critical for endothelial cell migration[79].

1.1.3 Remodeling Phase

This last phase of wound healing is essential for restoration of full functionality and a 'normal' appearance to the injured tissue[40]. This phase may last up to one or two years, or for an even more longer period[80]. At this stage, proliferation ceases and an equilibrium is reached between formation of new scar tissue, replacing the old matrix by a tightly regulated process involving balance between the proteolytic activities of MMP-1 (collagenase), MMP-2 and MMP-9 (gelatinases), & MMP-3 (stromelysin) and the inhibitory activity of tissue inhibitors of metalloproteinases (TIMP-1 & TIMP-2); all of which are secreted by fibroblasts[81]. During this period, the type III collagen deposited by granulation tissue fibroblasts is gradually replaced by type I collagen returning the dermis to stable preinjury phenotype, reaching up to 70% of its preinjury tensile strength[24]. This strength is achieved by organization of collagen molecules into fibers that are oriented between specialized cellular clefts and further reinforced by covalent cross-linking of the fibrillar collagen by an enzyme lysyl oxidase[82]. However, the final acquired strength generally does not equate to the original strength of tissue[80].

1.2 Chronic Wound Healing

By definition, wounds are termed as 'chronic', 'impaired' or 'compromised' when they fail to progress through the normal phases of healing as described in previous section and enter to a state of chronic pathologic inflammation[83]. Most chronic wounds can be classified into three major types: pressure ulcers, venous ulcers, and diabetic ulcers[84 85]. For the purpose of this dissertation only, diabetic wound healing is described subsequently.

1.2.1 Diabetic Wound Healing

Worldwide, diabetes is a major health problem and its prevalence is growing at a phenomenal rate due to a number of factors including urbanization, sedentary life style, aging, obesity and increase in other risk factors like smoking and overeating. The total

number of people with diabetes was projected to rise from 171 million in 2000 to 366 million in 2030[86]. However, a recent study suggested that the world prevalence of diabetes among adults (aged 20–79 years) will increase to 7.7%, and 439 million adults by 2030[87]. Development of chronic foot ulcers is one of the most debilitating complications of diabetes, affecting 15% of patients[88 89] and around 14-24% of the afflicted patients require amputation[89]. The rate of lower extremity amputation among diabetic patients is 17–40 times higher than in non-diabetics[90] and approximately 50,000–60,000 amputations are performed in diabetic patients each year in the USA[91]. Five-year mortality rates after new-onset diabetic ulceration have been reported between 43% and 55% and up to 74% for patients with lower-extremity amputation[92].

The global health expenditure on diabetes is expected to total at least USD 376 billion or ID 418 billion in 2010 and USD 490 billion or ID 561 billion in 2030[93]. Management of diabetic foot disease is very expensive and the cost of managing the diabetic foot complications is estimated to be in billions of US dollars[94-96]. In Europe the average cost per episode is €6,650 for leg ulcers and €10,000 for foot ulcers, which accounts for 2–4% of health-care budgets[97]. In an Irish hospital, the cost of managing diabetic foot ulceration per patient is € 23,000 per annum[98]. Apart from the cost, the delay in healing is associated with serious lifestyle impairment, huge negative psychological and social effect and a large emotional burden on the patients' caregivers[99 100]. In diabetes, the etiology of impaired healing is multifactorial and is still being fathomed. The various aspects of diabetic pathology are interrelated and affect wound healing adversely (Figure 1.1).

The major factors include intrinsic factors such as neuropathy, vascular pathology, other complicating systemic effects due to diabetes, and extrinsic factors such as wound infection, callus formation, and excessive pressure to the site[88 101]. Other risk factors include foot deformity causing high-pressure focal points; autonomic neuropathy causing fissure and integument and osseous hyperemia; limited joint mobility; obesity; impaired vision; poor control of blood glucose levels resulting in advanced glycosylation and impaired wound healing; smoking; poorly designed or poorly fitting

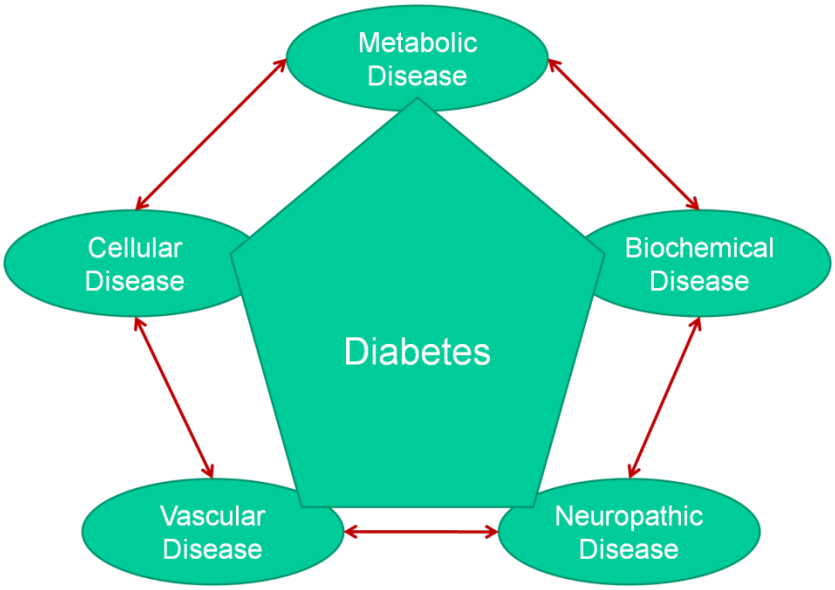

Figure 1.1: Schematic representing various facets of diabetic pathology which contribute to impaired and delayed wound healing seen in diabetic patients. The arrows suggest that all the factors are inter-related and influence each other to create a complex etiopathology of diabetic healing.

footwear inadequately protecting the foot or causing tissue breakdown; history of foot ulceration or amputation[102 103].

The diabetic wound healing can be understood at 'gross level' with disruption of all the normal wound healing phases or at 'cellular level' with dysfunction of all the cells involved in wound healing or at 'molecular level' with differential regulation of gene expression and subsequent protein production. The hallmark of diabetic wound healing is chronic inflammation[104]. Typically, there is decreased early cell infiltration required to clear up the debris and combat infection; and persistence of neutrophils and macrophages in the chronic, non-healing wounds leading to chronic inflammation[105]. It is understood that the chronic inflammation is a result of dysfunctional macrophages[104] and neutrophils[106]. Macro- and micro- angiopathy, central to diabetic pathology, also play a crucial role in delayed wound healing. Diabetes leads to delayed and inadequate formation of granulation tissue, reduced and abnormal angiogenesis, reduced collagen and glycosaminoglycan (GAG) content and low breaking strength[107-109]. Angiogenesis required for normal wound healing is disrupted in diabetes[107 110], probably due to an inhibitory effect of the high glucose and high glycation products[111]. Hypoxia induced stimulation of HIF-1α expression which regulates induction of angiogenic factors such as VEGF[70] is hampered in diabetes[112]. This also contributes to abnormal and insufficient angiogenesis in diabetic wound healing. Diabetic fibroblasts show a decreased proliferative response to growth factors[113-115] and selective impairments in cellular migration, VEGF production and response to hypoxia[116]. Reepithelialization is delayed in diabetes. The diabetic keratinocytes show reduced motility[117], probably as a result of sequential suppression of p-Stat-1 and α2β1integrin mediated MMP-1 pathways[118] and reduced expression of LM-3A32 (uncleaved, precursor of the α3 chain of laminin 5), a key molecule present on migrating epithelium[119]. Some studies have also shown imbalance between proliferation and differentiation of diabetic keratinocytes[119 120].

The altered molecular mechanisms leading to chronic healing are being extensively studied, unraveling the pathogenesis of diabetic wound healing. A dysregulated gene expression profile of proinflammatory cytokines such as IL-6 and IL-8 and their

receptors such as CXCR1, CXCR2 and GP130 contribute to the chronic inflammation[121]. In addition, high serum levels of TNF-α have been reported in type II diabetes[122] and prolonged TNF-α may disrupt cytokine networks for example, stimulation of monocytes chemotactic protein (MCP)-1, macrophage inflammatory protein (MIP)-2 and IL-1β secretion, leading to more persistent inflammation and to tissue damage[123 124]. High TGF-β3 levels in diabetic wounds can inhibit TGF-β1, leading to increased macrophage activity[125 126]. A number of growth factors such IGF-1[127-129], PDGF-A, PDGF-B[130], nerve growth factor (NGF)[131 132] and other neurotrophins/neuropeptides such as substance P and neurotrophin-3 (NT-3)[133] which play an important role in wound healing have reduced levels in diabetic wounds. In addition, a lack of up-regulation of IL-10 and IL-15 in keratinocytes and of EGF, basic fibroblast growth factor, and nitric oxide synthase-3 in endothelial cells in the diabetic ulcer has been reported[134]. Another important biochemical characteristic of chronic wound is sustained ROS production and decreased bioavailability of NO, leading to oxidative stress[135 136]. Numerous studies have linked impaired healing to NO and NOS deficiencies locally[137-141]. There is accumulating evidence of how the MMPs are affected in diabetes, supporting a growing notion that high proteolytic activity plays an important role in diabetic wound healing. A number of studies have reported increased levels of MMPs (e.g. MMP-1, 2, 3, 8, 9 and 26) and decreased levels of tissue inhibitors of MMPs (TIMP-1, 2) in chronic wounds including diabetic and pressure ulcers[43-45 50 53 142-149].

1.2.1.1 Management of Diabetic Wounds

Management of diabetic wounds poses a challenging clinical, economic and social problem. In general, the treatment of diabetic foot is difficult and clinical outcomes are often poor and disappointing. Hence, recently, a great deal of emphasis is being given to follow algorithms derived from evidence-based practices and protocols. The general guidelines for management of diabetic foot emphasize that diabetic foot should be managed by a multidisciplinary team[150-153]. A number of authors have extensively reviewed the standard therapies, practices, their advantages and limitations. In this section, a brief overview of standard treatments will be given while novel therapies will be discussed as possible avenues for the betterment of outcome.

1.2.1.1.1 Management of Infection

Infection is the most common complication of diabetic foot[154-157] and final determinant that leads to amputation[158], especially in developing nations[159] and can also serve as entry points for serious systemic infections, particularly so due to impaired immune system in diabetic patients[160 161]. Hence, apart from the routine signs of neuropathy and peripheral vascular disease, evidence of infection must be sought during the examination of a newly presenting diabetic wound and should be treated as a first priority in the management protocol. *S. aureus* and beta-hemolytic streptococci are widely recognized as pathogens in diabetic foot infections. Nevertheless, multiple organisms, both aerobic and anaerobic, are isolated upon use of proper methods for collection, transport, and culture[162]. Although a number antibiotic treatment regimens have been suggested[162-166], in general, mild soft tissue infection can be treated effectively with oral antibiotics, including dicloxacillin, cephalexin, and clindamycin. Whereas severe soft tissue infection can initially be treated intravenously with ciprofloxacin plus clindamycin; piperacillin/tazobactam; or imipenem/cilastatin, always keeping in mind the risk of methicillin-resistant *S. aureus* infection when choosing a regimen[167]. The initial empirical antibacterial regimen may be tailored based on the results of culture and sensitivity tests from properly obtained specimens[166]. Infection of bone (osteomyelitis) is another complication that affects around 20% of cases with diabetic foot infections[168] and markedly increases the likelihood of amputation[154 158]. Due to arterial and neural disease in diabetes, osteomyelitis may be present with little or no signs of infection, making the diagnosis difficult. Hence, the international working group on diabetic foot (IWGDF) has come up with a scheme to assess the likelihood of osteomyelitis in patients as ‘definite’, ‘probable’, ‘possible’ or ‘unlikely’ based on clinical, imaging and laboratory results[169]. The most difficult differential diagnosis is acute Charcot’s disease[170]. The principle of treatment is to administer appropriate antibiotics regimen[171 172] while removing dead, soft tissue and accessible dead bone[173]. Although urgent surgery is indicated in some patients with necrotizing fasciitis, deep soft-tissue abscess, or gangrene accompanying osteomyelitis[173], non-surgical management of those without limb-threatening infection is associated with a high rate of apparent remission[171 174].

1.2.1.1.2 Debridement

Along with treatment of infection, the wound management focus is generally on the wound bed preparation to stimulate healing. The Scottish intercollegiate guidelines network (SIGN) diabetic foot guidelines and the royal college of general practitioners' (RCGP) guidelines recommended debridement along with appropriate local therapy such as proper antibiotic regimen, pressure relief and appropriate dressings[175]. Debridement is widely practiced in diabetic foot care and involves the complete removal of all necrotic, dysvascular, and nonviable tissue in order to achieve a red, granular wound bed[176]. Furthermore, debridement provides the added advantage promoting dependent drainage and stimulating growth factors[94] and has been shown to heal the wounds faster[177]. Regular debridement and prevention measures by a skilled podiatrist have been shown to reduce amputation rates[178 179]. Sharp debridement using a scalpel, forceps, scissors, and/or curette is the most rapid and precise method, though the procedure may be painful even when local anesthetics are used[180] and can make the wound bigger unless certain amount of skill is employed[175]. Other debridement methods include enzymatic debridement using proteolytic enzymes such as papain or collagenase, wet-to-dry saline gauze method and maggots therapy[176].

1.2.1.1.3 Offloading

Since the diabetic ulcers have a predilection to high pressure areas of the relatively insensitive foot, reduction of pressure is essential, particularly in plantar ulcers. Pressure relief, termed as offloading, is an evidence-based treatment modality for patients with diabetic foot ulcers and is part of the standard protocol for treatment[181 182].Common offloading methods include bed rest, wheel chair, total contact casts, various ambulatory braces, splints, half shoes, modified therapeutic shoes and sandals[183-189]. These devices use various mechanisms for pressure relief, which include felted foam and other special dressings, polymeric molded insoles, rigid rockered outsoles and orthoses with load isolation areas[190-194]. Although the evidence base to support the use of footwear and offloading in the prevention and treatment of diabetic foot ulcers is meager[195], the most compelling evidence comes from use of total contact casts[188 196-198]. A controlled clinical trial has shown that non-infected neuropathic resistant ulcers heal in a total contact cast in 6 weeks[196]. Apart from the poor outcome in patients with combination

of peripheral arterial disease and infection, a prospective follow-up study also showed that casting therapy results in good healing rates in a wide range of patients[198]. Thus, the total contact casts have been aptly termed as the "gold standard" of offloading but studies have shown that very low percentage of patients actually receive this gold standard care[199 200], partly due to the difficult and time consuming procedure. A randomized control trial has shown that instant total contact casts are equally efficacious[201].

1.2.1.1.4 Dressings and Topical Antiseptics

Regular cleaning and dressing are crucial for proper local wound care. Traditionally, dressings were primarily used as barriers and to keep wound bed dry. A warm moist environment is now considered optimal for wound healing. Hence, the newer wound dressings, such as hydrogels, hydrocolloids, biomaterials such as alginates and collagen, aim at providing moist environment, which aids reperfusion and regeneration as well as protection from infection and reducing pain. Studies have shown that faster wound healing with better tissue quality is among the beneficial effects of moist dressings[202-204]. Although the use of antimicrobial products containing silver/iodine is widespread, their clinical benefits are yet to be proven by randomized controlled trials[176], since the only randomized control trial till date showed no difference between silver containing dressings and control groups[205]. Apart from newer dressings, delivery of growth factors, use of skin substitutes such as bioengineered matrices[206] and other novel approaches are being investigated[207].

1.2.1.1.5Negative Pressure Wound Therapy

Negative pressure wound therapy (NPWT) developed in 1990s at Wake Forest University, involves creation and maintenance of sub-atmospheric pressure, either intermittent or continuous, by use of a vacuum pump, which is connected to an open-cell foam dressing applied on the wound[208]. A multicenter randomized control trial performed on patients after partial diabetic foot amputation indicated that NPWT (using the VAC therapy system) seems to be a safe and effective treatment for complex diabetic foot wounds with a higher proportion of wounds that healed, faster healing rates, and potentially fewer re-amputations than with standard treatment[209]. Some

studies have even demonstrated that the NPWT is more effective than the moist wound dressings[210 211]. However, some of the recent systematic reviews concluded that the evidence to support the use of NPWT is not strong at the moment and more rigorous studies with proper controls are required for evaluating NPWT as treatment of chronic wounds[208 212 213].

1.2.1.1.6 Hyperbaric Oxygen Therapy

Hyperbaric oxygen (HBO) therapy has been used in the treatment of chronic wounds for decades. A cyclical therapy with oxygen at high and low pressure over 1 or 2 hours has beneficial effects by stimulating physiological angiogenesis as against abnormal angiogenesis with continuous HBO therapy over several days[214]. A prospective study reported that HBO doubles the mean healing rate of non-ischemic chronic wounds in selected diabetic patients who do not have major macroangiopathy[214]. Another randomized study concluded that the HBO when used in addition to aggressive multidisciplinary therapeutic protocol is effective in reducing major amputations in diabetic patients with severe ischemic foot ulcers[215]. Although a small double blinded randomized controlled trial (RCT) has proved the effectiveness of HBO[216] and there is data supporting the use of systemic HBO to avoid major amputations, for evidence based practice, research towards understanding the specific indications and clinical benefits of this expensive treatment is required. Specifically randomized placebo controlled clinical trials in large populations[217-219] would provide more reliable clinical data needed to establish HBO as appropriate adjunct therapy for chronic wounds[220].

1.2.1.1.7 Treatment with Bioactive Substances

As described earlier (section 1.2.1), a number of abnormalities at molecular and cellular levels lead to the delayed healing in diabetes. This fact has provided the impetus for investigating the modulation of these abnormalities by delivery of bioactive substances such as growth factors, cytokines and extracellular matrix substances in the form on biological dressings and cells involved in wound healing like fibroblasts, keratinocytes and even stem cells.

To date a number of studies have investigated the benefits of delivery of growth factors and cytokines, such as rhEGF, FGF-1, PDGF-BB, TGF-α, IGF-1, NGF, GM-CSF, to

diabetic wounds either as individual factors[221-229] or as a combination of factors[230-235] or treatment with platelet rich plasma in various forms as a source of numerous growth factors[236-241]. Since, the results of preclinical studies do not always translate faithfully in clinical scenario[242], rigorous randomized trials are required to establish the clinical benefits of these treatments. For example, the randomized trials exploring the GM-CSF therapy suggested that although the healing rates are not particularly enhanced, the overall amputation rates in patients with diabetic foot ulcers are reduced[243]. A small randomized placebo controlled double blinded study showed that RGD peptide matrix treatment can accelerate and promote wound healing in diabetic ulcers to a significant degree[244]. PDGF-BB is, by far, the most studied factor in the clinical set up[245-251]. It is the only FDA approved growth factor for human use as topical treatment with recombinant human PDGF (rhPDGF) which has shown significant improvement in healing in diabetic ulcers[245 252] with no adverse effects reported[253], albeit that recently there is concern over increased risk of cancer after treatment with more than three tubes of becaplermin[254]. In addition, it is an expensive medication and therefore future work on its safety is needed to justify its routine use[255].

Recently, there has been growing interest in delivery of cells, especially stem progenitor cells as either topical treatment or recruiting them from circulation to diabetic wounds[256 257]. A preclinical study reported improvement in wound healing after topical application of bone marrow derived stromal progenitor cells[258]. A large report recently suggested clinical benefit in limb salvage by delivery of peripheral mononuclear blood cells to diabetic wounds[259]. A combined treatment with autologous skin fibroblasts and autologous mesenchymal stem cells from bone marrow of patients has been shown to reduce wound size and increase vascularization[260]. Repeated regular applications of autologous keratinocytes have been shown to initiate wound healing in patients resistant to conventional therapy[261]. There is increasing evidence that mesenchymal stem cells (MSCs) have beneficial effects on skin wound healing and repair[262-265]. Thus, clinical benefits of enhanced healing have been observed in resistant chronic wounds with the application of autologous bone marrow stem cells[266 267]. Although the potential of MSCs to differentiate and regenerate skin tissues has been described[262 263], new findings suggest that the ability of MSCs to alter the tissue microenvironment via secretion of

soluble factors may contribute more significantly than their capacity for transdifferentiation in tissue repair[265]. In addition, the conditioned medium from amniotic fluid derived MSCs has been shown to accelerate wound healing in a mouse excisional wound model, reiterating the beneficial effects of paracrine function of MSCs in tissue repair[268]. Since the biomaterial helps not only to physically retain the cells at the wound site but also to provide protection against the hostile wound environment, the use of delivery systems such as fibrin spray[269] or collagen membrane[260] has been investigated as a safe and effective way to deliver the stem cells.

In recent years, a significant amount of research has been focused on the development of tissue engineered dressings for the treatment of chronic ulcers. Tissue engineered dressings generally act by filling the wound gap by extracellular matrix and inducing expression of cytokines and growth factors which accelerate wound healing[270]. These dressings have been investigated by combining natural or synthetic materials with wound therapeutics such as antimicrobial agents, growth factors and/or cytokines as pure protein or genes or live cells[271-273]. Amongst the various hydrogels and biomaterials such as collagen and fibrin have been the most popular ones for delivery of live cells[274-278]. Currently, a number of tissue engineered skin substitutes are commercially available: Integra™ (Collagen and Chondroitin 6 sulphate matrix overlaid with silicone sheet), Dermagraft™ (Cultured human fibroblasts on a polyglycolic acid or polyglactin mesh), Myskin™ (Cultured human autologous human keratinocytes on silicone polymer substrates), Apligraf™ (Bovine type I collagen with dermal fibroblasts suspension), Hyalograft 3-D™ (Cultured human fibroblasts on a laser microperforated membrane of benzyl hyaluronate), Laserskin™ (Human keratinocytes on a laser-microperforated membrane of benzyl hyaluronate), TranCyte™ (Polyglycolic acid/polylactic acid, extracellular matrix proteins derived from allogenic human fibroblasts and collagen) and Bioseed™ (Fibrin sealant and cultured autologous human keratinocytes)[279].

Another form of treatment that has been investigated extensively in recent years is gene delivery, majorly due to failure to achieve the clinical promise of growth factors/cytokines delivery despite of intensive research[280]. The limited success of

growth factors/cytokines delivery can be attributed to a number of factors which include their short half lives, degradation by proteases, toxicity at high doses and lack of effective delivery[281-285]. Gene therapy, on the other hand, provides several advantages in these respects since it uses the cell machinery to produce the required amount of protein and, even in presence of the gene delivered, cells act as intelligent factories, which know when to shut down the production. Therefore, the deficient protein is produced as long as it is needed and at a physiologically relevant level. A number of studies have shown promising results in normalizing various pathological aspects of diabetic wound healing. Some recent salient examples of these studies have been detailed in Table 1.1.

Table 1.1: Preclinical studies to treat diabetic wounds using gene therapy

Viral Vector	Gene	*In Vivo* Model	Wound Type	Significant Finding	Reference
Adeno-associated virus (AAV) vector	Simultaneous transfer of VEGF-A and fibroblast growth factor 4	C57BLKS mice homozygous for a mutation in the leptin receptor ($Lepr^{db}$)	Full-thickness excisional circular wounds (4 mm in diameter)	Simultaneous delivery VEGF-A and FGF-4 gene therapy leads to significantly faster wound closure, increased granulation tissue formation, vascularity and dermal matrix deposition	286
Recombinant AAV vector	Angiopoietin-1 (Ang-1)	C57BL/KsJLep^{db} mice	Full-thickness longitudinal incisions (4 cm) on dorsum	Ang-1 gene transfer improves the delayed wound repair in diabetes by stimulating angiogenesis, apparently without VEGF involvement	287
Adenovirus	c-Met gene	Organ cultured human diabetic corneas	5-mm epithelial wounds	Recombinant AV-driven c-met transduction into diabetic corneas appears to restore HGF signaling, normalize diabetic marker patterns, and accelerate wound healing	288

Table 1.1: Preclinical studies to treat diabetic wounds using gene therapy

Viral Vector	Gene	*In Vivo* Model	Wound Type	Significant Finding	Reference
Adenovirus in fibrin scaffold	eNOS	Alloxan induced diabetic New Zealand white rabbits	6-mm punch biopsy wounds on the ears	Fibrin delivery of AdeNOS resulted in enhanced eNOS expression, inflammatory response, and a faster rate of re-epithelialization	[289]
Adenovirus vector (ADV/VEGF165)	VEGF 165	BKS.Cg-m+/+Lepr^{db} type 2 diabetic mice	Full-thickness excisional wounds, 1.4 cm in diameter on the dorsum	ADV/VEGF165 improves healing enhancing tensile stiffness and/or increasing epithelialization and collagen deposition, as well as by decreasing time to wound closure	[290]
Adenovirus	Placenta growth factor (PlGF)	Streptozotocin induced diabetic C57Bl/6 male mice	6 mm-diameter full-thickness punch biopsy wound	PlGF gene transfer improved granulation tissue formation, maturation, and vascularization, as well as monocytes/macrophages local recruitment	[291]

Table 1.1: Preclinical studies to treat diabetic wounds using gene therapy

Viral Vector	Gene	*In Vivo* Model	Wound Type	Significant Finding	Reference
Adenovirus	PDGF-B	C57BLKS/J-m+/+Lepr(db) and streptozotocin induced	8 mm full-thickness flank wounds	Adenoviral mediated gene therapy with PDGF-B significantly enhanced wound healing and neovascularization in diabetic wounds with augmentation of EPC recruitment	292
Lentivirus	Stromal-derived growth factor-1α (SDF-1α)	BKS.Cg-$m^{+/+}$ $Lepr^{db}$/J mice	8-mm full-thickness wound	SDF-1α treatment exhibited a decrease in wound surface area with more cellular wounds and increased granulation tissue volume and resulted in complete epithelialization at two weeks	293
Lentivirus	PDGF-B	*db/db* mice	2 x 2-cm full-thickness dermal wound	Statistically significant increase in angiogenesis and substantially thicker, more coherently aligned collagen fibers	294, 295

Table 1.1: Preclinical studies to treat diabetic wounds using gene therapy

Non-viral Vector	Gene	*In Vivo* Model	Wound Type	Significant Finding	Reference
Naked plasmid injection	Heat shock protein 47 (HSP47)	Alloxan-induced diabetic rat	Excisional skin wounds	Increased collagen I production around the wound during repair process	296
Plasmid vector with electroporation	HIF-1α	BKS.Cg-m$^{+/+}$ Lepr^{db}/J mice	5-mm full-thickness circular excisional wounds on the dorsum	Electroporation with HIF-1α increased levels of HIF-1α mRNA on day 3 and increased levels of VEGF, PLGF, PDGF-B, and ANGPT2 mRNA on day 7 and ten folds increase in circulating angiogenic cells after HIF-1α treatment	297
Plasmid vector with electroporation	Keratinocyte growth factor-1 (KGF-1)	BKS.Cg-m. Lepr^{db-db} mice	Excisional wounds	Results showed improvement in healing rate, quality of epithelialization and density of new blood vessels	298, 299

Table 1.1: Preclinical studies to treat diabetic wounds using gene therapy

Non-viral Vector	Gene	*In Vivo* Model	Wound Type	Significant Finding	Reference
Sonoporation of minicircle DNA	$VEGF_{165}$	Streptozotocin-Induced diabetic C57BL/6J mice	6 mm punch biopsy wounds on the dorsum	Sonoporation of minicircle-$VEGF_{165}$ resulted in Accelerated wound closure with markedly increased skin blood perfusion and CD31 expression and full restoration of normal architecture	300
Plasmid pellet (1% methyl cellulose)	HOXA3	db/db mice	8-mm full thickness excisional wound on the dorsum	HOXA3 accelerates wound repair by mobilizing endothelial progenitor cells and attenuating the excessive inflammatory response of chronic wounds	301
DNA/Methylcellulose Pellets	Sonic hedgehog (Shh)	C57BLKS/J-$m^{+/+}$*Lepr*^{db} mice	8 mm full-thickness excisional skin wounds	Topical gene therapy resulted in acceleration of wound recovery with increased wound vascularity	302

Table 1.1: Preclinical studies to treat diabetic wounds using gene therapy

Non-viral Vector	Gene	*In Vivo* Model	Wound Type	Significant Finding	Reference
Gold particles and gene gun	Rat opioid growth factor receptor (OGFr) complementary DNA	Adult male rats	3-mm corneal abrasions	Excess OGFr delays reepithelialization, whereas attenuation of OGFr accelerates repair of the corneal surface	303
RGDK-lipopeptide	rhPDGF-B	Streptozotocin-Induced Diabetic Sprague-Dawley Rats	2.1 cm (radii) circular dorsal skin incision to the level of the loose subcutaneous tissues	A single subcutaneous administration of the electrostatic complex of RGDK-lipopeptide and rhPDGF-B plasmid is capable of healing incisional wounds in streptozotocin-induced diabetic rats with significantly higher degree of epithelialization, keratization, fibrocollagenation and blood vessel formation	304

Table 1.1: Preclinical studies to treat diabetic wounds using gene therapy

Non-viral Vector	Gene	*In Vivo* Model	Wound Type	Significant Finding	Reference
Lipofectin and Lipofectamine 2000	Human insulin-like growth factor (higf)-1 (with keratinocytes)	Streptozotocin-Induced Diabetic Yorkshire pigs	Full-thickness excisional Wounds (1.5 × 1.5 × 0.8 cm) on the dorsum	Nonviral gene transfer increased IGF-1 expression in diabetic wounds by up to 900-fold and 83% wound closure achieved with combined gene and cell therapy	305
Plasmid / Liposome	aFGF	db/db mouse	Excisional and incisional	Accelerated closure of excisional wounds and increased Wound breaking strength in incisional wounds	306
Plasmid in PEG-PLGA-PEG tri-block co-polymer	TGFβ1	db/db mouse	7 x 7 mm excisional	Enhanced closure, re-epithelialization and cell proliferation	307

1.3 Gene Delivery Systems

Successful gene therapy of acquired or inherited genetic diseases critically depends on the identification of defects at the molecular level, development of vectors that result in gene replacement, over-expression of a therapeutic gene, or suppression of key targets in cellular signaling cascades involved in disease progression and development of a suitable system to deliver the cargo. The advances in molecular biology, successful completion of the human genome project and innovative technologies such as gene arrays and protein arrays, have contributed tremendously to our knowledge of the molecular dynamics of diseased phenotypes and will continue to do so. However, the bottleneck in the success of gene therapy has been the development of a safe and efficient gene delivery system[308]. The myriad of delivery systems currently under development is testimony to the urgent need for advanced clinical treatment options for a wide variety of diseases. The salient advantages and disadvantages of frequently used vector systems for gene delivery are depicted in Figure 1.2.

Viral carriers are at one end of the spectrum, offering very high transfection efficiency, but with the potential risks of toxicity or immunogenicity, in addition to their other disadvantages, such as difficulty of large-scale production and limited capacity to carry DNA beyond a certain size. At the other end of the spectrum is naked plasmid DNA, exhibiting a very attractive safety profile, but extremely low efficiency. Non-viral carriers, which include liposomes and polymers, lie in middle of the spectrum with a moderate efficiency and safety profile. Research in the field of delivery systems over the past few decades has focused mainly on the development of an optimal delivery system, aiming to increase transfection efficiency towards the viral end of the spectrum, while reducing toxicity to exhibit a superior safety profile and reduce immunological concerns. The non-viral carriers are in vogue due to their superior safety profile, their broad acceptance as reliable treatment options for a variety of medical indications and their versatility.

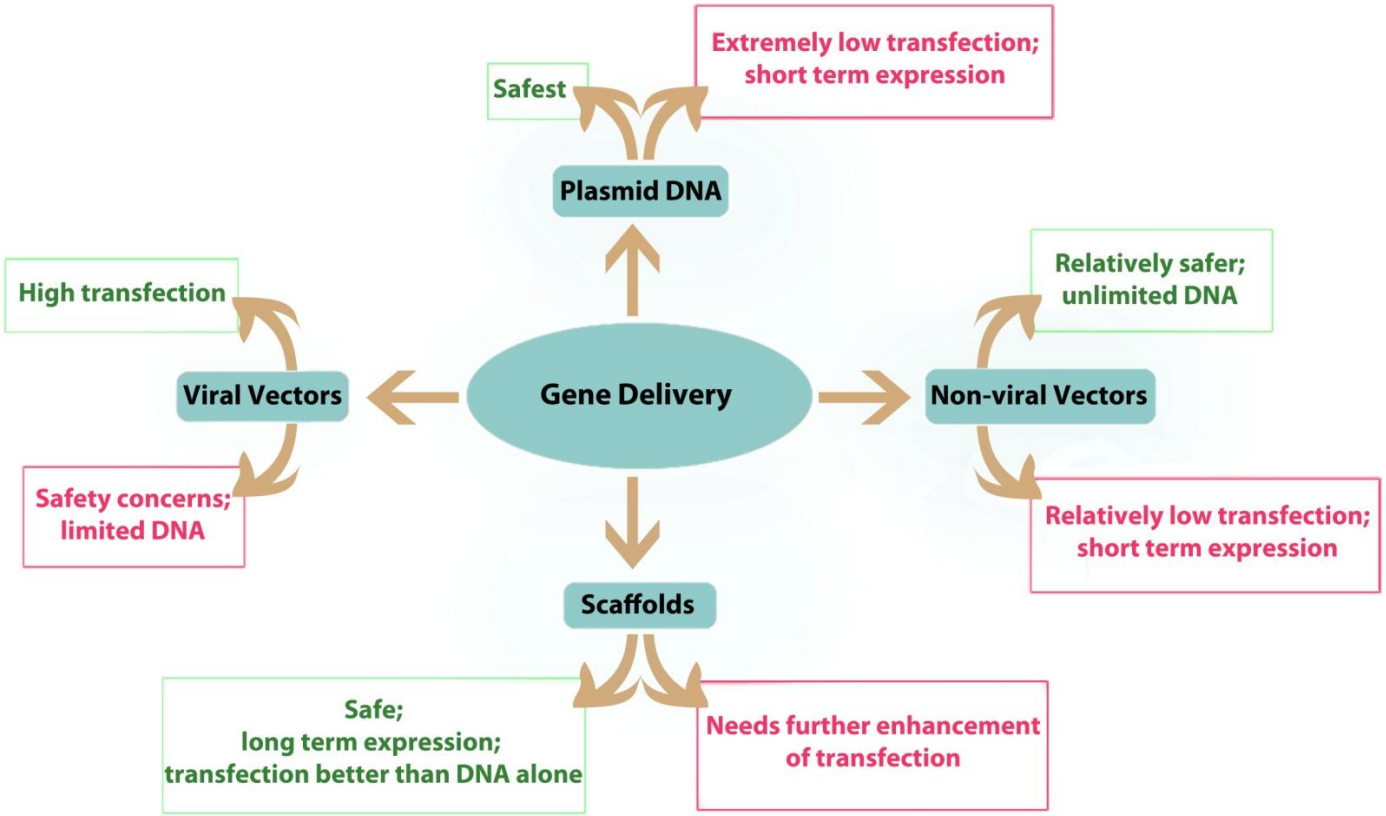

Figure 1.2: Schematic depiction of different options for gene delivery with their relevant advantages and disadvantages. It is clear from this schematic that there is not a single carrier system, which is safe and highly efficient at the same time. This scheme also illustrates that a combination of liposomes and tissue-engineered scaffolds would result in an approach with complementary benefits and reduced limitations.

The tissue-engineered scaffolds are being widely used as control release systems to deliver drugs, cells and/or bioactive agents such as growth factors and genes. When delivering genes, these slow-release systems can lengthen gene expression without risk of insertional mutagenesis as is the case in some of the viral carriers. However, the delivery of plasmid DNA from tissue-engineered scaffolds still poses the problem of low efficiency. Given the lack of a single superior delivery system that addresses all clinical requirements of high efficacy and a convincing safety profile, an increasing amount of research in recent years has focused on improving the delivery systems through a combinatorial approach whereby each component complements the others and thus might lead to an optimized outcome.

1.3.1 Liposomes: Multifaceted and Versatile Non-viral Delivery Systems

Liposomes are spherical lipid bilayers of diameters in the range of 50–1000 nm that have proven useful as convenient delivery vehicles for biologically active compounds[309]. Liposomal systems, despite being the oldest of the non-viral gene-delivery vehicles, remain attractive amid a surge of newer non-viral gene carriers. Their persisting popularity is not only due to advantages such as their unlimited load carrying capacity, relative safety and ease of large-scale production, but can also be attributed to their versatile nature in terms of possible functionalization and formulations. Despite the lower transfection rates of conventional liposomal systems (typically requiring 1,000 to 10,000 times more particles to achieve successful genetic modification of cells compared with viral counterparts), their potential for targeted delivery through functionalization, for example by conjugation with antibody (or fragments), peptides, sugars and so-called ‘stealthing’ i.*e.* polyethylene glycol (PEG)-ylation of lipids, and for escape from the reticuloendothelial system (RES) and, consequently, long-term circulation has proven to be a great advantage. Early progress during the 1970s and 1980s has led to the development of “stealth” liposomes with long circulation times after intravenous administration and decreased uptake by macrophages. These stealth liposomes are able to extravasate out of vasculature and to accumulate in other target tissues such as lung, kidney and liver, in therapeutically effective doses without rapid clearance from the blood stream, thus improving their bio-distribution[310]. Moreover, liposomes can be labeled with fluorescent tags for traceability *in vivo*. A variety of

stimuli such as pH, temperature, ultrasonic waves, magnetic fields and light are currently being investigated for improved gene delivery in various settings[311-314]. Co-application of liposomes with other polymers such as polyethyleneimine provides an avenue for improved transfection efficiency[315-317]. In Tables 1.2 and 1.3, only the recent major advances in gene delivery applications are listed.

1.3.1.1 Successful Liposomal Gene Delivery: Stumbling Blocks and Solutions

There are a number of extracellular and intracellular barriers to successful non-viral gene delivery. In systemic delivery, serum instability and sequestration by the RES due to uptake by macrophages are major problems. Various factors such as size, charge and surface hydration of the liposomes play important roles here. Cellular membranes pose another barrier to liposome uptake. The cationic liposomes show high transfection efficiency which can partly be attributed to interactions with negatively charged cell membranes. The structure and properties of cationic lipids, lipoplex assembly and endocytosis of lipoplexes have recently been described in detail[318]. The internalization of liposomes occurs most commonly by endocytosis in which the genetic material is subjected to degradation upon acidification in endolysosomes. Thus, the efficiency of liposomal uptake largely depends on their ability to escape the endosomal environment and to deliver their DNA/RNA content safely into the cytosol. This is also the reason why many research has been directed towards enhancing endosomal escape. Transfection efficiencies can be predicted from the structural phases of lipids and the morphologies of lipoplexes. For example, studies have shown that the presence of a non-bilayer-phase-preferring lipid, such as dioleoylphosphatidylethanolamine (DOPE) or cholesterol, promotes transition of liquid crystalline phase (L^{C}_{α}) to inverted hexagonal phase (H^{C}_{II}) and hence membrane fusion, indicating that increasing the weight fraction of DOPE might result in higher transfection efficiencies[319].

Table 1.2: Stimuli responsive liposomes in gene delivery: recent advances

Stimuli Responsive Element in Liposomes	Additional Modifications	Cell Types / Animal Model	*In Vitro* / *In Vivo*	Application	Reference
pH Sensitive Liposomes					
Acid-labile PEG-diorthoester (POD) lipids	Various PEG chain lengths	CV-1, B16F10 and U251	*In vitro*	Preparation of nanolipoparticles with high efficiency and low toxicity	320
Carbamate linkages between hydrocarbon chains and ammonium or tertiary amine head	Variable length of carbon chains and quaternary ammonium or neutral tertiary amine heads	-	*In vitro*	Synthesis of carbamate-linked lipids for gene delivery	321
GALA	-	COS-7, PC-12	*In vitro*	pH-sensitive fusogenic peptide mediated gene delivery	322

Table 1.2: Stimuli responsive liposomes in gene delivery: recent advances

Stimuli Responsive Element in Liposomes	Additional Modifications	Cell Types / Animal Model	*In Vitro* / *In Vivo*	Application	Reference
pH Sensitive Liposomes					
Methacrylic acid copolymers	Fluorescent labeling	A549	*In vitro*	Intracellular delivery of antisense oligonucleotides	323
DOPE	Polylysine	-	*In vitro*	Biophysical characterization using empirical phase diagrams	324
Histidine-modified galactosylated cholesterol derivative	-	HepG2 , NIH3T3	*In vitro*	Hepatocyte selective gene transfer	325
Histidine-lysine peptide in the complex	Modified hybrid (DNA-RNA) anti-HER-2 siRNA molecule	PANC-1, MDA-MB-435, MDA 435/LCC6 / PANC-1 s.c. tumors induced in female athymic nude (NCR nu/nu) mice	*In vitro* and *in vivo*	siRNA delivery via tumor targeting nanodelivery system	326

Table 1.2: Stimuli responsive liposomes in gene delivery: recent advances

Stimuli Responsive Element in Liposomes	Additional Modifications	Cell Types / Animal Model	*In Vitro* / *In Vivo*	Application	Reference
pH Sensitive Liposomes					
Hydrazone	PEG on TATp liposomes via pH/ non pH sensitive bonds	LLC tumors grown in nu/nu mice	*In vitro* and *in vivo*	Tumor specific intracellular gene delivery	311
DOPE and CHEMS	Pre-condensation of plasmid DNA with ALA and the incorporation of Tf into the formulations	HeLa	*In vitro*	DNA precondensation for enhanced gene delivery	327
Membrane-introduced Chol-GALA and a PEGylated GALA	Tf modified PEGylated liposomes	K562	*In vitro*	Development of artificial virus-like nanocarrier system	328

Table 1.2: Stimuli responsive liposomes in gene delivery: recent advances

Stimuli Responsive Element in Liposomes	Additional Modifications	Cell Types / Animal Model	*In Vitro* / *In Vivo*	Application	Reference
pH Sensitive Liposomes					
Synthetic analogue of a fusogenic peptide domain in glycoprotein H from herpes simplex virus	-	HepG2	*In vitro*	Fusogenic peptide for improved transfection efficiency	329
Polyethylene glycol-diorthoesterdistearoyl glycerol lipid	TATp modified PEGylated liposomes	U87-MG cells / Caudate putamen of healthy brains or U87-MG orthotopic tumors in athymic rats	*In vitro* and *in vivo*	TATp and convection enhanced delivery for gene delivery to brain and implanted tumors	330

Table 1.2: Stimuli responsive liposomes in gene delivery: recent advances

Stimuli Responsive Element in Liposomes	Additional Modifications	Cell Types / Animal Model	*In Vitro* / *In Vivo*	Application	Reference
pH Sensitive Liposomes					
Carboxylated poly(glycidol) derivatives	Varying hydrophobicities by reacting poly(glycidol) with glutaric anhydride, 3-methylglutaric anhydride, and 1,2-cyclohexanedicarboxylic anhydride	HeLa cells	*In vitro*	Preparation of pH-Sensitive Poly(glycidol) Derivatives with Varying Hydrophobicities	331
Poly(glycidol) with carboxyl groups	Tf and Mannan	DC2.4 cells	*In vitro*	Gene delivery to dendritic cells	332
Negatively charged cholesterol bearing two and four carboxylate moieties	The mixture of the cationic lipid and the negatively charged cholesterol at various ratio	B16 murine cells / C57Bl/6 mice bearing 3LL tumors	*In vitro* and *in vivo*	Liposomal delivery to lung tumors	333

Table 1.2: Stimuli responsive liposomes in gene delivery: recent advances

Stimuli Responsive Element in Liposomes	Additional Modifications	Cell Types / Animal Model	*In Vitro* / *In Vivo*	Application	Reference
pH Sensitive Liposomes					
DOPE and CHEMS (3:2 mol/mol)	DNA/PEI complexes and PEGylation	CV1-P cells	*In vitro*	Synthesis of glycosaminoglycan-resistant and pH-sensitive lipid-coated DNA complexes	334
Anionic LPD complexes	-	RAW 264.7	*In vitro*	Anionic lipid/peptide/DNA complexes for gene delivery	335
Oxime linkage that results from PEG coupling with aminoxycholesteryl lipid	-	Huh-7 / HBV transgenic mice	*In vitro* and *in vivo*	Anti HBV siRNA delivery	336
GALA	Avidin (68 kDa) and streptavidin-coated quantum dots (15-20 nm)	HeLa	*In vitro*	Cytosolic targeting of proteins and nanoparticles	337

Table 1.2: Stimuli responsive liposomes in gene delivery: recent advances

Stimuli Responsive Element in Liposomes	Additional Modifications	Cell Types / Animal Model	*In Vitro* / *In Vivo*	Application	Reference
Ultrasound Sensitive Liposomes					
Lipid coated microbubbles (perfluorobutane as filling gas)	Varying phospholipid and emulsifier Composition	-	*In vitro*	Role of shell composition in modulating the acoustic response of lipid-coated microbubbles	338
Bubble liposomes containing perfluoropropane	PEGylation	COS-7 / ddY mice	*In vitro* and *in vivo*	Combination of bubble liposomes and ultrasound exposure non-invasive gene delivery tool	339
Liposomes filled with CO_2 gas bubbles	-	-	*In vitro*	Preparation and characterization of bubble liposomes	340
Bubble liposomes entrapping perfluoropropane gas	-	COS-7 / i.a injection in mouse femoral artery	*In vitro* and *in vivo*	Bubble liposomes and ultrasound as non-invasive gene delivery	341

Table 1.2: Stimuli responsive liposomes in gene delivery: recent advances

Stimuli Responsive Element in Liposomes	Additional Modifications	Cell Types / Animal Model	*In Vitro* / *In Vivo*	Application	Reference
Ultrasound Sensitive Liposomes					
Lipid shelled decafluorobutane microbubbles	-	Ligation of left common iliac artery and small proximal branches in Sprague-Dawley rats	*In vivo*	Therapeutic arteriogenesis	312
Bubble liposomes containing perfluoropropane	PEGylation	S-180, Colon26, B16BL6, Jurkat, HUVEC, COS-7 / i. a. injection in mouse femoral artery	*In vitro* and *in vivo*	Tissue specific gene delivery	342
Bubble liposomes containing perfluoropropane	-	COS-7 / ddY mice with i.p. injection of S-180 cells / ddY mice with inoculation of S-180 cells in foot pad	*In vitro* and *in vivo*	Tumor specific delivery	343

Table 1.2: Stimuli responsive liposomes in gene delivery: recent advances

Stimuli Responsive Element in Liposomes	Additional Modifications	Cell Types / Animal Model	*In Vitro* / *In Vivo*	Application	Reference
Ultrasound Sensitive Liposomes					
Microbubbles with perfluorobutane	Loading microbubbles with PEGylated siRNA-liposomes complexes	HUH7, HUH7eGFPLuc	*In vitro*	Delivery of siRNA targeting firefly luciferase	344
Bubble liposomes containing perfluoropropane	PEGylation	COS-7, NIH3T3 and C2C12 / i.d., i.m. and intra-renal-parenchymal injection in ICR mice	*In vitro* and *in vivo*	Delivery of siRNA targeting luciferase and EGFP	345
Ultrasonic gas-filled liposomes	Varying wave intensity, ultrasound duration, gas-filled liposome concentration, and oligonucleotide concentration	SK-BR-3	*In vitro*	Downregulation of HER-2 expression by antisense oligonucleotide delivery	346

Table 1.2: Stimuli responsive liposomes in gene delivery: recent advances

Stimuli Responsive Element in Liposomes	Additional Modifications	Cell Types / Animal Model	*In Vitro* / *In Vivo*	Application	Reference
Magnetic Field Sensitive Liposomes					
Transferrin-associated cationic lipid-coated magnetic nanoparticles	Combined with PEI condensed plasmid DNA	KB cell line, Human EGFR cDNA transfected F98EGFR glioma cell line	*In vitro*	Enhanced gene transfer under influence of a magnetic field	[347]
Magnetite in cationic liposomes	Varying concentrations of magnetite	THLE-3 / i.v. injection in male wistar rats	*In vitro* and *in vivo*	Enhanced gene transfer under influence of a magnetic field	[313]

Table 1.2: Stimuli responsive liposomes in gene delivery: recent advances

Stimuli Responsive Element in Liposomes	Additional Modifications	Cell Types / Animal Model	*In Vitro* / *In Vivo*	Application	Reference
Light Sensitive Liposomes					
Hollow gold nanoshells (near infrared light)	Different coupling methods such as having the HGNs tethered to, encapsulated within, or suspended freely outside the liposomes	-	*In vitro*	Remote triggering by near infrared light for liposome release	314
Bilayer-incorporated [Methyl(PEG)2000MA] polymer (UV light)	PEGylation	-	*In vitro*	Light-sensitive fusion between polymer-coated liposomes	348

Table 1.3: Targeted liposomes in gene delivery: recent advances

Targeting Moiety	Targeted Tissue / Cells / Receptors	Additional Modifications	*In Vitro / In Vivo*	Application	Reference
PLAEIDGIELA; tenascin peptide sequence	Upper-airway epithelial cells/ alpha(9)beta(1)-integrin proteins	Liposome: Mu peptide: DNA platform	*In vitro*	Synthesis and application of integrin targeting lipopeptides	349
Endothelium-specific antibody (273-34A) via a distearoyl phosphatidyl ethanolamine-poly(ethylene glycol) spacer	Mouse lung endothelial cells	Ionisable amino lipid (1,2-dioleoyl-3-dimethylammonium propane) and an ethanol-containing buffer system for encapsulating large quantities of polyanionic ODN	*In vitro* and *in vivo*	Targeted delivery of oligodeoxynucleotides	350
Antibody-lipopolymer (anti-HER2 scFv (F5)-PEG-DSPE) conjugate	HER2 overexpressing SK-BR-3 breast cancer cells	PEGylation	*In vitro*	Self-assembling nucleic acid-lipid nanoparticles suitable for targeted gene delivery	351

Table 1.3: Targeted liposomes in gene delivery: recent advances

Targeting Moiety	Targeted Tissue / Cells / Receptors	Additional Modifications	*In Vitro / In Vivo*	Application	Reference
Biotinylated transferrin	HeLa cells/ transferrin receptor	Lipophilic cholesteryl-based biotin derivatives, biotinyl cholesteryl formylhydrazide (MSB1) and amino hexanoyl biotinyl cholesteryl formylhydrazide (MSB2) for docking streptavidin(bio3-transferrin) on cationic liposomes	*In vitro*	Lipoplexes with biotinylated transferrin accessories	352
Fucosylated cationic liposomes	Liver	-	*In vitro* and *in vivo*	NF kappa B decoy delivery	353
DSPE-PEG-anisamide	Lung cancer cells	Liposome-polycation-DNA nanoparticles	*In vitro*	AS-ODN and siRNA delivery	354
Galactosylated cationic liposomes	Liver / parenchymal cells	-	*In vitro* and *in vivo*	siRNA delivery	355

Table 1.3: Targeted liposomes in gene delivery: recent advances

Targeting Moiety	Targeted Tissue / Cells / Receptors	Additional Modifications	*In Vitro / In Vivo*	Application	Reference
DSPE-PEG-anisamide	Human lung cancer cells	PEGylated liposome-polycation-DNA nanoparticles	*In vitro* and *in vivo*	Liposome-polycation-DNA nanoparticles for tumor targeting	356
Sulfatide	Glioma cells/ tenascin-C	-	*In vitro*	siRNA delivery	357
Mannose 6-phosphate human serum albumin	Liver/ hepatic stellate cells	Fusion with HVJ envelopes	*In vitro* and *in vivo*	Antifibrotic therapy	358
Monoclonal antibodies: clones RI7 and 8D3	Mouse transferrin receptor	PEGylation	*In vitro*	Development of a PEG-stabilized immunoliposome formulation	359
Mannosylated cationic liposomes	Melanoma/ Mannose receptors	Melanoma associated antigen expressing pDNA	*In vitro* and *in vivo*	DNA vaccination	360

Table 1.3: Targeted liposomes in gene delivery: recent advances

Targeting Moiety	Targeted Tissue / Cells / Receptors	Additional Modifications	*In Vitro / In Vivo*	Application	Reference
Monoclonal antibodies: OKT9, 1.2 B6, 1.4 C3	Human transferrin receptor (CD71), E/P-selectin (CD62E/P), VCAM-1 (CD106) respectively	Complexes formed between viruses, liposomes, and antibodies	*In vitro*	Changing viral tropism	[361]
Monoclonal antibody: rat 8D3	Mouse transferring receptor	Trojan horse liposomes	*In vitro* and *in vivo*	Gene delivery to Brain	[362]
CRRETAWAC domain of peptide 3	$\alpha_5\beta_1$integrins	Polylysine component to condense DNA	*In vitro*	Biophysical characterization	[363]
C-terminal fragments of tetanus toxin (THC), botulinum toxin (BHC) or the truncated C-terminal domain of THC	Neuronal cell lines (human SH-5YSY and rat/mouse hybrid N18-RE105)/ GT1b receptor	PEGylation	*In vitro*	Gene delivery to CNS	[364]

Table 1.3: Targeted liposomes in gene delivery: recent advances

Targeting Moiety	Targeted Tissue / Cells / Receptors	Additional Modifications	*In Vitro / In Vivo*	Application	Reference
Monoclonal antibody: FIB504	Gut mononuclear leukocytes/ B_7integrins	Hyaluronan coating of liposomes and protamine condensation of siRNA	*In vitro* and *in vivo*	Systemic leukocyte-directed siRNA delivery	365
CRPPR peptide	Heart endothelium	PEGylation	*In vitro* and *in vivo*	Targeting of heart and dynamic imaging	366
Fab' fragments of recombinant humanized monoclonal antibody, HuCC49	TAG-72-overexpressing cancer cells	PEGylation	*In vitro* and *in vivo*	Systemic gene delivery to human colon cancer cells	367
DSPE-PEG2000-anisamide	B16F10 cells / Sigma receptor	PEGylation and protamine condensation	*In vitro* and *in vivo*	siRNA delivery to metastatic tumors	368

Table 1.3: Targeted liposomes in gene delivery: recent advances

Targeting Moiety	Targeted Tissue / Cells / Receptors	Additional Modifications	*In Vitro / In Vivo*	Application	Reference
K16GACSERSMNFCG	Lung/ human airway epithelial cell lines/ intercellular adhesion molecule-1 (ICAM-1)	PEGylation	*In vitro* and *in vivo*	Cystic fibrosis gene therapy	369
Folate	HeLa cells/ folate receptors	Series of novel di- and tetraether-type archaeal derivatives with a PEG chain	*In vitro*	Synthesis and transfection properties of folate equipped archaeal lipid derivatives	370
DSPE-PEG-anisamide	Sigma receptor over-expressed in the B16F10 melanoma cells	Liposomes-protamine-hyaluronic acid nanoparticle	*In vitro* and *in vivo*	siRNA delivery to tumors	371
Monoclonal antibody: 2G4	Myocardium/ myosin	TATp peptide	*In vitro* and *in vivo*	Gene delivery to ischemic myocardium	372

Table 1.3: Targeted liposomes in gene delivery: recent advances

Targeting Moiety	Targeted Tissue / Cells / Receptors	Additional Modifications	*In Vitro / In Vivo*	Application	Reference
Monoclonal antibody: 8D3	Brain/ transferrin receptor	Encapsulation of the PEI/ODN polyplexes into PEGylated liposomes	*In vivo*	Targeting brain	[373]
U11 peptide-lipid amphiphile	Prostate cancer cells (DU145 cells) / urokinase plasminogen activator receptor	PEGylation	*In vitro*	Targeting specific receptor overexpressed in breast and prostate cancers	[374]
Artificial cationic liposome-associated apolipoprotein A-I	Hepatocytes/ Scavenger receptor BI (SR-BI)	Construction of transient HCV model by hydrodynamic injection of plasmid DNA expressing viral structural proteins under hepatic control region and alpha1-antitrypsin promoter elements	*In vivo*	Targeted delivery of siRNA against hepatitis C virus	[375]

1.3.1.2 Peptides for Intracellular Delivery

Recently, peptides have been increasingly used with the aim to aid the intracellular delivery of the genes. Tat peptide (TATp) is by far the most commonly used cell penetrating peptide, or so-called protein transduction domain (PTD), and is derived from the transcriptional activator protein encoded by human immunodeficiency virus type 1 (HIV-1). Its mechanism has recently been elucidated as macropinocytosis, a nonclathrin noncaveolar endocytosis brought about by formation of large vacuoles that are generated by actin filaments[376]. TATp-mediated delivery of liposomes and DNA has recently been reviewed[376 377]. Octaarginine is another commonly used PTD that is thought to use cell surface heparin sulfate proteoglycans as non-specific receptors for uptake. Octaarginine-modified liposomes have been used for enhanced cellular uptake and controlled intracellular trafficking of plasmid DNA[378]. Apart from cell penetration, peptides are also being utilized for endosomal escape, which in turn results in higher transfection efficiency. Another cell-penetrating peptide is GALA, (a 30-amino acid synthetic peptide with a glutamic acid–alanine–leucine–alanine repeats), a fusogenic pH-sensitive peptide developed by Szoka and co-workers that aids cytosolic delivery by facilitating the disruption of endosomal membrane and release of DNA in cytoplasm. Kobayashi et al. and Sasaki et al. demonstrated enhanced endosomal escape of macromolecules via GALA and its derivatives[328 337].

While fusogenic peptides act upon acidification in endosomes, it has been recently shown that a stearylated INF7 peptide derivative enhanced gene expression in a fusion-independent manner and was able to rupture artificial membranes, both at acidic and neutral pH, extending the time the liposomes could escape endosomal degradation[379]. Once successful delivery of liposomes to the cytosol has been accomplished, liposome-mediated gene delivery faces additional obstacles such as the requirement of intracellular trafficking to the nucleus and uptake into the nucleus via the nuclear pore complexes. The potential of using nuclear localization signals (NLSs) for targeting to the nucleus has been studied by several groups and it was found that the efficiency of nuclear targeting depended on the valency (positive charges) associated with plasmid DNA and the number of NLS associated with a cargo such as plasmid DNA, proteins, liposomes and nanoparticles[380]. Different NLSs will bind to different receptors on

nuclear membranes such as importins[381] or farnesoid X receptor (FXR)[382], either directly or indirectly by forming complexes with other cytoplasmic proteins. A significant increase in gene expression that was mediated by liposomes and the means of using a NLS has been shown, both *in vitro* and *in vivo*[381 382]. Attempts have also been made to utilize the biological responses against liposomes such as cytokine production, for their increased uptake. TNF-α, which is induced by lipoplexes, is known to activate transcription factor nuclear factor κB (NF-κB), and NF-κB upon activation can aid nuclear transfer of DNA. It has been reported that if NF-κB binding sequences are incorporated in plasmid DNA, lipoplex-mediated transgene expression can be enhanced[383].

1.3.1.3 Short Term Expression and Toxicity Related to Liposomes

Short-term expression following liposomal gene delivery constitutes a major problem in clinical applications that requires sustained levels of transgene expression over months and years. Short-term expression is due to the cargo being either not integrated into the host genome, or integrated only in an unstable manner, and this limitation can be addressed with repeated doses of the gene, a practice, which, however, is not always feasible and/or practical. Here, gene delivery via release systems with an extended effect, such as tissue-engineered scaffolds, presents the opportunity of controlled DNA release over a long period as required for long-term expression. The toxicity of cationic lipids, which are frequently inflammatory, is another concern. This toxicity is dose-dependent and is based on to the exposure of the liposome to and its interactions with immune cells. The use of tissue-engineered scaffolds could address these issues as a topical delivery of liposomes via a tissue scaffold would reduce their exposure to immune cells.

1.3.2 Tissue-Engineered Scaffolds

The view of tissue-engineered scaffolds as gene delivery systems is a relatively novel concept. Initially, scaffolds were proposed for applications in tissue engineering and considered solely as inert structural support for tissue repair and regeneration. Over the last few years, this view has changed dramatically and scaffolds are no longer seen only as dynamic tools for mimicking biological environments but now are also regarded as

delivery vehicles for cells and/or bioactive agents. Tissue-engineered scaffolds provide a multitude of advantages such as safe profile, protection of cargo, and enhanced and extended gene expression and the ability to control a localized delivery of cargo, as depicted in Figure 1.3.

1.3.2.1 Tissue-engineered Scaffolds as Depots and Controlled-release Systems

Tissue-engineered scaffolds can be designed in order to physically and/or chemically control the release pattern of any incorporated bioactive agents. A controlled release of DNA will not only lead to extended periods of gene and thus protein expression, but will also minimize the risk of under- or over-dosing of the expressed protein. The major advantage of using natural scaffolds, such as collagen and fibrin, in addition to their safety profile, is their tunable degradation, which can be readily achieved either by varying the concentration of monomers and/or crosslinking agents and thus controls the long-term release of bioactive agents. As with ECM, fibrin-based biomaterials could also act as temporary depots for the sustained release of substances [384] which could be readily optimized by varying the concentrations of the fibrinogen and thrombin components[385]. The release profile of bioactive agents from collagen/gelatin scaffolds can also be further optimized by appropriate choice of crosslinking agents, such as microbial transglutaminase or *N*-ethyl-*N*-(3-diethylaminopropyl)-carbodiimide/*N*-hydroxysuccinimide (EDC/NHS), as well as the degree of crosslinking.

As an alternative to natural scaffolds, synthetic scaffolds have also been suggested as they are highly flexible in that they can be manufactured in any desired shape and size, with a tightly defined architecture and relevant parameters such as porosity. Some of these synthetic scaffolds such as polylactic acid (PLA) also have the additional advantage of a degradation within the body, which will only leave behind harmless breakdown products such as lactic acid[308]. By crosslinking of PLA with PEG, or by using co-polymers such as poly(lactic-*co*-glycolic acid) (PLGA), their degradation in the body can be further controlled[308].

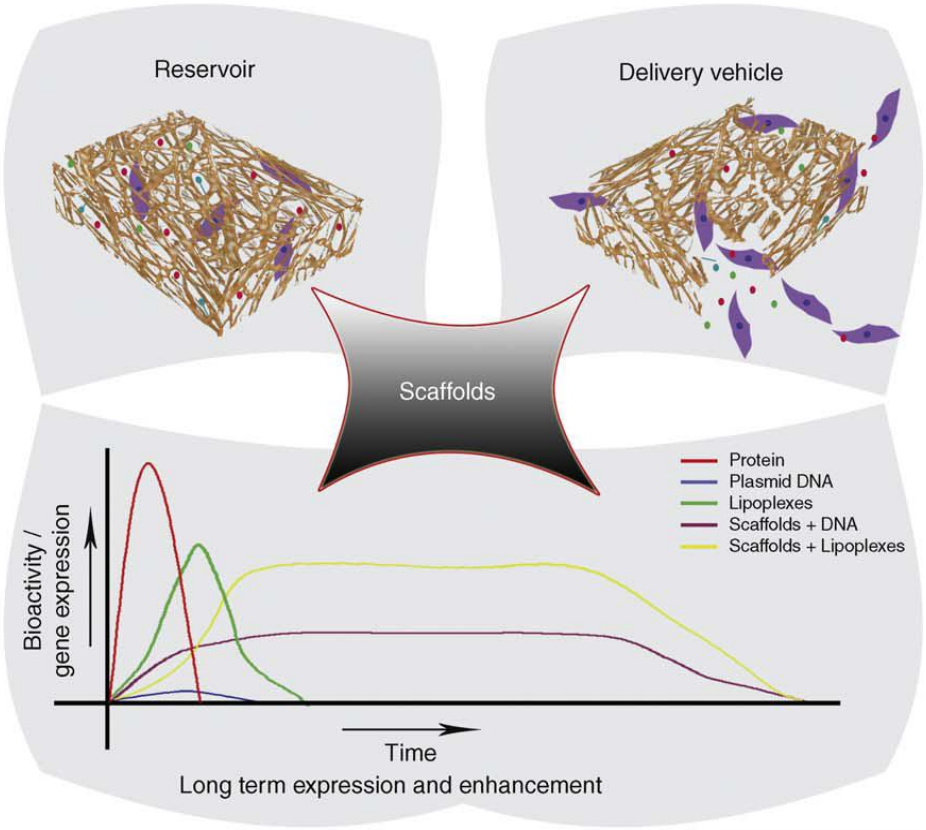

Figure 1.3: Schematic depiction of the role of tissue-engineered scaffolds in gene delivery. Tissue-engineered scaffolds can be employed either as reservoirs, or as sustained delivery systems. If they are used as reservoirs, the host tissue will integrate with the scaffold material and the contents of the scaffolds will exhibit their intended function in the context of the host tissue. In sustained delivery systems, the contents of the scaffolds are delivered as and when the scaffold material degrades. This sustained delivery results in gene expression over a longer period than would be the case with delivery by lipoplexes alone. As depicted in the graph shown below, tissue-engineered scaffold-mediated sustained gene delivery enhanced gene expression and a synergistic effect is observed when tissue-engineered scaffolds delivered lipoplexes (yellow curve) as opposed to naked plasmids (purple curve).

1.3.2.2 Need for Further Enhancement

Although, as depicted in Figure 1.3, the enhanced and sustained localized gene delivery that could be achieved via tissue-engineered scaffolds is certainly superior to that of naked plasmid delivery, further enhancement is required for therapeutic benefit. Towards this goal and as opposed to delivering naked plasmid DNA through scaffolds, a number of researchers have utilized different transfection reagents such as liposomes to first complex the DNA and to subsequently deliver these complexes via the scaffolds, as outlined below.

1.3.3 A Combined Liposome–scaffold Approach

As mentioned above, the combination of liposomal gene delivery systems with scaffold technologies is now being considered as being complementary. Table 1.4 summarizes a number of studies that have investigated tissue-engineered scaffold-mediated liposomal gene delivery. The various aspects and intrinsic benefits offered by this combined liposome-scaffold approach are discussed in detail below.

1.3.3.1 Long-term Expression

By far the most important advantage of combining tissue-engineered scaffolds with liposomal gene delivery is the possibility and flexibility of a well-controlled sustained delivery. This fact provides an opportunity to overcome short-term gene expression following liposomal delivery, although the release kinetics of the used lipoplexes would depend on various factors, such as their size and net charge, as well as their biomolecular and chemical interactions. The combination of tissue-engineered scaffolds with liposomes has already been utilized for sustained delivery of drugs. For example, a single application of fibrin-enmeshed tobramycin-bearing liposomes had a similar effect on reducing pseudomonas colonies when treating pseudomonas keratitis compared to 24 hourly doses of fortified topical tobramycin[386]. Subsequently, a number of studies have described sustained release systems using liposomes loaded with proteins or drugs and that had been incorporated in fibrin[387-390]. The biomedical applications of collagen, including a combination of liposomes with collagen for drug delivery, have been reviewed elsewhere[391].

Table 1.4: Combined liposome-scaffold approach for gene delivery

Scaffold/ Substrate	Liposomes	DNA	Application	Reference
Serum-coated tissue culture polystyrene	Lipofectamine ™ 2000	Plasmid- luciferase/ EGFP	Substrate mediated delivery	[392]
Porous poly (D,L-lactide) disks	FuGene® 6 lipophilic transfection reagent; 20 mM DOTAP: cholesterol (1:1) liposome	Plasmid- GFP	Bone repair	[393]
PLG matrices	Lipofectamine ™ 2000	Plasmid- luciferase/β-galactosidase/NGF/ NGF-GFP dual expression	Nerve regeneration	[394]
Type II collagen glycosaminoglycan scaffolds	GenePORTER® Reagent	Plasmid- insulin-like growth factor (IGF)-1	Cartilage repair	[395]
Fibrin	Lipofectamine™ and Plus Reagent	Plasmid- VEGF	Wound healing	[396]

Table 1.4: Combined liposome-scaffold approach for gene delivery

Scaffold/ Substrate	Liposomes	DNA	Application	Reference
Collagen	GenePORTER® Reagent	Plasmid- GDNF	Brain injury	397
Tissue culture polystyrene	Lipofectamine ™ 2000	Plasmid- EGFP-luciferase	Substrate mediated delivery	398
Polystyrene Plate	Lipofectamine™	Plasmid- luciferase	Substrate mediated delivery	399
Fibrin	Lipofectin ®Reagent	Plasmid- EGFP; luciferase + β-galactosidase	Simultaneous delivery of multiple genes to wound bed	400
ECM coated Multiple channel PLG bridges	TransFast™ Transfection Reagent	Plasmid- firefly luciferase and β-galactosidase	Spinal cord injury	401
Polydimethylsiloxane cured on patterned molds using photolithography	Lipofectamine ™ 2000	Plasmid- EGFP + luciferase; NGF	Nerve repair	402

The extended release of lipoplexes, and consequently the long-term expression of their delivered genes, has been demonstrated by a number of groups[393-395 400 401]. To achieve sustained delivery, different approaches were possible. For example, lipoplexes could be merely entrapped physically within the scaffolds by tailoring certain parameters, such as the degree of crosslinking and pore sizes. Alternatively, lipoplexes were specifically bound to components of the scaffolds. Recently, a fibrin-lipoplex system was described. This system made use of naturally-occurring interactions between liposomes and the fibrinogen components of the scaffold, which obviated the need for chemical conjugation[400].

Another approach for creating a sustained delivery system is the adsorption of lipoplexes on the surface of scaffolds[392 399 403]. To facilitate lipoplex adsorption, scaffold surfaces have been coated with various ECM proteins, and this has led to being able to transfect a higher number of cells while at the same time reducing the amount of DNA required. Several other strategies have been developed to associate lipoplexes or DNA complexes with the scaffold surface, including the specific binding of complexes to the scaffold through biotin–avidin interaction, gelatin entrapment, or by nonspecific adsorption[392].

1.3.3.2 Maintaining Lipoplex Stability

Another major advantage of the combining liposomes with scaffolds is that this approach maintains lipoplex stability, consequently prolonging bioactivity. An increased liposomal stability has been demonstrated in fibrin-encapsulated liposomes that were used as protein delivery system[404], as well as in biophysical studies of collagen-lipid interactions[405]. The local delivery of lipoplexes from a biomaterial scaffold, such as fibronectin-coated PLG, could have the ability to maintain lipoplex stability and therefore could increase the number of transfected cells and transgene expression[401]. In a spinal cord injury model, high transgene expression has been achieved by implanting fibronectin-coated-PLG bridges with multiple hollow channels that had been immobilized with lipoplexes[401]. However, the fabrication of the scaffold can also adversely affect the stability of lipoplexes. Therefore, special processing techniques, such as cryopreparation or carbohydrate stabilization as well as mild

processing conditions need to be adopted to avoid any detrimental effect on lipoplex stability, and thus the activity of incorporated DNA complexes[406]. On the other hand, if lipoplexes are immobilized on the surface of a scaffold, the need for careful processing steps is obviated as the lipoplexes are immobilized after the scaffold fabrication[407].

1.3.3.3 Moderating Lipoplex Toxicity

Although considered safer than viral delivery systems, lipoplexes are frequently associated with some degree of toxicity, typically in the form of inflammatory responses. The enhanced transgene expression observed via the combined liposome-scaffold approach reduces the required dose and this indirectly reduces dose-related toxicity. However, the cellular toxicity seen in direct bolus delivery of lipoplexes has been shown to be reduced significantly when they are delivered via gene activated matrix (GAM)[393]. This can be explained by the fact that, at any given time, only those lipoplexes that are released from, and that are only a fraction of the total amount incorporated in the scaffold, are exposed to the immune cells. This apparent 'fooling' of the immune system helps to reduce the observed toxicity of lipoplexes. Another postulation that can explain the observed reduction in toxicity is that the specific interaction of cells with scaffold material such as fibrin can lead to suppression of the caspase pathway which is involved in cell apoptosis and that of reactive oxygen species, which are typically activated by liposomes[408]. In addition, when compared to bolus delivery, this approach has been shown to transfect cells, which are otherwise hard to transfect such as primary cells, and with improved cellular viability[392]. Thus, with regard to toxicity, embedding the lipoplexes within the scaffold appears a particularly useful approach, whereas surface adsorption is beneficial in terms of flexibility of fabrication and stability. In addition, the possibility of a localized therapy as afforded by the use of scaffolds significantly reduces the occurrence of systemic toxicity.

1.3.3.4 Multiple Gene Delivery and Spatio-temporal Patterning

Combining liposomes with scaffolds also provides several additional advantages such as the possibility to deliver multiple genes simultaneously[400], or to create spatial[402] and temporal patterns of gene delivery. Recently, the successful simultaneous delivery of two reporter genes by means of a fibrin-lipoplex model system was demonstrated[400].

Such a system might prove particularly useful in diseases in which multiple genes are involved, or in which the local restoration of a specific gene function can result in therapeutic benefit, e.g. the compromised wound healing seen in diabetes mellitus. In most tissues in the body, a highly orchestrated spatio-temporal control of gene expression is established, particularly in neural and vascular networks. Recently, spatially-patterned expression of NGF was achieved using lipoplexes that had been immobilized in microfluidic networks of polydimethylsiloxane (PDMS) and this patterned expression of NGF led to neurite outgrowth and guidance[402]. Another means to control spatial gene expression is to immobilize lipoplexes to specific regions of the scaffold, which is the basis for transfected cell-arrays used in high-throughput functional genomics studies[403]. Here, patterned deposition of lipoplexes can be achieved by various techniques, such as spotting, printing, pinning and microfluidics[409]. Additionally, temporal control over gene expression can be achieved in a number of ways, such as by layer-by-layer assembly[410] of the scaffold with lipoplexes incorporated only in certain layers. Cell-controlled temporal expression patterns are also possible[408] in which the lipoplexes are confined within the scaffold, and only become available for transfection only upon cell-mediated degradation of scaffold. Another approach could be to simply mix polymer scaffolds that have different degradation profiles[409] or to fabricate a complex scaffold consisting of predetermined regions with different degradation rates, different porosity or different density of "homing" agents such as antibodies or peptide ligands. The success of spatial patterning depends largely on the stability and activity of DNA complexes after they have been deposited on or embedded in the scaffold, and thus, the differential concentration achieved on the pattern as against the non-patterned region of the scaffold[409].

On the other hand, lipoplexes have also been shown to enhance the transfection efficiency that can be achieved using only tissue-engineered scaffolds as demonstrated for the delivery of lipoplexes based on fibrin-scaffolds based in skin wound healing[396]. The authors of this study showed a significantly higher skin flap survival when it was treated with a fibrin-lipoplex system carrying vascular endothelial growth factor plasmid (pVEGF) as compared to using a fibrin gel carrying pVEGF. The enhanced gene expression upon liposome-scaffold delivery was synergistic and not merely

additive. Their claim could be substantiated by observations of six to seven-fold increase in protein production compared to control levels as long as two weeks after treatment of rat mesenchymal stem cells with a porous sponge-like collagen scaffold that had been embedded with lipoplexes carrying glial cell line-derived neurotrophic factor (GDNF) gene[397].

1.3.3.5 Potential for Clinical Translation

One of the most promising aspects of combining liposome with scaffold-based delivery is its potential for clinical translation in the near future. A range of tissue-engineered scaffolds has already been approved for human use and this list is ever increasing and some relevant examples are summarized in Table 1.5.

Currently, over a hundred clinical trials addressing liposomal gene delivery are underway and are at different phases of completion. Considering the advantageous regulatory status of tissue-engineered scaffolds and of liposomal approaches, a clinical realization of combined liposome-scaffold delivery could be anticipated within the next two decades.

Table 1.5: Examples of tissue-engineered scaffolds approved for human use

Major Component	Clinical Use	Market Name	Marketed By
Collagen	Skin repair	TransCyte®	Advanced Biohealing
		Apligraf®	Organogenesis
		Dermagraft®	Advanced Biohealing
		INTEGRA® dermal regeneration template	Integra Lifesciences
	Bone repair	INFUSE® bone graft	Medtronic
		OP-1™	Stryker
		VITOSS® Scaffold FOAM™	Orthovita and Kensey Nash
		FortrOss	Pioneer Surgical
		BioSet®-RTI	Pioneer Surgical and Regeneration Technologies
	Nerve conduit	NeuraGen®	Integra
	Cartilage repair	Menaflex™	Regenbiologics
		CaReS®	Arthro Kinetics
Fibrin	Sealant for wound management	TISSEEL™	Baxter International
Gelatin	Bone repair	Regenafil®	Exactech

1.4 Fibrin Scaffolds

For the assets discussed in section 1.3.4, tissue engineered scaffolds are being investigated increasingly for gene delivery experiments as tools for controlled extended and patterned release of the cargo. The fibrin scaffolds, in particular, have a number of unique advantages in their use as gene delivery vehicles. The biochemical machinery in the body for synthesis and degradation of fibrin is highly evolved making fibrin a highly malleable system to work with. Moreover, the ease at which the polymerization of its monomer and the subsequent gelation can be manipulated makes fibrin a surpassingly dynamic system. The chemical structure, physiological role, clinical application of fibrin and its role in tissue engineering research are discussed in this section.

1.4.1 Fibrin: Structure and Polymerization

Fibrinogen is the monomeric unit of fibrin. Fibrinogen has a unique structure (Figure 1.4) with a number of known and potential binding sites. Fibrinogen is a 340,000 Da hexamer synthesized by hepatocytes, approximately 45nm in length[411]. The molecule is a dimer composed of two sets of three polypeptide chains; two Aα chains, two Bβ chains and two γ chains[412]. Each monomer comprised of two end globular domains separated by a coiled-coil domain and consisting of one Aα, Bβ, and γ chain is stabilized by two disulfide ring structures on either end of the coiled-coil[413]. The homodimer is stabilized by a disulfide "knot" at the N-terminal region of each heterotrimeric monomer thus the fibrinogen dimer is configured in a "head-to-head" configuration with one central domain known as the N-terminal disulfide knot (NDSK) and two globular end domains each separated by the coiled-coil domains[414]. Thrombin, required for polymerization of fibrinogen, is formed from its precursor prothrombin by either intrinsic or extrinsic pathway. Thrombin acts by cleavage of fibrinopeptide A (FPA) and fibrinopeptide B (FPB) from the amino terminus of fibrinogen leading to exposure of binding sites needed for polymerization. The E_A binding site has two portions: one portion at N-terminus of α-chain and the other in the β-chain. Subsequently, the E_A binding site combines with complementary binding pocket that is located in the γ-chain of the D-domain of the neighboring molecules.

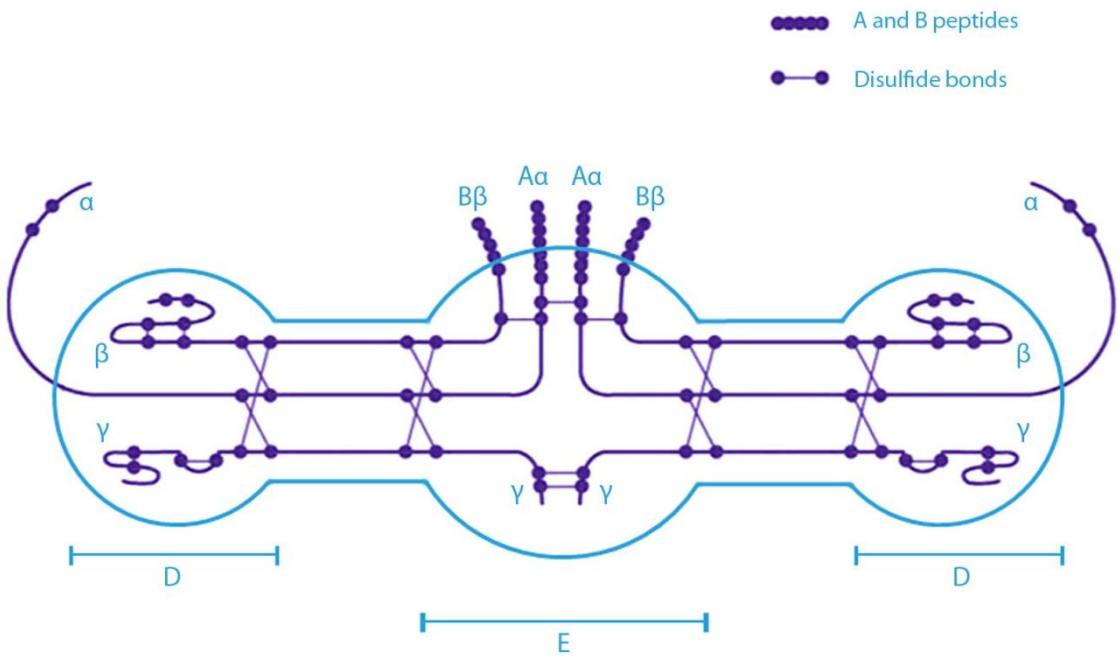

Figure 1.4: Tri-nodular structure of fibrinogen molecule. E domain, the middle domain, represents the amino-terminal disulfide knot of the six chains. D domains on the both sides of E domain represent the carboxyl terminal regions of Bβ and γ chains.

This interaction results in a staggered overlapping domain arrangement leading to a formation of twisting fibrils. The binding site E_B is located at the amino terminal of the β-chain and its combination with the complementary site at the C terminal of γ-chain resulting in lateral aggregation of fibrils. Intertwining of fibrin fibers leads to formation fibrin clot. The fibrin clot is stabilized by intermolecular covalent crosslinking of chains of adjacent strands carried out by factor XIIIa. Endothelial cells and fibroblasts, which bind to fibrin during the granulation tissue formation, produce tissue plasminogen activator (tPA) and urokinase plasminogen activator (uPA). tPA and uPA convert plasminogen to plasmin. This plasmin causes fibrinolysis leading to formation of fibrin degradation products.

1.4.2 Fibrin: Physiological Role

Fibrin is formed naturally during the wound healing, as discussed in section 1.1.1., as a measure to stabilize the platelet plug and stop bleeding. The blood coagulation cascade ends in the formation of cross-linked fibrin clot. This fibrin clot interacts with platelets, through the platelet membrane receptor GPIIb-IIIa[415]. Thus, fibrin gets incorporated in the wound tissue. Apart from acting as hemostatic plug, fibrin functions as a scaffold for cell migration and proliferation and as a reservoir for growth factors, proteolytic enzymes and their inhibitors. Endothelial cells and fibroblasts bind to fibrin via $\alpha_V\beta_3$integrins[416 417]. However, keratinocytes do not $\alpha_V\beta_3$ integrins and thus cannot bind to fibrinogen and fibrin[418]. This explains the migration of keratinocytes down the collagen rich wound bed avoiding the fibrin clot. Fibronectin, vitronectin and thombospondin which support cell migration bind to fibrinogen[419-421]. Various growth factors such as bFGF[422], $VEGF_{165}$[423], TGF-β1[424], PDGF-BB[425], IGF-1[425] and IL-1β[426] bind to fibrin either directly or indirectly through heparin which is bound to fibrin. Also, degrading enzymes such as plasminogen[427] and tPA[427], in parallel with plasminogen activator inhibitor[428] and thrombin[429], bind to the fibrin clot. This gives an opportunity to control balance between the further coagulation and lysis.

1.4.3 Fibrin: Clinical Application

Fibrin sealants became commercially available in Europe around 1978 and Tisseel® (or Tissucol®), marketed by Baxter Healthcare later was FDA approved in US in 1998.

Currently, around ten fibrin products are commercially available. As happens naturally, these fibrin sealants act as fibrin clots supporting fibroblast and endothelial cells infiltration and enhance wound healing. Depending on the local proteolytic mileu and concentrations of fibrinogen and thrombin used, the gelation rate and degradation rates of these sealants can be easily manipulated to suit a particular situation.

Major use of fibrin has been in hemostasis and tissue sealing in surgical practice[430], including extensive investigation in cardiovascular and cardiothoracic surgeries[431], urology[432], pneumothoracic surgery[433], neurosurgery[434], reconstructive surgery[435]. A number of clinical studies have been performed to investigate the use of fibrin in bypass operations, grafts, ventricular ruptures, suture reinforcement[436]. Patient derived fibrin sealants are also being investigated[437 438].

1.4.4 Fibrin: Tissue Engineering

Due to its biodegradability, nontoxic degradation products, flexibility in use, easy control over gelation, degradation, pore size, suitability for infiltration of host tissue and as delivery vehicle simply by manipulating the concentrations of thrombin and fibrinogen, and presence of FDA approved fibrin products in clinical and surgical practice; fibrin has been very popular in tissue engineering research. A vast body of research investigated fibrin as a delivery vehicle for cells, therapeutic drugs and bioactive molecules[439].

Keratinocytes[440] and fibroblasts[441] have been seeded on and then delivered through fibrin scaffolds to chronic wounds. In cardiac tissue engineering, cardiomyocytes or have been encapsulated in fibrin hydrogel[442 443]. In cartilage regeneration, chondrogenic precursor cells grown in fibrin showed increased expression of collagen type II and aggrecan[444]. Also, long term stable fibrin gels have been successfully investigated for cartilage tissue engineering by adjusting fibrinogen, thrombin and calcium concentrations and pH of the system[445]. In an *in vivo* study, 6 months after subcutaneous implantation of fibrin seeded with chondrocytes in a scaffold resulted in cartilage formation[446]. Recently, fibrin is being used for delivery of stem cells such as human umbilical cord stem cells[447], infrapatellar fat pad derived stem cells[448], bone mesenchymal stem cells[449]. Fibrin has also been utilized in tissue engineering in the

form of microbeads/microspheres as cell carriers due to being haptotactic to a number of cells such as endothelial cells, smooth muscle cells and fibroblasts and its use in this form in wound healing has been investigated[450]. Fibrin microbeads have also been used as cell carriers for a variety of other cells such as chondrocytes, periosteal-derived cells, and nucleus pulposus cells[451]. Recently, these microbeads have been extensively utilized for isolation, expansion and differentiation of mesenchymal stem cells [452-456] and investigated in a variety of applications such as bone tissue engineering[457], renal diseases[458].

Fibrin as delivery vehicle for bioactive molecules, genes and drugs has been a very successful research tool and has been recently reviewed[439]. The natural affinity of fibrin for growth factors has been put to work by several researchers[224 422 423 459-462] while others have resorted to enhancing the binding through various strategies such as incorporation of free[463] or tethered heparin[464 465], incorporation of bidomain peptide[466-468], or tethering growth factors to fibrin by creation of fusion proteins[469 470]. Recently, the use of fibrin scaffold for gene delivery has received much focus. The gene delivery through fibrin scaffold has been researched in various modalities such as naked DNA, viral vectors, non-viral vectors, or use of tethering techniques or incorporation of cells as gene vectors. While amongst viral vectors, fibrin has been utilized for lentiviral[471-473] or adeno-associated viral[474] gene delivery, adenovirus is the most commonly used viral vector fibrin mediated viral gene delivery[475-478]. Although fibrin has been used for delivery of naked DNA[479], delivery of non-viral vectors is more efficacious[480-482]. Various tethering techniques have also been employed in fibrin mediated viral/non-viral gene delivery[472 483]. Fibrin has been shown to mediate spatially arrayed and cell controlled gene delivery[408]. Delivery of combination of cells and biomolecules or transfected cells as gene vectors is in vogue in recent years[484-486]. Also, fibrin has been used as a part of a composite scaffold[471].

1.5 Hypotheses and Objectives

The ultimate aim of this project was to develop a gene therapy for compromised wounds using a non-viral gene delivery system. It was hypothesized that the fibrin-in-fibrin system encoding eNOS and Rab18 genes would enhance the wound healing in an

alloxan induced rabbit ear ulcer model of compromised wound healing. The enhancement in the wound healing would occur by means of the therapeutic effects of eNOS and Rab18 leading to functional angiogenesis and reduction in inflammation respectively.

The research goal had two strands. The first was the development of a suitable gene delivery system for controlled delivery of multiple genes, and the other was unleashing the molecular pathology of wounded keratinocytes grown in high and normal glucose conditions through an *in vitro* assay of multiple scratch wounds. The research areas were divided into four phases, each with specific objectives and hypotheses.

1.5.1 Phase One (Chapter Two):

Overall aim: To assess the feasibility of a fibrin gel to deliver lipoplexes that encodes multiple genes.

Hypotheses:

- There exists a biomolecular interaction between fibrin (ogen) and lipofectin which would allow lipoplexes to be held in the fibrin gel and released in a controlled fashion.
- The lipoplexes held within and released from fibrin gel can remain viable and can efficiently transfect *in vitro* and *in vivo* in a rabbit ear ulcer model.

Specific objectives:

- To investigate the *in vitro* release profile of lipoplexes from fibrin gel by measuring the released DNA with or without plasmin dissolution of fibrin gel using intercalation assay.
- To investigate the biomolecular interaction between components of fibrin-lipoplex system using surface plasmon resonance.
- To investigate the *in vitro* transfection efficiency of lipoplexes (encoding eGFP) released from fibrin gel by studying green fluorescence from GFP produced by transfected cells.

- To investigate the *in vivo* transfection efficiency of lipoplexes (encoding βGal and luciferase enzyme) released from fibrin gel in rabbit ear ulcer model.

1.5.2 Phase Two (Chapter Three):

Overall aim: To develop fibrin-in-fibrin (fibrin microspheres in fibrin gel) gene delivery system for increased DNA carrying capacity with respect to gelation time and control.

Hypotheses:

- Fibrin microspheres carrying lipoplexes can be fabricated by water-in-preheated oil emulsion method.
- The lipoplexes encapsulated within the fibrin microspheres remain functionally active.
- The fibrin microspheres can be fabricated to degrade with a profile different to that of the fibrin gel alone giving an opportunity to develop fibrin in fibrin gene delivery system (fibrin microspheres in fibrin gel) which can release DNA in a dynamically controlled manner.

Specific objectives:

- To fabricate fibrin microspheres carrying lipoplexes by modification of the water in preheated oil emulsion method and characterize them for morphology.
- To investigate the stability of DNA in the lipoplexes encapsulated within the fibrin microspheres by gel electrophoresis of DNA from the fibrin microspheres compared to the naked DNA.
- To investigate the functional integrity of the lipoplexes (encoding eNOS) from fibrin microspheres in an alloxan induced hyperglycemic rabbit ear ulcer model of compromised wound healing by investigating
    - mRNA expression by real time PCR.
    - Angiogenic effect of the proangiogenic eNOS seven days after post-wounding compared to control.
- To investigate the degradation fibrin microspheres vs. fibrin gel by scanning electron microscopy and densitometry analysis.

- To compare the *in vitro* release of DNA from fibrin microspheres vs. fibrin gel.

1.5.3 Phase Three (Chapter Four):

Overall aim: To assess the differential gene regulation in human keratinocytes grown in high and normal glucose conditions during an *in vitro* assay of multiple scratch wounds.

Hypotheses:

- Hyperglycemia affects the healing capacity of keratinocytes by altering their migration and/or proliferation.
- Hyperglycemia, at least in part, leads to altered gene regulation in keratinocytes during *in vitro* wound healing.

Specific objectives:

- To establish primary culture of human keratinocytes under normal (6 mM) and high (25 mM) glucose conditions.
- To develop an *in vitro* wound model of multiple scratch wounds on monolayers of keratinocytes grown under normal (6 mM) and high (25 mM) glucose conditions to allow 40 - 50 % of cells to contribute to an in *vitro* healing response.
- To assess the healing of scratch in the *in vitro* wound model of multiple scratch wounds under normal (6 mM) and high (25 mM) glucose conditions.
- To study gene regulation in wounded human keratinocytes grown under normal (6 mM) and high (25 mM) glucose conditions in comparison with non-wounded keratinocytes as control.
- To ascertain, by pathway analysis and gene ontology, a single downregulated gene which when delivered along with proangiogenic gene eNOS to a compromised wound will complement the therapeutic benefit of eNOS.

1.5.4 Phase Four (Chapter Five):

Overall aim: To evaluate the efficiency of fibrin-in-fibrin system encoding eNOS and Rab18 genes to promote wound healing in an alloxan induced hyperglycemic rabbit ear ulcer model of compromised wound healing.

Hypothesis:

- Fibrin in fibrin system, encoding eNOS and Rab18 genes, will enhance functional angiogenesis and reduce inflammation during wound healing in an alloxan induced hyperglycemic rabbit ear ulcer model of compromised wound healing.

Specific objectives:

- To assess the effect of eNOS and Rab18 gene delivery via fibrin-in-fibrin system, in terms of wound closure, angiogenesis and inflammatory response.
- To evaluate correlations between wound healing parameters, namely percent wound closure, epithelialization, volume fraction of inflammatory cells, surface and length density of blood vessels and radial diffusion distance.

1.6 References:

1. Buchanan EP, Longaker MT, Lorenz HP. Fetal skin wound healing. *Adv Clin Chem* 2009;48:137-61.

2. Yannas IV, Kwan MD, Longaker MT. Early fetal healing as a model for adult organ regeneration. *Tissue Eng* 2007;13(8):1789-98.

3. Lynch SE, Nixon JC, Colvin RB, Antoniades HN. Role of platelet-derived growth factor in wound healing: synergistic effects with other growth factors. *Proc Natl Acad Sci U S A* 1987;84(21):7696-700.

4. Eming SA, Krieg T, Davidson JM. Inflammation in wound repair: molecular and cellular mechanisms. *J Invest Dermatol* 2007;127(3):514-25.

5. Huber AR, Weiss SJ. Disruption of the subendothelial basement membrane during neutrophil diapedesis in an in vitro construct of a blood vessel wall. *J Clin Invest* 1989;83(4):1122-36.

6. Foxall C, Watson SR, Dowbenko D, Fennie C, Lasky LA, Kiso M, Hasegawa A, Asa D, Brandley BK. The three members of the selectin receptor family recognize a common carbohydrate epitope, the sialyl Lewis(x) oligosaccharide. *J Cell Biol* 1992;117(4):895-902.

7. Muller WA. Leukocyte-endothelial-cell interactions in leukocyte transmigration and the inflammatory response. *Trends Immunol* 2003;24(6):327-34.

8. Martin P, Leibovich SJ. Inflammatory cells during wound repair: the good, the bad and the ugly. *Trends Cell Biol* 2005;15(11):599-607.

9. Chavakis T, Preissner KT, Santoso S. Leukocyte trans-endothelial migration: JAMs add new pieces to the puzzle. *Thromb Haemost* 2003;89(1):13-7.

10. Schenkel AR, Mamdouh Z, Muller WA. Locomotion of monocytes on endothelium is a critical step during extravasation. *Nat Immunol* 2004;5(4):393-400.

11. Etzioni A, Doerschuk CM, Harlan JM. Of man and mouse: leukocyte and endothelial adhesion molecule deficiencies. *Blood* 1999;94(10):3281-8.

12. Brinkmann V, Reichard U, Goosmann C, Fauler B, Uhlemann Y, Weiss DS, Weinrauch Y, Zychlinsky A. Neutrophil extracellular traps kill bacteria. *Science* 2004;303(5663):1532-5.

13. Sen CK. The general case for redox control of wound repair. *Wound Repair Regen* 2003;11(6):431-8.

14. Finkel T. Redox-dependent signal transduction. *FEBS Lett* 2000;476(1-2):52-4.

15. Finkel T, Holbrook NJ. Oxidants, oxidative stress and the biology of ageing. *Nature* 2000;408(6809):239-47.

16. Gamaley IA, Klyubin IV. Roles of reactive oxygen species: signaling and regulation of cellular functions. *Int Rev Cytol* 1999;188:203-55.

17. Droge W. Free radicals in the physiological control of cell function. *Physiol Rev* 2002;82(1):47-95.

18. Schafer M, Werner S. Oxidative stress in normal and impaired wound repair. *Pharmacol Res* 2008;58(2):165-71.

19. Martin CW, Muir IF. The role of lymphocytes in wound healing. *Br J Plast Surg* 1990;43(6):655-62.

20. Boyce DE, Jones WD, Ruge F, Harding KG, Moore K. The role of lymphocytes in human dermal wound healing. *Br J Dermatol* 2000;143(1):59-65.

21. Keen D. A review of research examining the regulatory role of lymphocytes in normal wound healing. *J Wound Care* 2008;17(5):218-20, 22.

22. Ng MF. The role of mast cells in wound healing. *Int Wound J* 2010;7(1):55-61.

23. Gurtner GC, Werner S, Barrandon Y, Longaker MT. Wound repair and regeneration. *Nature* 2008;453(7193):314-21.

24. Li J, Chen J, Kirsner R. Pathophysiology of acute wound healing. *Clin Dermatol* 2007;25(1):9-18.

25. Werner S, Grose R. Regulation of wound healing by growth factors and cytokines. *Physiol Rev* 2003;83(3):835-70.

26. Singer AJ, Clark RA. Cutaneous wound healing. *N Engl J Med* 1999;341(10):738-46.

27. Singh P, Chen C, Pal-Ghosh S, Stepp MA, Sheppard D, Van De Water L. Loss of integrin alpha9beta1 results in defects in proliferation, causing poor re-epithelialization during cutaneous wound healing. *J Invest Dermatol* 2009;129(1):217-28.

28. Falanga V. Growth factors and wound healing. *Dermatol Clin* 1993;11(4):667-75.

29. Schaffer MR, Tantry U, Gross SS, Wasserburg HL, Barbul A. Nitric oxide regulates wound healing. *J Surg Res* 1996;63(1):237-40.

30. Soneja A, Drews M, Malinski T. Role of nitric oxide, nitroxidative and oxidative stress in wound healing. *Pharmacol Rep* 2005;57 Suppl:108-19.

31. Witte MB, Barbul A. Role of nitric oxide in wound repair. *Am J Surg* 2002;183(4):406-12.

32. Amadeu TP, Costa AM. Nitric oxide synthesis inhibition alters rat cutaneous wound healing. *J Cutan Pathol* 2006;33(7):465-73.

33. Schulz G, Stechmiller J. Wound healing and nitric oxide production: too little or too much may impair healing and cause chronic wounds. *Int J Low Extrem Wounds* 2006;5(1):6-8.

34. Dhaunsi GS, Ozand PT. Nitric oxide promotes mitogen-induced dna synthesis in human dermal fibroblasts through cGMP. *Clin Exp Pharmacol Physiol* 2004;31(1-2):46-9.

35. Schaffer MR, Efron PA, Thornton FJ, Klingel K, Gross SS, Barbul A. Nitric oxide, an autocrine regulator of wound fibroblast synthetic function. *J Immunol* 1997;158(5):2375-81.

36. Witte MB, Thornton FJ, Efron DT, Barbul A. Enhancement of fibroblast collagen synthesis by nitric oxide. *Nitric Oxide* 2000;4(6):572-82.

37. Gill SE, Parks WC. Metalloproteinases and their inhibitors: regulators of wound healing. *Int J Biochem Cell Biol* 2008;40(6-7):1334-47.

38. Raja, Sivamani K, Garcia MS, Isseroff RR. Wound re-epithelialization: modulating keratinocyte migration in wound healing. *Front Biosci* 2007;12:2849-68.

39. Diegelmann RF, Evans MC. Wound healing: an overview of acute, fibrotic and delayed healing. *Front Biosci* 2004;9:283-9.

40. Shaw TJ, Martin P. Wound repair at a glance. *J Cell Sci* 2009;122(Pt 18):3209-13.

41. Armstrong DG, Jude EB. The role of matrix metalloproteinases in wound healing. *J Am Podiatr Med Assoc* 2002;92(1):12-8.

42. Ravanti L, Kahari VM. Matrix metalloproteinases in wound repair (review). *Int J Mol Med* 2000;6(4):391-407.

43. Lobmann R, Schultz G, Lehnert H. Proteases and the diabetic foot syndrome: mechanisms and therapeutic implications. *Diabetes Care* 2005;28(2):461-71.

44. Muller M, Trocme C, Lardy B, Morel F, Halimi S, Benhamou PY. Matrix metalloproteinases and diabetic foot ulcers: the ratio of MMP-1 to TIMP-1 is a predictor of wound healing. *Diabet Med* 2008;25(4):419-26.

45. Wall SJ, Sampson MJ, Levell N, Murphy G. Elevated matrix metalloproteinase-2 and -3 production from human diabetic dermal fibroblasts. *Br J Dermatol* 2003;149(1):13-6.

46. Sternlicht MD, Werb Z. How matrix metalloproteinases regulate cell behavior. *Annu Rev Cell Dev Biol* 2001;17:463-516.

47. Xue M, Le NT, Jackson CJ. Targeting matrix metalloproteases to improve cutaneous wound healing. *Expert Opin Ther Targets* 2006;10(1):143-55.

48. Mirastschijski U, Schnabel R, Claes J, Schneider W, Agren MS, Haaksma C, Tomasek JJ. Matrix metalloproteinase inhibition delays wound healing and blocks the latent transforming growth factor-beta1-promoted myofibroblast formation and function. *Wound Repair Regen* 2010;18(2):223-34.

49. Hattori N, Mochizuki S, Kishi K, Nakajima T, Takaishi H, D'Armiento J, Okada Y. MMP-13 plays a role in keratinocyte migration, angiogenesis, and contraction in mouse skin wound healing. *Am J Pathol* 2009;175(2):533-46.

50. Liu Y, Min D, Bolton T, Nube V, Twigg SM, Yue DK, McLennan SV. Increased matrix metalloproteinase-9 predicts poor wound healing in diabetic foot ulcers. *Diabetes Care* 2009;32(1):117-9.

51. Hartenstein B, Dittrich BT, Stickens D, Heyer B, Vu TH, Teurich S, Schorpp-Kistner M, Werb Z, Angel P. Epidermal development and wound healing in matrix metalloproteinase 13-deficient mice. *J Invest Dermatol* 2006;126(2):486-96.

52. Ovington LG. Overview of matrix metalloprotease modulation and growth factor protection in wound healing. Part 1. *Ostomy Wound Manage* 2002;48(6 Suppl):3-7.

53. Ladwig GP, Robson MC, Liu R, Kuhn MA, Muir DF, Schultz GS. Ratios of activated matrix metalloproteinase-9 to tissue inhibitor of matrix

metalloproteinase-1 in wound fluids are inversely correlated with healing of pressure ulcers. *Wound Repair Regen* 2002;10(1):26-37.

54. Steffensen B, Hakkinen L, Larjava H. Proteolytic events of wound-healing--coordinated interactions among matrix metalloproteinases (MMPs), integrins, and extracellular matrix molecules. *Crit Rev Oral Biol Med* 2001;12(5):373-98.
55. Frossing S, Rono B, Hald A, Romer J, Lund LR. Skin wound healing in MMP2-deficient and MMP2 / plasminogen double-deficient mice. *Exp Dermatol* 2010;19(8):e234-40.
56. Peled ZM, Phelps ED, Updike DL, Chang J, Krummel TM, Howard EW, Longaker MT. Matrix metalloproteinases and the ontogeny of scarless repair: the other side of the wound healing balance. *Plast Reconstr Surg* 2002;110(3):801-11.
57. Pilcher BK, Wang M, Qin XJ, Parks WC, Senior RM, Welgus HG. Role of matrix metalloproteinases and their inhibition in cutaneous wound healing and allergic contact hypersensitivity. *Ann N Y Acad Sci* 1999;878:12-24.
58. Agren MS, Mirastschijski U, Karlsmark T, Saarialho-Kere UK. Topical synthetic inhibitor of matrix metalloproteinases delays epidermal regeneration of human wounds. *Exp Dermatol* 2001;10(5):337-48.
59. Gawronska-Kozak B. Scarless skin wound healing in FOXN1 deficient (nude) mice is associated with distinctive matrix metalloproteinase expression. *Matrix Biol* 2011;30(4):290-300.
60. Loffek S, Schilling O, Franzke CW. Biological role of matrix metalloproteinases: a critical balance. *Eur Respir J* 2011;38(1):191-208.
61. Soo C, Shaw WW, Zhang X, Longaker MT, Howard EW, Ting K. Differential expression of matrix metalloproteinases and their tissue-derived inhibitors in cutaneous wound repair. *Plast Reconstr Surg* 2000;105(2):638-47.
62. Li J, Zhang YP, Kirsner RS. Angiogenesis in wound repair: angiogenic growth factors and the extracellular matrix. *Microsc Res Tech* 2003;60(1):107-14.
63. Knighton DR, Phillips GD, Fiegel VD. Wound healing angiogenesis: indirect stimulation by basic fibroblast growth factor. *J Trauma* 1990;30(12 Suppl):S134-44.

64. Lees VC, Fan TP. A freeze-injured skin graft model for the quantitative study of basic fibroblast growth factor and other promoters of angiogenesis in wound healing. *Br J Plast Surg* 1994;47(5):349-59.

65. Iruela-Arispe ML, Sage EH. Endothelial cells exhibiting angiogenesis in vitro proliferate in response to TGF-beta 1. *J Cell Biochem* 1993;52(4):414-30.

66. Phillips GD, Whitehead RA, Stone AM, Ruebel MW, Goodkin ML, Knighton DR. Transforming growth factor beta (TGF-B) stimulation of angiogenesis: an electron microscopic study. *J Submicrosc Cytol Pathol* 1993;25(2):149-55.

67. Ma J, Wang Q, Fei T, Han JD, Chen YG. MCP-1 mediates TGF-beta-induced angiogenesis by stimulating vascular smooth muscle cell migration. *Blood* 2007;109(3):987-94.

68. Kurosaka M, Suzuki T, Hosono K, Kamata Y, Fukamizu A, Kitasato H, Fujita Y, Majima M. Reduced angiogenesis and delay in wound healing in angiotensin II type 1a receptor-deficient mice. *Biomed Pharmacother* 2009;63(9):627-34.

69. Liu ZJ, Snyder R, Soma A, Shirakawa T, Ziober BL, Fairman RM, Herlyn M, Velazquez OC. VEGF-A and alphaVbeta3 integrin synergistically rescue angiogenesis via N-Ras and PI3-K signaling in human microvascular endothelial cells. *FASEB J* 2003;17(13):1931-3.

70. Hickey MM, Simon MC. Regulation of angiogenesis by hypoxia and hypoxia-inducible factors. *Curr Top Dev Biol* 2006;76:217-57.

71. Chen L, Endler A, Shibasaki F. Hypoxia and angiogenesis: regulation of hypoxia-inducible factors via novel binding factors. *Exp Mol Med* 2009;41(12):849-57.

72. Breen EC. VEGF in biological control. *J Cell Biochem* 2007;102(6):1358-67.

73. Bao P, Kodra A, Tomic-Canic M, Golinko MS, Ehrlich HP, Brem H. The role of vascular endothelial growth factor in wound healing. *J Surg Res* 2009;153(2):347-58.

74. Bates DO. Vascular endothelial growth factors and vascular permeability. *Cardiovasc Res* 2010;87(2):262-71.

75. Montrucchio G, Lupia E, de Martino A, Battaglia E, Arese M, Tizzani A, Bussolino F, Camussi G. Nitric oxide mediates angiogenesis induced in vivo by platelet-

activating factor and tumor necrosis factor-alpha. *Am J Pathol* 1997;151(2):557-63.

76. Ziche M, Morbidelli L, Masini E, Amerini S, Granger HJ, Maggi CA, Geppetti P, Ledda F. Nitric oxide mediates angiogenesis in vivo and endothelial cell growth and migration in vitro promoted by substance P. *J Clin Invest* 1994;94(5):2036-44.
77. Ziche M, Morbidelli L, Masini E, Granger H, Geppetti P, Ledda F. Nitric oxide promotes DNA synthesis and cyclic GMP formation in endothelial cells from postcapillary venules. *Biochem Biophys Res Commun* 1993;192(3):1198-203.
78. Daher Z, Boulay PL, Desjardins F, Gratton JP, Claing A. Vascular endothelial growth factor receptor-2 activates ADP-ribosylation factor 1 to promote endothelial nitric-oxide synthase activation and nitric oxide release from endothelial cells. *J Biol Chem* 2010;285(32):24591-9.
79. Pi X, Wu Y, Ferguson JE, 3rd, Portbury AL, Patterson C. SDF-1alpha stimulates JNK3 activity via eNOS-dependent nitrosylation of MKP7 to enhance endothelial migration. *Proc Natl Acad Sci U S A* 2009;106(14):5675-80.
80. Velnar T, Bailey T, Smrkolj V. The wound healing process: an overview of the cellular and molecular mechanisms. *J Int Med Res* 2009;37(5):1528-42.
81. Childress BB, Stechmiller JK. Role of nitric oxide in wound healing. *Biol Res Nurs* 2002;4(1):5-15.
82. Robson MC, Steed DL, Franz MG. Wound healing: biologic features and approaches to maximize healing trajectories. *Curr Probl Surg* 2001;38(2):72-140.
83. Menke NB, Ward KR, Witten TM, Bonchev DG, Diegelmann RF. Impaired wound healing. *Clin Dermatol* 2007;25(1):19-25.
84. Mustoe TA, O'Shaughnessy K, Kloeters O. Chronic wound pathogenesis and current treatment strategies: a unifying hypothesis. *Plast Reconstr Surg* 2006;117(7 Suppl):35S-41S.
85. Nwomeh BC, Yager DR, Cohen IK. Physiology of the chronic wound. *Clin Plast Surg* 1998;25(3):341-56.

86. Wild S, Roglic G, Green A, Sicree R, King H. Global prevalence of diabetes: estimates for the year 2000 and projections for 2030. *Diabetes Care* 2004;27(5):1047-53.

87. Shaw JE, Sicree RA, Zimmet PZ. Global estimates of the prevalence of diabetes for 2010 and 2030. *Diabetes Res Clin Pract* 2010;87(1):4-14.

88. Liu ZJ, Velazquez OC. Hyperoxia, endothelial progenitor cell mobilization, and diabetic wound healing. *Antioxid Redox Signal* 2008;10(11):1869-82.

89. Consensus Development Conference on Diabetic Foot Wound Care: 7-8 April 1999, Boston, Massachusetts. American Diabetes Association. *Diabetes Care* 1999;22(8):1354-60.

90. Fard AS, Esmaelzadeh M, Larijani B. Assessment and treatment of diabetic foot ulcer. *Int J Clin Pract* 2007;61(11):1931-8.

91. Nagoba BS, Gandhi RC, Wadher BJ, Rao A, Hartalkar AR, Selkar SP. A simple and effective approach for the treatment of diabetic foot ulcers with different Wagner grades. *Int Wound J* 2010;7(3):153-8.

92. Robbins JM, Strauss G, Aron D, Long J, Kuba J, Kaplan Y. Mortality rates and diabetic foot ulcers: is it time to communicate mortality risk to patients with diabetic foot ulceration? *J Am Podiatr Med Assoc* 2008;98(6):489-93.

93. Zhang P, Zhang X, Brown J, Vistisen D, Sicree R, Shaw J, Nichols G. Global healthcare expenditure on diabetes for 2010 and 2030. *Diabetes Res Clin Pract* 2010;87(3):293-301.

94. Giurini JM, Lyons TE. Diabetic foot complications: diagnosis and management. *Int J Low Extrem Wounds* 2005;4(3):171-82.

95. Dorresteijn JA, Kriegsman DM, Valk GD. Complex interventions for preventing diabetic foot ulceration. *Cochrane Database Syst Rev* 2010(1):CD007610.

96. Wukich DK. Current concepts review: diabetic foot ulcers. *Foot Ankle Int* 2010;31(5):460-7.

97. Gottrup F, Apelqvist J, Price P. Outcomes in controlled and comparative studies on non-healing wounds: recommendations to improve the quality of evidence in wound management. *J Wound Care* 2010;19(6):237-68.

98. Smith D, Cullen M, Nolan J. The cost of managing diabetic foot ulceration

in an Irish hospital. *Irish Journal of Medical Science* 2004;173(2):89-92.

99. Goodridge D, Trepman E, Embil JM. Health-related quality of life in diabetic patients with foot ulcers: literature review. *J Wound Ostomy Continence Nurs* 2005;32(6):368-77.
100. Ribu L, Hanestad BR, Moum T, Birkeland K, Rustoen T. A comparison of the health-related quality of life in patients with diabetic foot ulcers, with a diabetes group and a nondiabetes group from the general population. *Qual Life Res* 2007;16(2):179-89.
101. Falanga V. Wound healing and its impairment in the diabetic foot. *Lancet* 2005;366(9498):1736-43.
102. Ogbera OA, Osa E, Edo A, Chukwum E. Common clinical features of diabetic foot ulcers: perspectives from a developing nation. *Int J Low Extrem Wounds* 2008;7(2):93-8.
103. Hess CT. Diabetic foot ulcers. *Adv Skin Wound Care* 2008;21(6):296.
104. Khanna S, Biswas S, Shang Y, Collard E, Azad A, Kauh C, Bhasker V, Gordillo GM, Sen CK, Roy S. Macrophage dysfunction impairs resolution of inflammation in the wounds of diabetic mice. *PLoS One* 2010;5(3):e9539.
105. Ochoa O, Torres FM, Shireman PK. Chemokines and diabetic wound healing. *Vascular* 2007;15(6):350-5.
106. Delamaire M, Maugendre D, Moreno M, Le Goff MC, Allannic H, Genetet B. Impaired leucocyte functions in diabetic patients. *Diabet Med* 1997;14(1):29-34.
107. Martin A, Komada MR, Sane DC. Abnormal angiogenesis in diabetes mellitus. *Med Res Rev* 2003;23(2):117-45.
108. Li YJ, Guan H, Hazarika S, Liu CW, Annex BH. Impaired angiogenesis following hind-limb ischemia in diabetes mellitus mice. *Chin Med Sci J* 2007;22(4):232-7.
109. Cechowska-Pasko M, Palka J, Bankowski E. Decrease in the glycosaminoglycan content in the skin of diabetic rats. The role of IGF-I, IGF-binding proteins and proteolytic activity. *Mol Cell Biochem* 1996;154(1):1-8.
110. Brem H, Jacobs T, Vileikyte L, Weinberger S, Gibber M, Gill K, Tarnovskaya A, Entero H, Boulton AJ. Wound-healing protocols for diabetic foot and pressure ulcers. *Surg Technol Int* 2003;11:85-92.

111. Teixeira AS, Andrade SP. Glucose-induced inhibition of angiogenesis in the rat sponge granuloma is prevented by aminoguanidine. *Life Sci* 1999;64(8):655-62.

112. Catrina SB, Okamoto K, Pereira T, Brismar K, Poellinger L. Hyperglycemia regulates hypoxia-inducible factor-1alpha protein stability and function. *Diabetes* 2004;53(12):3226-32.

113. Loots MA, Lamme EN, Mekkes JR, Bos JD, Middelkoop E. Cultured fibroblasts from chronic diabetic wounds on the lower extremity (non-insulin-dependent diabetes mellitus) show disturbed proliferation. *Arch Dermatol Res* 1999;291(2-3):93-9.

114. Loot MA, Kenter SB, Au FL, van Galen WJ, Middelkoop E, Bos JD, Mekkes JR. Fibroblasts derived from chronic diabetic ulcers differ in their response to stimulation with EGF, IGF-I, bFGF and PDGF-AB compared to controls. *Eur J Cell Biol* 2002;81(3):153-60.

115. Hehenberger K, Kratz G, Hansson A, Brismar K. Fibroblasts derived from human chronic diabetic wounds have a decreased proliferation rate, which is recovered by the addition of heparin. *J Dermatol Sci* 1998;16(2):144-51.

116. Lerman OZ, Galiano RD, Armour M, Levine JP, Gurtner GC. Cellular dysfunction in the diabetic fibroblast: impairment in migration, vascular endothelial growth factor production, and response to hypoxia. *Am J Pathol* 2003;162(1):303-12.

117. Lan CC, Liu IH, Fang AH, Wen CH, Wu CS. Hyperglycaemic conditions decrease cultured keratinocyte mobility: implications for impaired wound healing in patients with diabetes. *Br J Dermatol* 2008;159(5):1103-15.

118. Lan CC, Wu CS, Kuo HY, Huang SM, Chen GS. Hyperglycaemic conditions hamper keratinocyte locomotion via sequential inhibition of distinct pathways: new insights on poor wound closure in patients with diabetes. *Br J Dermatol* 2009;160(6):1206-14.

119. Usui ML, Mansbridge JN, Carter WG, Fujita M, Olerud JE. Keratinocyte migration, proliferation, and differentiation in chronic ulcers from patients with diabetes and normal wounds. *J Histochem Cytochem* 2008;56(7):687-96.

120. Spravchikov N, Sizyakov G, Gartsbein M, Accili D, Tennenbaum T, Wertheimer E. Glucose effects on skin keratinocytes: implications for diabetes skin complications. *Diabetes* 2001;50(7):1627-35.

121. Pradhan L, Nabzdyk C, Andersen ND, LoGerfo FW, Veves A. Inflammation and neuropeptides: the connection in diabetic wound healing. *Expert Rev Mol Med* 2009;11:e2.

122. Mishima Y, Kuyama A, Tada A, Takahashi K, Ishioka T, Kibata M. Relationship between serum tumor necrosis factor-alpha and insulin resistance in obese men with Type 2 diabetes mellitus. *Diabetes Res Clin Pract* 2001;52(2):119-23.

123. Naguib G, Al-Mashat H, Desta T, Graves DT. Diabetes prolongs the inflammatory response to a bacterial stimulus through cytokine dysregulation. *J Invest Dermatol* 2004;123(1):87-92.

124. Acosta JB, del Barco DG, Vera DC, Savigne W, Lopez-Saura P, Guillen Nieto G, Schultz GS. The pro-inflammatory environment in recalcitrant diabetic foot wounds. *Int Wound J* 2008;5(4):530-9.

125. Jude EB, Blakytny R, Bulmer J, Boulton AJ, Ferguson MW. Transforming growth factor-beta 1, 2, 3 and receptor type I and II in diabetic foot ulcers. *Diabet Med* 2002;19(6):440-7.

126. Tsunawaki S, Sporn M, Ding A, Nathan C. Deactivation of macrophages by transforming growth factor-beta. *Nature* 1988;334(6179):260-2.

127. Blakytny R, Jude EB, Martin Gibson J, Boulton AJ, Ferguson MW. Lack of insulin-like growth factor 1 (IGF1) in the basal keratinocyte layer of diabetic skin and diabetic foot ulcers. *J Pathol* 2000;190(5):589-94.

128. Velander P, Theopold C, Hirsch T, Bleiziffer O, Zuhaili B, Fossum M, Hoeller D, Gheerardyn R, Chen M, Visovatti S, Svensson H, Yao F, Eriksson E. Impaired wound healing in an acute diabetic pig model and the effects of local hyperglycemia. *Wound Repair Regen* 2008;16(2):288-93.

129. Bitar MS, Labbad ZN. Transforming growth factor-beta and insulin-like growth factor-I in relation to diabetes-induced impairment of wound healing. *J Surg Res* 1996;61(1):113-9.

130. Doxey DL, Ng MC, Dill RE, Iacopino AM. Platelet-derived growth factor levels in wounds of diabetic rats. *Life Sci* 1995;57(11):1111-23.

131. Yiangou Y, Facer P, Sinicropi DV, Boucher TJ, Bennett DL, McMahon SB, Anand P. Molecular forms of NGF in human and rat neuropathic tissues: decreased NGF precursor-like immunoreactivity in human diabetic skin. *J Peripher Nerv Syst* 2002;7(3):190-7.

132. Graiani G, Emanueli C, Desortes E, Van Linthout S, Pinna A, Figueroa CD, Manni L, Madeddu P. Nerve growth factor promotes reparative angiogenesis and inhibits endothelial apoptosis in cutaneous wounds of Type 1 diabetic mice. *Diabetologia* 2004;47(6):1047-54.

133. Galkowska H, Olszewski WL, Wojewodzka U, Rosinski G, Karnafel W. Neurogenic factors in the impaired healing of diabetic foot ulcers. *J Surg Res* 2006;134(2):252-8.

134. Galkowska H, Wojewodzka U, Olszewski WL. Chemokines, cytokines, and growth factors in keratinocytes and dermal endothelial cells in the margin of chronic diabetic foot ulcers. *Wound Repair Regen* 2006;14(5):558-65.

135. Ennis WJ, Lee C, Meneses P. A biochemical approach to wound healing through the use of modalities. *Clin Dermatol* 2007;25(1):63-72.

136. Hink U, Li H, Mollnau H, Oelze M, Matheis E, Hartmann M, Skatchkov M, Thaiss F, Stahl RA, Warnholtz A, Meinertz T, Griendling K, Harrison DG, Forstermann U, Munzel T. Mechanisms underlying endothelial dysfunction in diabetes mellitus. *Circ Res* 2001;88(2):E14-22.

137. Isenberg JS, Ridnour LA, Espey MG, Wink DA, Roberts DD. Nitric oxide in wound-healing. *Microsurgery* 2005;25(5):442-51.

138. Schaffer MR, Tantry U, Efron PA, Ahrendt GM, Thornton FJ, Barbul A. Diabetes-impaired healing and reduced wound nitric oxide synthesis: a possible pathophysiologic correlation. *Surgery* 1997;121(5):513-9.

139. Witte MB, Kiyama T, Barbul A. Nitric oxide enhances experimental wound healing in diabetes. *Br J Surg* 2002;89(12):1594-601.

140. Witte MB, Thornton FJ, Tantry U, Barbul A. L-Arginine supplementation enhances diabetic wound healing: involvement of the nitric oxide synthase and arginase pathways. *Metabolism* 2002;51(10):1269-73.

141. Stallmeyer B, Anhold M, Wetzler C, Kahlina K, Pfeilschifter J, Frank S. Regulation of eNOS in normal and diabetes-impaired skin repair: implications for tissue regeneration. *Nitric Oxide* 2002;6(2):168-77.

142. Mast BA, Schultz GS. Interactions of cytokines, growth factors, and proteases in acute and chronic wounds. *Wound Repair Regen* 1996;4(4):411-20.

143. Lobmann R, Ambrosch A, Schultz G, Waldmann K, Schiweck S, Lehnert H. Expression of matrix-metalloproteinases and their inhibitors in the wounds of diabetic and non-diabetic patients. *Diabetologia* 2002;45(7):1011-6.

144. Bullen EC, Longaker MT, Updike DL, Benton R, Ladin D, Hou Z, Howard EW. Tissue inhibitor of metalloproteinases-1 is decreased and activated gelatinases are increased in chronic wounds. *J Invest Dermatol* 1995;104(2):236-40.

145. Lobmann R, Zemlin C, Motzkau M, Reschke K, Lehnert H. Expression of matrix metalloproteinases and growth factors in diabetic foot wounds treated with a protease absorbent dressing. *J Diabetes Complications* 2006;20(5):329-35.

146. Nwomeh BC, Liang HX, Cohen IK, Yager DR. MMP-8 is the predominant collagenase in healing wounds and nonhealing ulcers. *J Surg Res* 1999;81(2):189-95.

147. Pirila E, Korpi JT, Korkiamaki T, Jahkola T, Gutierrez-Fernandez A, Lopez-Otin C, Saarialho-Kere U, Salo T, Sorsa T. Collagenase-2 (MMP-8) and matrilysin-2 (MMP-26) expression in human wounds of different etiologies. *Wound Repair Regen* 2007;15(1):47-57.

148. Terasaki K, Kanzaki T, Aoki T, Iwata K, Saiki I. Effects of recombinant human tissue inhibitor of metalloproteinases-2 (rh-TIMP-2) on migration of epidermal keratinocytes in vitro and wound healing in vivo. *J Dermatol* 2003;30(3):165-72.

149. Wall SJ, Bevan D, Thomas DW, Harding KG, Edwards DR, Murphy G. Differential expression of matrix metalloproteinases during impaired wound healing of the diabetes mouse. *J Invest Dermatol* 2002;119(1):91-8.

150. Standards of medical care in diabetes--2007. *Diabetes Care* 2007;30 Suppl 1:S4-S41.

151. Foster A. An evaluation of NICE guidelines on foot care for patients with diabetes. *Nurs Times* 2004;100(22):52-3.

152. Kalish J, Hamdan A. Management of diabetic foot problems. *J Vasc Surg* 2010;51(2):476-86.

153. Sumpio BE, Aruny J, Blume PA. The multidisciplinary approach to limb salvage. *Acta Chir Belg* 2004;104(6):647-53.

154. Lavery LA, Armstrong DG, Wunderlich RP, Mohler MJ, Wendel CS, Lipsky BA. Risk factors for foot infections in individuals with diabetes. *Diabetes Care* 2006;29(6):1288-93.

155. Esposito S, Leone S, Noviello S, Fiore M, Ianniello F, Felaco FM, Romagnoli F, Sarli E. Foot infections in diabetes (DFIs) in the out-patient setting: an Italian multicentre observational survey. *Diabet Med* 2008;25(8):979-84.

156. Lipsky BA, Berendt AR, Deery HG, Embil JM, Joseph WS, Karchmer AW, LeFrock JL, Lew DP, Mader JT, Norden C, Tan JS. Diagnosis and treatment of diabetic foot infections. *Plast Reconstr Surg* 2006;117(7 Suppl):212S-38S.

157. Miller AO, Henry M. Update in diagnosis and treatment of diabetic foot infections. *Phys Med Rehabil Clin N Am* 2009;20(4):611-25.

158. Lipsky BA, Berendt AR, Deery HG, Embil JM, Joseph WS, Karchmer AW, LeFrock JL, Lew DP, Mader JT, Norden C, Tan JS. Diagnosis and treatment of diabetic foot infections. *Clin Infect Dis* 2004;39(7):885-910.

159. Ince P, Abbas ZG, Lutale JK, Basit A, Ali SM, Chohan F, Morbach S, Mollenberg J, Game FL, Jeffcoate WJ. Use of the SINBAD classification system and score in comparing outcome of foot ulcer management on three continents. *Diabetes Care* 2008;31(5):964-7.

160. Park S, Rich J, Hanses F, Lee JC. Defects in innate immunity predispose C57BL/6J-Leprdb/Leprdb mice to infection by Staphylococcus aureus. *Infect Immun* 2009;77(3):1008-14.

161. Rich J, Lee JC. The pathogenesis of Staphylococcus aureus infection in the diabetic NOD mouse. *Diabetes* 2005;54(10):2904-10.

162. Citron DM, Goldstein EJ, Merriam CV, Lipsky BA, Abramson MA. Bacteriology of moderate-to-severe diabetic foot infections and in vitro activity of antimicrobial agents. *J Clin Microbiol* 2007;45(9):2819-28.

163. Nelson EA, O'Meara S, Golder S, Dalton J, Craig D, Iglesias C. Systematic review of antimicrobial treatments for diabetic foot ulcers. *Diabet Med* 2006;23(4):348-59.

164. Clay PG, Graham MR, Lindsey CC, Lamp KC, Freeman C, Glaros A. Clinical efficacy, tolerability, and cost savings associated with the use of open-label metronidazole plus ceftriaxone once daily compared with ticarcillin/clavulanate every 6 hours as empiric treatment for diabetic lower-extremity infections in older males. *Am J Geriatr Pharmacother* 2004;2(3):181-9.

165. Lipsky BA, Stoutenburgh U. Daptomycin for treating infected diabetic foot ulcers: evidence from a randomized, controlled trial comparing daptomycin with vancomycin or semi-synthetic penicillins for complicated skin and skin-structure infections. *J Antimicrob Chemother* 2005;55(2):240-5.

166. Rao N, Lipsky BA. Optimising antimicrobial therapy in diabetic foot infections. *Drugs* 2007;67(2):195-214.

167. Bader MS. Diabetic foot infection. *Am Fam Physician* 2008;78(1):71-9.

168. Shone A, Burnside J, Chipchase S, Game F, Jeffcoate W. Probing the validity of the probe-to-bone test in the diagnosis of osteomyelitis of the foot in diabetes. *Diabetes Care* 2006;29(4):945.

169. Berendt AR, Peters EJ, Bakker K, Embil JM, Eneroth M, Hinchliffe RJ, Jeffcoate WJ, Lipsky BA, Senneville E, Teh J, Valk GD. Diabetic foot osteomyelitis: a progress report on diagnosis and a systematic review of treatment. *Diabetes Metab Res Rev* 2008;24 Suppl 1:S145-61.

170. Berendt AR, Lipsky B. Is this bone infected or not? Differentiating neuro-osteoarthropathy from osteomyelitis in the diabetic foot. *Curr Diab Rep* 2004;4(6):424-9.

171. Game FL, Jeffcoate WJ. Primarily non-surgical management of osteomyelitis of the foot in diabetes. *Diabetologia* 2008;51(6):962-7.

172. Embil JM, Rose G, Trepman E, Math MC, Duerksen F, Simonsen JN, Nicolle LE. Oral antimicrobial therapy for diabetic foot osteomyelitis. *Foot Ankle Int* 2006;27(10):771-9.

173. Berendt AR, Peters EJ, Bakker K, Embil JM, Eneroth M, Hinchliffe RJ, Jeffcoate WJ, Lipsky BA, Senneville E, Teh J, Valk GD. Specific guidelines for treatment of diabetic foot osteomyelitis. *Diabetes Metab Res Rev* 2008;24 Suppl 1:S190-1.

174. Aragon-Sanchez J. Treatment of diabetic foot osteomyelitis: A surgical critique. *Int J Low Extrem Wounds* 2010;9(1):37-59.

175. Edwards J, Stapley S. Debridement of diabetic foot ulcers. *Cochrane Database Syst Rev* 2010(1):CD003556.

176. Dinh TL, Veves A. Treatment of diabetic ulcers. *Dermatol Ther* 2006;19(6):348-55.

177. Steed DL, Donohoe D, Webster MW, Lindsley L. Effect of extensive debridement and treatment on the healing of diabetic foot ulcers. Diabetic Ulcer Study Group. *J Am Coll Surg* 1996;183(1):61-4.

178. Plank J, Haas W, Rakovac I, Gorzer E, Sommer R, Siebenhofer A, Pieber TR. Evaluation of the impact of chiropodist care in the secondary prevention of foot ulcerations in diabetic subjects. *Diabetes Care* 2003;26(6):1691-5.

179. Ronnemaa T, Hamalainen H, Toikka T, Liukkonen I. Evaluation of the impact of podiatrist care in the primary prevention of foot problems in diabetic subjects. *Diabetes Care* 1997;20(12):1833-7.

180. Fonder MA, Lazarus GS, Cowan DA, Aronson-Cook B, Kohli AR, Mamelak AJ. Treating the chronic wound: A practical approach to the care of nonhealing wounds and wound care dressings. *J Am Acad Dermatol* 2008;58(2):185-206.

181. Brem H, Sheehan P, Boulton AJ. Protocol for treatment of diabetic foot ulcers. *Am J Surg* 2004;187(5A):1S-10S.

182. Bell D. Evidence-based rationale for offloading treatment modalities. *Surg Technol Int* 2008;17:113-7.

183. Baumhauer JF, Wervey R, McWilliams J, Harris GF, Shereff MJ. A comparison study of plantar foot pressure in a standardized shoe, total contact cast, and prefabricated pneumatic walking brace. *Foot Ankle Int* 1997;18(1):26-33.

184. Beuker BJ, van Deursen RW, Price P, Manning EA, van Baal JG, Harding KG. Plantar pressure in off-loading devices used in diabetic ulcer treatment. *Wound Repair Regen* 2005;13(6):537-42.

185. Hissink RJ, Manning HA, van Baal JG. The MABAL shoe, an alternative method in contact casting for the treatment of neuropathic diabetic foot ulcers. *Foot Ankle Int* 2000;21(4):320-3.

186. Knowles EA, Armstrong DG, Hayat SA, Khawaja KI, Malik RA, Boulton AJ. Offloading diabetic foot wounds using the scotchcast boot: a retrospective study. *Ostomy Wound Manage* 2002;48(9):50-3.

187. Birke JA, Novick A, Graham SL, Coleman WC, Brasseaux DM. Methods of treating plantar ulcers. *Phys Ther* 1991;71(2):116-22.

188. Armstrong DG, Nguyen HC, Lavery LA, van Schie CH, Boulton AJ, Harkless LB. Off-loading the diabetic foot wound: a randomized clinical trial. *Diabetes Care* 2001;24(6):1019-22.

189. Chantelau E. Half-shoes for off-loading diabetic plantar ulcers. *Diabetes Care* 2001;24(11):2016.

190. Brown D, Wertsch JJ, Harris GF, Klein J, Janisse D. Effect of rocker soles on plantar pressures. *Arch Phys Med Rehabil* 2004;85(1):81-6.

191. Zimny S, Schatz H, Pfohl U. The effects of applied felted foam on wound healing and healing times in the therapy of neuropathic diabetic foot ulcers. *Diabet Med* 2003;20(8):622-5.

192. Zimny S, Meyer MF, Schatz H, Pfohl M. Applied felted foam for plantar pressure relief is an efficient therapy in neuropathic diabetic foot ulcers. *Exp Clin Endocrinol Diabetes* 2002;110(7):325-8.

193. Zimny S, Reinsch B, Schatz H, Pfohl M. Effects of felted foam on plantar pressures in the treatment of neuropathic diabetic foot ulcers. *Diabetes Care* 2001;24(12):2153-4.

194. Caravaggi C, Faglia E, De Giglio R, Mantero M, Quarantiello A, Sommariva E, Gino M, Pritelli C, Morabito A. Effectiveness and safety of a nonremovable fiberglass off-bearing cast versus a therapeutic shoe in the treatment of

neuropathic foot ulcers: a randomized study. *Diabetes Care* 2000;23(12):1746-51.

195. Bus SA, Valk GD, van Deursen RW, Armstrong DG, Caravaggi C, Hlavacek P, Bakker K, Cavanagh PR. The effectiveness of footwear and offloading interventions to prevent and heal foot ulcers and reduce plantar pressure in diabetes: a systematic review. *Diabetes Metab Res Rev* 2008;24 Suppl 1:S162-80.
196. Mueller MJ, Diamond JE, Sinacore DR, Delitto A, Blair VP, 3rd, Drury DA, Rose SJ. Total contact casting in treatment of diabetic plantar ulcers. Controlled clinical trial. *Diabetes Care* 1989;12(6):384-8.
197. Nabuurs-Franssen MH, Huijberts MS, Sleegers R, Schaper NC. Casting of recurrent diabetic foot ulcers: effective and safe? *Diabetes Care* 2005;28(6):1493-4.
198. Nabuurs-Franssen MH, Sleegers R, Huijberts MS, Wijnen W, Sanders AP, Walenkamp G, Schaper NC. Total contact casting of the diabetic foot in daily practice: a prospective follow-up study. *Diabetes Care* 2005;28(2):243-7.
199. Fife CE, Carter MJ, Walker D. Why is it so hard to do the right thing in wound care? *Wound Repair Regen* 2010;18(2):154-8.
200. Wu SC, Jensen JL, Weber AK, Robinson DE, Armstrong DG. Use of pressure offloading devices in diabetic foot ulcers: do we practice what we preach? *Diabetes Care* 2008;31(11):2118-9.
201. Katz IA, Harlan A, Miranda-Palma B, Prieto-Sanchez L, Armstrong DG, Bowker JH, Mizel MS, Boulton AJ. A randomized trial of two irremovable off-loading devices in the management of plantar neuropathic diabetic foot ulcers. *Diabetes Care* 2005;28(3):555-9.
202. Piaggesi A, Baccetti F, Rizzo L, Romanelli M, Navalesi R, Benzi L. Sodium carboxyl-methyl-cellulose dressings in the management of deep ulcerations of diabetic foot. *Diabet Med* 2001;18(4):320-4.
203. Nemeth AJ, Eaglstein WH, Taylor JR, Peerson LJ, Falanga V. Faster healing and less pain in skin biopsy sites treated with an occlusive dressing. *Arch Dermatol* 1991;127(11):1679-83.

204. Eaglstein WH. Moist wound healing with occlusive dressings: a clinical focus. *Dermatol Surg* 2001;27(2):175-81.

205. Jude EB, Apelqvist J, Spraul M, Martini J. Prospective randomized controlled study of Hydrofiber dressing containing ionic silver or calcium alginate dressings in non-ischaemic diabetic foot ulcers. *Diabet Med* 2007;24(3):280-8.

206. Marston WA, Hanft J, Norwood P, Pollak R. The efficacy and safety of Dermagraft in improving the healing of chronic diabetic foot ulcers: results of a prospective randomized trial. *Diabetes Care* 2003;26(6):1701-5.

207. Dang CN, Boulton AJ. Changing perspectives in diabetic foot ulcer management. *Int J Low Extrem Wounds* 2003;2(1):4-12.

208. Gregor S, Maegele M, Sauerland S, Krahn JF, Peinemann F, Lange S. Negative pressure wound therapy: a vacuum of evidence? *Arch Surg* 2008;143(2):189-96.

209. Armstrong DG, Lavery LA. Negative pressure wound therapy after partial diabetic foot amputation: a multicentre, randomised controlled trial. *Lancet* 2005;366(9498):1704-10.

210. Blume PA, Walters J, Payne W, Ayala J, Lantis J. Comparison of negative pressure wound therapy using vacuum-assisted closure with advanced moist wound therapy in the treatment of diabetic foot ulcers: a multicenter randomized controlled trial. *Diabetes Care* 2008;31(4):631-6.

211. Vuerstaek JD, Vainas T, Wuite J, Nelemans P, Neumann MH, Veraart JC. State-of-the-art treatment of chronic leg ulcers: A randomized controlled trial comparing vacuum-assisted closure (V.A.C.) with modern wound dressings. *J Vasc Surg* 2006;44(5):1029-37; discussion 38.

212. Ubbink DT, Westerbos SJ, Evans D, Land L, Vermeulen H. Topical negative pressure for treating chronic wounds. *Cochrane Database Syst Rev* 2008(3):CD001898.

213. Ubbink DT, Westerbos SJ, Nelson EA, Vermeulen H. A systematic review of topical negative pressure therapy for acute and chronic wounds. *Br J Surg* 2008;95(6):685-92.

214. Kessler L, Bilbault P, Ortega F, Grasso C, Passemard R, Stephan D, Pinget M, Schneider F. Hyperbaric oxygenation accelerates the healing rate of

nonischemic chronic diabetic foot ulcers: a prospective randomized study. *Diabetes Care* 2003;26(8):2378-82.

215. Faglia E, Favales F, Aldeghi A, Calia P, Quarantiello A, Oriani G, Michael M, Campagnoli P, Morabito A. Adjunctive systemic hyperbaric oxygen therapy in treatment of severe prevalently ischemic diabetic foot ulcer. A randomized study. *Diabetes Care* 1996;19(12):1338-43.
216. Abidia A, Laden G, Kuhan G, Johnson BF, Wilkinson AR, Renwick PM, Masson EA, McCollum PT. The role of hyperbaric oxygen therapy in ischaemic diabetic lower extremity ulcers: a double-blind randomised-controlled trial. *Eur J Vasc Endovasc Surg* 2003;25(6):513-8.
217. Hunter S, Langemo DK, Anderson J, Hanson D, Thompson P. Hyperbaric oxygen therapy for chronic wounds. *Adv Skin Wound Care* 2010;23(3):116-9.
218. Wunderlich RP, Peters EJ, Lavery LA. Systemic hyperbaric oxygen therapy: lower-extremity wound healing and the diabetic foot. *Diabetes Care* 2000;23(10):1551-5.
219. Roeckl-Wiedmann I, Bennett M, Kranke P. Systematic review of hyperbaric oxygen in the management of chronic wounds. *Br J Surg* 2005;92(1):24-32.
220. Thackham JA, McElwain DL, Long RJ. The use of hyperbaric oxygen therapy to treat chronic wounds: A review. *Wound Repair Regen* 2008;16(3):321-30.
221. Fernandez-Montequin JI, Valenzuela-Silva CM, Diaz OG, Savigne W, Sancho-Soutelo N, Rivero-Fernandez F, Sanchez-Penton P, Morejon-Vega L, Artaza-Sanz H, Garcia-Herrera A, Gonzalez-Benavides C, Hernandez-Canete CM, Vazquez-Proenza A, Berlanga-Acosta J, Lopez-Saura PA. Intra-lesional injections of recombinant human epidermal growth factor promote granulation and healing in advanced diabetic foot ulcers: multicenter, randomised, placebo-controlled, double-blind study. *Int Wound J* 2009;6(6):432-43.
222. Fernandez-Montequin JI, Infante-Cristia E, Valenzuela-Silva C, Franco-Perez N, Savigne-Gutierrez W, Artaza-Sanz H, Morejon-Vega L, Gonzalez-Benavides C, Eliseo-Musenden O, Garcia-Iglesias E, Berlanga-Acosta J, Silva-Rodriguez R, Betancourt BY, Lopez-Saura PA. Intralesional injections of Citoprot-P

(recombinant human epidermal growth factor) in advanced diabetic foot ulcers with risk of amputation. *Int Wound J* 2007;4(4):333-43.

223. Saba AA, Freedman BM, Gaffield JW, Mackay DR, Ehrlich HP. Topical platelet-derived growth factor enhances wound closure in the absence of wound contraction: an experimental and clinical study. *Ann Plast Surg* 2002;49(1):62-6; discussion 66.

224. Pandit AS, Wilson DJ, Feldman DS, Thompson JA. Fibrin scaffold as an effective vehicle for the delivery of acidic fibroblast growth factor (FGF-1). *Journal of Biomaterials Applications* 2000;14(3):229-42.

225. Mustoe TA, Pierce GF, Morishima C, Deuel TF. Growth factor-induced acceleration of tissue repair through direct and inductive activities in a rabbit dermal ulcer model. *J Clin Invest* 1991;87(2):694-703.

226. Judith R, Nithya M, Rose C, Mandal AB. Application of a PDGF-containing novel gel for cutaneous wound healing. *Life Sci* 2010;87(1-2):1-8.

227. Li H, Fu X, Zhang L, Huang Q, Wu Z, Sun T. Research of PDGF-BB gel on the wound healing of diabetic rats and its pharmacodynamics. *J Surg Res* 2008;145(1):41-8.

228. Matsuda H, Koyama H, Sato H, Sawada J, Itakura A, Tanaka A, Matsumoto M, Konno K, Ushio H, Matsuda K. Role of nerve growth factor in cutaneous wound healing: accelerating effects in normal and healing-impaired diabetic mice. *J Exp Med* 1998;187(3):297-306.

229. Fang Y, Shen J, Yao M, Beagley KW, Hambly BD, Bao S. Granulocyte-macrophage colony-stimulating factor enhances wound healing in diabetes via upregulation of proinflammatory cytokines. *Br J Dermatol* 2010;162(3):478-86.

230. Kiritsy CP, Antoniades HN, Carlson MR, Beaulieu MT, D'Andrea M. Combination of platelet-derived growth factor-BB and insulin-like growth factor-I is more effective than platelet-derived growth factor-BB alone in stimulating complete healing of full-thickness wounds in "older" diabetic mice. *Wound Repair Regen* 1995;3(3):340-50.

231. Greenhalgh DG, Hummel RP, Albertson S, Breeden MP. Synergistic actions of platelet-derived growth factor and the insulin-like growth factors in vivo. *Wound Repair Regen* 1993;1(2):69-81.

232. Brown RL, Breeden MP, Greenhalgh DG. PDGF and TGF-alpha act synergistically to improve wound healing in the genetically diabetic mouse. *J Surg Res* 1994;56(6):562-70.

233. Davidson JM, Broadley KN, Quaglino D. Reversal of the Wound Healing Deficit in Diabetic Rats by Combined Basic Fibroblast Growth and Transforming Factor-Beta1 Therapy. *Wound Repair Regen* 1997;5:77-88.

234. Jazwa A, Kucharzewska P, Leja J, Zagorska A, Sierpniowska A, Stepniewski J, Kozakowska M, Taha H, Ochiya T, Derlacz R, Vahakangas E, Yla-Herttuala S, Jozkowicz A, Dulak J. Combined vascular endothelial growth factor-A and fibroblast growth factor 4 gene transfer improves wound healing in diabetic mice. *Genet Vaccines Ther* 2010;8(1):6.

235. Cao L, Arany PR, Kim J, Rivera-Feliciano J, Wang YS, He Z, Rask-Madsen C, King GL, Mooney DJ. Modulating Notch signaling to enhance neovascularization and reperfusion in diabetic mice. *Biomaterials* 2010;31(34):9048-56.

236. Akingboye AA, Giddins S, Gamston P, Tucker A, Navsaria H, Kyriakides C. Application of autologous derived-platelet rich plasma gel in the treatment of chronic wound ulcer: diabetic foot ulcer. *J Extra Corpor Technol* 2010;42(1):20-9.

237. Lacci KM, Dardik A. Platelet-rich plasma: support for its use in wound healing. *Yale J Biol Med* 2010;83(1):1-9.

238. Jeong SH, Han SK, Kim WK. Treatment of diabetic foot ulcers using a blood bank platelet concentrate. *Plast Reconstr Surg* 2010;125(3):944-52.

239. Villela DL, Santos VL. Evidence on the use of platelet-rich plasma for diabetic ulcer: a systematic review. *Growth Factors* 2010;28(2):111-6.

240. Pietramaggiori G, Scherer SS, Mathews JC, Alperovich M, Yang HJ, Neuwalder J, Czeczuga JM, Chan RK, Wagner CT, Orgill DP. Healing modulation induced

by freeze-dried platelet-rich plasma and micronized allogenic dermis in a diabetic wound model. *Wound Repair Regen* 2008;16(2):218-25.

241. Driver VR, Hanft J, Fylling CP, Beriou JM, Autologel Diabetic Foot Ulcer Study G. A prospective, randomized, controlled trial of autologous platelet-rich plasma gel for the treatment of diabetic foot ulcers. *Ostomy Wound Manage* 2006;52(6):68-70, 72, 74 passim.
242. Cross KJ, Mustoe TA. Growth factors in wound healing. *Surg Clin North Am* 2003;83(3):531-45, vi.
243. Cruciani M, Lipsky BA, Mengoli C, de Lalla F. Are granulocyte colony-stimulating factors beneficial in treating diabetic foot infections?: A meta-analysis. *Diabetes Care* 2005;28(2):454-60.
244. Steed DL, Ricotta JJ, Prendergast JJ, Kaplan RJ, Webster MW, McGill JB, Schwartz SL. Promotion and acceleration of diabetic ulcer healing by arginine-glycine-aspartic acid (RGD) peptide matrix. RGD Study Group. *Diabetes Care* 1995;18(1):39-46.
245. Wieman TJ, Smiell JM, Su Y. Efficacy and safety of a topical gel formulation of recombinant human platelet-derived growth factor-BB (becaplermin) in patients with chronic neuropathic diabetic ulcers. A phase III randomized placebo-controlled double-blind study. *Diabetes Care* 1998;21(5):822-7.
246. Margolis DJ, Bartus C, Hoffstad O, Malay S, Berlin JA. Effectiveness of recombinant human platelet-derived growth factor for the treatment of diabetic neuropathic foot ulcers. *Wound Repair Regen* 2005;13(6):531-6.
247. Barrientos S, Stojadinovic O, Golinko MS, Brem H, Tomic-Canic M. Growth factors and cytokines in wound healing. *Wound Repair Regen* 2008;16(5):585-601.
248. Mulder G, Tallis AJ, Marshall VT, Mozingo D, Phillips L, Pierce GF, Chandler LA, Sosnowski BK. Treatment of nonhealing diabetic foot ulcers with a platelet-derived growth factor gene-activated matrix (GAM501): results of a phase 1/2 trial. *Wound Repair Regen* 2009;17(6):772-9.
249. Steed DL, Goslen JB, Holloway GA, Malone JM, Bunt TJ, Webster MW. Randomized prospective double-blind trial in healing chronic diabetic foot

ulcers. CT-102 activated platelet supernatant, topical versus placebo. *Diabetes Care* 1992;15(11):1598-604.

250. Koveker GB. Growth factors in clinical practice. *Int J Clin Pract* 2000;54(9):590-3.

251. Smiell JM. Clinical safety of becaplermin (rhPDGF-BB) gel. Becaplermin Studies Group. *Am J Surg* 1998;176(2A Suppl):68S-73S.

252. Embil JM, Papp K, Sibbald G, Tousignant J, Smiell JM, Wong B, Lau CY. Recombinant human platelet-derived growth factor-BB (becaplermin) for healing chronic lower extremity diabetic ulcers: an open-label clinical evaluation of efficacy. *Wound Repair Regen* 2000;8(3):162-8.

253. Nagai MK, Embil JM. Becaplermin: recombinant platelet derived growth factor, a new treatment for healing diabetic foot ulcers. *Expert Opin Biol Ther* 2002;2(2):211-8.

254. Papanas N, Maltezos E. Benefit-risk assessment of becaplermin in the treatment of diabetic foot ulcers. *Drug Saf* 2010;33(6):455-61.

255. Papanas N, Maltezos E. Becaplermin gel in the treatment of diabetic neuropathic foot ulcers. *Clin Interv Aging* 2008;3(2):233-40.

256. Conrad C, Huss R. Adult stem cell lines in regenerative medicine and reconstructive surgery. *J Surg Res* 2005;124(2):201-8.

257. Badiavas EV, Abedi M, Butmarc J, Falanga V, Quesenberry P. Participation of bone marrow derived cells in cutaneous wound healing. *J Cell Physiol* 2003;196(2):245-50.

258. Javazon EH, Keswani SG, Badillo AT, Crombleholme TM, Zoltick PW, Radu AP, Kozin ED, Beggs K, Malik AA, Flake AW. Enhanced epithelial gap closure and increased angiogenesis in wounds of diabetic mice treated with adult murine bone marrow stromal progenitor cells. *Wound Repair Regen* 2007;15(3):350-9.

259. Kawamura A, Horie T, Tsuda I, Ikeda A, Egawa H, Imamura E, Iida J, Sakata H, Tamaki T, Kukita K, Meguro J, Yonekawa M, Kasai M. Prevention of limb amputation in patients with limbs ulcers by autologous peripheral blood mononuclear cell implantation. *Ther Apher Dial* 2005;9(1):59-63.

260. Vojtassak J, Danisovic L, Kubes M, Bakos D, Jarabek L, Ulicna M, Blasko M. Autologous biograft and mesenchymal stem cells in treatment of the diabetic foot. *Neuro Endocrinol Lett* 2006;27 Suppl 2:134-7.

261. Moustafa M, Bullock AJ, Creagh FM, Heller S, Jeffcoate W, Game F, Amery C, Tesfaye S, Ince Z, Haddow DB, MacNeil S. Randomized, controlled, single-blind study on use of autologous keratinocytes on a transfer dressing to treat nonhealing diabetic ulcers. *Regen Med* 2007;2(6):887-902.

262. Sasaki M, Abe R, Fujita Y, Ando S, Inokuma D, Shimizu H. Mesenchymal stem cells are recruited into wounded skin and contribute to wound repair by transdifferentiation into multiple skin cell type. *J Immunol* 2008;180(4):2581-7.

263. Wu Y, Chen L, Scott PG, Tredget EE. Mesenchymal stem cells enhance wound healing through differentiation and angiogenesis. *Stem Cells* 2007;25(10):2648-59.

264. Mansilla E, Marin GH, Sturla F, Drago HE, Gil MA, Salas E, Gardiner MC, Piccinelli G, Bossi S, Petrelli L, Iorio G, Ramos CA, Soratti C. Human mesenchymal stem cells are tolerized by mice and improve skin and spinal cord injuries. *Transplant Proc* 2005;37(1):292-4.

265. Phinney DG, Prockop DJ. Concise review: mesenchymal stem/multipotent stromal cells: the state of transdifferentiation and modes of tissue repair--current views. *Stem Cells* 2007;25(11):2896-902.

266. Bartsch T, Brehm M, Falke T, Kogler G, Wernet P, Strauer BE. [Rapid healing of a therapy-refractory diabetic foot after transplantation of autologous bone marrow stem cells]. *Med Klin (Munich)* 2005;100(10):676-80.

267. Badiavas EV, Falanga V. Treatment of chronic wounds with bone marrow-derived cells. *Arch Dermatol* 2003;139(4):510-6.

268. Yoon BS, Moon JH, Jun EK, Kim J, Maeng I, Kim JS, Lee JH, Baik CS, Kim A, Cho KS, Lee HH, Whang KY, You S. Secretory profiles and wound healing effects of human amniotic fluid-derived mesenchymal stem cells. *Stem Cells Dev* 2010;19(6):887-902.

269. Falanga V, Iwamoto S, Chartier M, Yufit T, Butmarc J, Kouttab N, Shrayer D, Carson P. Autologous bone marrow-derived cultured mesenchymal stem cells

delivered in a fibrin spray accelerate healing in murine and human cutaneous wounds. *Tissue Eng* 2007;13(6):1299-312.

270. Veves A, Falanga V, Armstrong DG, Sabolinski ML. Graftskin, a human skin equivalent, is effective in the management of noninfected neuropathic diabetic foot ulcers: a prospective randomized multicenter clinical trial. *Diabetes Care* 2001;24(2):290-5.
271. Andreadis ST, Geer DJ. Biomimetic approaches to protein and gene delivery for tissue regeneration. *Trends Biotechnol* 2006;24(7):331-7.
272. Horch RE, Kopp J, Kneser U, Beier J, Bach AD. Tissue engineering of cultured skin substitutes. *J Cell Mol Med* 2005;9(3):592-608.
273. Supp DM, Boyce ST. Engineered skin substitutes: practices and potentials. *Clin Dermatol* 2005;23(4):403-12.
274. Hoffman AS. Hydrogels for biomedical applications. *Adv Drug Deliv Rev* 2002;54(1):3-12.
275. Hoffman AS. Hydrogels for biomedical applications. *Ann N Y Acad Sci* 2001;944:62-73.
276. Ruszczak Z. Effect of collagen matrices on dermal wound healing. *Adv Drug Deliv Rev* 2003;55(12):1595-611.
277. Grant I, Warwick K, Marshall J, Green C, Martin R. The co-application of sprayed cultured autologous keratinocytes and autologous fibrin sealant in a porcine wound model. *Br J Plast Surg* 2002;55(3):219-27.
278. Mogford JE, Tawil B, Jia S, Mustoe TA. Fibrin sealant combined with fibroblasts and platelet-derived growth factor enhance wound healing in excisional wounds. *Wound Repair Regen* 2009;17(3):405-10.
279. Boateng JS, Matthews KH, Stevens HN, Eccleston GM. Wound healing dressings and drug delivery systems: a review. *J Pharm Sci* 2008;97(8):2892-923.
280. Eming SA, Krieg T, Davidson JM. Gene transfer in tissue repair: status, challenges and future directions. *Expert Opin Biol Ther* 2004;4(9):1373-86.
281. Steed DL. Modifying the wound healing response with exogenous growth factors. *Clin Plast Surg* 1998;25(3):397-405.

282. Grinnell F, Ho CH, Wysocki A. Degradation of fibronectin and vitronectin in chronic wound fluid: analysis by cell blotting, immunoblotting, and cell adhesion assays. *J Invest Dermatol* 1992;98(4):410-6.

283. Barrick B, Campbell EJ, Owen CA. Leukocyte proteinases in wound healing: roles in physiologic and pathologic processes. *Wound Repair Regen* 1999;7(6):410-22.

284. Lauer G, Sollberg S, Cole M, Flamme I, Sturzebecher J, Mann K, Krieg T, Eming SA. Expression and proteolysis of vascular endothelial growth factor is increased in chronic wounds. *J Invest Dermatol* 2000;115(1):12-8.

285. Bowler PG. Wound pathophysiology, infection and therapeutic options. *Ann Med* 2002;34(6):419-27.

286. Jazwa A, Kucharzewska P, Leja J, Zagorska A, Sierpniowska A, Stepniewski J, Kozakowska M, Taha H, Ochiya T, Derlacz R, Vahakangas E, Yla-Herttuala S, Jozkowicz A, Dulak J. Combined vascular endothelial growth factor-A and fibroblast growth factor 4 gene transfer improves wound healing in diabetic mice. *Genet Vaccines Ther* 2010;8:6.

287. Bitto A, Minutoli L, Galeano MR, Altavilla D, Polito F, Fiumara T, Calo M, Lo Cascio P, Zentilin L, Giacca M, Squadrito F. Angiopoietin-1 gene transfer improves impaired wound healing in genetically diabetic mice without increasing VEGF expression. *Clin Sci (Lond)* 2008;114(12):707-18.

288. Saghizadeh M, Kramerov AA, Yu FS, Castro MG, Ljubimov AV. Normalization of wound healing and diabetic markers in organ cultured human diabetic corneas by adenoviral delivery of c-Met gene. *Invest Ophthalmol Vis Sci* 2010;51(4):1970-80.

289. Breen AM DP, O'Brien T, Pandit AS. The use of therapeutic gene eNOS delivered via a fibrin scaffold enhances wound healing in a compromised wound model. *Biomaterials* 2008;29(21):3143-51.

290. Brem H, Kodra A, Golinko MS, Entero H, Stojadinovic O, Wang VM, Sheahan CM, Weinberg AD, Woo SL, Ehrlich HP, Tomic-Canic M. Mechanism of sustained release of vascular endothelial growth factor in accelerating experimental diabetic healing. *J Invest Dermatol* 2009;129(9):2275-87.

291. Cianfarani F, Zambruno G, Brogelli L, Sera F, Lacal PM, Pesce M, Capogrossi MC, Failla CM, Napolitano M, Odorisio T. Placenta growth factor in diabetic wound healing: altered expression and therapeutic potential. *Am J Pathol* 2006;169(4):1167-82.

292. Keswani SG, Katz AB, Lim FY, Zoltick P, Radu A, Alaee D, Herlyn M, Crombleholme TM. Adenoviral mediated gene transfer of PDGF-B enhances wound healing in type I and type II diabetic wounds. *Wound Repair Regen* 2004;12(5):497-504.

293. Badillo AT, Chung S, Zhang L, Zoltick P, Liechty KW. Lentiviral gene transfer of SDF-1alpha to wounds improves diabetic wound healing. *J Surg Res* 2007;143(1):35-42.

294. Lee JA, Conejero JA, Mason JM, Parrett BM, Wear-Maggitti KD, Grant RT, Breitbart AS. Lentiviral transfection with the PDGF-B gene improves diabetic wound healing. *Plast Reconstr Surg* 2005;116(2):532-8.

295. Man LX, Park JC, Terry MJ, Mason JM, Burrell WA, Liu F, Kimball BY, Moorji SM, Lee JA, Breitbart AS. Lentiviral gene therapy with platelet-derived growth factor B sustains accelerated healing of diabetic wounds over time. *Ann Plast Surg* 2005;55(1):81-6; discussion 86.

296. Wang Z, Li L. The plasmid encoding HSP47 enhances collagen expression and promotes skin wound healing in an alloxan-induced diabetic model. *Cell Biol Int* 2009;33(7):705-10.

297. Liu L, Marti GP, Wei X, Zhang X, Zhang H, Liu YV, Nastai M, Semenza GL, Harmon JW. Age-dependent impairment of HIF-1alpha expression in diabetic mice: Correction with electroporation-facilitated gene therapy increases wound healing, angiogenesis, and circulating angiogenic cells. *J Cell Physiol* 2008;217(2):319-27.

298. Marti GP, Mohebi P, Liu L, Wang J, Miyashita T, Harmon JW. KGF-1 for wound healing in animal models. *Methods Mol Biol* 2008;423:383-91.

299. Marti G, Ferguson M, Wang J, Byrnes C, Dieb R, Qaiser R, Bonde P, Duncan MD, Harmon JW. Electroporative transfection with KGF-1 DNA improves wound healing in a diabetic mouse model. *Gene Ther* 2004;11(24):1780-5.

300. Yoon CS, Jung HS, Kwon MJ, Lee SH, Kim CW, Kim MK, Lee M, Park JH. Sonoporation of the minicircle-VEGF(165) for wound healing of diabetic mice. *Pharm Res* 2009;26(4):794-801.

301. Mace KA, Restivo TE, Rinn JL, Paquet AC, Chang HY, Young DM, Boudreau NJ. HOXA3 modulates injury-induced mobilization and recruitment of bone marrow-derived cells. *Stem Cells* 2009;27(7):1654-65.

302. Asai J, Takenaka H, Kusano KF, Ii M, Luedemann C, Curry C, Eaton E, Iwakura A, Tsutsumi Y, Hamada H, Kishimoto S, Thorne T, Kishore R, Losordo DW. Topical sonic hedgehog gene therapy accelerates wound healing in diabetes by enhancing endothelial progenitor cell-mediated microvascular remodeling. *Circulation* 2006;113(20):2413-24.

303. Zagon IS, Sassani JW, Malefyt KJ, McLaughlin PJ. Regulation of corneal repair by particle-mediated gene transfer of opioid growth factor receptor complementary DNA. *Arch Ophthalmol* 2006;124(11):1620-4.

304. Bhattacharyya J, Mondal G, Madhusudana K, Agawane SB, Ramakrishna S, Gangireddy SR, Madhavi RD, Reddy PK, Konda VR, Rao SR, Udaykumar P, Chaudhuri A. Single subcutaneous administration of RGDK-lipopeptide:rhPDGF-B gene complex heals wounds in streptozotocin-induced diabetic rats. *Mol Pharm* 2009;6(3):918-27.

305. Hirsch T, Spielmann M, Velander P, Zuhaili B, Bleiziffer O, Fossum M, Steinstraesser L, Yao F, Eriksson E. Insulin-like growth factor-1 gene therapy and cell transplantation in diabetic wounds. *J Gene Med* 2008;10(11):1247-52.

306. Sun L, Xu L, Chang H, Henry FA, Miller RM, Harmon JM, Nielsen TB. Transfection with aFGF cDNA improves wound healing. *J Invest Dermatol* 1997;108(3):313-8.

307. Lee PY, Li Z, Huang L. Thermosensitive hydrogel as a Tgf-beta1 gene delivery vehicle enhances diabetic wound healing. *Pharm Res* 2003;20(12):1995-2000.

308. Agarwal A, Mallapragada SK. Synthetic sustained gene delivery systems. *Curr Top Med Chem* 2008;8(4):311-0.

309. Banerjee R. Liposomes: applications in medicine. *J Biomater Appl* 2001;16(1):3-21.

310. Samad A, Sultana Y, Aqil M. Liposomal drug delivery systems: an update review. *Curr Drug Deliv* 2007;4(4):297-305.

311. Kale AA, Torchilin VP. Enhanced transfection of tumor cells in vivo using "Smart" pH-sensitive TAT-modified pegylated liposomes. *J Drug Target* 2007;15(7-8):538-45.

312. Leong-Poi H, Kuliszewski MA, Lekas M, Sibbald M, Teichert-Kuliszewska K, Klibanov AL, Stewart DJ, Lindner JR. Therapeutic arteriogenesis by ultrasound-mediated VEGF165 plasmid gene delivery to chronically ischemic skeletal muscle. *Circ Res* 2007;101(3):295-303.

313. Zheng X, Lu J, Deng L, Xiong Y, Chen J. Preparation and characterization of magnetic cationic liposome in gene delivery. *Int J Pharm* 2009;366(1-2):211-7.

314. Wu G, Mikhailovsky A, Khant HA, Fu C, Chiu W, Zasadzinski JA. Remotely triggered liposome release by near-infrared light absorption via hollow gold nanoshells. *J Am Chem Soc* 2008;130(26):8175-7.

315. Hanzlikova M, Soininen P, Lampela P, Mannisto PT, Raasmaja A. The role of PEI structure and size in the PEI/liposome-mediated synergism of gene transfection. *Plasmid* 2009;61(1):15-21.

316. Lampela P, Soininen P, Urtti A, Mannisto PT, Raasmaja A. Synergism in gene delivery by small PEIs and three different nonviral vectors. *Int J Pharm* 2004;270(1-2):175-84.

317. Lee CH, Ni YH, Chen CC, Chou C, Chang FH. Synergistic effect of polyethylenimine and cationic liposomes in nucleic acid delivery to human cancer cells. *Biochim Biophys Acta* 2003;1611(1-2):55-62.

318. Wasungu L, Hoekstra D. Cationic lipids, lipoplexes and intracellular delivery of genes. *J Control Release* 2006;116(2):255-64.

319. Ma B, Zhang S, Jiang H, Zhao B, Lv H. Lipoplex morphologies and their influences on transfection efficiency in gene delivery. *J Control Release* 2007;123(3):184-94.

320. Li W, Huang Z, MacKay JA, Grube S, Szoka FC, Jr. Low-pH-sensitive poly(ethylene glycol) (PEG)-stabilized plasmid nanolipoparticles: effects of

PEG chain length, lipid composition and assembly conditions on gene delivery. *J Gene Med* 2005;7(1):67-79.

321. Liu D, Hu J, Qiao W, Li Z, Zhang S, Cheng L. Synthesis of carbamate-linked lipids for gene delivery. *Bioorg Med Chem Lett* 2005;15(12):3147-50.
322. Futaki S, Masui Y, Nakase I, Sugiura Y, Nakamura T, Kogure K, Harashima H. Unique features of a pH-sensitive fusogenic peptide that improves the transfection efficiency of cationic liposomes. *J Gene Med* 2005;7(11):1450-8.
323. Yessine MA, Meier C, Petereit HU, Leroux JC. On the role of methacrylic acid copolymers in the intracellular delivery of antisense oligonucleotides. *Eur J Pharm Biopharm* 2006;63(1):1-10.
324. Ruponen M, Braun CS, Middaugh CR. Biophysical characterization of polymeric and liposomal gene delivery systems using empirical phase diagrams. *J Pharm Sci* 2006;95(10):2101-14.
325. Shigeta K, Kawakami S, Higuchi Y, Okuda T, Yagi H, Yamashita F, Hashida M. Novel histidine-conjugated galactosylated cationic liposomes for efficient hepatocyte-selective gene transfer in human hepatoma HepG2 cells. *J Control Release* 2007;118(2):262-70.
326. Pirollo KF, Rait A, Zhou Q, Hwang SH, Dagata JA, Zon G, Hogrefe RI, Palchik G, Chang EH. Materializing the potential of small interfering RNA via a tumor-targeting nanodelivery system. *Cancer Res* 2007;67(7):2938-43.
327. Rosa M, Penacho N, Simoes S, Lima MC, Lindman B, Miguel MG. DNA pre-condensation with an amino acid-based cationic amphiphile. A viable approach for liposome-based gene delivery. *Mol Membr Biol* 2008;25(1):23-34.
328. Sasaki K, Kogure K, Chaki S, Nakamura Y, Moriguchi R, Hamada H, Danev R, Nagayama K, Futaki S, Harashima H. An artificial virus-like nano carrier system: enhanced endosomal escape of nanoparticles via synergistic action of pH-sensitive fusogenic peptide derivatives. *Anal Bioanal Chem* 2008;391(8):2717-27.
329. Tu Y, Kim JS. A fusogenic segment of glycoprotein H from herpes simplex virus enhances transfection efficiency of cationic liposomes. *J Gene Med* 2008;10(6):646-54.

330. MacKay JA, Li W, Huang Z, Dy EE, Huynh G, Tihan T, Collins R, Deen DF, Szoka FC, Jr. HIV TAT peptide modifies the distribution of DNA nanolipoparticles following convection-enhanced delivery. *Mol Ther* 2008;16(5):893-900.

331. Sakaguchi N, Kojima C, Harada A, Kono K. Preparation of pH-sensitive poly(glycidol) derivatives with varying hydrophobicities: their ability to sensitize stable liposomes to pH. *Bioconjug Chem* 2008;19(5):1040-8.

332. Yuba E, Kojima C, Sakaguchi N, Harada A, Koiwai K, Kono K. Gene delivery to dendritic cells mediated by complexes of lipoplexes and pH-sensitive fusogenic polymer-modified liposomes. *J Control Release* 2008;130(1):77-83.

333. Mignet N, Richard C, Seguin J, Largeau C, Bessodes M, Scherman D. Anionic pH-sensitive pegylated lipoplexes to deliver DNA to tumors. *Int J Pharm* 2008;361(1-2):194-201.

334. Lehtinen J, Hyvonen Z, Subrizi A, Bunjes H, Urtti A. Glycosaminoglycan-resistant and pH-sensitive lipid-coated DNA complexes produced by detergent removal method. *J Control Release* 2008;131(2):145-9.

335. Sun P, Zhong M, Shi X, Li Z. Anionic LPD complexes for gene delivery to macrophage: preparation, characterization and transfection in vitro. *J Drug Target* 2008;16(9):668-78.

336. Carmona S, Jorgensen MR, Kolli S, Crowther C, Salazar FH, Marion PL, Fujino M, Natori Y, Thanou M, Arbuthnot P, Miller AD. Controlling HBV Replication in Vivo by Intravenous Administration of Triggered PEGylated siRNA-Nanoparticles. *Mol Pharm* 2009;6(3):706-17.

337. Kobayashi S, Nakase I, Kawabata N, Yu HH, Pujals S, Imanishi M, Giralt E, Futaki S. Cytosolic targeting of macromolecules using a pH-dependent fusogenic peptide in combination with cationic liposomes. *Bioconjug Chem* 2009;20(5):953-9.

338. Borden MA, Kruse DE, Caskey CF, Zhao S, Dayton PA, Ferrara KW. Influence of lipid shell physicochemical properties on ultrasound-induced microbubble destruction. *IEEE Trans Ultrason Ferroelectr Freq Control* 2005;52(11):1992-2002.

339. Suzuki R, Takizawa T, Negishi Y, Hagisawa K, Tanaka K, Sawamura K, Utoguchi N, Nishioka T, Maruyama K. Gene delivery by combination of novel liposomal bubbles with perfluoropropane and ultrasound. *J Control Release* 2007;117(1):130-6.

340. Liu R, Wei X, Yao Y, Chai Q, Chen Y, Xu Y. The preparation and characterization of gas bubble containing liposomes. *Conf Proc IEEE Eng Med Biol Soc* 2005;4:3998-4001.

341. Maruyama K, Suzuki R, Takizawa T, Utoguchi N, Negishi Y. [Drug and gene delivery by "bubble liposomes" and ultrasound]. *Yakugaku Zasshi* 2007;127(5):781-7.

342. Suzuki R, Takizawa T, Negishi Y, Utoguchi N, Maruyama K. Effective gene delivery with liposomal bubbles and ultrasound as novel non-viral system. *J Drug Target* 2007;15(7-8):531-7.

343. Suzuki R, Takizawa T, Negishi Y, Utoguchi N, Sawamura K, Tanaka K, Namai E, Oda Y, Matsumura Y, Maruyama K. Tumor specific ultrasound enhanced gene transfer in vivo with novel liposomal bubbles. *J Control Release* 2008;125(2):137-44.

344. Vandenbroucke RE, Lentacker I, Demeester J, De Smedt SC, Sanders NN. Ultrasound assisted siRNA delivery using PEG-siPlex loaded microbubbles. *J Control Release* 2008;126(3):265-73.

345. Negishi Y, Endo Y, Fukuyama T, Suzuki R, Takizawa T, Omata D, Maruyama K, Aramaki Y. Delivery of siRNA into the cytoplasm by liposomal bubbles and ultrasound. *J Control Release* 2008;132(2):124-30.

346. Luo YK, Zhao YZ, Lu CT, Tang J, Li XK. Application of ultrasonic gas-filled liposomes in enhancing transfer for breast cancer-related antisense oligonucleotides: an experimental study. *J Liposome Res* 2008;18(4):341-51.

347. Pan X, Guan J, Yoo JW, Epstein AJ, Lee LJ, Lee RJ. Cationic lipid-coated magnetic nanoparticles associated with transferrin for gene delivery. *Int J Pharm* 2008;358(1-2):263-70.

348. Kostarelos K, Emfietzoglou D, Tadros TF. Light-sensitive fusion between polymer-coated liposomes following physical anchoring of polymerisable

polymers onto lipid bilayers by self-assembly. *Faraday Discuss* 2005;128:379-88.

349. Waterhouse JE, Harbottle RP, Keller M, Kostarelos K, Coutelle C, Jorgensen MR, Miller AD. Synthesis and application of integrin targeting lipopeptides in targeted gene delivery. *Chembiochem* 2005;6(7):1212-23.

350. Wilson A, Zhou W, Champion HC, Alber S, Tang ZL, Kennel S, Watkins S, Huang L, Pitt B, Li S. Targeted delivery of oligodeoxynucleotides to mouse lung endothelial cells in vitro and in vivo. *Mol Ther* 2005;12(3):510-8.

351. Hayes ME, Drummond DC, Kirpotin DB, Zheng WW, Noble CO, Park JW, Marks JD, Benz CC, Hong K. Genospheres: self-assembling nucleic acid-lipid nanoparticles suitable for targeted gene delivery. *Gene Ther* 2006;13(7):646-51.

352. Singh M, Hawtrey A, Ariatti M. Lipoplexes with biotinylated transferrin accessories: novel, targeted, serum-tolerant gene carriers. *Int J Pharm* 2006;321(1-2):124-37.

353. Higuchi Y, Kawakami S, Yamashita F, Hashida M. The potential role of fucosylated cationic liposome/NFkappaB decoy complexes in the treatment of cytokine-related liver disease. *Biomaterials* 2007;28(3):532-9.

354. Li SD, Huang L. Targeted delivery of antisense oligodeoxynucleotide and small interference RNA into lung cancer cells. *Mol Pharm* 2006;3(5):579-88.

355. Sato A, Takagi M, Shimamoto A, Kawakami S, Hashida M. Small interfering RNA delivery to the liver by intravenous administration of galactosylated cationic liposomes in mice. *Biomaterials* 2007;28(7):1434-42.

356. Li SD, Huang L. Surface-modified LPD nanoparticles for tumor targeting. *Ann N Y Acad Sci* 2006;1082:1-8.

357. Shao K, Hou Q, Go ML, Duan W, Cheung NS, Feng SS, Wong KP, Yoram A, Zhang W, Huang Z, Li QT. Sulfatide-tenascin interaction mediates binding to the extracellular matrix and endocytic uptake of liposomes in glioma cells. *Cell Mol Life Sci* 2007;64(4):506-15.

358. Adrian JE, Kamps JA, Poelstra K, Scherphof GL, Meijer DK, Kaneda Y. Delivery of viral vectors to hepatic stellate cells in fibrotic livers using HVJ envelopes fused with targeted liposomes. *J Drug Target* 2007;15(1):75-82.

359. Rivest V, Phivilay A, Julien C, Belanger S, Tremblay C, Emond V, Calon F. Novel liposomal formulation for targeted gene delivery. *Pharm Res* 2007;24(5):981-90.

360. Lu Y, Kawakami S, Yamashita F, Hashida M. Development of an antigen-presenting cell-targeted DNA vaccine against melanoma by mannosylated liposomes. *Biomaterials* 2007;28(21):3255-62.

361. Tan PH, Xue SA, Wei B, Holler A, Voss RH, George AJ. Changing viral tropism using immunoliposomes alters the stability of gene expression: implications for viral vector design. *Mol Med* 2007;13(3-4):216-26.

362. Zhang Y, Wang Y, Boado RJ, Pardridge WM. Lysosomal enzyme replacement of the brain with intravenous non-viral gene transfer. *Pharm Res* 2008;25(2):400-6.

363. Mustapa MF, Bell PC, Hurley CA, Nicol A, Guenin E, Sarkar S, Writer MJ, Barker SE, Wong JB, Pilkington-Miksa MA, Papahadjopoulos-Sternberg B, Shamlou PA, Hailes HC, Hart SL, Zicha D, Tabor AB. Biophysical characterization of an integrin-targeted lipopolyplex gene delivery vector. *Biochemistry* 2007;46(45):12930-44.

364. Andreu A, Fairweather N, Miller AD. Clostridium neurotoxin fragments as potential targeting moieties for liposomal gene delivery to the CNS. *Chembiochem* 2008;9(2):219-31.

365. Peer D, Park EJ, Morishita Y, Carman CV, Shimaoka M. Systemic leukocyte-directed siRNA delivery revealing cyclin D1 as an anti-inflammatory target. *Science* 2008;319(5863):627-30.

366. Zhang H, Kusunose J, Kheirolomoom A, Seo JW, Qi J, Watson KD, Lindfors HA, Ruoslahti E, Sutcliffe JL, Ferrara KW. Dynamic imaging of arginine-rich heart-targeted vehicles in a mouse model. *Biomaterials* 2008;29(12):1976-88.

367. Kim KS, Lee YK, Kim JS, Koo KH, Hong HJ, Park YS. Targeted gene therapy of LS174 T human colon carcinoma by anti-TAG-72 immunoliposomes. *Cancer Gene Ther* 2008;15(5):331-40.

368. Li SD, Chono S, Huang L. Efficient oncogene silencing and metastasis inhibition via systemic delivery of siRNA. *Mol Ther* 2008;16(5):942-6.

369. Tagalakis AD, McAnulty RJ, Devaney J, Bottoms SE, Wong JB, Elbs M, Writer MJ, Hailes HC, Tabor AB, O'Callaghan C, Jaffe A, Hart SL. A receptor-targeted nanocomplex vector system optimized for respiratory gene transfer. *Mol Ther* 2008;16(5):907-15.

370. Laine C, Mornet E, Lemiegre L, Montier T, Cammas-Marion S, Neveu C, Carmoy N, Lehn P, Benvegnu T. Folate-equipped pegylated archaeal lipid derivatives: synthesis and transfection properties. *Chemistry* 2008;14(27):8330-40.

371. Chono S, Li SD, Conwell CC, Huang L. An efficient and low immunostimulatory nanoparticle formulation for systemic siRNA delivery to the tumor. *J Control Release* 2008;131(1):64-9.

372. Ko YT, Hartner WC, Kale A, Torchilin VP. Gene delivery into ischemic myocardium by double-targeted lipoplexes with anti-myosin antibody and TAT peptide. *Gene Ther* 2009;16(1):52-9.

373. Ko YT, Bhattacharya R, Bickel U. Liposome encapsulated polyethylenimine/ODN polyplexes for brain targeting. *J Control Release* 2009;133(3):230-7.

374. Wang M, Lowik DW, Miller AD, Thanou M. Targeting the urokinase plasminogen activator receptor with synthetic self-assembly nanoparticles. *Bioconjug Chem* 2009;20(1):32-40.

375. Kim SI, Shin D, Lee H, Ahn BY, Yoon Y, Kim M. Targeted delivery of siRNA against hepatitis C virus by apolipoprotein A-I-bound cationic liposomes. *J Hepatol* 2009;50(3):479-88.

376. Torchilin VP. Cell penetrating peptide-modified pharmaceutical nanocarriers for intracellular drug and gene delivery. *Biopolymers* 2008;90(5):604-10.

377. Torchilin VP. Tat peptide-mediated intracellular delivery of pharmaceutical nanocarriers. *Adv Drug Deliv Rev* 2008;60(4-5):548-58.

378. Khalil IA, Kogure K, Futaki S, Harashima H. Octaarginine-modified liposomes: enhanced cellular uptake and controlled intracellular trafficking. *Int J Pharm* 2008;354(1-2):39-48.

379. El-Sayed A, Masuda T, Khalil I, Akita H, Harashima H. Enhanced gene expression by a novel stearylated INF7 peptide derivative through fusion independent endosomal escape. *J Control Release* 2009;138(2):160-7.

380. Sung M, Poon GM, Gariepy J. The importance of valency in enhancing the import and cell routing potential of protein transduction domain-containing molecules. *Biochim Biophys Acta* 2006;1758(3):355-63.

381. Vaysse L, Gregory LG, Harbottle RP, Perouzel E, Tolmachov O, Coutelle C. Nuclear-targeted minicircle to enhance gene transfer with non-viral vectors in vitro and in vivo. *J Gene Med* 2006;8(6):754-63.

382. Liu F, Conwell CC, Yuan X, Shollenberger LM, Huang L. Novel nonviral vectors target cellular signaling pathways: regulated gene expression and reduced toxicity. *J Pharmacol Exp Ther* 2007;321(2):777-83.

383. Kuramoto T, Nishikawa M, Thanaketpaisarn O, Okabe T, Yamashita F, Hashida M. Use of lipoplex-induced nuclear factor-kappaB activation to enhance transgene expression by lipoplex in mouse lung. *J Gene Med* 2006;8(1):53-62.

384. Morton TJ, Furst W, van Griensven M, Redl H. Controlled release of substances bound to fibrin-anchors or of DNA. *Drug Deliv* 2009;16(2):102-7.

385. Breen A, Strappe P, Kumar A, O'Brien T, Pandit A. Optimization of a fibrin scaffold for sustained release of an adenoviral gene vector. *J Biomed Mater Res A* 2006;78(4):702-8.

386. Frucht-Perry J, Assil KK, Ziegler E, Douglas H, Brown SI, Schanzlin DJ, Weinreb RN. Fibrin-enmeshed tobramycin liposomes: single application topical therapy of Pseudomonas keratitis. *Cornea* 1992;11(5):393-7.

387. Meyenburg S, Lilie H, Panzner S, Rudolph R. Fibrin encapsulated liposomes as protein delivery system Studies on the in vitro release behaviour. *J Control Release* 2000;69:159-68.

388. Giannoni P, Hunziker EB. Release kinetics of transforming growth factor-beta1 from fibrin clots. *Biotechnol Bioeng* 2003;83(1):121-3.

389. Chung TW, Yang MC, Tsai WJ. A fibrin encapsulated liposomes-in-chitosan matrix (FLCM) for delivering water-soluble drugs. Influences of the surface properties of liposomes and the crosslinked fibrin network. *Int J Pharm* 2006;311(1-2):122-9.

390. Wang SS, Yang MC, Chung TW. Liposomes/chitosan scaffold/human fibrin gel composite systems for delivering hydrophilic drugs--release behaviors of tirofiban in vitro. *Drug Deliv* 2008;15(3):149-57.

391. Lee CH, Singla A, Lee Y. Biomedical applications of collagen. *Int J Pharm* 2001;221(1-2):1-22.

392. Bengali Z, Pannier AK, Segura T, Anderson BC, Jang JH, Mustoe TA, Shea LD. Gene delivery through cell culture substrate adsorbed DNA complexes. *Biotechnol Bioeng* 2005;90(3):290-302.

393. Winn SR, Chen JC, Gong X, Bartholomew SV, Shreenivas S, Ozaki W. Non-viral-mediated gene therapy approaches for bone repair. *Orthod Craniofac Res* 2005;8(3):183-90.

394. Whittlesey KJ, Shea LD. Nerve growth factor expression by PLG-mediated lipofection. *Biomaterials* 2006;27(11):2477-86.

395. Capito RM, Spector M. Collagen scaffolds for nonviral IGF-1 gene delivery in articular cartilage tissue engineering. *Gene Ther* 2007;14(9):721-32.

396. Michlits W, Mittermayr R, Schafer R, Redl H, Aharinejad S. Fibrin-embedded administration of VEGF plasmid enhances skin flap survival. *Wound Repair Regen* 2007;15(3):360-7.

397. Bolliet C, Bohn MC, Spector M. Non-viral delivery of the gene for glial cell line-derived neurotrophic factor to mesenchymal stem cells in vitro via a collagen scaffold. *Tissue Eng Part C Methods* 2008;14(3):207-19.

398. Bengali Z, Rea JC, Gibly RF, Shea LD. Efficacy of immobilized polyplexes and lipoplexes for substrate-mediated gene delivery. *Biotechnol Bioeng* 2009;102(6):1679-91.

399. Rea JC, Gibly RF, Barron AE, Shea LD. Self-assembling peptide-lipoplexes for substrate-mediated gene delivery. *Acta Biomater* 2009;5(3):903-12.

400. Kulkarni M, Breen A, Greiser U, O'Brien T, Pandit A. Fibrin-lipoplex system for controlled topical delivery of multiple genes. *Biomacromolecules* 2009;10(6):1650-4.

401. De Laporte L, Yan AL, Shea LD. Local gene delivery from ECM-coated poly(lactide-co-glycolide) multiple channel bridges after spinal cord injury. *Biomaterials* 2009;30(12):2361-8.

402. Houchin-Ray T, Huang A, West ER, Zelivyanskaya M, Shea LD. Spatially patterned gene expression for guided neurite extension. *J Neurosci Res* 2009;87(4):844-56.

403. Bengali Z, Shea LD. Gene Delivery by Immobilization to Cell-Adhesive Substrates. *MRS Bull* 2005;30(9):659-62.

404. Meyenburg S, Lilie H, Panzner S, Rudolph R. Fibrin encapsulated liposomes as protein delivery system. Studies on the in vitro release behavior. *J Control Release* 2000;69(1):159-68.

405. Mady MM. Biophysical studies on collagen-lipid interaction. *J Biosci Bioeng* 2007;104(2):144-8.

406. Pannier AK, Shea LD. Controlled release systems for DNA delivery. *Mol Ther* 2004;10(1):19-26.

407. Houchin-Ray T, Swift LA, Jang JH, Shea LD. Patterned PLG substrates for localized DNA delivery and directed neurite extension. *Biomaterials* 2007;28(16):2603-11.

408. Lei P, Padmashali RM, Andreadis ST. Cell-controlled and spatially arrayed gene delivery from fibrin hydrogels. *Biomaterials* 2009;30(22):3790-9.

409. De Laporte L, Shea LD. Matrices and scaffolds for DNA delivery in tissue engineering. *Adv Drug Deliv Rev* 2007;59(4-5):292-307.

410. Yamauchi F, Kato K, Iwata H. Layer-by-layer assembly of poly(ethyleneimine) and plasmid DNA onto transparent indium-tin oxide electrodes for temporally and spatially specific gene transfer. *Langmuir* 2005;21(18):8360-7.

411. Mosesson MW, Siebenlist KR, Meh DA. The structure and biological features of fibrinogen and fibrin. *Ann N Y Acad Sci* 2001;936:11-30.

412. Doolittle RF. Some notes on crystallizing fibrinogen and fibrin fragments. *Biophys Chem* 2003;100(1-3):307-13.

413. Laurens N, Koolwijk P, de Maat MP. Fibrin structure and wound healing. *J Thromb Haemost* 2006;4(5):932-9.

414. Clarke RAF. *The Molecular and Cellular Biology of Wound Repair*. Second ed. New York: Plenum Press, 1996.

415. Podolnikova NP, Gorkun OV, Loreth RM, Yee VC, Lord ST, Ugarova TP. A cluster of basic amino acid residues in the gamma370-381 sequence of fibrinogen comprises a binding site for platelet integrin alpha(IIb)beta3 (glycoprotein IIb/IIIa). *Biochemistry* 2005;44(51):16920-30.

416. Cheresh DA. Human endothelial cells synthesize and express an Arg-Gly-Asp-directed adhesion receptor involved in attachment to fibrinogen and von Willebrand factor. *Proc Natl Acad Sci U S A* 1987;84(18):6471-5.

417. Gailit J, Clarke C, Newman D, Tonnesen MG, Mosesson MW, Clark RA. Human fibroblasts bind directly to fibrinogen at RGD sites through integrin alpha(v)beta3. *Exp Cell Res* 1997;232(1):118-26.

418. Kubo M, Van de Water L, Plantefaber LC, Mosesson MW, Simon M, Tonnesen MG, Taichman L, Clark RA. Fibrinogen and fibrin are anti-adhesive for keratinocytes: a mechanism for fibrin eschar slough during wound repair. *J Invest Dermatol* 2001;117(6):1369-81.

419. Makogonenko E, Tsurupa G, Ingham K, Medved L. Interaction of fibrin(ogen) with fibronectin: further characterization and localization of the fibronectin-binding site. *Biochemistry* 2002;41(25):7907-13.

420. Podor TJ, Campbell S, Chindemi P, Foulon DM, Farrell DH, Walton PD, Weitz JI, Peterson CB. Incorporation of vitronectin into fibrin clots. Evidence for a binding interaction between vitronectin and gamma A/gamma' fibrinogen. *J Biol Chem* 2002;277(9):7520-8.

421. Bacon-Baguley T, Ogilvie ML, Gartner TK, Walz DA. Thrombospondin binding to specific sequences within the A alpha- and B beta-chains of fibrinogen. *J Biol Chem* 1990;265(4):2317-23.

422. Sahni A, Odrljin T, Francis CW. Binding of basic fibroblast growth factor to fibrinogen and fibrin. *J Biol Chem* 1998;273(13):7554-9.

423. Sahni A, Francis CW. Vascular endothelial growth factor binds to fibrinogen and fibrin and stimulates endothelial cell proliferation. *Blood* 2000;96(12):3772-8.

424. Grainger DJ, Wakefield L, Bethell HW, Farndale RW, Metcalfe JC. Release and activation of platelet latent TGF-beta in blood clots during dissolution with plasmin. *Nat Med* 1995;1(9):932-7.

425. Dohan DM, Choukroun J, Diss A, Dohan SL, Dohan AJ, Mouhyi J, Gogly B. Platelet-rich fibrin (PRF): a second-generation platelet concentrate. Part II: platelet-related biologic features. *Oral Surg Oral Med Oral Pathol Oral Radiol Endod* 2006;101(3):e45-50.

426. Sahni A, Guo M, Sahni SK, Francis CW. Interleukin-1beta but not IL-1alpha binds to fibrinogen and fibrin and has enhanced activity in the bound form. *Blood* 2004;104(2):409-14.

427. Tsurupa G, Medved L. Identification and characterization of novel tPA- and plasminogen-binding sites within fibrin(ogen) alpha C-domains. *Biochemistry* 2001;40(3):801-8.

428. Wagner OF, de Vries C, Hohmann C, Veerman H, Pannekoek H. Interaction between plasminogen activator inhibitor type 1 (PAI-1) bound to fibrin and either tissue-type plasminogen activator (t-PA) or urokinase-type plasminogen activator (u-PA). Binding of t-PA/PAI-1 complexes to fibrin mediated by both the finger and the kringle-2 domain of t-PA. *J Clin Invest* 1989;84(2):647-55.

429. Pospisil CH, Stafford AR, Fredenburgh JC, Weitz JI. Evidence that both exosites on thrombin participate in its high affinity interaction with fibrin. *J Biol Chem* 2003;278(24):21584-91.

430. Jackson MR. Fibrin sealants in surgical practice: An overview. *Am J Surg* 2001;182(2):1s-7s.

431. Albala DM. Fibrin sealants in clinical practice. *Cardiovasc Surg* 2003;11 Suppl 1:5-11.

432. Kumar U, Albala DM. Fibrin glue applications in urology. *Curr Urol Rep* 2001;2(1):79-82.

433. Goussard P, Gie RP, Kling S, Kritzinger FE, van Wyk J, Janson J, Andronikou S. Fibrin glue closure of persistent bronchopleural fistula following pneumonectomy for post-tuberculosis bronchiectasis. *Pediatr Pulmonol* 2008;43(7):721-5.

434. Patel MR, Louie W, Rachlin J. Postoperative cerebrospinal fluid leaks of the lumbosacral spine: management with percutaneous fibrin glue. *AJNR Am J Neuroradiol* 1996;17(3):495-500.

435. Currie LJ, Sharpe JR, Martin R. The use of fibrin glue in skin grafts and tissue-engineered skin replacements: a review. *Plast Reconstr Surg* 2001;108(6):1713-26.

436. Kjaergard HK, Fairbrother JE. Controlled clinical studies of fibrin sealant in cardiothoracic surgery--a review. *Eur J Cardiothorac Surg* 1996;10(9):727-33.

437. Kjaergard HK. Patient-derived fibrin sealant: clinical, preclinical, and biophysical aspects. *Dan Med Bull* 2003;50(4):293-309.

438. Kjaergard HK, Trumbull HR. Vivostat system autologous fibrin sealant: preliminary study in elective coronary bypass grafting. *Ann Thorac Surg* 1998;66(2):482-6.

439. Breen A, O'Brien T, Pandit A. Fibrin as a delivery system for therapeutic drugs and biomolecules. *Tissue Eng Part B Rev* 2009;15(2):201-14.

440. Currie LJ, Martin R, Sharpe JR, James SE. A comparison of keratinocyte cell sprays with and without fibrin glue. *Burns* 2003;29(7):677-85.

441. Cox S, Cole M, Tawil B. Behavior of human dermal fibroblasts in three-dimensional fibrin clots: dependence on fibrinogen and thrombin concentration. *Tissue Eng* 2004;10(5-6):942-54.

442. Yuan Ye K, Sullivan KE, Black LD. Encapsulation of cardiomyocytes in a fibrin hydrogel for cardiac tissue engineering. *J Vis Exp* 2011(55).

443. Liau B, Christoforou N, Leong KW, Bursac N. Pluripotent stem cell-derived cardiac tissue patch with advanced structure and function. *Biomaterials* 2011;32(35):9180-7.

444. Dare EV, Vascotto SG, Carlsson D, Hincke MT, Griffith M. Differentiation of a fibrin gel encapsulated chondrogenic cell line. *Int J Artif Organs* 2007;30(7):619-27.

445. Eyrich D, Brandl F, Appel B, Wiese H, Maier G, Wenzel M, Staudenmaier R, Goepferich A, Blunk T. Long-term stable fibrin gels for cartilage engineering. *Biomaterials* 2007;28(1):55-65.

446. Eyrich D, Wiese H, Maier G, Skodacek D, Appel B, Sarhan H, Tessmar J, Staudenmaier R, Wenzel MM, Goepferich A, Blunk T. In vitro and in vivo cartilage engineering using a combination of chondrocyte-seeded long-term stable fibrin gels and polycaprolactone-based polyurethane scaffolds. *Tissue Eng* 2007;13(9):2207-18.

447. Chen W, Zhou H, Tang M, Weir MD, Bao C, Xu HH. Gas-Foaming Calcium Phosphate Cement Scaffold Encapsulating Human Umbilical Cord Stem Cells. *Tissue Eng Part A* 2011.

448. Ahearne M, Buckley CT, Kelly DJ. A growth factor delivery system for chondrogenic induction of infrapatellar fat pad-derived stem cells in fibrin hydrogels. *Biotechnol Appl Biochem* 2011;58(5):345-52.

449. Zhao Z, Hao C, Zhao H, Liu J, Shao L. Injectable allogeneic bone mesenchymal stem cells: A potential minimally invasive therapy for atrophic nonunion. *Med Hypotheses* 2011;77(5):912-3.

450. Gorodetsky R, Clark RA, An J, Gailit J, Levdansky L, Vexler A, Berman E, Marx G. Fibrin microbeads (FMB) as biodegradable carriers for culturing cells and for accelerating wound healing. *J Invest Dermatol* 1999;112(6):866-72.

451. Perka C, Arnold U, Spitzer RS, Lindenhayn K. The use of fibrin beads for tissue engineering and subsequential transplantation. *Tissue Eng* 2001;7(3):359-61.

452. Kassis I, Zangi L, Rivkin R, Levdansky L, Samuel S, Marx G, Gorodetsky R. Isolation of mesenchymal stem cells from G-CSF-mobilized human peripheral blood using fibrin microbeads. *Bone Marrow Transplant* 2006;37(10):967-76.

453. Zangi L, Rivkin R, Kassis I, Levdansky L, Marx G, Gorodetsky R. High-yield isolation, expansion, and differentiation of rat bone marrow-derived mesenchymal stem cells with fibrin microbeads. *Tissue Eng* 2006;12(8):2343-54.

454. Rivkin R, Ben-Ari A, Kassis I, Zangi L, Gaberman E, Levdansky L, Marx G, Gorodetsky R. High-yield isolation, expansion, and differentiation of murine bone marrow-derived mesenchymal stem cells using fibrin microbeads (FMB). *Cloning Stem Cells* 2007;9(2):157-75.

455. Gorodetsky R. The use of fibrin based matrices and fibrin microbeads (FMB) for cell based tissue regeneration. *Expert Opin Biol Ther* 2008;8(12):1831-46.

456. Shainer R, Gaberman E, Levdansky L, Gorodetsky R. Efficient isolation and chondrogenic differentiation of adult mesenchymal stem cells with fibrin microbeads and micronized collagen sponges. *Regen Med* 2010;5(2):255-65.

457. Ben-Ari A, Rivkin R, Frishman M, Gaberman E, Levdansky L, Gorodetsky R. Isolation and implantation of bone marrow-derived mesenchymal stem cells with fibrin micro beads to repair a critical-size bone defect in mice. *Tissue Eng Part A* 2009;15(9):2537-46.

458. Shimony N, Gorodetsky R, Marx G, Gal D, Rivkin R, Ben-Ari A, Landsman A, Haviv YS. Fibrin microbeads (FMB) as a 3D platform for kidney gene and cell therapy. *Kidney Int* 2006;69(3):625-33.

459. Cole M, Cox S, Inman E, Chan C, Mana M, Helgerson S, Tawil B. Fibrin as a delivery vehicle for active macrophage activator lipoprotein-2 peptide: in vitro studies. *Wound Repair Regen* 2007;15(4):521-9.

460. Iwakawa M, Mizoi K, Tessler A, Itoh Y. Intraspinal implants of fibrin glue containing glial cell line-derived neurotrophic factor promote dorsal root regeneration into spinal cord. *Neurorehabil Neural Repair* 2001;15(3):173-82.

461. Mackenzie DJ, Sipe R, Buck D, Burgess W, Hollinger J. Recombinant human acidic fibroblast growth factor and fibrin carrier regenerates bone. *Plast Reconstr Surg* 2001;107(4):989-96.

462. Wong C IE, Spaethe R, Helgerson S. Fibrin-based biomaterials to deliver human growth factors. *Thromb Haemost* 2003;89(3):573-82.

463. Jeon O, Ryu SH, Chung JH, Kim BS. Control of basic fibroblast growth factor release from fibrin gel with heparin and concentrations of fibrinogen and thrombin. *J Control Release* 2005;105(3):249-59.

464. Yang HS, La WG, Bhang SH, Jeon JY, Lee JH, Kim BS. Heparin-conjugated fibrin as an injectable system for sustained delivery of bone morphogenetic protein-2. *Tissue Eng Part A* 2010;16(4):1225-33.

465. Sakiyama-Elbert SE, Hubbell JA. Controlled release of nerve growth factor from a heparin-containing fibrin-based cell ingrowth matrix. *J Control Release* 2000;69(1):149-58.

466. Schense JC, Hubbell JA. Cross-linking exogenous bifunctional peptides into fibrin gels with factor XIIIa. *Bioconjugate Chemistry* 1999;10(1):75-81.

467. Ehrbar M, Djonov VG, Schnell C, Tschanz SA, Martiny-Baron G, Schenk U, Wood J, Burri PH, Hubbell JA, Zisch AH. Cell-demanded liberation of VEGF121 from fibrin implants induces local and controlled blood vessel growth. *Circ Res* 2004;94(8):1124-32.

468. Ehrbar M, Metters A, Zammaretti P, Hubbell JA, Zisch AH. Endothelial cell proliferation and progenitor maturation by fibrin-bound VEGF variants with differential susceptibilities to local cellular activity. *J Control Release* 2005;101(1-3):93-109.

469. Zhao W, Han Q, Lin H, Gao Y, Sun W, Zhao Y, Wang B, Chen B, Xiao Z, Dai J. Improved neovascularization and wound repair by targeting human basic fibroblast growth factor (bFGF) to fibrin. *J Mol Med (Berl)* 2008;86(10):1127-38.

470. Zhao W, Han Q, Lin H, Sun W, Gao Y, Zhao Y, Wang B, Wang X, Chen B, Xiao Z, Dai J. Human basic fibroblast growth factor fused with Kringle4 peptide binds to a fibrin scaffold and enhances angiogenesis. *Tissue Eng Part A* 2009;15(5):991-8.

471. Kidd ME, Shin S, Shea LD. Fibrin hydrogels for lentiviral gene delivery in vitro and in vivo. *J Control Release* 2011.

472. Padmashali RM, Andreadis ST. Engineering fibrinogen-binding VSV-G envelope for spatially- and cell-controlled lentivirus delivery through fibrin hydrogels. *Biomaterials* 2011;32(12):3330-9.

473. Raut SD, Lei P, Padmashali RM, Andreadis ST. Fibrin-mediated lentivirus gene transfer: implications for lentivirus microarrays. *J Control Release* 2010;144(2):213-20.

474. Lee HH, Haleem AM, Yao V, Li J, Xiao X, Chu CR. Release of bioactive adeno-associated virus from fibrin scaffolds: effects of fibrin glue concentrations. *Tissue Eng Part A* 2011;17(15-16):1969-78.

475. Breen A, Dockery P, O'Brien T, Pandit A. Fibrin scaffold promotes adenoviral gene transfer and controlled vector delivery. *J Biomed Mater Res A* 2009;89(4):876-84.

476. Breen A, Dockery P, O'Brien T, Pandit A. The use of therapeutic gene eNOS delivered via a fibrin scaffold enhances wound healing in a compromised wound model. *Biomaterials* 2008;29(21):3143-51.

477. Escamez MJ, Carretero M, Garcia M, Martinez-Santamaria L, Mirones I, Duarte B, Holguin A, Garcia E, Garcia V, Meana A, Jorcano JL, Larcher F, Del Rio M. Assessment of optimal virus-mediated growth factor gene delivery for human cutaneous wound healing enhancement. *J Invest Dermatol* 2008;128(6):1565-75.

478. Teraishi F UT, Saito T, Tsukagoshi T, Tanaka N, Fujiwara T. A novel method for gene delivery and expression in esophageal epithelium with fibrin glues containing replication-deficient adenovirus vector. *Surg Endosc* 2003;17(11):1845-8.

479. Jozkowicz A, Fugl A, Nanobashvili J, Neumayer C, Dulak J, Valentini D, Funovics P, Polterauer P, Redl H, Huk I. Delivery of high dose VEGF plasmid using fibrin carrier does not influence its angiogenic potency. *Int J Artif Organs* 2003;26(2):161-9.

480. des Rieux A, Shikanov A, Shea LD. Fibrin hydrogels for non-viral vector delivery in vitro. *J Control Release* 2009;136(2):148-54.

481. Lei Y, Rahim M, Ng Q, Segura T. Hyaluronic acid and fibrin hydrogels with concentrated DNA/PEI polyplexes for local gene delivery. *J Control Release* 2011;153(3):255-61.

482. Lei Y, Huang S, Sharif-Kashani P, Chen Y, Kavehpour P, Segura T. Incorporation of active DNA/cationic polymer polyplexes into hydrogel scaffolds. *Biomaterials* 2010;31(34):9106-16.

483. Trentin D, Hall H, Wechsler S, Hubbell JA. Peptide-matrix-mediated gene transfer of an oxygen-insensitive hypoxia-inducible factor-1alpha variant for local induction of angiogenesis. *Proc Natl Acad Sci U S A* 2006;103(8):2506-11.

484. Gelse K, von der Mark K, Aigner T, Park J, Schneider H. Articular cartilage repair by gene therapy using growth factor-producing mesenchymal cells. *Arthritis Rheum* 2003;48(2):430-41.

485. Torio-Padron N, Borges J, Momeni A, Mueller MC, Tegtmeier FT, Stark GB. Implantation of VEGF transfected preadipocytes improves vascularization of fibrin implants on the cylinder chorioallantoic membrane (CAM) model. *Minim Invasive Ther Allied Technol* 2007;16(3):155-62.

486. Lee TC, Ho JT, Hung KS, Chen WF, Chung YH, Yang YL. Bone morphogenetic protein gene therapy using a fibrin scaffold for a rabbit spinal-fusion experiment. *Neurosurgery* 2006;58(2):373-80; discussion 73-80.

Chapter Two

Ability of Fibrin Gel to Deliver Two Reporter Genes Simultaneously in an *In Vivo* Model of Rabbit Ear Ulcer

Contents of this chapter have previously been published:

Kulkarni M., Breen A. Greiser U., O'Brien T. and Pandit A. **'**Fibrin-lipoplex System for Controlled Topical Delivery of Multiple Genes.' *Biomacromolecules* 2009;10(6):1650-4.

2.1 Introduction

Biodegradable scaffolds have a prominent role to play in various tissue engineering approaches. Natural macromolecules like collagen and fibrin can be used as tools for controlled release of various therapeutic agents. Apart from traditional use of fibrin as a sealant[1-4], fibrin is being increasingly used as a scaffold for delivery of cells[5], drugs[6], plasmids[7] and, more recently, gene vectors[8-11]. As highly efficient gene delivery carriers, viruses have been studied by many investigators for various clinical applications such as wound healing, bone tissue engineering and cartilage. Recently, it has been shown that fibrin enhances the delivery of adenovirus vector to chronic wounds[12].

However, there is a need to investigate non-viral systems of gene delivery in order to minimize possible immunogenic response associated with viral vectors. Non-viral systems offer the advantage of safety and can transfer therapeutically relevant amounts of DNA[13]. Non-viral delivery usually does not result in insertion of the transgene in the host genome. This removes the risk of insertional mutagenesis, but on the other hand, this necessitates repeated administration. Thus, although non-viral carriers are generally considered safer compared to the viral counterparts, the need for repeated doses along with the issue of low transfection efficiency are some of the major disadvantages of non-viral gene therapy. Although in most cases, higher transfection efficiency can be achieved at higher dose, this also proportionally increases the risk of toxicity. Thus, efficiency and toxicity of non-viral vectors is dose related and represents a significant concern. These risks associated with high loads and subsequent toxicity of non-viral vectors when used on their own can be eliminated by use of a extracellular matrix based biodegradable scaffold, like fibrin, mediated delivery of non-viral vectors. Also, the use of such scaffold based delivery prolongs the gene delivery. Thus, effectively, the use of scaffolds enables the delivery at lower doses with enhanced prolonged therapeutic response and has the potential to significantly impact the safety profiles of the vectors embedded in the scaffolds.

Although some investigators have reported the use of fibrin based delivery systems previously for plasmid, drug or protein delivery[8 14 15], the simultaneous delivery of

multiple genes using non-viral gene carriers via fibrin scaffold has not been reported and thus remains to be fully characterized and investigated.

Fibrin plays an important role in hemostasis and wound healing. The physiological hemostatic not only plays an indispensable role in clot formation, but is a natural tissue engineering/regenerative medicine scaffold which has been shown to act as a reservoir for growth factors, extracellular matrix molecules, and platelets and responds to various microenvironmental cues in a highly orchestrated manner. It is one of the few natural biomolecules found in the body as stable monomer precursors and polymerizes only when needed and degrades in a highly controlled manner, leaving behind chemotactic and mitogenic degradation products.

Liposomes, as explained in detail in chapter one (section 1.3.1), are multifaceted versatile non-viral gene delivery systems which are spherical lipid bilayers of diameters generally in the range of 50–1000 nm. Depending on the net charge on the surface of liposomes, they are classified as cationic, anionic or neutral. Cationic liposomes have been the most popular liposomal formulations used in gene delivery experiments, probably on account of their opposite charge compared to that on cell surface, convenience and efficacy. Cationic liposomes interact with negatively charged DNA molecules to make stable complexes called lipoplexes. In general, they contain one cationic lipid and a helper lipid such as dioleoylphosphatidylethanolamine (DOPE) or dioleoylphosphatidylcholine (DOPC). The helper lipids help in stabilization of lipoplexes. Lipofectin® is the commercially available cationic lipid formulation, reported by Phil Felgner in 1987. Lipofectin® is a 1:1 (w/w) liposome formulation of the cationic lipid N-[1-(2, 3-dioleyloxy) propyl]-n, n, n-trimethyl ammonium chloride (DOTMA) and DOPE in membrane filtered water. Lipofectin® has been used to deliver linear/plasmid DNA to a variety of cells in culture and also to variety of tissues *in vivo*.

The aim of this study was to develop a safe, efficient gene delivery system using fibrin as a scaffold, capable of delivering genes in a sustained fashion and lipoplexes as complementary non-viral gene carriers. In this initial study, the suitability of fibrin as a scaffold to deliver genes over an extended period of time by using a liposome based

gene delivery system was investigated. Specifically, an analysis of the interaction of the fibrinogen component of fibrin with lipofectin was studied qualitatively. This analysis was done using surface plasmon resonance (SPR), which is a well-established method for studying bimolecular interactions[16]. The bioactivity of the released complexes was tested by *in vitro* transfection studies. In addition, the efficacy of this fibrin-based non-viral gene delivery system to deliver two reporter genes simultaneously was investigated in an *in vivo* model of a rabbit ear ulcer. Figure 2.1 schematically depicts the steps taken in this phase of the project.

2.2 Materials and Methods

2.2.1 Fibrin-lipoplex System Fabrication

Fibrin scaffold was fabricated using fibrin kits (TISSEEL, Baxter Healthcare, Vienna, Austria), kindly donated by Baxter Healthcare, Vienna. Fibrinogen component was reconstituted with aprotinin (3000KIU) and subsequently diluted with fibrinogen dilution buffer to a concentration of 60mg/ml. Thrombin component was reconstituted with calcium chloride (40μM) to a concentration of 4IU. Large scale plasmid preparations were performed utilizing the Gigaprep kits (Qiagen) according to the manufacturers' instructions. Prior to scaffold fabrication, the lipoplexes were prepared using lipofectin (Invitrogen) and plasmid DNA, encoding either green fluorescent protein for the *in vitro* transfection study or β-galactosidase and firefly luciferase for the *in vivo* study. The lipoplexes were mixed with thrombin solution. In the *in vivo* study, polymerization of the scaffold was carried out by delivering fibrinogen solution and thrombin-lipoplex solution simultaneously to the wounded area.

2.2.2 Stability of DNA

The stability of plasmid DNA was checked by agarose gel electrophoresis. Agarose gel electrophoresis was performed in 0.7% (w/v) agarose gels containing 0.01% SYBR safe for visualization, for 30 min at 100V. The resultant gels were visualized under UV transilluminator at wavelength of 365 nm.

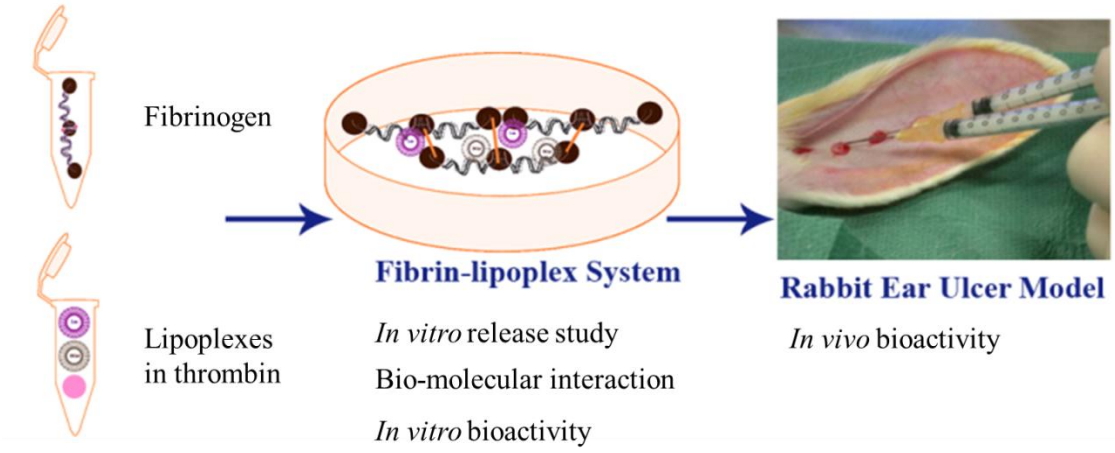

Figure 2.1: Schematic representation of the experimental steps taken in the phase I. The fibrin-lipoplex system was fabricated and characterized *in vitro* and *in vivo*.

2.2.3 *In Vitro* Release Study

Fibrin-lipoplex system was fabricated as described above and incubated at 37^0C. Dulbecco's Modified Eagles medium (Sigma) supplemented with 10% Fetal Bovine Serum (Sigma), 2mM Glutamine (Sigma), 1% Penicillin (Sigma) and 1% Streptomycin (Sigma) was used to cover the scaffold surface. The supernatant was collected from the scaffold at 24, 48, 96, 120 and 144 hours of incubation, and the DNA was quantified after triton-X dissolution of the released lipoplexes. Finally, at 144 hours of incubation, the fibrin scaffolds were dissolved by 100nM plasmin, and the DNA content was quantified again by PicoGreen® assay using manufacturer's guidelines (Invitrogen).

2.2.4 Biomolecular Interaction Analysis (BIA)

All the materials required for surface plasmon studies such as sensor chip CM3 and an amine immobilization kit containing *N*-hydroxysuccinimide (NHS), *N*-ethyl-*N*-(3-diethylaminopropyl)-carbodiimide (EDC), 1 M ethanolamine-HCl (pH 8.5), HEPES buffer and Glycine HCl (pH 2.5) were obtained from Biacore (UK).The interaction of fibrin (ogen) and lipofectin was evaluated with surface plasmon resonance (SPR) technology using the Biacore 2000 system (Biacore). Fibrinogen was immobilized covalently to the dextran matrix of the flow-cell 2 (Fc2) or flow-cell 4 (Fc4) in a sensor chip CM3 using the amine-coupling procedure as per manufacturer's instructions. Flow-cell 1 (Fc1) or flow-cell 3 (Fc3) was used as reference in all measurements. The SPR responses were reported in response units (RU). To determine the binding between fibrinogen and lipofectin, lipofectin diluted in 10 mM HEPES pH 7.4 (1:1 v/v) was injected over the surface at a flow rate of 5µL/min and 25°C, and the SPR response was recorded. To study the effect of different concentrations on the binding, lipofectin at high (0.5 mg/ml) and low (0.05 mg/ml) concentrations was injected over the surface at a flow rate of 30 µL/min and 25°C. High flow rates were used to reduce mass transfer of lipids to the surface.

2.2.5 *In Vitro* Transfection Study

NIH-3T3 cells were cultured in Dulbecco's Modified Eagles medium (Sigma) supplemented with 10% Fetal Bovine Serum (Sigma), 2mM Glutamine (Sigma), 1% Penicillin (Sigma) and 1% Streptomycin (Sigma). The cells were seeded in a 24-well

plate at a concentration of 50,000 cells per well. All the transfections were done in triplicates and at 37^0C. The study was done in two phases. In the first phase, the cells were transfected by the supernatant from the fibrin-lipoplex system at 48 and 96 hours of incubation. In the second phase, the fibrin scaffolds were dissolved at 48 and 96 hours of incubation by human plasmin, and then the cells were transfected. Fluorescent microscopy was used to study transfection at 48 hours.

2.2.6 *In Vivo* Model

New Zealand white rabbits (3-5 kg, male) were used in the study. The study was conducted under a license granted by the Department of Health and Children, Dublin, Ireland, and the protocol was approved by the Research Ethics Committee of the National University of Ireland, Galway. Hair was removed from the rabbit ear by shaving 24 hours prior to surgery. Animals were anesthetized using ketamine (0.3 mg/kg) and xylazine (0.35 mg/kg) and maintained by 2% isofluorane for the duration of surgery. Four 6mm punch biopsy wounds were created in each ear, exposing bare cartilage. Each wound was treated with one of the four randomized treatment groups: no treatment, fibrin scaffold alone, lipoplexes alone or the fibrin-lipoplex system. The lipoplexes used were a mix of two lipoplexes, containing plasmids encoding β-galactosidase (2.5 μg) and firefly luciferase (2.5 μg). Wounds were observed for 7 days. At 7 days, rabbits were anesthetized and euthanized using sodium pentobarbital (100-150 mg/kg). Ears were surgically removed after sacrifice. Wounds were cut across the centerline, and one of the halves was fixed in neutral-buffered formalin fixative. Tissue was processed and then embedded in paraffin. Five micrometer sections were saved for histological and immunohistochemical analysis at the midlevel. The other halves were stored immediately in liquid nitrogen.

2.2.7 β-galactosidase Transgene Expression

Immunohistochemistry was carried out to detect β-galactosidase transgene expression. Slides were cleared in xylene and rehydrated. Enzymatic antigen retrieval was carried out using 1× proteinase K (20 μg/mL, Sigma Aldrich) solution in TE buffer (50 m*M* Tris Base, 1 m*M* EDTA, pH 8.0, Sigma Aldrich) at 37°C in a humidity chamber for 30 min before cooling at room temperature for 10 min. Slides were blocked using normal

goat serum (2% goat serum, 1% bovine serum albumin, 0.1% cold fish skin gelatin, 0.1% Triton X-100 and 0.05% Tween 20 in 0.01*M* PBS, pH 7.2, all from Sigma Aldrich, Ireland) for 40 min at room temperature. Mouse primary anti-βGal (AbCam, UK) (1:100 in 0.01*M* PBS containing 1%BSA and 0.1% cold fish skin gelatin) was added to the slides for 2 hours at room temperature. Blocking buffer was added to three slides as negative control. Endogenous peroxidase was blocked with 3% hydrogen peroxide (Sigma Aldrich) for 10 min at room temperature. Secondary goat anti-mouse IgG (1:200 in 0.01*M* PBS, DakoCytomation, Ireland) was applied for 45 min at room temperature followed by strepatavidin-avidin biotin complex HRP (DakoCytomation, Ireland) for 20 min. DAB chromagen (Sigma Aldrich, Ireland) was added to slides for 3-5 min. Slides were rinsed, dehydrated, cleared in xylene and then mounted using DPX mounting media. Slides were rinsed between every step in PBST (0.05% Tween 20, Sigma Aldrich) solution for 2- to 3-min time periods. Slides were not rinsed after blocking. Sections were viewed under a bright light microscope (Olympus® dp70, Ireland). Four fields of view were captured at a magnification of 400× for each section using image analysis software (Image Pro®, Media Cybernetics, UK). The volume fraction of cells staining positive, as identified by brown cytoplasm, was measured using a 192-point grid. A 192-point grid was overlaid on each field of view, and the number of brown cells that intersected with a grid point was counted. The volume fraction (V_v) of brown cells was calculated using the equation

$$V_v = \left(\frac{P_p}{P_T} \right)$$

Where P_P is the number of brown cells intersecting a grid point and P_T is the total number of grid points intersecting the tissue. The cumulative volume fraction for four fields of view was calculated for each section by dividing the total number of brown cells intersecting the grid points by the total number of grid points for all the fields.

2.2.8 Luciferase Transgene Expression

The tissue stored in liquid nitrogen was assayed for luciferase transgene expression by luciferase assay system (Promega, UK). The tissue sample was homogenized by probes Tissue Ruptor™ (Promega, UK) in 500 μl of cell culture lysis buffer. The tissue

extracts were then subjected to three cycles of freeze thaw (3 min in liquid nitrogen and 3 min at 37^0C) and centrifuged at 10,000 rpm at 4^0C in a bench-top microfuge for 10 min. 50 µl of the supernatant was mixed with 100 µl of luciferase assay buffer, and the light units were immediately measured (Wallac Multi-label Counter, PerkinElmer).

2.3 Results

2.3.1 *In Vitro* Release Study

The release profile of lipoplexes was studied for 144 hours of incubation. The percent of DNA released from the fibrin scaffold was calculated by PicoGreen® assay. As can be seen in Figure 2.2 (A), only very small amount of plasmid DNA was released in 144 hours of incubation. After plasmin dissolution of the scaffold, almost all the plasmid DNA content was released from the scaffold indicating complete encapsulation and long term storage of lipoplexes inside the scaffold. It is important for the plasmid to remain intact to be effective in transfection. To check the integrity of the plasmid, 2-D gel electrophoresis was performed. It was found that the plasmid DNA released from the scaffold at 144 hours was intact when compared with plasmid DNA released form freshly formed lipoplexes and plasmid DNA alone (Figure 2.2 B). This result suggests that the plasmid DNA is held safely within the fibrin scaffold.

2.3.2 Biomolecular Interaction Analysis (BIA)

Fibrinogen was successfully immobilized on a sensor chip CM3 using amine coupling. Figure 2.3 shows binding of immobilized fibrinogen with lipofectin. The baseline is the response after immobilization of fibrinogen. The surface was saturated with fibrinogen. The peaks 1 and 2 are responses after lipofectin at high concentration was passed sequentially. These positive peaks suggest binding of lipofectin to fibrinogen. Then the surface was regenerated and lipofectin at low concentration was passed. This time the response was a positive peak (peak 3) but less than that observed at high concentration.

2.3.3 *In Vitro* Transfection Study

Figure 2.4 shows the fluorescent microscopic images of transfection studies on fibroblasts. The transfection was done in two phases – with and without plasmin dissolution of the scaffold.

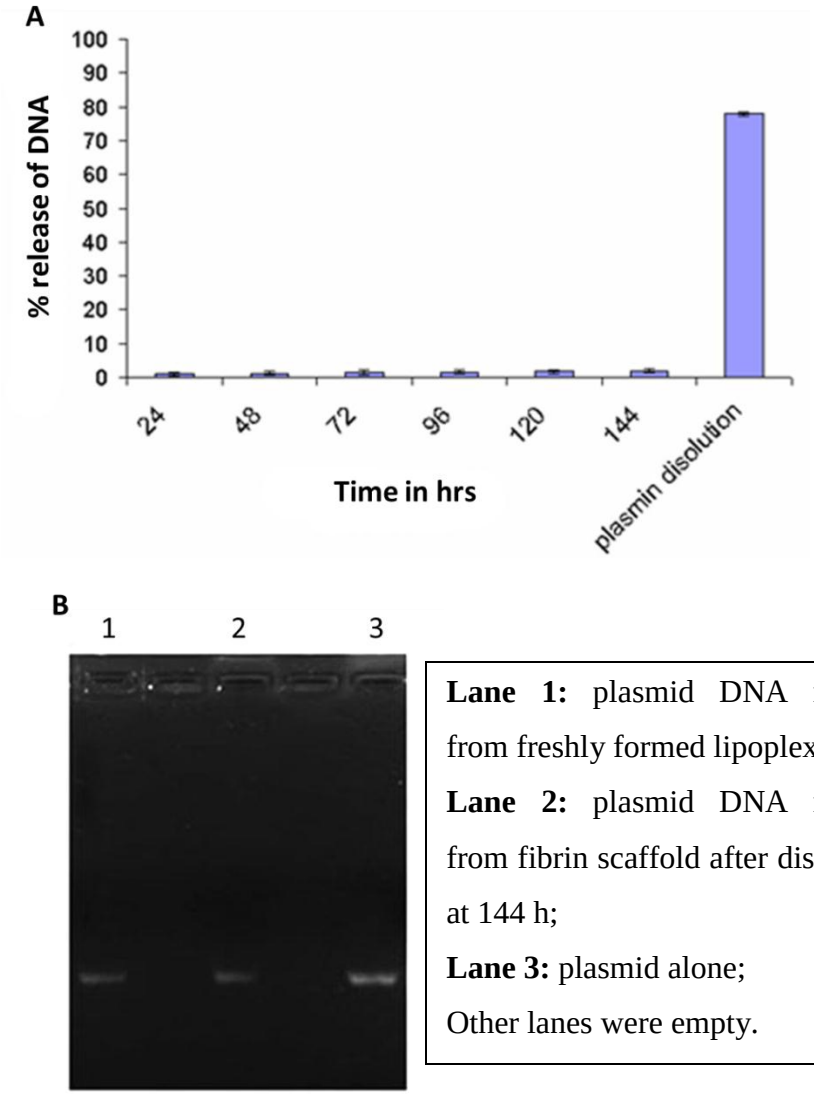

Figure 2.2: *In vitro* release profile of plasmid DNA from the fibrin-lipoplex system under static conditions, measured over a period of 144 hours by PicoGreen® assay. (A) Minimal release of plasmid DNA was observed up to 144 hours after fibrin-lipoplex fabrication. PicoGreen® assays performed after plasmin dissolution of the scaffolds confirmed that most of the DNA is retained within the scaffold. The percentage of plasmid DNA within the fibrin-lipoplex system at 0 hour is arbitrarily set as 100%. (B) On gel electrophoresis, the released plasmid DNA after dissolution of scaffold was found to be intact when compared to plasmid DNA from freshly formed lipoplexes and plasmid alone.

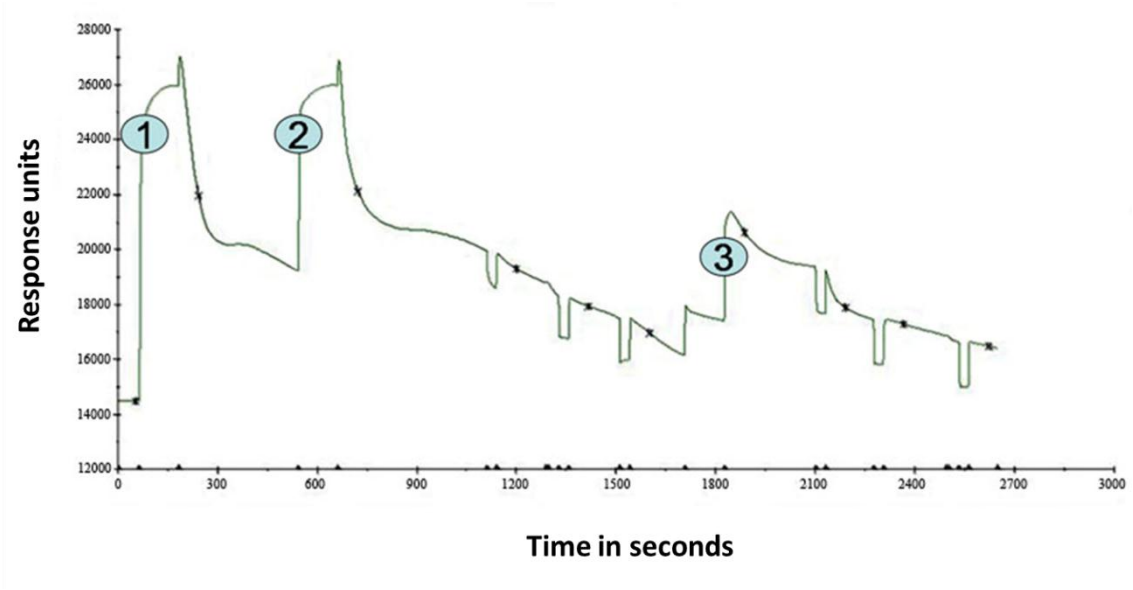

Figure 2.3: Sensorgram of response unit changes observed during the injection of lipofectin over immobilized fibrinogen. The peaks 1 and 2 are responses observed by binding of lipofectin to immobilized fibrinogen at high concentration and peak 3 shows binding at low concentration. The negative peaks are due to regeneration of the surface by 10 mM glycine, pH 2.5. Thus, lipofectin binds to fibrinogen in concentration dependent manner.

There was no transfection observed from samples not treated with plasmin (Figure 2.4 A & B) due to the very small amount of the lipoplexes released from the scaffold during this time period. However, transfection was observed after dissolution of scaffolds with plasmin (Figure 2.4 C & D) indicating that the encapsulated lipoplexes maintained their ability to transfect fibroblasts when compared to freshly formed lipoplexes (Figure 2.4 E)

2.3.4 *In Vivo* Transfection

The expression of the two reporter genes delivered simultaneously, through the fibrin-lipoplex system to rabbit ear ulcer model, 7 days post-surgery was investigated, quantified and compared with the background expression and by lipoplexes alone. Figure 2.5 shows representative immunohistochemistry images of β-Gal expression by transfected cells from the rabbit ear. These images indicate a higher transfection level achieved by fibrin-lipoplex system (Figure 2.5 D; brown cells) than seen in lipoplexes alone (Figure 2.5 C). These animal studies also included negative control groups such as a "no treatment" group (Figure 2.5 A) and a "fibrin alone" treatment group (Figure 2.5 B). The expression was quantified using a well-established stereological parameter, volume fraction (Figure 2.6). The expression in the fibrin-lipoplex group was significantly higher than that seen in lipoplexes alone. The results of the luciferase assay (Figure 2.7) also suggest that at day 7 the transfection mediated by fibrin-lipoplex system was significantly higher than the lipoplexes alone. Thus, the expression of both the reporter genes was significantly higher in the fibrin-lipoplex system than all the other groups.

2.4 Discussion

This study is critical in the development of a non-viral gene delivery system using fibrin as scaffold. The components of fibrin-lipoplex system investigated in this study are complementary to each other. Although use of plasmid DNA has its own advantages, the extremely low transfection efficiency and short term expression render them inefficient for any therapeutic benefit[17]. Studies have shown the beneficial effect of biodegradable scaffold[7 18] which acts as a reservoir that protects the DNA and releases it in a sustained fashion. Fibrin is one such highly promising scaffold.

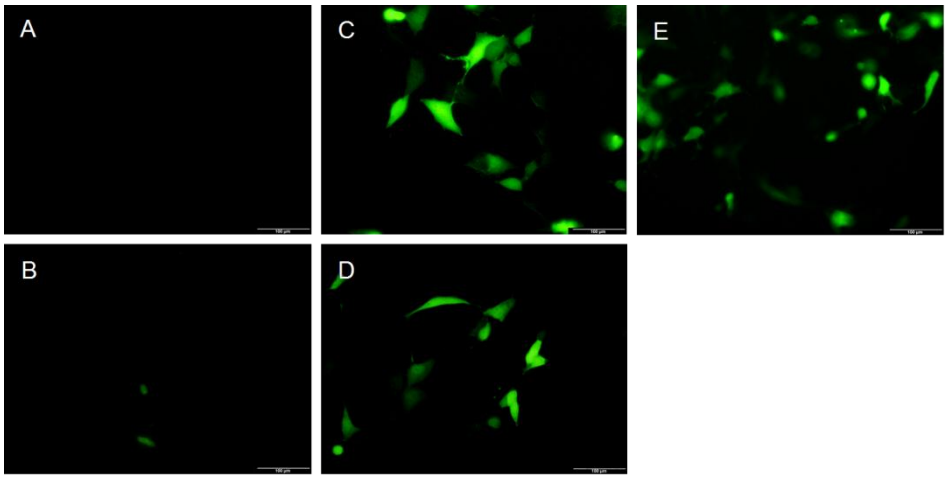

Figure 2.4: Representative fluorescent images of fibroblasts expressing green fluorescent protein (GFP). Very low transfection efficiencies were observed when the supernatant from the fibrin-lipoplex system was used for transfection at 48 and 96 hours of incubation (A & B). When the fibrin scaffold was dissolved, the released lipoplexes were used for transfection and cells expressed GFP (C & D) which is comparable to transfection by freshly prepared lipoplexes (E). The scale bars represent 100 µm.

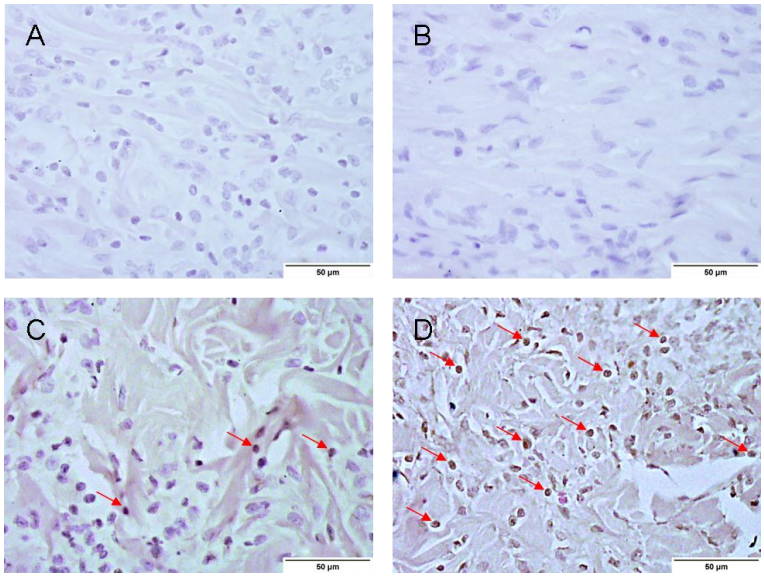

Figure 2.5: Immunohistochemistry for βGal expression at day seven of treatment. Brown cells indicate positive expression of βGal. Examples of positively stained cells are highlighted by arrows. (A) no treatment, (B) fibrin alone, (C) lipoplexes alone and (D) fibrin-lipoplex system. The scale bars represent 50 µm.

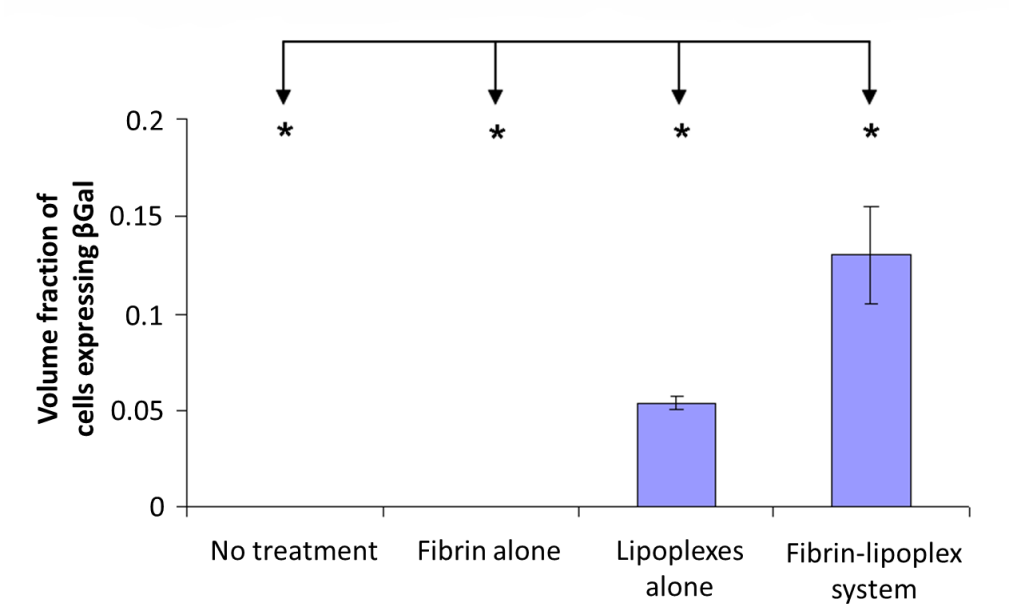

Figure 2.6: Volume fraction of cells stained positively for βGal at 7 days. βGal expression was significantly higher in the fibrin-lipoplex system than all other treatment groups. * indicates statistical significance by one-way ANOVA (*P*< 0.05, n=4).

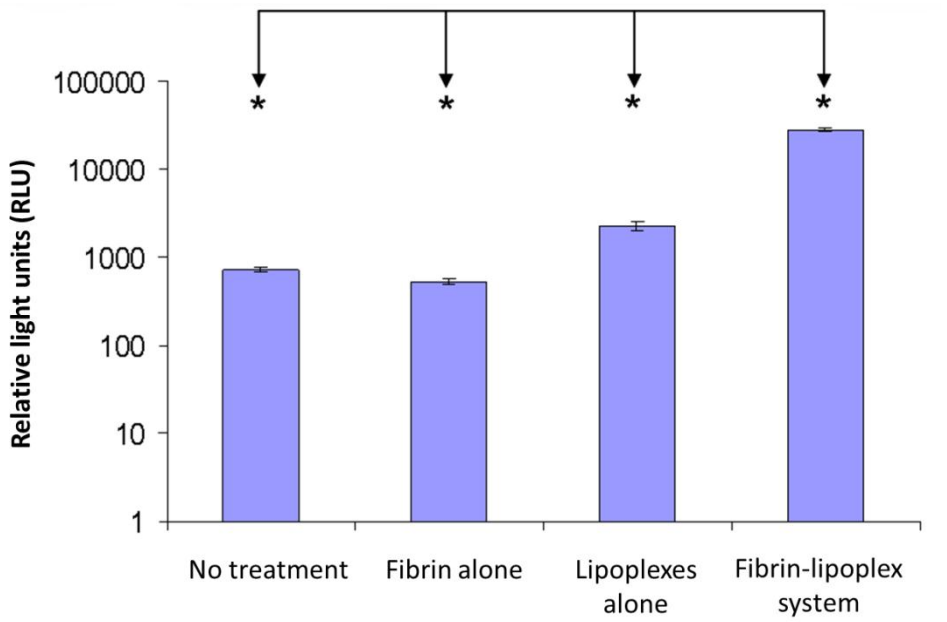

Figure 2.7: Analysis of luciferase expression at day seven post-treatment. The luciferase expression was significantly higher in fibrin-lipoplex system than in all other treatment groups. * indicates statistical significance by one-way ANOVA (*P*< 0.05, n=4).

When complemented by non-viral transfection reagents such as liposomes, plasmid DNA can be taken up more efficiently by cells and thus improving transfection efficiency without raising the safety issues related with use of viruses. Michlits *et al* have shown that use of lipofectin can enhance the beneficial effect of scaffold, by improving transfection efficiency[8]. Thus, considering the potential benefits of the combination, the fibrin-lipoplex system was investigated for topical delivery of two reporter genes simultaneously. Initially, the aim was to investigate if the fibrin scaffold will hold the lipoplexes within the scaffold matrix and release them in a sustained fashion. Furthermore, it was desirable to determine if the lipoplexes held in fibrin remained viable and could transfect cells. To answer the first question, an *in vitro* release study was performed. The results suggested that the lipoplexes were held in the scaffold for up to 144 hours of incubation at 37^0C.

Controlled release of bioactive agents via tissue engineered scaffolds can be achieved chemically by bio-conjugation or physically by hindrance. A binding interaction between the scaffold and the active agents obviates the need for additional conjugation and provides a natural bio-conjugation for controlled release. It is known that the polymerized fibrin acts as a scaffold for cell migration and proliferation, and as a reservoir for growth factors, proteases, and protease inhibitors. In terms of interactions, platelet membrane receptor GPIIb-IIIa mediates interaction of fibrin with platelets[19 20]. Fibrinogen contains a number of known and potential integrin binding sites[21], two of which bind $\alpha_V\beta_3$ present on endothelial cells[22] and fibroblasts[23]. Fibrinogen is the "sticky" component of the fibrin gel Matrix proteins which interact with and bind fibrinogen and fibrin clots include fibronectin[24], vitronectin[25] and thrombospondin[26] and effectively support tissue cell migration.[27] Fibrinogen has also been shown to bind various other biomolecules such as myosin[28], basic fibroblast growth factor (bFGF)[29], TGF-β[30] and VEGF[31]. Considering this, the interaction of fibrinogen with lipofectin was studied, hoping to understand why lipoplexes were retained inside the scaffold. The surface plasmon resonance studies clearly indicate, at least qualitatively that there is interaction between the two bio-molecules and this might explain the *in vitro* release pattern of the lipofectin from the fibrin scaffold. The lipofectin is a two component

liposome and also fibrinogen is known to have more than one binding sites. Hence the quantification of such an interaction is difficult. A more elaborate study with single lipid components and pure fragments of fibrinogen molecule is required to determine the exact degree and specificity of binding. Thus, from the combination of the preliminary SPR data and release profile, it can be presumed that the lipoplexes are naturally bound to fibrin, thereby providing a natural solution as opposed to physical or chemical tethering methods for retaining any bioactive agent within a scaffold[32-34].

Data obtained from the *in vitro* release studies resemble closely to previously reported studies on the fibrin- liposome system[15 35] while other studies have shown different release profiles[6 14]. These differences could be due to the fact that the interaction between fibrinogen and lipofectin is very specific and the composition of liposomes plays an important role. Another influential factor could be the concentrations of fibrinogen and liposomes. It has been shown that this interaction is concentration-dependent. Therefore, at low concentrations of fibrinogen and liposomes the release pattern will be different. Other factors such as pore sizes, surface charge of liposomes and cross-linking may also influence the release profile. In fact, this variability of affecting parameters provides an opportunity to tailor the fibrin scaffold for controlled release of lipoplexes.

Having investigated the bio-molecular interaction, the next step was to investigate the bioactivity of the released complexes *in vitro* and *in vivo*. The results of the *in vitro* transfection study suggest that the lipoplexes retain their bioactivity within the scaffold and, when released, are capable of transfection, comparable to that seen with freshly formed lipoplexes. The scenario in the *in vitro* setup is entirely different when compared to that in an *in vivo* setup as the fibrin scaffold is degraded naturally *in vivo* in a controlled manner. For this reason, the efficacy of the fibrin-lipoplex system in the *in vivo* model of rabbit ear wound was studied. Preliminary results suggest that the fibrin lipoplex system is able to deliver genes in a time-dependent manner. The expression of β-Gal transgene was quantified by volume fraction, a stereological parameter and that of luciferase was quantified by quantitative assay. Stereology provides solution to the major problem of sampling, i.e. loss of dimension as it enables to draw three-

dimensional information based on observations made in two-dimensional sections[36]. The reference (wound volume) being the same, volume fraction provided reliable information on the relative fraction of positive cells in various treatment groups. Thus, the quantification of the relative expression of both the reporter genes reliably suggested that the transgene expression in the fibrin-lipoplex system at seven days of surgery was significantly higher than the lipoplexes alone. The comparison of fibrin-lipoplex system versus fibrin-plasmid system has been done previously by Michlits *et al* where it has been shown that fibrin-lipoplex system had significantly higher transfection for VEGF plasmid when compared with fibrin-plasmid system[8]. In this study, the fibrin-lipoplex system was compared versus the lipoplexes alone. Thus, the fibrin-lipoplex system is able to deliver two genes simultaneously. This is particularly important when dealing with diseases involving multiple gene defects, wherein simultaneous delivery of multiple genes can be extremely rewarding.

2.5 Conclusion

The results of this study suggest that a fibrin-lipoplex system is an excellent choice for sustained gene delivery and that it can potentially be utilized for delivery of multiple genes. In conclusion, it was shown that lipoplexes are released for extended period of 7 days from a fibrin-lipoplex system; probably on account of biomolecular interaction and these released complexes are capable of transfection both *in vitro* and *in vivo*. Thus, it is evident that the fibrin-lipoplex system provides an enhanced method of extended transfer of multiple genes for topical applications.

2.5 References

1. Garcia-Villarreal OA, Casillas-Covarrubias LE. Fibrin sealant for left ventricular rupture after mitral valve replacement. *Asian Cardiovasc Thorac Ann* 2008;16(2):152-3.

2. Foster JA, Holck DE, Perry JD, Wulc AE, Burns JA, Cahill KV, Morgenstern KE. Fibrin sealant for Muller muscle-conjunctiva resection ptosis repair. *Ophthal Plast Reconstr Surg* 2006;22(3):184-7.

3. Anidjar M, Desgrandchamps F, Martin L, Cochand-Priollet B, Cussenot O, Teillac P, Le Duc A. Laparoscopic fibrin glue ureteral anastomosis: experimental study in the porcine model. *J Endourol* 1996;10(1):51-6.

4. Hetherington VJ, Park JB, Park SH, Carnett JA, Patterson BA, Bratkiewicz L, Kessler DA. Effects of fibrin sealant on the fixation of porous titanium and pyrolytic carbon implants. *J Foot Surg* 1989;28(2):145-50.

5. Lee OK. Fibrin glue as a vehicle for mesenchymal stem cell delivery in bone regeneration. *J Chin Med Assoc* 2008;71(2):59-61.

6. Chung TW, Yang MC, Tsai WJ. A fibrin encapsulated liposomes-in-chitosan matrix (FLCM) for delivering water-soluble drugs. Influences of the surface properties of liposomes and the crosslinked fibrin network. *Int J Pharm* 2006;311(1-2):122-9.

7. Andree C, Voigt M, Wenger A, Erichsen T, Bittner K, Schaefer D, Walgenbach KJ, Borges J, Horch RE, Eriksson E, Stark B. Plasmid gene delivery to human keratinocytes through a fibrin-mediated transfection system. *Tissue Eng* 2001;7(6):757-66.

8. Michlits W, Mittermayr R, Schafer R, Redl H, Aharinejad S. Fibrin-embedded administration of VEGF plasmid enhances skin flap survival. *Wound Repair Regen* 2007;15(3):360-7.

9. Breen A, Dockery P, O'Brien T, Pandit A. Fibrin scaffold promotes adenoviral gene transfer and controlled vector delivery. *J Biomed Mater Res A* 2009;89(4):876-84.

10. Teraishi F, Umeoka T, Saito T, Tsukagoshi T, Tanaka N, Fujiwara T. A novel method for gene delivery and expression in esophageal epithelium with fibrin

glues containing replication-deficient adenovirus vector. *Surg Endosc* 2003;17(11):1845-8.

11. Schillinger U, Wexel G, Hacker C, Kullmer M, Koch C, Gerg M, Vogt S, Ueblacker P, Tischer T, Hensler D, Wilisch J, Aigner J, Walch A, Stemberger A, Plank C. A fibrin glue composition as carrier for nucleic acid vectors. *Pharm Res* 2008;25(12):2946-62.
12. Breen A, Dockery P, O'Brien T, Pandit A. The use of therapeutic gene eNOS delivered via a fibrin scaffold enhances wound healing in a compromised wound model. *Biomaterials* 2008;29(21):3143-51.
13. Saul JM, Linnes MP, Ratner BD, Giachelli CM, Pun SH. Delivery of non-viral gene carriers from sphere-templated fibrin scaffolds for sustained transgene expression. *Biomaterials* 2007;28(31):4705-16.
14. Wang SS, Yang MC, Chung TW. Liposomes/chitosan scaffold/human fibrin gel composite systems for delivering hydrophilic drugs--release behaviors of tirofiban in vitro. *Drug Deliv* 2008;15(3):149-57.
15. Meyenburg S, Lilie H, Panzner S, Rudolph R. Fibrin encapsulated liposomes as protein delivery system Studies on the in vitro release behaviour. *J Control Release* 2000;69:159-68.
16. Besenicar M, Macek P, Lakey JH, Anderluh G. Surface plasmon resonance in protein–membrane interactions. *Chemistry and Physics of Lipids* 2006;141(Issues 1-2):169-78.
17. Bonadio J. Tissue engineering via local gene delivery. *J Mol Med* 2000;78(6):303-11.
18. Bonadio J, Smiley E, Patil P, Goldstein S. Localized, direct plasmid gene delivery in vivo: prolonged therapy results in reproducible tissue regeneration. *Nat Med* 1999;5(7):753-9.
19. Charo IF, Bekeart LS, Phillips DR. Platelet glycoprotein IIb-IIIa-like proteins mediate endothelial cell attachment to adhesive proteins and the extracellular matrix. *J Biol Chem* 1987;262(21):9935-8.
20. Podolnikova NP, Gorkun OV, Loreth RM, Yee VC, Lord ST, Ugarova TP. A cluster of basic amino acid residues in the gamma370-381 sequence of

fibrinogen comprises a binding site for platelet integrin alpha(IIb)beta3 (glycoprotein IIb/IIIa). *Biochemistry* 2005;44(51):16920-30.

21. Plow EF, Haas TA, Zhang L, Loftus J, Smith JW. Ligand binding to integrins. *J Biol Chem* 2000;275(29):21785-8.
22. Cheresh DA. Human endothelial cells synthesize and express an Arg-Gly-Asp-directed adhesion receptor involved in attachment to fibrinogen and von Willebrand factor. *Proc Natl Acad Sci U S A* 1987;84(18):6471-5.
23. Gailit J, Clarke C, Newman D, Tonnesen MG, Mosesson MW, Clark RA. Human fibroblasts bind directly to fibrinogen at RGD sites through integrin alpha(v)beta3. *Experimental cell research* 1997;232(1):118-26.
24. Makogonenko E, Tsurupa G, Ingham K, Medved L. Interaction of fibrin(ogen) with fibronectin: further characterization and localization of the fibronectin-binding site. *Biochemistry* 2002;41(25):7907-13.
25. Podor TJ, Campbell S, Chindemi P, Foulon DM, Farrell DH, Walton PD, Weitz JI, Peterson CB. Incorporation of vitronectin into fibrin clots. Evidence for a binding interaction between vitronectin and gamma A/gamma' fibrinogen. *J Biol Chem* 2002;277(9):7520-8.
26. Bacon-Baguley T, Ogilvie ML, Gartner TK, Walz DA. Thrombospondin binding to specific sequences within the A alpha- and B beta-chains of fibrinogen. *J Biol Chem* 1990;265(4):2317-23.
27. Clark RA. Fibrin is a many splendored thing. *J Invest Dermatol* 2003;121(5):xxi-xxii.
28. Kolev K, Tenekedjiev K, Ajtai K, Kovalszky I, Gombas J, Varadi B, Machovich R. Myosin: a noncovalent stabilizer of fibrin in the process of clot dissolution. *Blood* 2003;101(11):4380-6.
29. Peng H, Sahni A, Fay P, Bellum S, Prudovsky I, Maciag T, Francis CW. Identification of a binding site on human FGF-2 for fibrinogen. *Blood* 2004;103(6):2114-20.
30. Catelas I, Dwyer JF, Helgerson S. Controlled release of bioactive transforming growth factor Beta-1 from fibrin gels in vitro. *Tissue Eng Part C Methods* 2008;14(2):119-28.

31. Sahni A, Francis CW. Vascular endothelial growth factor binds to fibrinogen and fibrin and stimulates endothelial cell proliferation. *Blood* 2000;96(12):3772-8.

32. Wood MD, Borschel GH, Sakiyama-Elbert SE. Controlled release of glial-derived neurotrophic factor from fibrin matrices containing an affinity-based delivery system. *J Biomed Mater Res A* 2009;89(4):909-18.

33. Liang JF, Song H, Li YT, Yang VC. A novel heparin/protamine-based pro-drug type delivery system for protease drugs. *J Pharm Sci* 2000;89(5):664-73.

34. Trentin D, Hall H, Wechsler S, Hubbell JA. Peptide-matrix-mediated gene transfer of an oxygen-insensitive hypoxia-inducible factor-1alpha variant for local induction of angiogenesis. *Proc Natl Acad Sci U S A* 2006;103(8):2506-11.

35. Giannoni P, Hunziker EB. Release kinetics of transforming growth factor-beta1 from fibrin clots. *Biotechnol Bioeng* 2003;83(1):121-3.

36. Garcia Y, Breen A, Burugapalli K, Dockery P, Pandit A. Stereological methods to assess tissue response for tissue-engineered scaffolds. *Biomaterials* 2007;28(2):175-86.

Chapter Three

A Temporal Gene Delivery System Based on Fibrin Microspheres

Contents of this chapter have previously been published:

Kulkarni M., Greiser U, O'Brien T and Pandit A. 'A Temporal Gene Delivery System Based on Fibrin Microspheres.' *Mol Pharm* 2011;8(2):439-46.

3.1 Introduction

In recent years, gene therapy, involving manipulation of genetic make-up either to replace a defective gene or up- or down-regulate the dysregulated genes/molecular pathways has become a common and promising research approach. This surge can be attributed to a number of factors such as better diagnostic tools and advances in molecular biology to identify genetic diseases or diseases with plausible genetic element. However, the translation of gene therapy from laboratory to clinics is stalled due to lack of an ideal gene delivery system with high transfection efficiency, extended but easily controllable gene expression and optimal safety profile. One of the research avenues towards solving this issue, being investigated recently, is to employ complementary delivery systems, such as non-viral carriers and tissue engineering scaffolds in a combinatorial approach[1].

Fibrin is a polymer formed in the body on need basis and degraded in highly controlled manner. Thus, the host has full machinery to degrade fibrin scaffolds in a very systematic manner, highly is desirable in tissue engineering applications. Also, fibrin scaffolds have not been reported to elicit any untoward inflammatory response, abnormal foreign body reaction, tissue necrosis, or fibrosis[2]. Fibrin is highly versatile and can be fabricated in various forms such as simple or composite gel[3-5], sphere-templated scaffolds[6], as gels with extracellular protein coated spheres[7] or as fibrin microspheres[8-11]. Although liposomal systems have been shown to be safer than viral carriers, the factors hindering the success of liposomal approach appear to be instability of the liposome-DNA complex (lipoplex), toxicity of the cationic lipid, and short half-life of the complexed DNA[12]. The use of scaffolds not only provides opportunity, by virtue of their macro- and micro- structure, to manipulate dynamics of liposomal gene delivery, creating controlled extended[13-15] or spatiotemporal release systems[16-19] and/or reservoir systems but also enhances stability of liposomes[20 21] while reducing its toxicity[17 22]. In order to exploit this complementary benefit, a scaffold that has the complimentary benefits of fibrin and lipoplexes was decided to be fabricated.

A fibrin-lipoplex system has previously been described to deliver two reporter genes simultaneously for an extended period of seven days post-surgery[14]. Towards

improvement of this system for therapeutic use, it was hypothesized that a fibrin-in-fibrin system, devised by incorporation of another fibrin system in the form of microspheres within the fibrin gel would not only enhance the DNA carrying capacity of the system but at the same time may open newer avenues for development of concentration gradients or temporal release system as against simultaneous delivery. A number of studies have exploited geometry of microspheres fabricated from either natural or synthetic materials for gene delivery. This spherical/spheroid geometry along with suitable size provides certain advantages such as high surface area and easy fabrication of composite scaffolds. So, to realize the hypothesis, the primary objective of this "proof of concept" study was to fabricate fibrin microspheres capable of encapsulating lipoplexes for gene delivery. This is probably the first study describing use fibrin microspheres for gene delivery. Towards this goal, fibrin microspheres encapsulating lipoplexes were fabricated by modified "preheated oil emulsion" method developed in our laboratory. This study investigates the structural and functional integrity of the DNA to establish that the fabrication procedure doesn't affect the integrity of the DNA. As a step towards development of proposed fibrin-in-fibrin system, the degradation of fibrin microspheres and release of DNA was studied in comparison with fibrin scaffold to fathom the plausibility of spatiotemporal control over the release kinetics from the system. Figure 3.1 is a schematic representation of the contents of this chapter.

3.2 Materials and Methods

3.2.1 Fabrication of Fibrin Microspheres with Lipoplexes

Fibrinogen and thrombin were sourced from Baxter Healthcare, Vienna. Fibrin microspheres (FM) were fabricated by modification of a "preheated oil emulsion" method[8]. Briefly, fibrinogen solution (20 mg/ml) and thrombin solution (4 IU), containing lipoplexes (with 25 µg of pDNA) were mixed. Prior to formation of gel, while it is still in liquid phase, the solution was poured drop-wise into a pre-heated mineral oil at 75^0C and stirred over night at 250 rpm to evaporate the water phase.

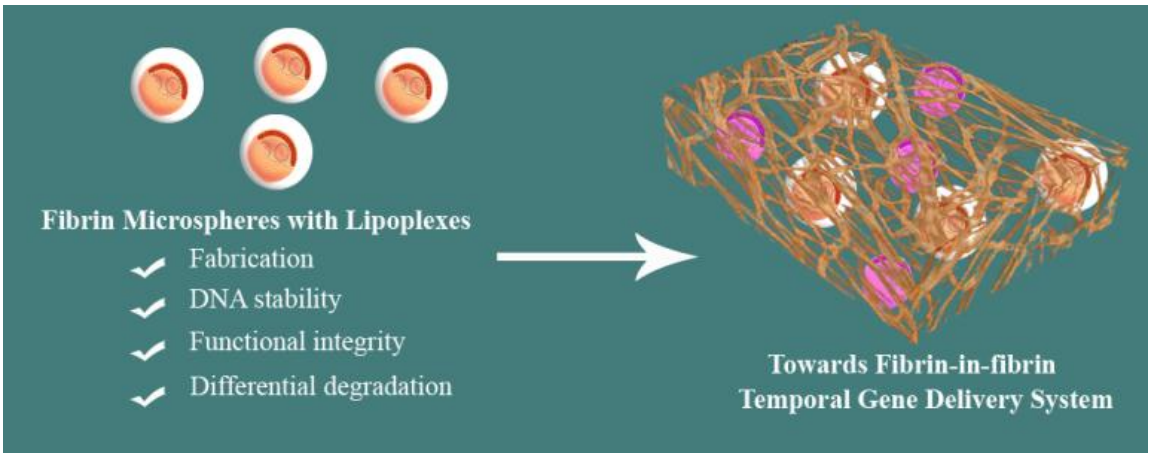

Figure 3.1: Schematic summarizing the research steps taken in the phase II of the project

Two surfactants were used. Tween20 was used in water phase and Spam80 was used in oil phase. After overnight stirring, the oil was decanted. This was done in two phases, first at low speed (1000 rpm) centrifugation and then at high speed (4500 rpm). The FM were washed by ethanol, hexane and then air dried.

3.2.2 Transmission and Scanning Electron Microscopy and Size Analysis

Formation of microspheres was confirmed by transmission electron microscopy (TEM). The FM were resuspended in water and a drop was placed directly on a formvar carbon coated grid (Agar Scientific) and viewed under TEM (Hitachi H7500 transmission electron microscope)**.**In addition, scanning electron microscopy (SEM) was used for surface morphological analysis. The samples were first gold coated and visualized under vacuum using SEM **(**Hitachi S-4700 Scanning Electron Microscope). The mean size of FM was measured by laser light diffraction using zetasizer (Nano ZS, Malvern). The air dried FM were suspended indirectly in water and vortexed gently. Three experimental replicates were used for these measurements. The particle size was expressed as mean diameter (± standard deviation).

3.2.3 Plasmid DNA Labeling and Confocal Microscopy

Plasmid DNA was labeled by Cy™ 5 using *Label* IT® Cy™ 5 Labeling Kit (Mirus Bio, Madison, WI) using manufacturer's instructions. Briefly, plasmid DNA and Cy™ 5 marker were mixed together and incubated at 37^{o}C for 1 hour, with a quick spin after 30 minutes to reduce the effect of evaporation. The labeled plasmid DNA was then extracted by using spin column provided in the kit and stored at -20^{o}C until use. Fibrin microspheres fabricated with the labeled DNA complexes were then studied under confocal microscope (Zeiss LSM 510 Axiovert Inverted Confocal Microscope) to confirm encapsulation of DNA. Fibrin microspheres with labeled DNA complexes were further labeled by FITC and were also studied under confocal microscope (Zeiss LSM 510 Axiovert Inverted confocal microscope).

3.2.4 Stability of DNA

The integrity of plasmid DNA within the FM was assessed by agarose gel electrophoresis. The fibrin microspheres were dissolved in 100 nM human plasmin for

45 minutes and the released lipoplexes were treated with triton-X to get free DNA. Agarose gel electrophoresis was then performed in 0.7% (w/v) agarose gels containing 0.01% SYBR safe for visualization for 30 min at 100 V. 1kb DNA ladder was also run. The resultant gels were visualized under UV transilluminator at wavelength of 365 nm.

3.2.5 *In Vivo* Model

The ability of FM to deliver the gene of interest *in vivo* was investigated qualitatively. Alloxan induced hyperglycemic model of rabbit ear ulcer was utilized for this purpose. Two New Zealand white rabbits (3-3.5 kg) were used in the study. The protocol was approved by the ethics committee of the National University of Ireland, Galway, and the study was conducted under a license granted by the Department of Health and Children, Dublin, Ireland. Rabbits were housed in individual cages with a 12 h light/dark cycle and controlled temperature and humidity. Rabbits were fed a standard chow diet and water ad libitum.

3.2.6 Induction of Hyperglycemia

Rabbits were sedated with subcutaneous injection of 1 ml/kg acepromazine. Hair was shaved off at the back of the ears, and an anesthetic cream (EMLA, AstraZeneca, USA) was rubbed into the back of the ear and left in situ for 20 min. Alloxan (150 mg/kg) (Sigma–Aldrich, Ireland) in 30 ml saline was prepared and administered via an ear vein using a butterfly syringe, at a rate of 1.5 ml/min. Alloxan is known to cause necrosis of pancreatic islets, thereby inducing hyperglycemia[23]. After alloxan treatment, water containing one tablespoon of glucose per liter was given to the rabbits for a 48 h period, to avoid possible hypoglycemia. Blood glucose readings were taken daily, using blood glucose test strips and meter (Accu-chek® test advantage meter, Accu-chek® advantage II strips, Roche Diagnostics, United Kingdom). Food and water intakes were monitored daily. Hyperglycemia was confirmed if blood glucose readings were in the range of 20–28 mmol/l. Insulin treatment was not required to control hyperglycemia in any animals.

3.2.7 Surgical Procedure

Four weeks post-alloxan treatment; rabbits were anesthetized using intramuscular injection of 0.1 ml/kg xylazine and 0.12 ml/kg ketamine. This is half the dose of

anesthesia, as full dose will likely prove fatal under hyperglycemic conditions. Two 6 mm punch biopsy wounds were created in each ear, using sterile disposable 6 mm diameter punch biopsies (Panvet, Ireland), exposing bare cartilage. Each wound was treated with one of two randomized treatment groups: No treatment, fibrin gel containing fibrin microspheres encapsulating lipoplexes with eNOS plasmid DNA. Wounds were covered with polyurethane dressing (Opsite™, Smith and Nephew Ltd) until day 7. At day 7, rabbits were euthanized. At necropsy, ears were surgically removed and cut across the center-line. One half of the ear was fixed in formalin for histological and immunohistochemical analysis, in order that a cross-section of the wound could be analyzed. The other half was stored in RNA *later* at - 80^0C for further analysis.

3.2.8 Histology and Immunohistochemistry

Formalin fixed paraffin embedded sections were cut at 5 mm thickness. Six consecutive sections were saved from the block, as soon as the tissue was reached in the block. This ensured that all sections were saved at the cross-section of the wound. Identification of blood vessels was confirmed by immunohistochemistry with endothelial cell marker CD31 using standard protocol.

Briefly, enzymatic antigen retrieval was carried out at 37^0C using 1X proteinase K (20 mg/ml, Sigma–Aldrich) solution in TE buffer (50 mM Tris Base, 1 mM EDTA, pH 8.0, Sigma–Aldrich). Primary antibody used was monoclonal mouse anti-CD31 (DakoCytomation, Dublin, Ireland) (1:30 in 0.01 M PBS containing 1% BSA, 0.1% cold fish skin gelatin), with an incubation time of 90 min at room temperature. Blocking buffer was added to three slides as negative control. Endogenous peroxidase was blocked with 3% hydrogen peroxide (Sigma–Aldrich). Secondary goat anti-mouse IgG (1:100 in 0.01 M PBS, DakoCytomation, Ireland) was applied for 45 min at room temperature, followed by streptavidin–avidin biotin complex HRP (DakoCytomation, Ireland), and developed using DAB chromagen (Sigma–Aldrich, Ireland).

3.2.9 RNA Isolation and Real Time PCR

For isolating RNA, the wound tissue from treated and control groups was first crushed in pestle and mortar under liquid nitrogen and then homogenized in 1ml of Tri-Reagent per sample. RNA was separated by chloroform and precipitated by ethanol. The samples were then applied to Qiagen RNAeasy column and RNA was extracted according to manufacturer's instructions (Qiagen RNAeasy kit). RNA was collected in RNase free water and the purity and concentration were checked using spectrophotometer (ND-1000 UV-Vis, NanoDrop Technologies, USA). The extracted RNA was reverse-transcribed using ImProm-II™ Reverse Transcription System (Promega) to obtain cDNA. Real time PCR was then carried out using StepOne Plus™ Real-Time PCR System, software version 2.1 (Applied Biosystems). The relative expression of eNOS was normalized to 18S ribosomal RNA as endogenous control and calculated by comparative CT method. Table 3.1 details the specific primer sequences used.

3.2.10 Degradation of Fibrin Microspheres vs. Fibrin Gel

To compare the degradation of FM with fibrin gel, 1 mg of FM were incubated with 2 ml of 0.1 N NaOH for 24 hours at room temperature. The supernatant was collected and subjected to reduced 4-12% gradient SDS-PAGE. Supernatant from fibrin gel under same conditions was used as control. Next, the supernatant from FM in 0.1 N NaOH was discarded and FM were visualized under scanning electron microscope to qualitatively assess the degradation.

3.2.11 *In Vitro* Release Study

Cumulative DNA release from fibrin gel and microspheres was assayed to compare their DNA release profile. For this study, fibrin gel and microspheres containing lipoplexes were incubated with 0.1 N NaOH at 37^0C with continuous shaking. Samples from supernatant collected at 0, ½, 1, 6, 12, 24, and 48 h and stored at -20^0C.

Table 3.1: Primer sequences used in the qPCR

eNOS_forward	5’- CTG AGA GAC CAG CAG AGA TAC CAC -3’
eNOS_reverse	5’- CTG AAG CTC TGG GTC CTG AT -3’
18S_forward	5’- GTA ACC CGT TGA ACC CCA TT -3’
18S_reverse	5’- CCA TCC AAT CGG TAG TAG CG -3’

Equal amounts of fresh 0.1N NaOH were replaced each time the samples were collected. The quantity of DNA in each collected sample was assessed using PicoGreen assay using manufacturer's instructions (Quant-iT™ PicoGreen® dsDNA Reagent, Invitrogen). All the experiments were done in triplicates.

3.3 Results and Discussion

Over a decade ago, fibrin microspheres, termed then as fibrin derived microbeads, were first developed as cell carriers. These fibrin microbeads were shown to be haptotactic to cells such as endothelial cells, smooth muscle cells and fibroblasts and their use in wound healing was investigated[8]. Fibrin microbeads have also been used as cell carriers for a variety of cells such as chondrocytes, periosteal-derived cells, and nucleus pulposus cells[11]. Recently, these microbeads have been extensively utilized for isolation, expansion and differentiation of mesenchymal stem cells [10] [24-27]and investigated in a variety of applications such as bone tissue engineering[28], renal diseases[29]. However, as described earlier, in the present study, for the first time, fibrin microspheres have been fabricated for gene delivery, mainly to investigate their ability to encapsulate and deliver DNA complexes without damage to the structural and functional integrity.

3.3.1 Fabrication of Fibrin Microspheres

For fabricating FM suitable for gene delivery, the preheated oil emulsion method was modified. Previously, in FM fabrication, studies have used a variety of oil phase such as mixture of corn oil and isooctane[8], vegetable oil[9], medium chain triglyceride oil[29] or recently mineral oil[28]. It is preferable to use mineral oil or vegetable oil as continuous phase to encapsulate water soluble drug[30] and in this study DNA complexes. Mineral oil is commonly used as a preferred oil of choice in fabrication of a variety of microspheres[31-34], hence in this study, mineral oil was chosen as oil phase. To achieve more stable emulsion, two surfactants, one for each phase, were utilized. The dynamics of surfactants at the water-oil interface directly influence the stability of emulsion, since they affect the fundamental processes occurring during emulsification, namely droplet rupture and droplet recoalescence[35]. And since the fibrin microspheres were being

fabricated with plasmid DNA complexes, the stability of emulsion was of utmost importance in order to protect the DNA. So, two surfactants were used simultaneously, namely Tween20 in water phase and Spam80 in oil phase. Formation of microspheres was confirmed TEM (Figure 3.2 A) and SEM (Figure 3.2 B). The size analysis revealed two peaks; ~750nm and ~1000nm (Figure 3.2 C). The fibrin microspheres, used as cell carriers, are generally 50 – 200 μm in size. It was notable that the microspheres obtained by the modified method were much smaller. This smaller size provides with a number of advantages such as higher surface area, ease of uniform or gradient distribution as required within the scaffold.

3.3.2 Encapsulation and Stability of DNA

Another challenge was to encapsulate the DNA complexes within the microspheres without causing any degradation of the plasmid DNA. To confirm encapsulation, labeled DNA complexes were used as described in the methods section. The confocal microscopy (Figure 3.3 A) showed fluorescent microspheres suggesting that the labeled DNA complexes were encapsulated within. To further confirm that the fluorescence seen was indeed from the microspheres, we labeled the microspheres with FITC. The green signal from microspheres and the red signal from DNA complexes co-localized to give yellow signal (Figure 3.3 B). This confirmed the encapsulation of the DNA complexes within the microspheres.

In view of the high temperature at which the fabrication procedure was carried out, the stability and integrity of plasmid DNA was assessed by performing gel electrophoresis of the DNA released from fibrin microspheres. The distinct bands seen in lane with DNA from FM were similar to those seen in lane with control plasmid DNA (Figure 3.4) suggesting that the integrity of the plasmid DNA is maintained. We have previously shown that there exists a biomolecular interaction between fibrinogen and lipofectin[14]. It was presumed that on account of this interaction, the plasmid DNA complexes get physically covered by the fibrin (or fibrinogen) even before formation of microspheres and thus remain protected from undue exposure to high temperature and hence from degradation.

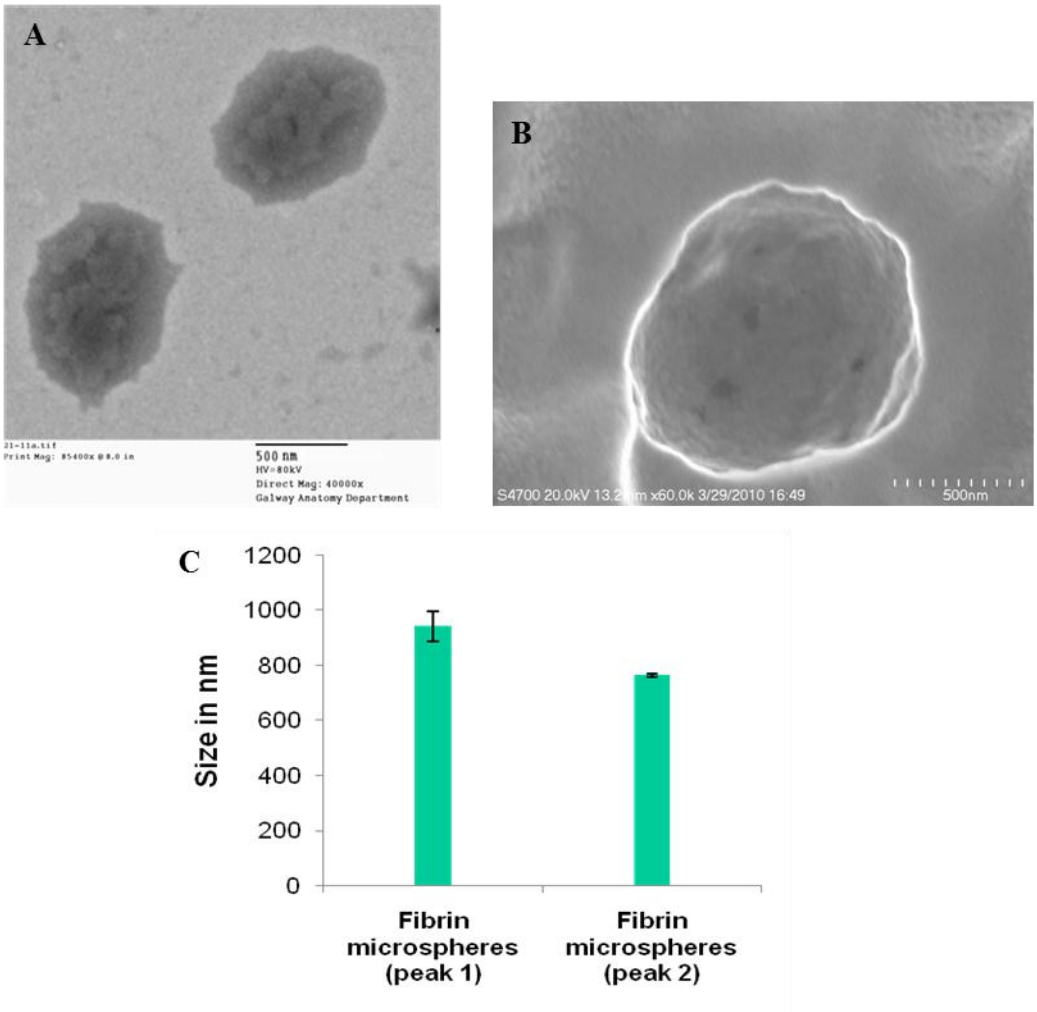

Figure 3.2: Formation of fibrin microspheres. (A) TEM and (B) SEM micrographs showing fibrin microspheres. (C) Graph showing the results of size analysis (n = 3, error bars represent standard deviation). Two peak sizes ~700 nm and ~1000 nm were observed.

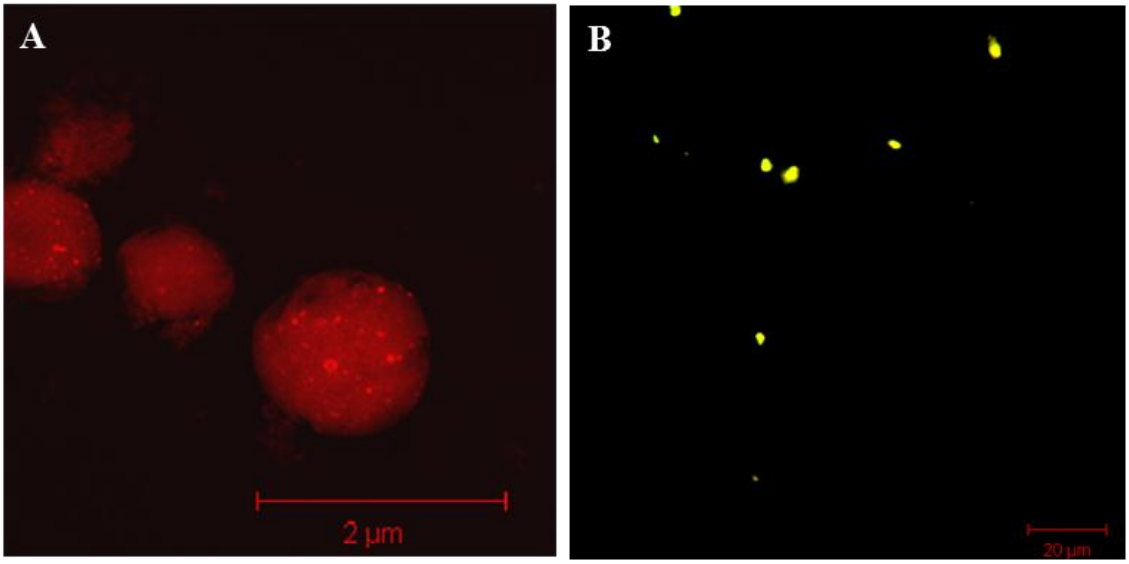

Figure 3.3: Confocal microscopy of (A) unlabeled and (B) FITC labeled fibrin microspheres encapsulating CY5 labeled DNA complexes. Fluorescence from the fibrin microspheres confirms encapsulation of DNA complexes.

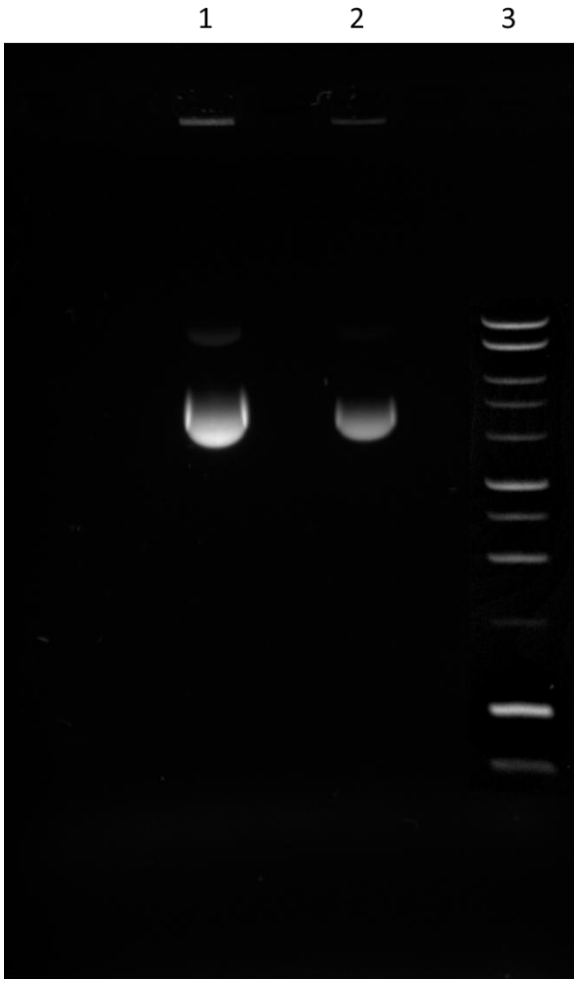

Lane 1: plasmid DNA released from freshly formed lipoplexes;
Lane 2: plasmid DNA released from fibrin microspheres;
Lane 3: DNA ladder (1 kb);
Other lanes were empty.

Figure 3.4: Gel electrophoresis of DNA eluted from the fibrin microspheres. The presence of distinct band similar to control DNA confirms the integrity of the plasmid DNA within the fibrin microspheres.

3.3.3 Functional Integrity in the *In Vivo* Model

With an aim to investigate the efficacy of fibrin microspheres for gene delivery and establish functional integrity of plasmid DNA, a pilot *in vivo* study was performed. The results of real time PCR (Figure 3.5) suggest that at seven days post-delivery the levels of eNOS mRNA is 28 folds higher than in the control group. It is known that eNOS knockouts have defects in angiogenesis[36] and studies have previously shown that eNOS delivery enhances angiogenesis[36-38]. Therefore, in order to assess the functional integrity of eNOS delivered via FM, it was decided to investigate the effect on angiogenesis in an alloxan induced compromised wound model of rabbit ear ulcer, which has been shown to have defects in angiogenesis[39]. The FFPE wound tissues from eNOS treated and control groups were analyzed histologically by H & E staining. Wounds treated with eNOS via FM showed a number of blood vessel-like structures when compared to control group (Figure 3.6). To confirm that these structures were indeed blood vessels, immunohistochemistry was performed for CD31, which is a specific endothelial cell marker. The brown staining seen in eNOS treated wounds (Figure 3.6 D & E) suggests that these cells are CD31 positive, confirming them to be endothelial cells forming blood vessels after eNOS delivery via fibrin microspheres.

3.3.4 A Step towards Fibrin-in-fibrin System

Having investigated the feasibility of FM for gene delivery, this study will form the basis of the overall idea of exploiting the potential of FM to extend the capacity of fibrin scaffold to deliver genes. The amount of DNA that can be carried in a fibrin scaffold is limited by the dilution factor added by liquid phase of the lipoplexes. FM carrying lipoplexes can be embedded within fibrin scaffold, allowing higher load of DNA to be carried in the system without adding dilution factor. This fibrin-in-fibrin system can provide at least one more very crucial advantage by virtue of the differential degradation of its components. To test this hypothesis, FM and fibrin scaffold were degraded in 0.1 N NaOH for 24 hours. Scanning electron microscopy of FM after 24 hr incubation with 0.1 N NaOH showed FM were only partially degraded (Figure 3.7). The densitometry analysis of SDS-PAGE (Figure 3.8) from the supernatant of partially degraded FM showed higher number of peaks than fibrin gel.

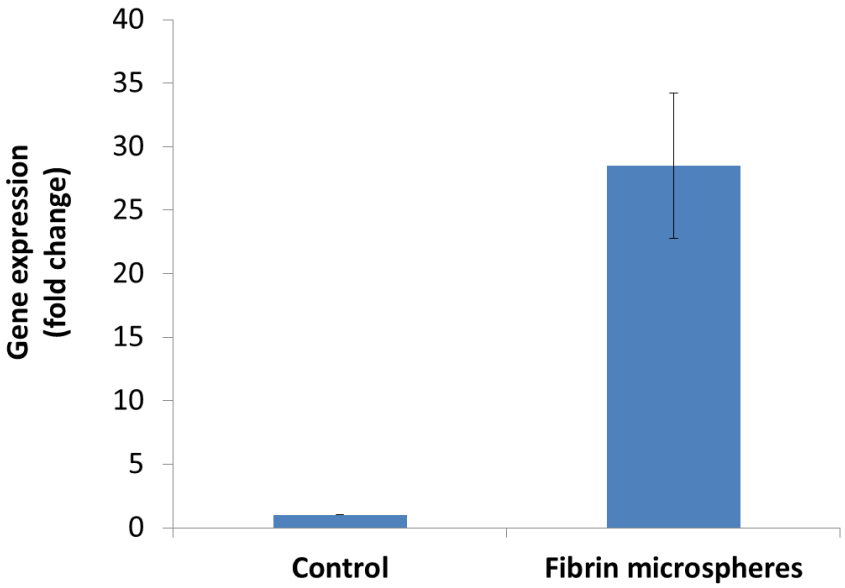

Figure 3.5: Real time PCR showing ~28 fold increase in eNOS mRNA following treatment with fibrin microspheres carrying eNOS gene as compared to control.

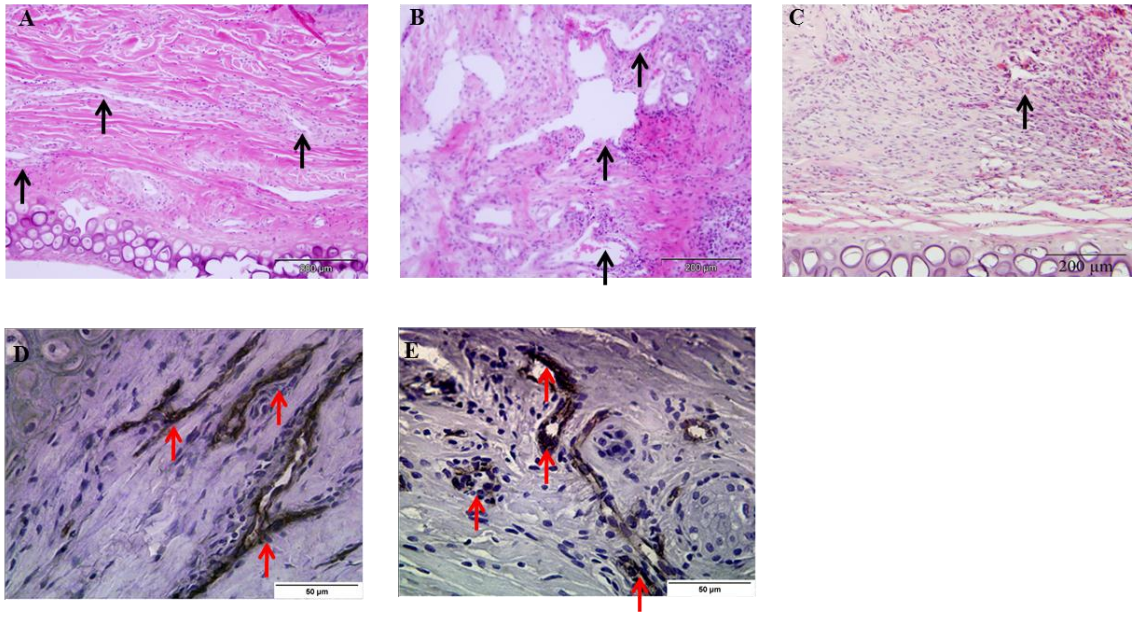

Figure 3.6: Functional integrity of eNOS, as observed by angiogenesis in response of eNOS delivered via fibrin microspheres. A number of blood vessel like structures seen in wounds treated with fibrin microspheres carrying eNOS (A, B) while only modest angiogenesis seen in control wounds (C) as shown by black arrows. CD31 immunohistochemistry (D & E) confirmed that these structures indeed endothelial cells. CD31 positive cells stained brown as indicated by red arrows.

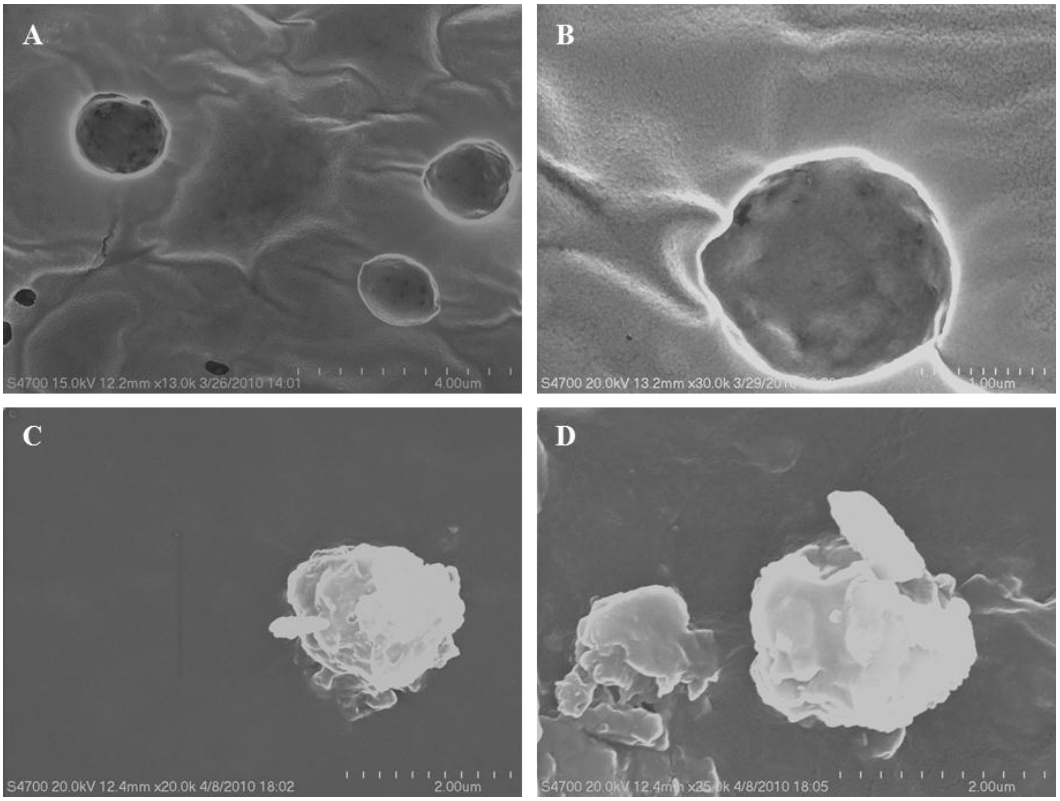

Figure 3.7: SEM micrographs of fibrin microspheres in water (A & B) and in 0.1 N NaOH for 24 hours (C & D). Partially degraded microspheres can be seen (C & D) after incubation with 0.1 N NaOH for 24 hours.

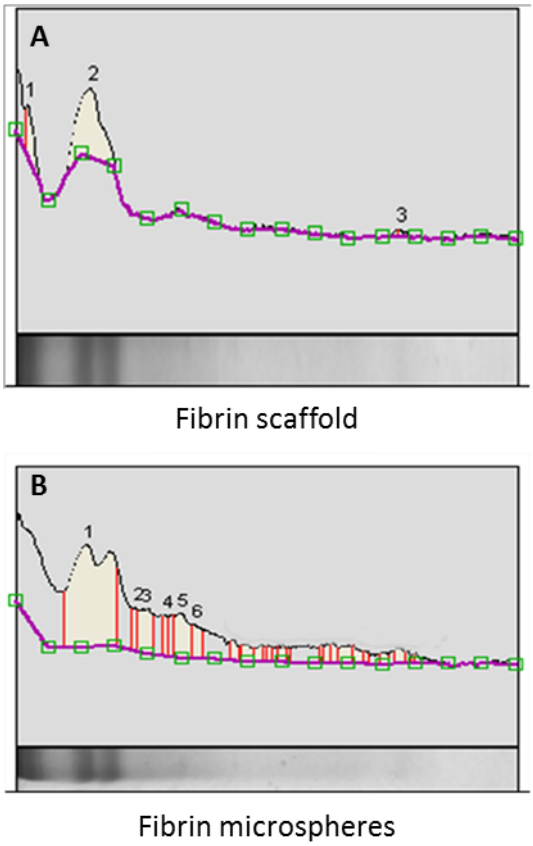

Figure 3.8: Densitometry curves from the SDS PAGE performed on the supernatant from (A) fibrin scaffold and (B) fibrin microspheres after 24 hours of incubation in 0.1 N NaOH solution at room temperature. High degree of cross-linking in fibrin microspheres is evident by the presence of high number of peaks representing high and low molecular weight fractions.

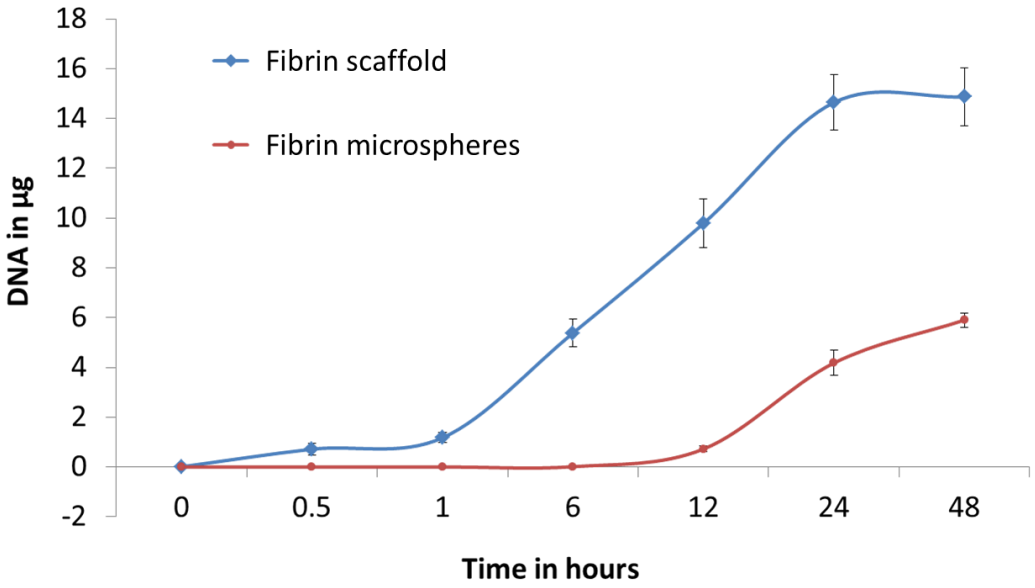

Figure 3.9: *In vitro* release of DNA from fibrin scaffold and fibrin microspheres. Significantly lower DNA released from fibrin microspheres from 30 min to 48 h suggests possibility of using fibrin microspheres embedded in fibrin scaffold as a temporal release system. Statistical significance was tested using t test ($p < 0.05$, $n = 3$).

Generally, in the process of normal clotting, fibrin loses α and γ bands and also α-α multimers and only show γ-γ dimers[8] whereas the presence of multiple peaks of both high and low molecular weight fragments in the FM lane suggests that FM has more cross-links than fibrin scaffold. A previous study has observed similar results[8]. It is believed that this high cross linking accounts for the slower degradation of FM. An *in vitro* release study comparing the DNA release profiles of fibrin scaffold and FM was performed. The quantification of released DNA (Figure 3.9) suggested that indeed fibrin scaffold and FM had different the release profiles. After 30 min of incubation, fibrin scaffold showed almost linear release profile of DNA and by 24 h almost all DNA was released from fibrin scaffold. Whereas DNA released from FM was significantly lower at all data points from 30 min onwards. Moreover, it is thought that the release from FM will be even slower when embedded in fibrin scaffold. Thus, potentially the fibrin-in-fibrin system can be utilized as simple temporal release system where DNA complexes from fibrin scaffold will be released first followed by temporal release of DNA complexes from FM.

Thus, in conclusion, fibrin microspheres of around one micron size can be fabricated by modified preheated oil emulsion method. This study showed that fibrin microspheres are capable of encapsulating DNA complexes without any degradation of DNA. It can also be concluded that these microspheres are able to deliver genes *in vivo* up to 7 days with the functional integrity of genes maintained. The differential degradation of fibrin microspheres compared to fibrin gel can be exploited to design the fibrin-in-fibrin system which can potentially be used as temporal release system.

3.4 References

1. Kulkarni M, Greiser U, O'Brien T, Pandit A. Liposomal gene delivery mediated by tissue-engineered scaffolds. *Trends Biotechnol* 2010;28(1):28-36.
2. Breen A, Strappe P, Kumar A, O'Brien T, Pandit A. Optimization of a fibrin scaffold for sustained release of an adenoviral gene vector. *J Biomed Mater Res A* 2006;78(4):702-8.
3. Wang SS, Yang MC, Chung TW. Liposomes/chitosan scaffold/human fibrin gel composite systems for delivering hydrophilic drugs--release behaviors of tirofiban in vitro. *Drug Deliv* 2008;15(3):149-57.
4. Zhao H, Ma L, Gong Y, Gao C, Shen J. A polylactide/fibrin gel composite scaffold for cartilage tissue engineering: fabrication and an in vitro evaluation. *J Mater Sci Mater Med* 2009;20(1):135-43.
5. Munirah S, Kim SH, Ruszymah BH, Khang G. The use of fibrin and poly(lactic-co-glycolic acid) hybrid scaffold for articular cartilage tissue engineering: an in vivo analysis. *Eur Cell Mater* 2008;15:41-52.
6. Saul JM, Linnes MP, Ratner BD, Giachelli CM, Pun SH. Delivery of non-viral gene carriers from sphere-templated fibrin scaffolds for sustained transgene expression. *Biomaterials* 2007;28(31):4705-16.
7. Nakatsu MN, Davis J, Hughes CC. Optimized fibrin gel bead assay for the study of angiogenesis. *J Vis Exp* 2007(3):186.
8. Gorodetsky R, Clark RA, An J, Gailit J, Levdansky L, Vexler A, Berman E, Marx G. Fibrin microbeads (FMB) as biodegradable carriers for culturing cells and for accelerating wound healing. *J Invest Dermatol* 1999;112(6):866-72.
9. Gurevich O, Vexler A, Marx G, Prigozhina T, Levdansky L, Slavin S, Shimeliovich I, Gorodetsky R. Fibrin microbeads for isolating and growing bone marrow-derived progenitor cells capable of forming bone tissue. *Tissue Eng* 2002;8(4):661-72.
10. Gorodetsky R. The use of fibrin based matrices and fibrin microbeads (FMB) for cell based tissue regeneration. *Expert Opin Biol Ther* 2008;8(12):1831-46.

11. Perka C, Arnold U, Spitzer RS, Lindenhayn K. The use of fibrin beads for tissue engineering and subsequential transplantation. *Tissue Eng* 2001;7(3):359-61.
12. Leong KW, Mao HQ, Truong-Le VL, Roy K, Walsh SM, August JT. DNA-polycation nanospheres as non-viral gene delivery vehicles. *J Control Release* 1998;53(1-3):183-93.
13. Capito RM, Spector M. Collagen scaffolds for nonviral IGF-1 gene delivery in articular cartilage tissue engineering. *Gene Ther* 2007;14(9):721-32.
14. Kulkarni M, Breen A, Greiser U, O'Brien T, Pandit A. Fibrin-lipoplex system for controlled topical delivery of multiple genes. *Biomacromolecules* 2009;10(6):1650-4.
15. Whittlesey KJ, Shea LD. Nerve growth factor expression by PLG-mediated lipofection. *Biomaterials* 2006;27(11):2477-86.
16. Wu G, Mikhailovsky A, Khant HA, Fu C, Chiu W, Zasadzinski JA. Remotely triggered liposome release by near-infrared light absorption via hollow gold nanoshells. *J Am Chem Soc* 2008;130(26):8175-7.
17. Lei P, Padmashali RM, Andreadis ST. Cell-controlled and spatially arrayed gene delivery from fibrin hydrogels. *Biomaterials* 2009;30(22):3790-9.
18. Houchin-Ray T, Whittlesey KJ, Shea LD. Spatially patterned gene delivery for localized neuron survival and neurite extension. *Mol Ther* 2007;15(4):705-12.
19. Houchin-Ray T, Huang A, West ER, Zelivyanskaya M, Shea LD. Spatially patterned gene expression for guided neurite extension. *J Neurosci Res* 2009;87(4):844-56.
20. Meyenburg S, Lilie H, Panzner S, Rudolph R. Fibrin encapsulated liposomes as protein delivery system. Studies on the in vitro release behavior. *J Control Release* 2000;69(1):159-68.
21. De Laporte L, Yan AL, Shea LD. Local gene delivery from ECM-coated poly(lactide-co-glycolide) multiple channel bridges after spinal cord injury. *Biomaterials* 2009;30(12):2361-8.

22. Winn SR, Chen JC, Gong X, Bartholomew SV, Shreenivas S, Ozaki W. Non-viral-mediated gene therapy approaches for bone repair. *Orthod Craniofac Res* 2005;8(3):183-90.

23. Lenzen S, Panten U. Alloxan: history and mechanism of action. *Diabetologia* 1988;31(6):337-42.

24. Kassis I, Zangi L, Rivkin R, Levdansky L, Samuel S, Marx G, Gorodetsky R. Isolation of mesenchymal stem cells from G-CSF-mobilized human peripheral blood using fibrin microbeads. *Bone Marrow Transplant* 2006;37(10):967-76.

25. Zangi L, Rivkin R, Kassis I, Levdansky L, Marx G, Gorodetsky R. High-yield isolation, expansion, and differentiation of rat bone marrow-derived mesenchymal stem cells with fibrin microbeads. *Tissue Eng* 2006;12(8):2343-54.

26. Rivkin R, Ben-Ari A, Kassis I, Zangi L, Gaberman E, Levdansky L, Marx G, Gorodetsky R. High-yield isolation, expansion, and differentiation of murine bone marrow-derived mesenchymal stem cells using fibrin microbeads (FMB). *Cloning Stem Cells* 2007;9(2):157-75.

27. Shainer R, Gaberman E, Levdansky L, Gorodetsky R. Efficient isolation and chondrogenic differentiation of adult mesenchymal stem cells with fibrin microbeads and micronized collagen sponges. *Regen Med* 2010;5(2):255-65.

28. Ben-Ari A, Rivkin R, Frishman M, Gaberman E, Levdansky L, Gorodetsky R. Isolation and implantation of bone marrow-derived mesenchymal stem cells with fibrin micro beads to repair a critical-size bone defect in mice. *Tissue Eng Part A* 2009;15(9):2537-46.

29. Shimony N, Gorodetsky R, Marx G, Gal D, Rivkin R, Ben-Ari A, Landsman A, Haviv YS. Fibrin microbeads (FMB) as a 3D platform for kidney gene and cell therapy. *Kidney Int* 2006;69(3):625-33.

30. Zinutti C, Kedzierewicz F, Hoffman M, Maincent P. Preparation and characterization of ethylcellulose microspheres containing 5-fluorouracil. *J Microencapsul* 1994;11(5):555-63.

31. Sanghvi SP, Nairn JG. A method to control particle size of cellulose acetate trimellitate microspheres. *J Microencapsul* 1993;10(2):181-94.

32. Fundueanu G, Constantin M, Stanciu C, Theodoridis G, Ascenzi P. pH- and temperature-sensitive polymeric microspheres for drug delivery: the dissolution of copolymers modulates drug release. *J Mater Sci Mater Med* 2009;20(12):2465-75.

33. Esposito E, Menegatti E, Cortesi R. Hyaluronan-based microspheres as tools for drug delivery: a comparative study. *Int J Pharm* 2005;288(1):35-49.

34. Eroglu M, Kursaklioglu H, Misirli Y, Iyisoy A, Acar A, Isin Dogan A, Denkbas EB. Chitosan-coated alginate microspheres for embolization and/or chemoembolization: in vivo studies. *J Microencapsul* 2006;23(4):367-76.

35. Baret JC, Kleinschmidt F, El Harrak A, Griffiths AD. Kinetic aspects of emulsion stabilization by surfactants: a microfluidic analysis. *Langmuir* 2009;25(11):6088-93.

36. Yu J, deMuinck ED, Zhuang Z, Drinane M, Kauser K, Rubanyi GM, Qian HS, Murata T, Escalante B, Sessa WC. Endothelial nitric oxide synthase is critical for ischemic remodeling, mural cell recruitment, and blood flow reserve. *Proc Natl Acad Sci U S A* 2005;102(31):10999-1004.

37. Namba T, Koike H, Murakami K, Aoki M, Makino H, Hashiya N, Ogihara T, Kaneda Y, Kohno M, Morishita R. Angiogenesis induced by endothelial nitric oxide synthase gene through vascular endothelial growth factor expression in a rat hindlimb ischemia model. *Circulation* 2003;108(18):2250-7.

38. Smith RS, Jr., Lin KF, Agata J, Chao L, Chao J. Human endothelial nitric oxide synthase gene delivery promotes angiogenesis in a rat model of hindlimb ischemia. *Arterioscler Thromb Vasc Biol* 2002;22(8):1279-85.

39. Breen A, Mc Redmond G, Dockery P, O'Brien T, Pandit A. Assessment of wound healing in the alloxan-induced diabetic rabbit ear model. *J Invest Surg* 2008;21(5):261-9.

Chapter Four

Assessment of Differential Gene Regulation in Keratinocytes during Compromised Wound Healing

Contents of this chapter are currently under preparation for manuscript submission:

Kulkarni M., O'Loughlin A., Vazquez R., Mashayekhi K., Greiser U., O'Toole E., O'Brien T., Malagon M. and Pandit A. 'Towards Developing a Pro-angiogenic and Secretory Control Therapy for Compromised Wound Healing.'

4.1 Introduction

Hyperglycemia, the defining biochemical phenomenon of diabetes mellitus, predisposes the patients to chronic complications[1] in multiple organs including skin. The dermatological complications are those least studied[2], especially at molecular level. Such studies are deemed necessary due to the fact that, in healthy skin wound healing, a highly regulated series of changes in gene expression, which trigger events leading to tissue repair, are orchestrated during the overlapping phases of inflammation, proliferation and remodeling. Response to epidermal injury is essentially a homeostatic one designed to rapidly seal the wound site[3]. In the epithelial cells, the orderly events of migration and proliferation occur to re-epithelialize the wound[4-6]. The process of migration begins with marked phenotypic changes in the epidermal cells such as retraction of intracellular tonofilaments[5]. Adherens junctions are then severed, followed by hyperproliferative response and cell migration[7]. There is redistribution of the actin cytoskeleton leading to formation of lamellipodia[8]. The dissolution of hemidesmosomal junctions between epidermal and dermal cells allows the lateral movement of epidermal cells[5]. The leading edge keratinocytes begin to secrete laminin-5 and show altered expression of integrins to which laminin-5 ligates to mediate migration[9]. Integrin expression also allows interaction with the matrix proteins such as fibronectin which helps migration. The proteolysis of extracellular matrix is necessary for the migration of keratinocytes[10]. This migration of keratinocytes occurs through the line of dissection between fibrin clot on top and collagenous dermis underneath. This process is facilitated by another highly controlled process of induction and expression of MMPs and their inhibitors[11-13].

Thus, reepithelialization which involves proliferation and migration of keratinocytes is a very complex yet crucial phase of wound healing. To investigate this phase in keratinocytes both at gross and molecular level when exposed to high glucose levels, an *in vitro* model of multiple scratch wounds was designed. The effect of hyperglycemia on keratinocytes was studied in terms of their capacity to heal scratch wounds and differential regulation of gene expression compared to wound healing in normal glucose conditions, through microarray analysis. The results of microarray are discussed, with

particular attention to the identified potential target gene which holds promise of therapeutic benefit.

4.2 Materials and Methods

4.2.1 Cell Culture

Normal human epidermal keratinocytes (NHEK) were purchased from Promocell. The cells were cultured in serum free, low calcium nutrient medium, supplemented by growth factors (Keratinocyte growth medium, Promocell) at normal (6 mM) and high (25 mM) glucose level.

4.2.2 Cell Proliferation Assay

Cell Proliferation ELISA BrdU (Colorimetric) assay was performed according to the manufacturer's instruction (Roche). Briefly, human keratinocytes grown in normal and high glucose conditions were plated in 96-well microplates in triplicates at density of 2000 cells/well and grown for 24 hrs. Then, BrdU labeling solution was added to each well and incubated at 37^0C and 5% CO_2 for 2 hours. The culture medium was removed and the cells denatured, and the anti-BrdU-POD added. This binds to the BrdU incorporated into cellular DNA. The level of incorporation is detected by means of a colorimetric substrate reaction. Quantification of the bound anti-BrdU-POD was accomplished by adding 100 µl TMB to each well and a further 20 minute incubation time at room temperature. 25 µl 0.1M H_2SO_4 was then added, incubated for 1 minute and shaken at 300 rpm to stop the reaction. The Plate was analyzed using the Wallac Victor Fluorescent Plate Reader (450-550 nm) protocol and measured absorbance for 2 minutes at room temperature.

4.2.3 *In Vitro* Scratch Wound Model

NHEK were plated on 60 mm cell culture dishes at density of 10^5 cells/dish and grown to confluence in keratinocyte growth medium 2 (Promocell) either with high glucose (25mM) or normal glucose (6.5mM) for 7 days. Then, multiple scratch wounds (4 scratch wounds per dish each passing through the center of dish and at an angle of 45 degrees) were created using 200 µl pipette tips on the confluent monolayer of cells. The cells were allowed to heal the scratch wounds for 36 hours. All the experiments were

conducted in triplicate. Five predetermined fields of vision were photographed using a digital camera and the average distance between the edges of the scratch wound was calculated using image analysis software (Image Pro Plus 7.0, Media Cybernetics). The percentage recovery of scratch wounds was then quantified. The normoglycemic cells were seen to heal the wounds significantly better than the hyperglycemic cells. At this stage, RNA was isolated from both types of cells and also from non-wounded cells in both conditions.

4.2.4 Microarray Study

For isolation of RNA, cells were homogenized by Trizol and then phase separated in chloroform. RNA was isolated using RNeasy® Micro Kit (Qiagen), following the manufacturer's protocol. The quantity of RNA isolated was checked spectrophotometrically using a NanoDrop. The quality was checked using Agilent RNA 6000 Nano Chips and Agilent 2100 Bioanalyser. Microarrays were then performed on three biological replicates using GeneChip Human Genome U133 Plus 2.0 Array (Affymetrix) at Karolinska Biomic Center, Stockholm. The data analysis was performed using GeneSpring GX software (Agilent). For validating the microarray data, real time PCR was performed. The isolated RNA was first reverse transcribed using ImProm-II™ Reverse Transcription System (Promega). The cDNA thus obtained was then used for real time PCR reaction (ABI StepOnePlus™ Real-Time PCR System, software v2.1) with specific designed primers and Fast SYBR® Green Master Mix (Applied Biosystems), under standard conditions.

4.3 Results

4.3.1 Keratinocytes in High Glucose Condition

The effect of hyperglycemia on the morphology, proliferation and migration of cultured keratinocytes was investigated. The morphology of the keratinocytes was seen to be altered when the cells were in culture at low density (Figure 4.1 A). The cells were wider and more spread out. This morphological change was transient and was not apparent on confluence. The proliferation also seemed to be affected as seen by the trends but no statistical difference was seen (Figure 4.1 B).

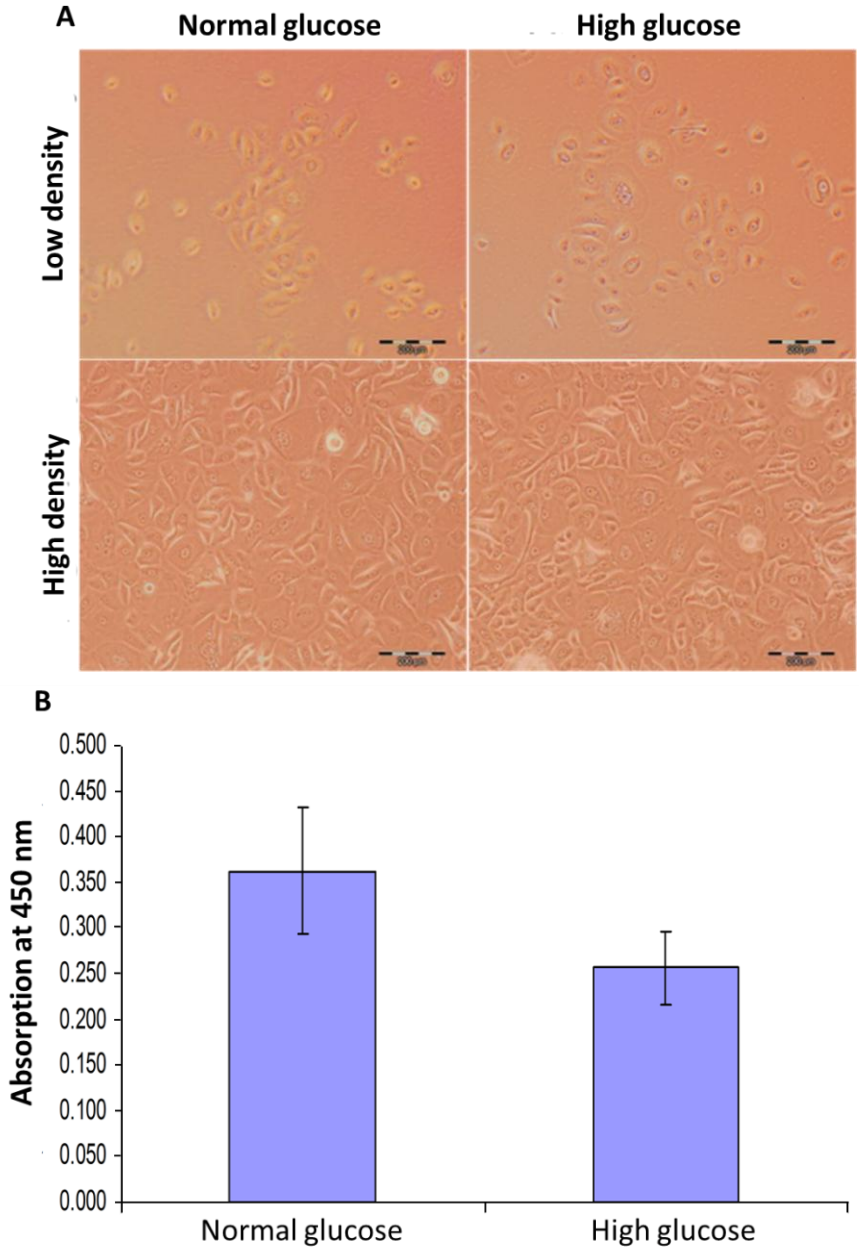

Figure 4.1: Effect of hyperglycemia on morphology and proliferation of primary human keratinocytes. Primary human keratinocytes were grown in normal glucose (6.5 mM) and high glucose (25 mM) conditions for 7 days. (A) The morphology of the keratinocytes was affected at low density. This effect was not apparent at high density. (B) BrdU assay results showed trends towards efficient proliferation of keratinocytes in normal glucose than high glucose; although no statistical difference was observed (n=3).

4.3.2 In vitro Scratch Wound

The migration of keratinocytes was assessed by the *in vitro* scratch assay. The percentage recovery of the scratched wound was quantified using Image-Pro software. The cells grown in high glucose showed poor mobility with only 16% of the scratch area recovered as compared to 68% recovery in case of cells grown under normal glucose conditions (Figure 4.2).

Keratinocytes grown under high glucose conditions were compromised in their ability to heal the scratch wound. It is known that re-epithelialization is delayed in diabetes. Studies have shown that diabetic keratinocytes show reduced motility[14], probably as a result of sequential suppression of p-Stat-1 and α2β1integrin mediated MMP-1 pathways[2] and reduced expression of LM-3A32 (uncleaved, precursor of the a3 chain of laminin 5), a key molecule present on migrating epithelium[9]. Some studies have also shown imbalance between proliferation and differentiation of diabetic keratinocytes[1 9]. So, in order to further understand the pathology at the molecular level, a microarray analysis was performed. Towards this goal, RNA was isolated from wounded keratinocytes grown under both high and normal glucose conditions in three separate experiments. Non-wounded cells grown under normal and high glucose conditions acted as controls.

4.3.3 Gene Expression Analysis

Microarray data analysis revealed that a number of genes and molecular signaling pathways involved in wound healing were altered under high glucose wounded conditions. Figure 4.3 shows an example of heat map of one of the comparisons made in the study. Figure 4.4 is an attempt to represent the number of genes found altered in the microarray analysis. With fold change of more than or equal to five, 1035 genes were upregulated in normal wounded keratinocytes when compared to normal non-wounded keratinocytes while 623 genes were upregulated in hyperglycemic wounded keratinocytes when compared to hyperglycemic non-wounded keratinocytes. Only 9 of these genes were common. This gives an insight to the extent to which wound healing in high glucose differs from that in normal glucose at molecular level.

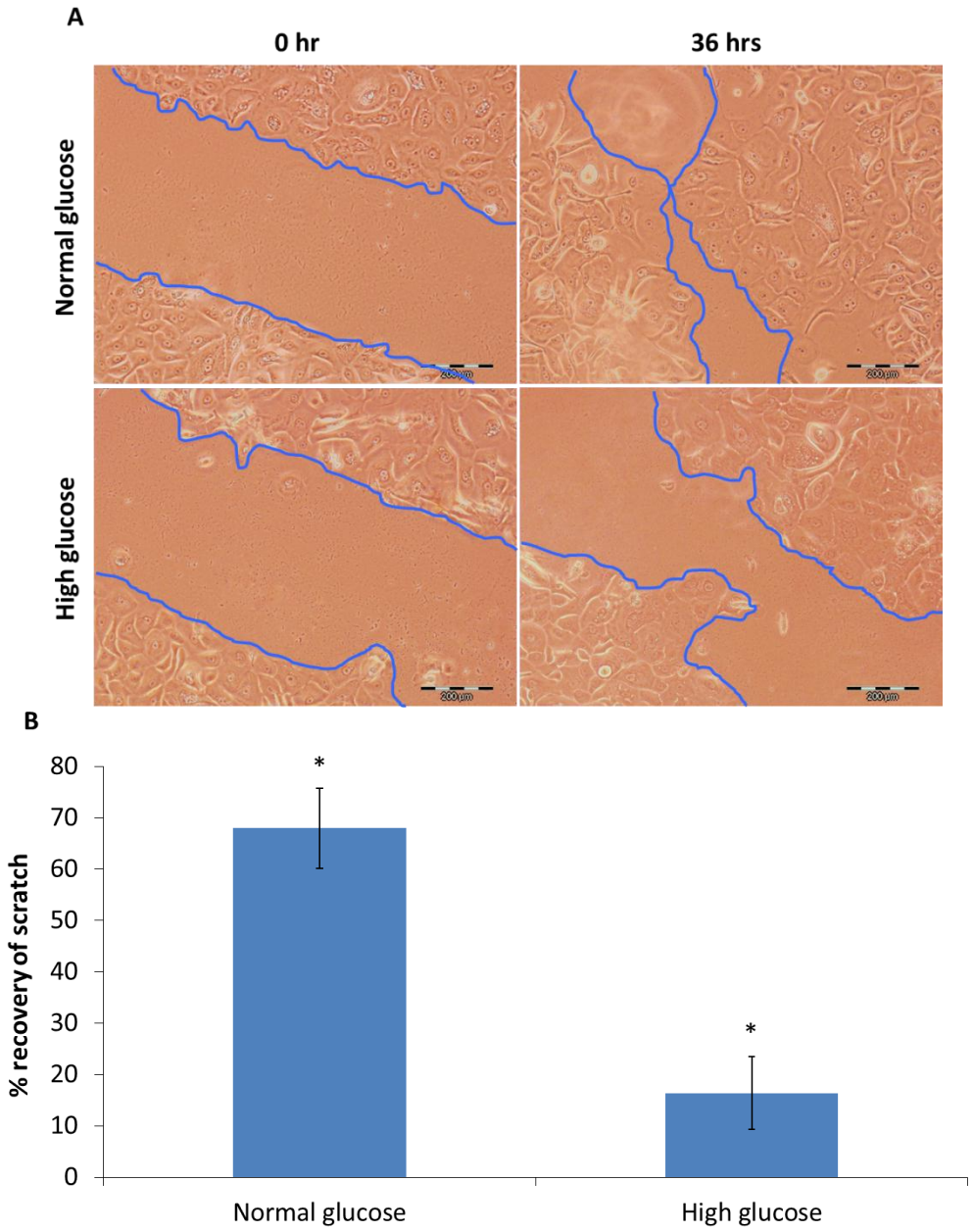

Figure 4.2: *In vitro* scratch assay. Multiple scratch wounds at predefined positions were created on the confluent monolayer of primary human keratinocytes grown under normal and high glucose concentrations and allowed to heal for 36 hours (A). The blue lines represent the edges of the scratch wound. (B) The percentage recovery of the scratch wound was quantified. The cells grown in normal glucose healed the scratch wound significantly better than the cells grown under high glucose conditions. * indicates statistical significance by one-way ANOVA ($P < 0.05$, $n = 3$).

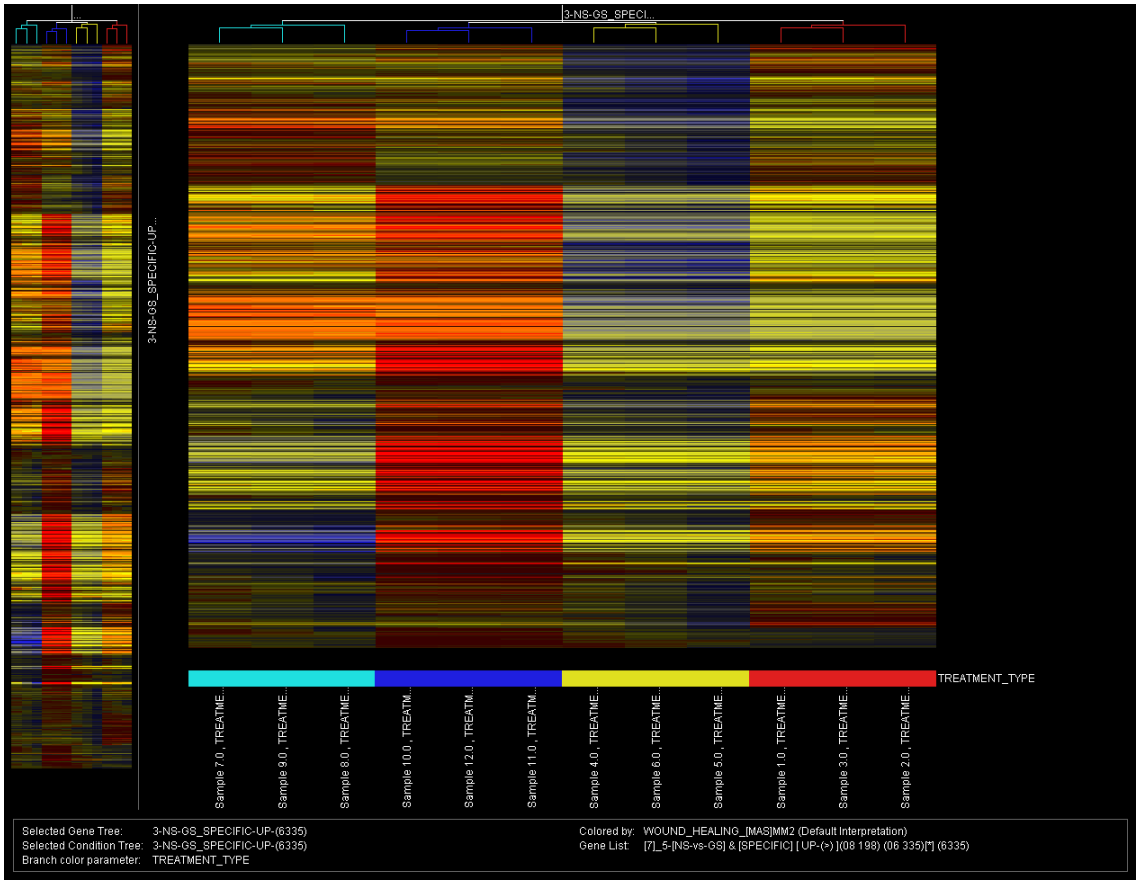

Figure 4.3: An example of a heat map of all twelve samples in the microarray study, with the gene tree relating to the specific genes down regulated in the hyperglycemic wounded keratinocytes compared with wounded normoglycemic keratinocytes (NS = Wounded keratinocytes under normal glucose conditions; GS = Wounded keratinocytes under high glucose conditions).

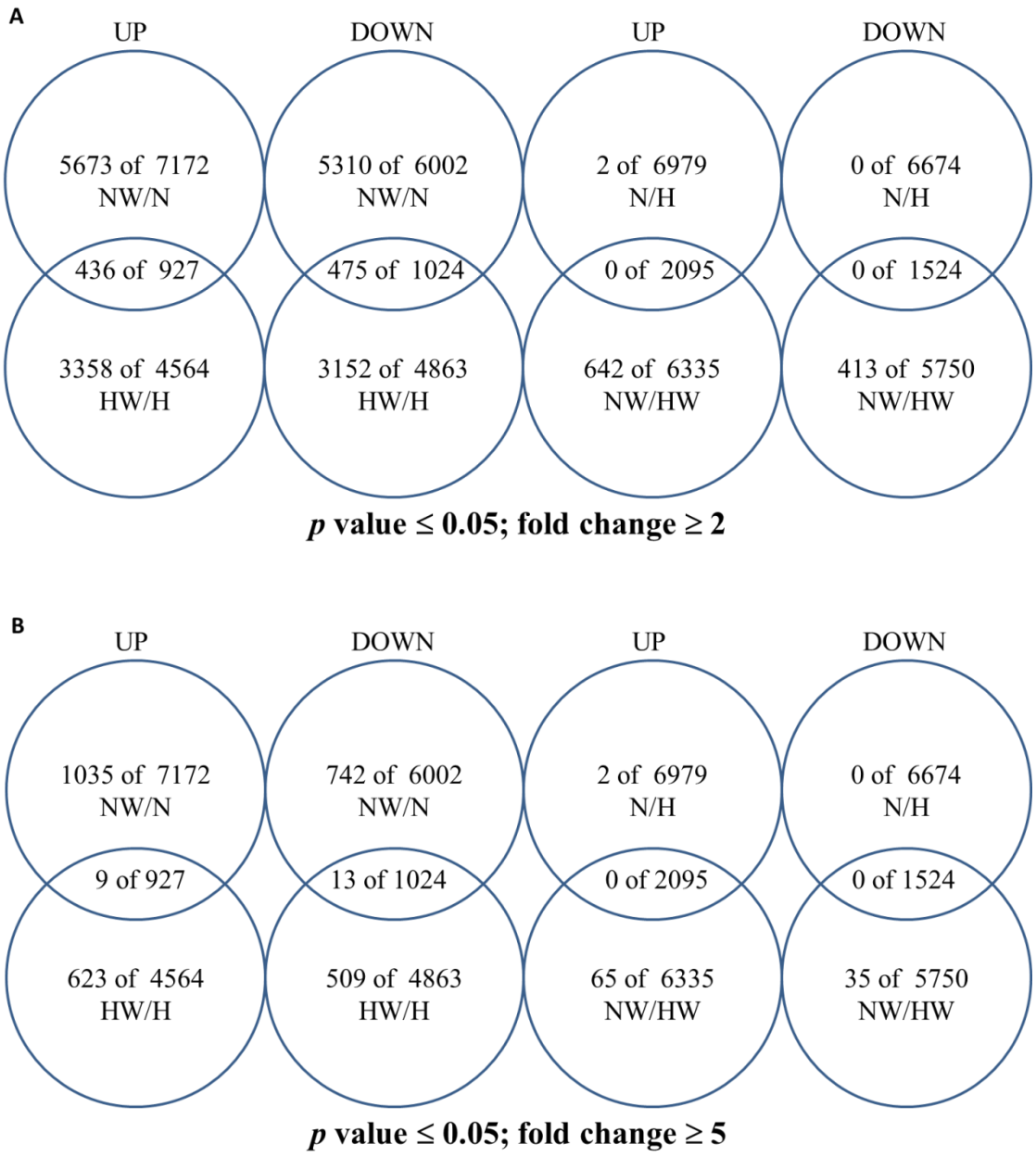

Figure 4.4: Overview of number of genes altered in the different comparisons studied in the microarray analysis with fold change cut off being (A) 2 and (B) 5 and p value ≤ 0.05.

For further analysis, genes up and downregulated in normal wounded keratinocytes compared to hyperglycemic wounded keratinocytes were focused on. Microarray data analysis showed that a total of 6,335 specific genes were down regulated in wounded keratinocytes grown under high glucose conditions compared with wounded keratinocytes grown under normal glucose conditions, 65 of which were down regulated by five or more folds (with p value of less than 0.05). A few examples of these downregulated genes are detailed in Table 4.1 A. Similarly, a total of 5,750 specific genes were upregulated in wounded keratinocytes grown under high glucose conditions compared with wounded keratinocytes grown under normal glucose conditions, 35 of which were upregulated by five or more folds (with p value of less than 0.05). A few examples are detailed in Table 4.1 B. Upon performing pathway analysis, it was found that numerous molecular pathways including TGF-β signaling pathway, WNT signaling pathway and G13 signaling pathway were shown to be dysregulated (Figure U1., Appendices). Sixty five genes were downregulated more than or equal to five folds in hyperglycemic wounded keratinocytes compared to normoglycemic wounded keratinocytes. These genes were focused upon since the hypothesis underlying the approach is that by manipulating down regulated genes under hyperglycemic conditions to normal levels using the fibrin-in-fibrin non-viral gene delivery system (described in chapter 3, section 3.3.4), diabetic wound healing can be normalized. Real time PCR was performed to validate the top 10 downregulated genes.

4.4 Discussion

In this chapter, the differential regulation of genes in keratinocytes during wound healing in hyperglycemic conditions was assessed using microarray analysis. Hyperglycemia is a key factor that affects various pathological manifestations of diabetes and has been shown to directly affect the wound healing cells such as macrophages[15], fibroblasts[16]. A number of studies have reported that the migration and proliferation of keratinocytes is hampered by hyperglycemia[1 2 14 17-20]. Prolonged exposure to high glucose has been shown to directly reduce the proliferation of human epidermal keratinocytes *in vitro*[1 19]. Keratinocyte motility is also significantly reduced along with downregulation of integrin expression and suppression of K16 the keratinocyte activation marker upon treatment with high glucose[2].

Table 4.1A: Examples of gene downregulated in wounded keratinocytes grown in high glucose conditions compared to wounded keratinocytes grown in normal glucose

Gene Symbol	Fold Decrease	P Value	Biological Process
MBNL1	42.17	0.026	Embryonic development, myoblast differentiation
TGFBR1	31.89	0.0206	Positive regulation of cell proliferation
LPHN3	22.11	0.0426	Cell adhesion
PRKRA	16.02	0.0283	Negative regulation of cell proliferation
EDNRA	12.75	0.027	Cell proliferation
LRCH3	12.55	0.0285	Protein binding
NUPL2	12.34	0.0225	Protein export from nucleus
FLJ10808	11.49	0.0427	Protein modification process, ubiquitin cycle
ATP5J	11.43	0.0482	ATP synthesis coupled proton transport
TRIM4	10.85	0.0173	Ubiquitin-protein ligase activity, zinc ion binding
PHCA	10.63	0.0268	Hydrolase activity

Table 4.1B: Examples of gene upregulated in wounded keratinocytes grown in high glucose conditions compared to wounded keratinocytes grown in normal glucose

Gene Symbol	Fold Increase	P Value	Biological Process
VNN3	17.26	0.0355	Pantetheinase activity; nitrogen compound metabolism
ZNF343	17.11	0.0481	Regulation of transcription
IGSF4D	14.58	0.0457	Extracellular recognition and intercellular adhesion
AMICA1	10.37	0.027	Cell adhesion
PTK2	9.333	0.0173	Cell growth and intracellular signal transduction
TNFAIP6	7.867	0.0301	Cell adhesion; cell migration
GDF15	6.725	0.0288	Tissue differentiation and maintenance
WNT10A	6.53	0.0307	Wnt receptor signaling pathway, calcium modulating pathway
IFITM1	5.816	0.029	Regulation of progression through cell cycle; negative regulation of cell proliferation

With an aim of studying the molecular basis of these changes in keratinocytes exposed to hyperglycemia, microarray study was performed on wounded and non-wounded keratinocytes grown in normal and high glucose conditions. It was found that a number of genes are up- and down- regulated in wounded keratinocytes grown in high glucose conditions compared to those grown in normal glucose conditions. *In vitro* model of multiple scratch wounds was used in this study. *In vitro* scratch model is an established model of wound healing[21]. However, a limitation in the classical scratch wound model arises from the fact that only around 5% of the seeded cells are involved in the healing process. To avoid this, a multiple scratch wound model was utilized in this study, which allows participation of 40-50% of cells. This makes the microarray data more representative. A previous study investigated the early changes in gene expression in keratinocytes during normal wound healing[22]. To the best of the authors' knowledge, this is the first study to compare the gene expression during wound healing in keratinocytes grown in normal and high glucose conditions.

RNA samples from wounded and non-wounded keratinocytes grown in high and normal glucose conditions were utilized for microarray study. Three biological replicates from each of the four samples were studied making a number of comparisons possible. When non-wounded cells grown in high and normal glucose conditions were compared, only couple genes were found to be more than two folds upregulated in cells grown in normal glucose conditions ($p<0.05$). However, comparisons between the wounded and non-wounded cells grown in either high or normal glucose conditions revealed thousands of genes that were up- and down-regulated (Figure 4.4). This finding was expected as wound healing process involves a number changes in gene expression profile. Of particular interest, though, was the comparison between wounded hyperglycemic keratinocytes and wounded normoglycemic keratinocytes because the study of these genes holds a promise to identify a plausible therapeutic molecule which when successfully delivered can normalize the up- and/or down-regulated genes in hyperglycemic wound healing. In this comparison, downregulated genes were further focused on to find out a possibility to deliver a plasmid DNA complex to replenish it for therapeutic benefit.

4.4.1 Rab18 as Potential Target

Intriguingly, one of the most significantly downregulated genes was identified to be the highly homologous Rab18 gene. Rab18 is a member of ras-related small GTPases, with particular relevance to membrane trafficking[23]. These GTPases are intracellular membrane organizers and act as membrane bound molecular switches[24]. Rab18 has been shown to be associated with secretory granules which inhibit their mobilization and thus reduce the secretory capacity of neuroendocrine cells[24 25]. Although, one previous study has shown therapeutic benefit of Rab18 delivery in acromegaly[26], the secretory control function of Rab18 has not been exploited.

With regard to the pathogenesis of diabetic wound healing, various studies have previously attempted to unravel the altered molecular mechanisms leading to chronic healing[27-30]. Chronic inflammation is the hallmark of diabetic wound healing[31]. A dysregulated gene expression profile of proinflammatory cytokines such as IL-6 and IL-8 and their receptors such as CXCR1, CXCR2 and GP130 contribute to the chronic inflammation[32]. Also, high serum levels of TNF-α have been seen in type II diabetes[33] and prolonged TNF-α may disrupt cytokine networks for example, stimulation of MCP-1, MIP-2 and IL-1β secretion, leading to more persistent inflammation and tissue damage[34 35]. High TGF-β3 levels in diabetic wounds can inhibit TGF-β1, leading to increased macrophage activity[36 37]. Also, there is increasing evidence that MMPs are affected in diabetes, supporting a growing notion that high proteolytic activity plays an important role in diabetic wound healing. A number of studies have reported increased levels of MMPs (e.g. MMP-1, 2, 3, 8, 9 and 26) and decreased levels of tissue inhibitors of MMPs (TIMP-1, 2) in chronic wounds including diabetic and pressure wounds[38-50]. Thus, hyper secretion can be looked at as a major pathology in diabetic wound healing. Combining the findings of the role of Rab18 in neuroendocrine cells and the microarray data in keratinocytes, it was hypothesized that Rab18 delivery to diabetic wounds potentially can revert the hyper secretion in diabetic wounds to the normal scenario, if Rab18 plays a similar secretory regulation role and in turn, can help reduce the chronic inflammation and proteolytic environment thus normalizing the wound healing, at least to some extent. Figure 4.5 shows a schematic depicting the hypothesis of the proposed role of Rab18 in diabetic wound healing.

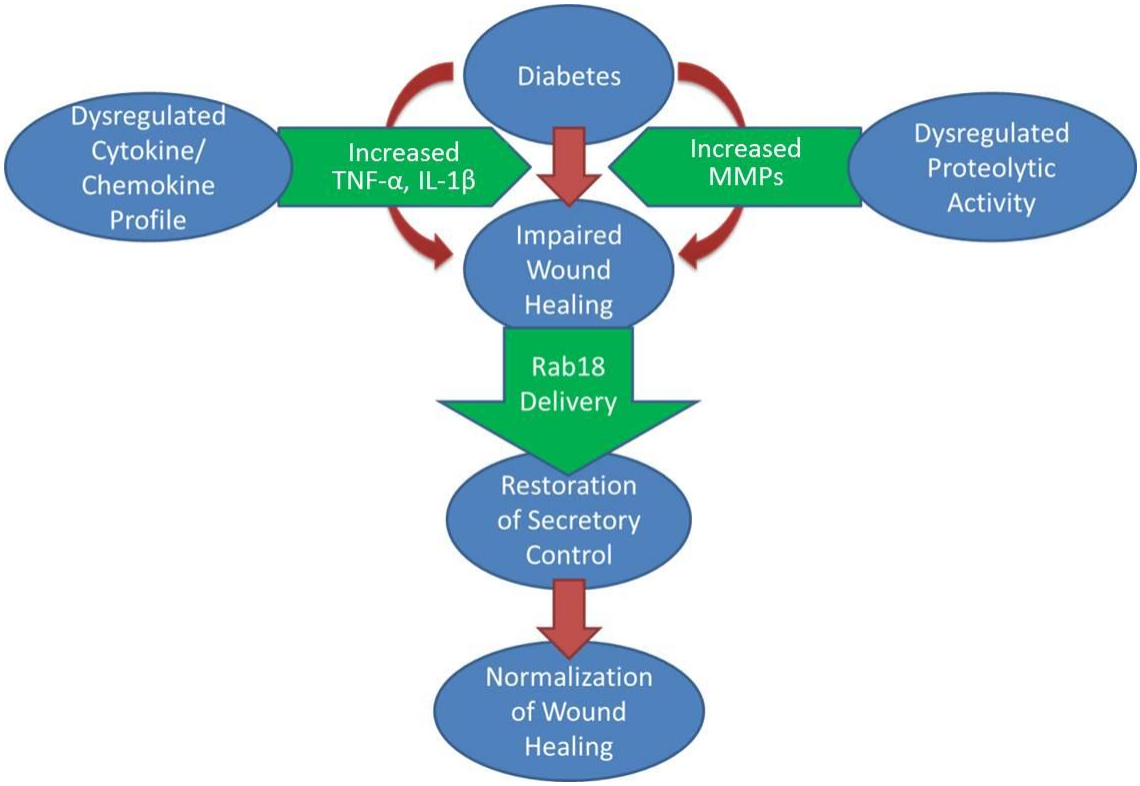

Figure 4.5: Schematic representation of the proposed role of Rab18 therapy in impaired wound healing.

4.5 References

1. Spravchikov N, Sizyakov G, Gartsbein M, Accili D, Tennenbaum T, Wertheimer E. Glucose effects on skin keratinocytes: implications for diabetes skin complications. *Diabetes* 2001;50(7):1627-35.

2. Lan CC, Wu CS, Kuo HY, Huang SM, Chen GS. Hyperglycaemic conditions hamper keratinocyte locomotion via sequential inhibition of distinct pathways: new insights on poor wound closure in patients with diabetes. *Br J Dermatol* 2009;160(6):1206-14.

3. Coulombe PA. Towards a molecular definition of keratinocyte activation after acute injury to stratified epithelia. *Biochem Biophys Res Commun* 1997;236(2):231-8.

4. Woodley DT, Chen JD, Kim JP, Sarret Y, Iwasaki T, Kim YH, O'Keefe EJ. Re-epithelialization. Human keratinocyte locomotion. *Dermatol Clin* 1993;11(4):641-6.

5. Singer AJ, Clark RA. Cutaneous wound healing. *N Engl J Med* 1999;341(10):738-46.

6. Santoro MM, Gaudino G. Cellular and molecular facets of keratinocyte reepithelization during wound healing. *Exp Cell Res* 2005;304(1):274-86.

7. Fuchs E. Scratching the surface of skin development. *Nature* 2007;445(7130):834-42.

8. O'Toole EA. Extracellular matrix and keratinocyte migration. *Clin Exp Dermatol* 2001;26(6):525-30.

9. Usui ML, Mansbridge JN, Carter WG, Fujita M, Olerud JE. Keratinocyte migration, proliferation, and differentiation in chronic ulcers from patients with diabetes and normal wounds. *J Histochem Cytochem* 2008;56(7):687-96.

10. Salonurmi T, Parikka M, Kontusaari S, Pirila E, Munaut C, Salo T, Tryggvason K. Overexpression of TIMP-1 under the MMP-9 promoter interferes with wound healing in transgenic mice. *Cell Tissue Res* 2004;315(1):27-37.

11. Ravanti L, Kahari VM. Matrix metalloproteinases in wound repair (review). *Int J Mol Med* 2000;6(4):391-407.

12. Loffek S, Schilling O, Franzke CW. Biological role of matrix metalloproteinases: a critical balance. *Eur Respir J* 2011;38(1):191-208.

13. Soo C, Shaw WW, Zhang X, Longaker MT, Howard EW, Ting K. Differential expression of matrix metalloproteinases and their tissue-derived inhibitors in cutaneous wound repair. *Plast Reconstr Surg* 2000;105(2):638-47.
14. Lan CC, Liu IH, Fang AH, Wen CH, Wu CS. Hyperglycaemic conditions decrease cultured keratinocyte mobility: implications for impaired wound healing in patients with diabetes. *Br J Dermatol* 2008;159(5):1103-15.
15. Sun C, Sun L, Ma H, Peng J, Zhen Y, Duan K, Liu G, Ding W, Zhao Y. The phenotype and functional alterations of macrophages in mice with hyperglycemia for long term. *J Cell Physiol* 2011.
16. Hehenberger K, Kratz G, Hansson A, Brismar K. Fibroblasts derived from human chronic diabetic wounds have a decreased proliferation rate, which is recovered by the addition of heparin. *J Dermatol Sci* 1998;16(2):144-51.
17. Deveci M, Gilmont RR, Dunham WR, Mudge BP, Smith DJ, Marcelo CL. Glutathione enhances fibroblast collagen contraction and protects keratinocytes from apoptosis in hyperglycaemic culture. *Br J Dermatol* 2005;152(2):217-24.
18. Lu SL, Qiao L, Xie T, Yang YM, Jin SW, Qing C. [Effects of the cutaneous and blood contents of glucose on wound healing in diabetic rats with superficial partial thickness scalding]. *Zhonghua Yi Xue Za Zhi* 2005;85(27):1899-902.
19. Terashi H, Izumi K, Deveci M, Rhodes LM, Marcelo CL. High glucose inhibits human epidermal keratinocyte proliferation for cellular studies on diabetes mellitus. *Int Wound J* 2005;2(4):298-304.
20. Portugal-Cohen M, Kohen R. Exposure of human keratinocytes to ischemia, hyperglycemia and their combination induces oxidative stress via the enzymes inducible nitric oxide synthase and xanthine oxidase. *J Dermatol Sci* 2009;55(2):82-90.
21. Liang CC, Park AY, Guan JL. In vitro scratch assay: a convenient and inexpensive method for analysis of cell migration in vitro. *Nat Protoc* 2007;2(2):329-33.
22. Dayem MA, Moreilhon C, Turchi L, Magnone V, Christen R, Ponzio G, Barbry P. Early gene expression in wounded human keratinocytes revealed by DNA microarray analysis. *Comp Funct Genomics* 2003;4(1):47-55.

23. Dejgaard SY, Murshid A, Erman A, Kizilay O, Verbich D, Lodge R, Dejgaard K, Ly-Hartig TB, Pepperkok R, Simpson JC, Presley JF. Rab18 and Rab43 have key roles in ER-Golgi trafficking. *J Cell Sci* 2008;121(Pt 16):2768-81.

24. Vazquez-Martinez R, Cruz-Garcia D, Duran-Prado M, Peinado JR, Castano JP, Malagon MM. Rab18 inhibits secretory activity in neuroendocrine cells by interacting with secretory granules. *Traffic* 2007;8(7):867-82.

25. Malagon MM, Cruz-Garcia D, Diaz-Ruiz A, Peinado JR, Pulido MR, Araujo J, Garcia-Navarro S, Gracia-Navarro F, Castano JP, Vazquez-Martinez R. Identification of novel genes involved in the plasticity of pituitary melanotropes in amphibians. *Ann N Y Acad Sci* 2009;1163:233-40.

26. Vazquez-Martinez R, Martinez-Fuentes AJ, Pulido MR, Jimenez-Reina L, Quintero A, Leal-Cerro A, Soto A, Webb SM, Sucunza N, Bartumeus F, Benito-Lopez P, Galvez-Moreno MA, Castano JP, Malagon MM. Rab18 is reduced in pituitary tumors causing acromegaly and its overexpression reverts growth hormone hypersecretion. *J Clin Endocrinol Metab* 2008;93(6):2269-76.

27. Blakytny R, Jude EB. Altered molecular mechanisms of diabetic foot ulcers. *Int J Low Extrem Wounds* 2009;8(2):95-104.

28. Blakytny R, Jude E. The molecular biology of chronic wounds and delayed healing in diabetes. *Diabet Med* 2006;23(6):594-608.

29. Brem H, Tomic-Canic M. Cellular and molecular basis of wound healing in diabetes. *J Clin Invest* 2007;117(5):1219-22.

30. Galkowska H, Wojewodzka U, Olszewski WL. Chemokines, cytokines, and growth factors in keratinocytes and dermal endothelial cells in the margin of chronic diabetic foot ulcers. *Wound Repair Regen* 2006;14(5):558-65.

31. Khanna S, Biswas S, Shang Y, Collard E, Azad A, Kauh C, Bhasker V, Gordillo GM, Sen CK, Roy S. Macrophage dysfunction impairs resolution of inflammation in the wounds of diabetic mice. *PLoS One* 2010;5(3):e9539.

32. Pradhan L, Nabzdyk C, Andersen ND, LoGerfo FW, Veves A. Inflammation and neuropeptides: the connection in diabetic wound healing. *Expert Rev Mol Med* 2009;11:e2.

33. Mishima Y, Kuyama A, Tada A, Takahashi K, Ishioka T, Kibata M. Relationship between serum tumor necrosis factor-alpha and insulin resistance in obese men with Type 2 diabetes mellitus. *Diabetes Res Clin Pract* 2001;52(2):119-23.

34. Naguib G, Al-Mashat H, Desta T, Graves DT. Diabetes prolongs the inflammatory response to a bacterial stimulus through cytokine dysregulation. *J Invest Dermatol* 2004;123(1):87-92.

35. Acosta JB, del Barco DG, Vera DC, Savigne W, Lopez-Saura P, Guillen Nieto G, Schultz GS. The pro-inflammatory environment in recalcitrant diabetic foot wounds. *Int Wound J* 2008;5(4):530-9.

36. Jude EB, Blakytny R, Bulmer J, Boulton AJ, Ferguson MW. Transforming growth factor-beta 1, 2, 3 and receptor type I and II in diabetic foot ulcers. *Diabet Med* 2002;19(6):440-7.

37. Tsunawaki S, Sporn M, Ding A, Nathan C. Deactivation of macrophages by transforming growth factor-beta. *Nature* 1988;334(6179):260-2.

38. Lobmann R, Ambrosch A, Schultz G, Waldmann K, Schiweck S, Lehnert H. Expression of matrix-metalloproteinases and their inhibitors in the wounds of diabetic and non-diabetic patients. *Diabetologia* 2002;45(7):1011-6.

39. Mast BA, Schultz GS. Interactions of cytokines, growth factors, and proteases in acute and chronic wounds. *Wound Repair Regen* 1996;4(4):411-20.

40. Bullen EC, Longaker MT, Updike DL, Benton R, Ladin D, Hou Z, Howard EW. Tissue inhibitor of metalloproteinases-1 is decreased and activated gelatinases are increased in chronic wounds. *J Invest Dermatol* 1995;104(2):236-40.

41. Liu Y, Min D, Bolton T, Nube V, Twigg SM, Yue DK, McLennan SV. Increased matrix metalloproteinase-9 predicts poor wound healing in diabetic foot ulcers. *Diabetes Care* 2009;32(1):117-9.

42. Ladwig GP, Robson MC, Liu R, Kuhn MA, Muir DF, Schultz GS. Ratios of activated matrix metalloproteinase-9 to tissue inhibitor of matrix metalloproteinase-1 in wound fluids are inversely correlated with healing of pressure ulcers. *Wound Repair Regen* 2002;10(1):26-37.

43. Lobmann R, Zemlin C, Motzkau M, Reschke K, Lehnert H. Expression of matrix metalloproteinases and growth factors in diabetic foot wounds treated with a protease absorbent dressing. *J Diabetes Complications* 2006;20(5):329-35.

44. Muller M, Trocme C, Lardy B, Morel F, Halimi S, Benhamou PY. Matrix metalloproteinases and diabetic foot ulcers: the ratio of MMP-1 to TIMP-1 is a predictor of wound healing. *Diabet Med* 2008;25(4):419-26.

45. Lobmann R, Schultz G, Lehnert H. Proteases and the diabetic foot syndrome: mechanisms and therapeutic implications. *Diabetes Care* 2005;28(2):461-71.

46. Wall SJ, Sampson MJ, Levell N, Murphy G. Elevated matrix metalloproteinase-2 and -3 production from human diabetic dermal fibroblasts. *Br J Dermatol* 2003;149(1):13-6.

47. Nwomeh BC, Liang HX, Cohen IK, Yager DR. MMP-8 is the predominant collagenase in healing wounds and nonhealing ulcers. *J Surg Res* 1999;81(2):189-95.

48. Pirila E, Korpi JT, Korkiamaki T, Jahkola T, Gutierrez-Fernandez A, Lopez-Otin C, Saarialho-Kere U, Salo T, Sorsa T. Collagenase-2 (MMP-8) and matrilysin-2 (MMP-26) expression in human wounds of different etiologies. *Wound Repair Regen* 2007;15(1):47-57.

49. Terasaki K, Kanzaki T, Aoki T, Iwata K, Saiki I. Effects of recombinant human tissue inhibitor of metalloproteinases-2 (rh-TIMP-2) on migration of epidermal keratinocytes in vitro and wound healing in vivo. *J Dermatol* 2003;30(3):165-72.

50. Wall SJ, Bevan D, Thomas DW, Harding KG, Edwards DR, Murphy G. Differential expression of matrix metalloproteinases during impaired wound healing of the diabetes mouse. *J Invest Dermatol* 2002;119(1):91-8.

Chapter Five

Delivery of Therapeutic Genes – eNOS and Rab18 – via Fibrin-in-fibrin System Enhances Wound Healing in Alloxan Induced Hyperglycemic Rabbit Ear Ulcer Model of Compromised Wound Healing

Contents of this chapter are currently under preparation for manuscript submission:

Kulkarni M., O'Loughlin A., Vazquez R., Mashayekhi K., Greiser U., O'Toole E., O'Brien T., Malagon M. and Pandit A. 'Towards Developing a Pro-angiogenic and Secretory Control Therapy for Compromised Wound Healing.'

5.1 Introduction

Angiogenesis required for normal wound healing is disrupted in diabetes[1 2]. Impaired wound healing in diabetes has been associated with reduced levels of NO[3-5]. The reduced NO synthesis in vascular endothelial cells by high glucose has been held responsible, at least partly, for diabetic angiopathy[6]. NO is a small pleotropic free radical that was found to play important role in regulation of vascular tone[7]. A number of studies have demonstrated the role of NO in wound healing[8-11]. It has been demonstrated to represent an important mediator in skin biology involved in homeostasis through regulation of blood flow[12]. The relation of NO and diabetic wound healing has been further supported by several reports showing enhanced wound healing after NO treatment[13-19] via a number of mechanisms which include altering MMPs[20-22], affecting the synthesis function in fibroblasts[14 23] or acting as effector molecule[24-27].

NO diffuses freely and has a half life in the order of seconds[28]. This can pose a problem in use of NO as therapeutic molecule. This can justify increased research in the upstream molecules such as nitric oxide synthases (NOSs). NOSs control the production of NO by oxidation of L-arginine. Three main isoforms of NOSs have been identified in mammals: inducible NOS (iNOS), neuronal NOS (nNOS) and endothelial NOS (eNOS)[29]. iNOS, as the name suggests, is induced only under certain stimuli such as infection, hypoxia and cytokines, resulting in NO production but in basal state it is not detectable. On the other hand, nNOS and eNOS are constitutionally produced and are fully active in the presence of factors such as tetrahydrobiopterin (BH4), flavine mononucleotide (FMN), nicotinamide-adeninedinucleotide phosphate (NADPH) and oxygen[30] as well as increasing Ca^{2+} levels via calmodulin[11]. eNOS, a constitutionally active enzyme that is involved in production of NO, plays a critical role in regulation of mobilization of endothelial progenitor cells (EPC)[7 31], a process that is considered indispensable for neovascularization. Furthermore, a previous study has shown therapeutic benefit of fibrin based viral gene delivery of eNOS in a preclinical model[32].

Besides reduced angiogenesis, increased inflammation and proteolysis are major pathological hallmarks of diabetic wound healing. A dysregulated gene expression profile of proinflammatory cytokines such as IL-6 and IL-8 and their receptors such as

CXCR1, CXCR2 and GP130 contribute to the chronic inflammation[33]. Also, high serum levels of TNF-α have been seen in type II diabetes[34]. High TGF-β3 levels in diabetic wounds can inhibit TGF-β1, leading to increased macrophage activity[35 36]. Also, there is increasing evidence that MMPs are affected in diabetes, supporting a growing notion that high proteolytic activity plays an important role in diabetic wound healing. A number of studies have reported increased levels of MMPs (e.g. MMP-1, 2, 3, 8, 9 and 26) and decreased levels of tissue inhibitors of MMPs (TIMP-1, 2) in chronic wounds including diabetic and pressure wounds[37-49]. Thus, hyper secretion of proinflammatory cytokines and proteolytic enzymes can be considered as a major pathology in diabetic wound healing. Therefore, as described in the previous chapter, Rab18, a negative regulator of secretion can address the issue of high proteolytic enzymes and inflammatory cytokines in diabetic wound healing.

Enhanced angiogenesis, along with the reduction of pro-inflammatory cytokines and proteolytic enzymes, can augment the process of normalization of wound healing. With this hypothesis in consideration, fibrin-in-fibrin system was employed to deliver eNOS and Rab18 genes to the full thickness wounds in an alloxan induced rabbit ear ulcer model of compromised wound healing. Stereological methods were utilized to quantify various parameters of wound healing response such as wound closure, angiogenesis and inflammation.

5.2 Materials and Methods

5.2.1 Fibrin-in-fibrin Delivery System

Fibrin microspheres with Rab18 lipoplexes were fabricated as described previously[50]. Briefly, fibrinogen solution (20 mg/ml) and thrombin solution (4 IU) containing lipoplexes (with 10 μg of Rab18 plasmid DNA) were mixed. Prior to formation of the gel, while it was still in liquid phase, the solution was poured drop wise into a pre-heated mineral oil at 75^0C and stirred over night at 250 rpm to evaporate the water phase. Two surfactants were used. Tween20 was used in the water phase and spam80 was used in the oil phase. After overnight stirring, the oil was decanted. This was done in two phases, first at low speed (1,000 rpm) centrifugation and then at high speed (4,500 rpm) centrifugation. The fibrin microspheres were washed by ethanol, hexane

and acetone and then air dried. The Rab18 containing fibrin microspheres were then dispersed in fibrinogen solution (60 mg/ml) and the eNOS lipoplexes were dispersed in thrombin solution (4 IU). The two solutions were mixed just before being applied on the wound where they formed a gel. In the eNOS in fibrin treatment group, eNOS lipoplexes (10 µg) were mixed in a thrombin solution (4 IU) and mixed with fibrinogen solution (60 mg/ml) before being applied immediately on the wound. The fibrin alone treatment consisted of fibrin microspheres (FM) added to a fibrinogen (60 mg/ml) and thrombin (4 IU) solution which was applied on the wound. Lipoplexes treatment had only Rab18 and eNOS lipoplexes without fibrin scaffold. The "no treatment" group where the wounds were left untreated acted as a control.

5.2.2 *In Vivo* Model

The ability of fibrin-in-fibrin system to deliver genes of interest *in vivo* was investigated. An alloxan induced hyperglycemic rabbit ear ulcer model was utilized for this purpose. New Zealand white rabbits (3-3.5 kg) were used in the study. The protocol was approved by the ethics committee of the National University of Ireland, Galway, and the study was conducted under a license granted by the Department of Health and Children, Dublin, Ireland. Rabbits were housed in individual cages with a 12-hour light/dark cycle under controlled temperature and humidity conditions. Rabbits were fed a standard chow diet and had access to water ad libitum.

5.2.3 Induction of Hyperglycemia

Rabbits were sedated with a subcutaneous injection of 1 ml/kg acepromazine. Hair was shaved off at the back of the ears, and an anesthetic cream (EMLA, AstraZeneca, USA) was rubbed into the back of the ear and left in situ for 20 minutes. Alloxan (150 mg/kg) (Sigma–Aldrich, Ireland) in 30 ml saline solution was prepared and administered via an ear vein using a butterfly syringe, at a flow rate of 1.5 ml/min. Alloxan is known to cause necrosis of pancreatic islets, thereby inducing hyperglycemia[51]. After treatment, water containing one tablespoon of glucose per liter was given to the rabbits for a 48 hour period, to avoid possible hypoglycemia. Blood glucose readings were taken daily, using blood glucose test strips and meter (Accu-Chek test advantage meter, Accu-Chek test strips advantage II, Roche Diagnostics, United Kingdom). Food and water intakes

were monitored daily. Hyperglycemia was confirmed if blood glucose readings were in the range of 20–28 mmol/l. Insulin treatment was not required to control hyperglycemia in any animals.

5.2.4 Surgical Procedure

Four weeks post-alloxan treatment; rabbits were anesthetized using an intramuscular injection of 0.1 ml/kg xylazine and 0.12 ml/kg ketamine. This is half dose anesthesia, as full dose may prove fatal under hyperglycemic conditions. Four "6 mm" punch biopsy wounds were created in each ear, using sterile disposable 6 mm diameter punch biopsies (Panvet, Ireland), exposing bare cartilage. Each wound was treated with one of five randomized treatment groups (Table 5.1). Wounds were covered with a polyurethane dressing (Opsite™, Smith and Nephew Ltd) until day 7 (n = 8) and day 14 (n = 8).

At days 7 and 14, rabbits were euthanized. At necropsy, ears were surgically removed and the wounds (using a ruler with clear markings) were photographed using a digital camera. The wounds were dissected across the center-line in a predetermined axis. One half of the ear was fixed in formalin for histological and immunohistochemical analysis, in order that a cross-section of the wound could be analyzed. The other half was stored in RNA *later* at - 80^0C for further analysis.

5.2.5 Wound Closure Measurements

Digital images of wounds were analyzed for wound closure using image processing software (Image J, NIH). The scale of measurement was set using the known distance in the image. The mean diameter of each wound was measured by averaging the diameter at four predetermined axes. The wound closure was then measured by using the following equation:

$$\text{Percent closure } (\%C) = \left(\frac{D_o - D_i}{D_o} \right) \times 100$$

Where D_i = Diameter of the wound at day of sacrifice

D_0 = Diameter of wound at day zero

Table 5.1: Randomized treatment groups applied on the wounds in alloxan induced rabbit ear ulcer model of compromised wound healing

	Treatment group	7 days (N)	14 days (N)
1	No treatment control	8	8
2	Fibrin gel with fibrin microspheres alone	8	8
3	Fibrin-in-fibrin system, carrying eNOS and Rab18	8	8
4	Fibrin-lipoplex system, carrying eNOS	8	8
5	Lipoplexes carrying eNOS and Rab18	8	8

5.2.6 Histology and Immunohistochemistry

Formalin fixed paraffin embedded sections were cut at 5 mm thickness. Six consecutive sections were saved from the block, as soon as the tissue was reached in the block. This ensured that all sections were saved at the cross-section of the wound. Six more sections were taken, three each at 100 µm intervals from the surface. Slides were stained with H & E stains using standard protocol. The criteria for identification of inflammatory cells and blood vessels were set at 400X magnification in the beginning for consistency.

Identification of blood vessels was confirmed by immunohistochemistry with endothelial cell marker CD31 using standard protocol. Briefly, enzymatic antigen retrieval was carried out at 37^0C using 1X proteinase K (20 mg/ml, Sigma–Aldrich) solution in TE buffer (50 mM Tris Base, 1 mM EDTA, pH 8.0, Sigma–Aldrich). Primary antibody used was monoclonal mouse anti-CD31 (DakoCytomation, Dublin, Ireland) (1:30 in 0.01 M PBS containing 1% BSA, 0.1% cold fish skin gelatin), with an incubation time of 90 min at room temperature. Blocking buffer was added to three slides as negative control. Endogenous peroxidase was blocked with 3% hydrogen peroxide (Sigma–Aldrich). Secondary goat anti-mouse IgG (1:100 in 0.01 M PBS, DakoCytomation, Ireland) was applied for 45 min at room temperature, followed by streptavidin–avidin biotin complex HRP (DakoCytomation, Ireland), and developed using DAB chromagen (Sigma–Aldrich, Ireland) and counterstained with filtered Harris hematoxylin solution.

Identification of macrophages was confirmed by immunohistochemistry using a standard protocol. Briefly, enzymatic antigen retrieval was carried out at 37^0C using 1X proteinase K (20 mg/ml, Sigma–Aldrich) solution in TE buffer (50 mM Tris Base, 1 mM EDTA, pH 8.0, Sigma–Aldrich). Primary antibody used was mouse monoclonal anti-rabbit macrophage clone Ram11 (Dako, Dublin, Ireland) (1:100 in 0.01 M PBS containing 1% BSA, 0.1% cold fish skin gelatin), with an overnight incubation at 4°C.Blocking buffer was added to three slides as negative control. Endogenous peroxidase was blocked with 3% hydrogen peroxide (Sigma–Aldrich). Biotinylated secondary anti-mouse horse radish peroxidase conjugated antibody (Calbiochem) was applied for 40 min at room temperature. Following rinsing the staining was developed

using DAB chromagen (Sigma–Aldrich, Ireland) and counterstained with filtered Harris hematoxylin solution.

5.2.7 Stereology

Six fields of view of H & E stained slides were captured at 400X magnification. The volume fraction of inflammatory cells was measured using a 192-point grid. The surface density and length density of blood vessels were measured using a cycloidal line grid.

5.2.7.1 Inflammation

Volume fraction (V_V) is a relative parameter best estimated by point counting[52]. The number of neutrophil and macrophage cell nuclei intersecting grid points was counted (P_P). This number was divided by the total number of grid points for each field of view (P_T), and a cumulative volume fraction of inflammatory cells calculated for the six fields of view on each section.

$$V_v = \left(\frac{P_p}{P_T} \right)$$

5.2.7.2 Angiogenesis

Since skin is a stratified organ and vertical sections of known orientation were saved, isotropy was emulated through use of cycloidal test lines of known radii and distance[32]. A cycloidal grid of 40 microns radius was overlaid on each field of view so that underlying cartilage of the ear section was always parallel to the major grid axis. The grid consisted of six test lines, each comprising 10 cycloid arcs. Therefore, the total length (L_T) of cycloid arcs was 2400 mm. The number of times a blood vessel intersected (I) an arc was counted, and the following standard equation was used to measure the surface density (S_V)

$$S_V = 2 \times \frac{I}{L_T}$$

Length density of blood vessels was measured by rotating each captured field of view by 90 degrees. The cycloidal grid was placed in the same orientation as described above, so that the underlying cartilage layer was perpendicular to the major grid axis. The grid now consisted of eight test lines, each comprising eight cycloid arcs of radius 40 microns. The total length of test line (L_T) was therefore 2560 mm. The number of intersections between blood vessels (I_L) and test line was counted, and the length density (Lv) of blood vessels was calculated using the following equation, where T_S is the thickness of the section.

$$L_T = \frac{(2 \times I_L)}{T_S}$$

Also, radial diffusion distance (R_{diff}) between the blood vessels was calculated using following equation:

$$R_{diff} = \frac{1}{\sqrt{\pi \times Lv}}$$

This distance is critical to determine the efficiency of new blood vessels as it measures the zone of diffusion around blood vessels.

5.3 Results

5.3.1 Wound Closure

The wound closure is determined as described in the methods section. At day 7 post-surgery, Rab18-eNOStreated groups showed 43% wound closure while eNOS and fibrin treated groups showed 41% wound closure. The control and lipoplexes treated groups showed 26% and 27% mean wound closure respectively. However, these differences were not statistically significant. At day 14 post-surgery, the Rab18-eNOS treatment showed a 92% mean wound closure which was significantly enhanced over the mean wound closure in treatment groups of lipoplexes alone (40%) and no treatment control (61%) (Figure 5.1).

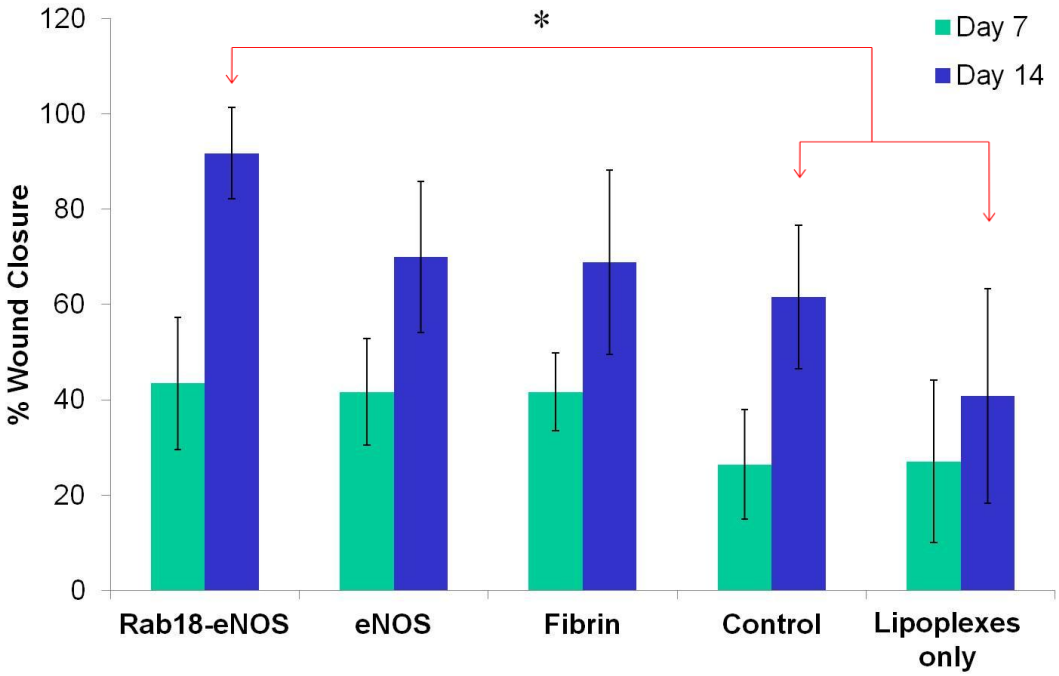

Figure 5.1: Wound closure measurements in a rabbit ear ulcer at day 7 and day 14. No significant differences were found at day 7 while at day 14, the fibrin-in-fibrin treatment group with Rab18 and eNOS was found to significantly enhance wound closure relative to lipoplexes alone and control "no treatment" groups. * represents statistical significance by one way ANOVA (n = 8, p < 0.05)

5.3.2 Stereology

It is important to look histologically at angiogenesis and inflammation. The sections were stained by H & E stains. Figure 5.2 shows representative pictures of H & E staining for the various treatments. Stereological methods were used for quantification. As described in methods section, angiogenesis was quantified by calculating surface density, length density and radial diffusion distance. Inflammation was quantified by calculating volume fraction of inflammatory cells.

5.3.2.1 Angiogenesis

Representative images of CD31 immunostaining for detection of endothelial cells is shown in Figure 5.3. The results of surface density analysis of blood vessels are depicted in Figure 5.4. At day 7 post-surgery, Rab18-eNOS treatment on average resulted in 58% and 56% increase in surface density of blood vessels over that seen in control and lipoplexes treated groups respectively while eNOS treatment resulted in 55% and 53% increase over that seen in control and lipoplexes treated groups respectively. At day14 post-surgery, surface density of blood vessels was 35% higher in Rab18-eNOS treated group than that in lipoplexes and fibrin treated groups while 41% higher than that in control group. The surface density of blood vessels was not statistically different between Rab18-eNOS treatment and eNOS alone treatment at both time points.

The length density and radial diffusion distance parameters determine the functional efficiency of the blood vessels rather than just the number of blood vessels in surface density measurement. At day 7 post-surgery, the length density of blood vessels in Rab18-eNOS treated group was 20%, 41%, 58% and 62% higher than that in eNOS treated, fibrin treated, lipoplexes treated and control groups respectively (Figure 5.5 A). In parallel, the mean radial diffusion distance in Rab18-eNOS treated group (0.011mm) was significantly decreased compared to that seen in eNOS treated, fibrin treated, lipoplexes treated and control groups by 12%, 26%, 38% and 41% respectively (Figure 5.5 B).

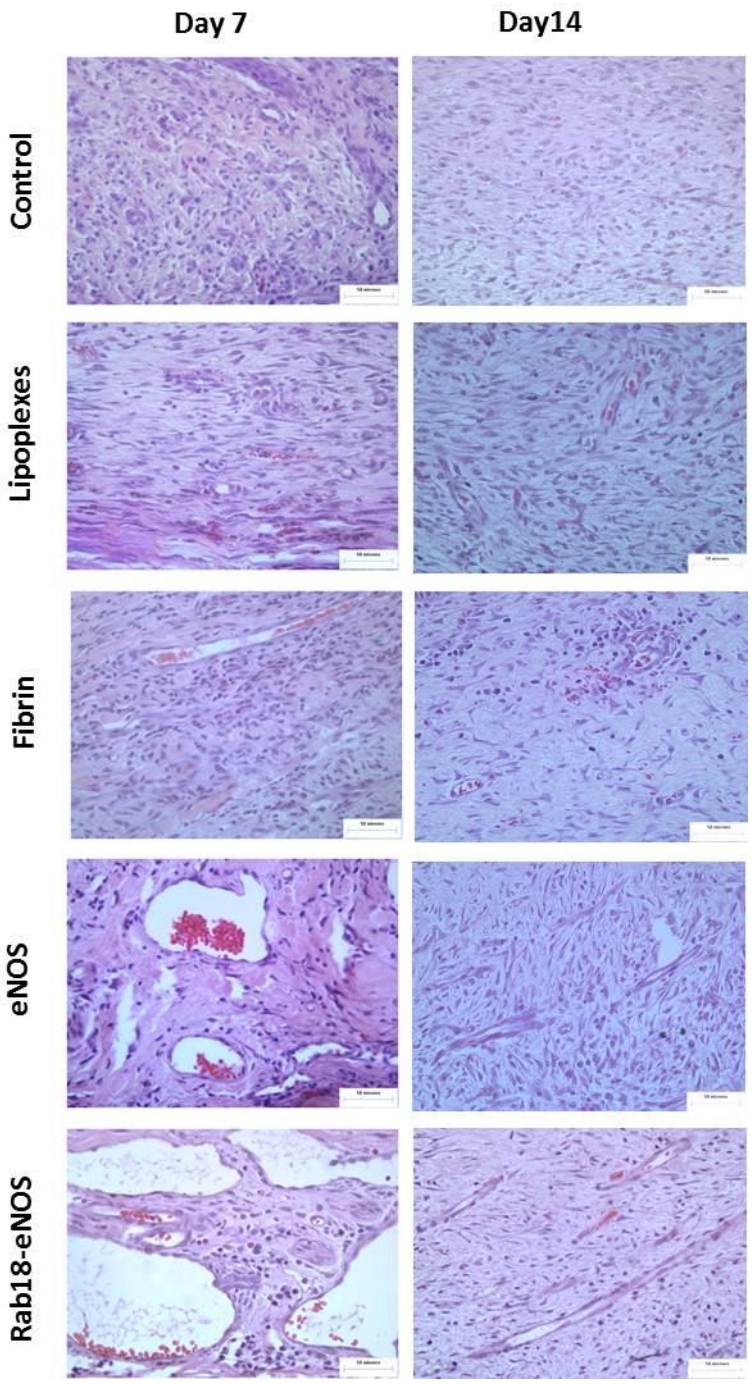

Figure 5.2: Representative images of H & E staining. The scale bars represent 50 µm.

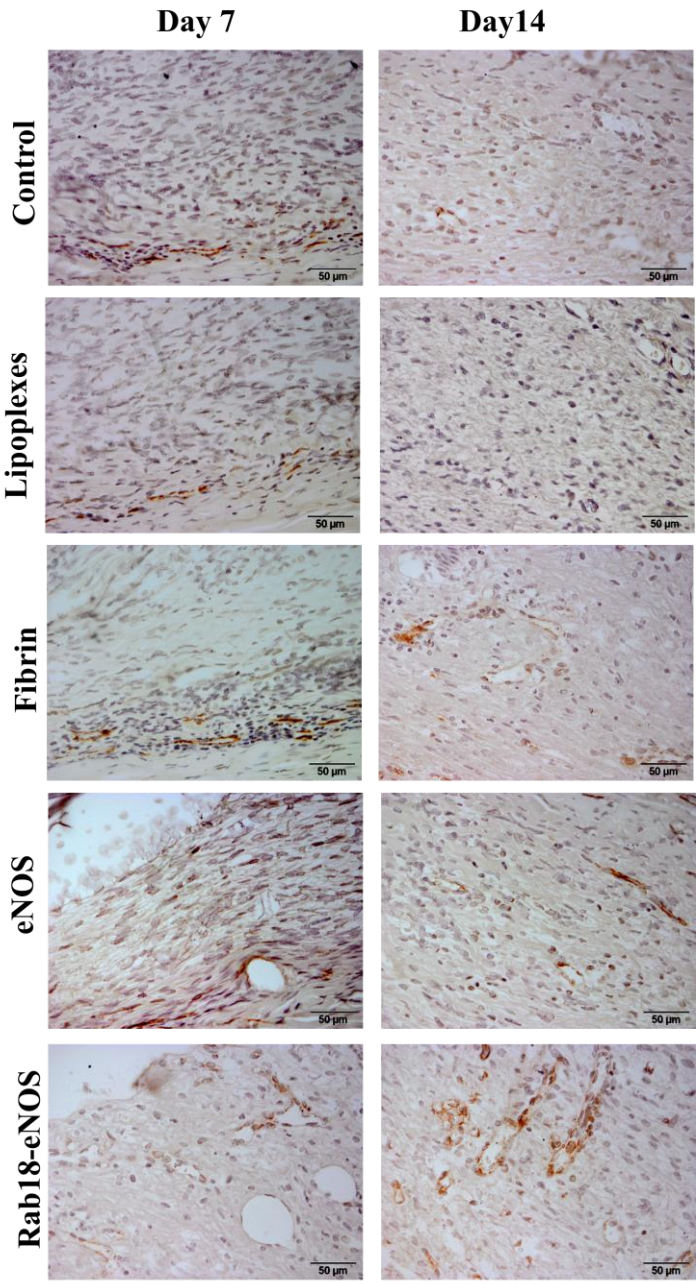

Figure 5.3: CD31 immunostaining showing endothelial cells (stained as brown cells) lining the blood vessels in various treatments at day 7 and 14. Hematoxylin was used for counterstaining. The scale bars represent 50 µm.

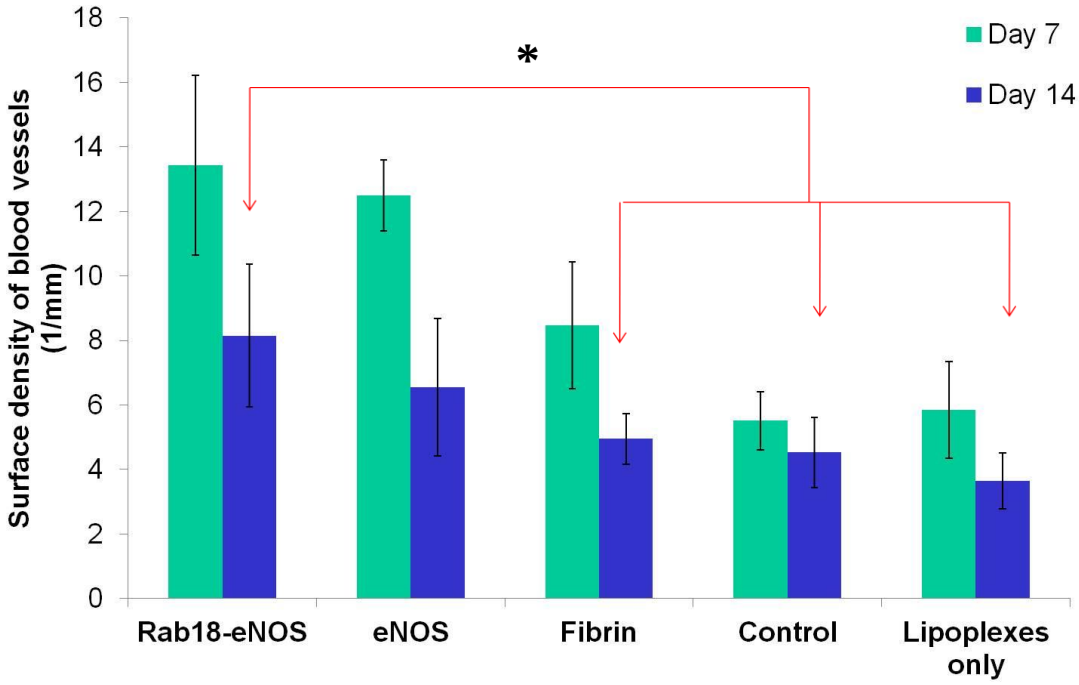

Figure 5.4: Surface density of blood vessels in wounds. At day 14 post-surgery, the surface density in Rab18-eNOS treatment group was significantly higher than fibrin, lipoplexes and no treatment control. * represents statistical significance by one way ANOVA (n = 8, $p < 0.05$).

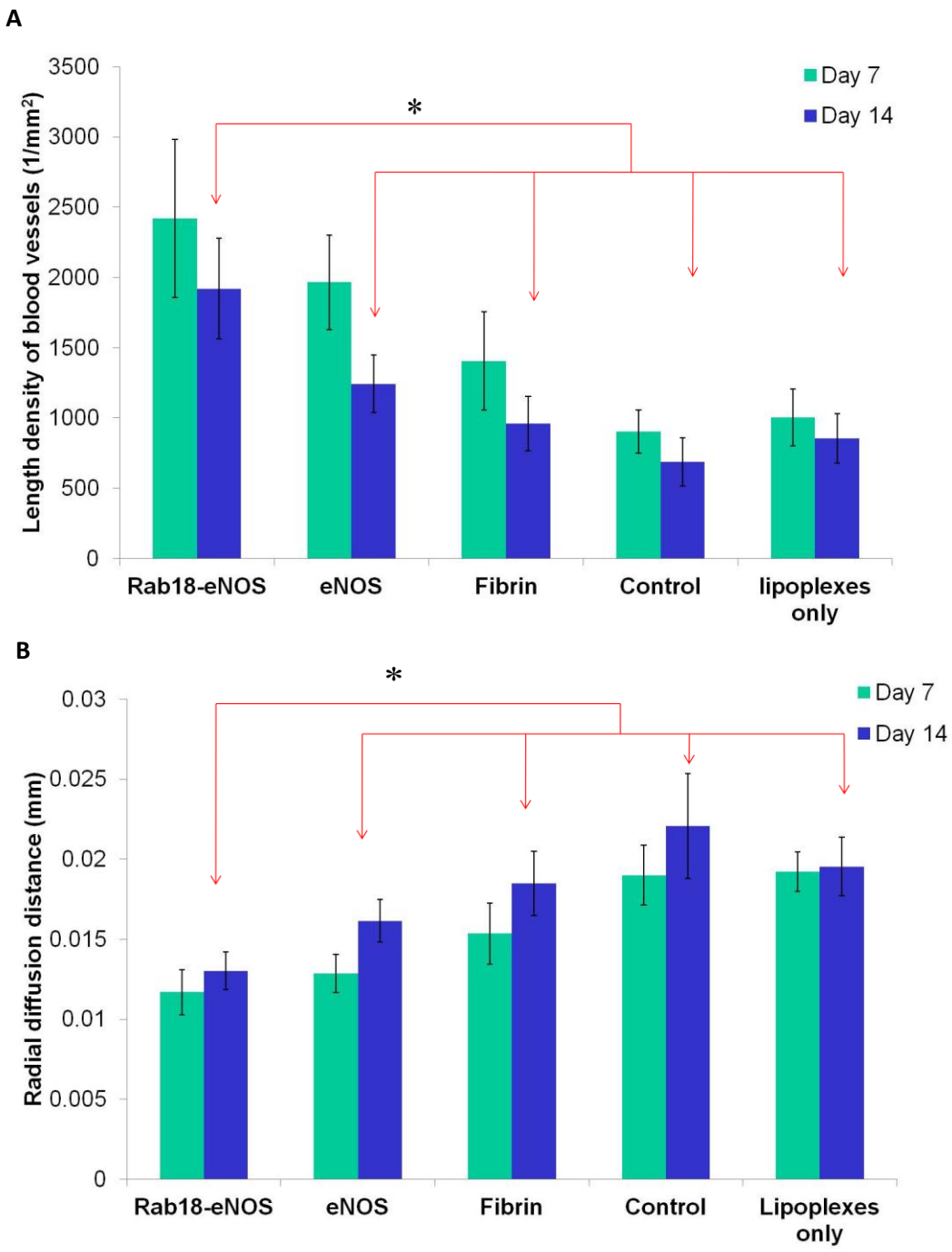

Figure 5.5: Length density (A) and radial diffusion distance (B) in the wounds. At day 14 post-surgery, addition of RAB18 to eNOS enhances the length density and reduces radial diffusion distance compared to eNOS alone, fibrin, control and lipoplexes alone treatment. * represents statistical significance by one way ANOVA (n = 8, p < 0.05).

At day 14 post-surgery, while the significant differences between Rab18-eNOS treated and fibrin treated, lipoplexes treated and control groups were still maintained, Rab18-eNOS treated group showed significant increase (39%) in length density and significant decrease (22%) in radial diffusion distance compared to eNOS treated group suggesting that the addition of Rab18 to eNOS aids in increasing the functional blood vessels.

There were no significant differences between the results of control and lipoplexes alone. However, fibrin had effect on its own. The significantly higher surface density (34%) and length density (35%) of blood vessels at day 7 in fibrin alone treated group compared to control group (Figure 5.4 & 5.5 A) suggest the ingenious angiogenic effect of fibrin on its own.

5.3.2.2 Inflammation

Representative images showing immunostaining for macrophages in various treatments at day 7 and 14 are shown in Figure 5.6. Inflammatory reaction to various treatments was quantified by measuring the volume fraction of inflammatory cells namely the macrophages and neutrophils. The results of volume fraction of inflammatory cells are depicted in Figure 5.7. At day 7 post-surgery, no significant differences were observed between the treatments although there was a trend towards increased inflammation in all fibrin containing treatments. By day 14 post-surgery, Rab18-eNOS treated group showed 58% reduction in volume fraction of inflammatory cells while there was no reduction in inflammation in control and lipoplexes treated groups. At day 14 post-surgery, Rab18-eNOS showed significantly lower volume fraction of inflammatory cells compared to eNOS treated, fibrin treated, lipoplexes treated and control groups by 42%, 43%, 47% and 50% respectively.

5.3.3 Relationship between Wound Healing Parameters

Pearson's correlations were obtained in order to compare how different healing parameters correlated in the different treatment groups (Table 5.2). The radial diffusion distance, which indicates state of perfusion, was negatively correlated with the percent epithelialization, length density of blood vessels and inflammation in the Rab18-eNOS treated group while the percent epithelialization in the Rab18-eNOS treated group was positively correlated with inflammation.

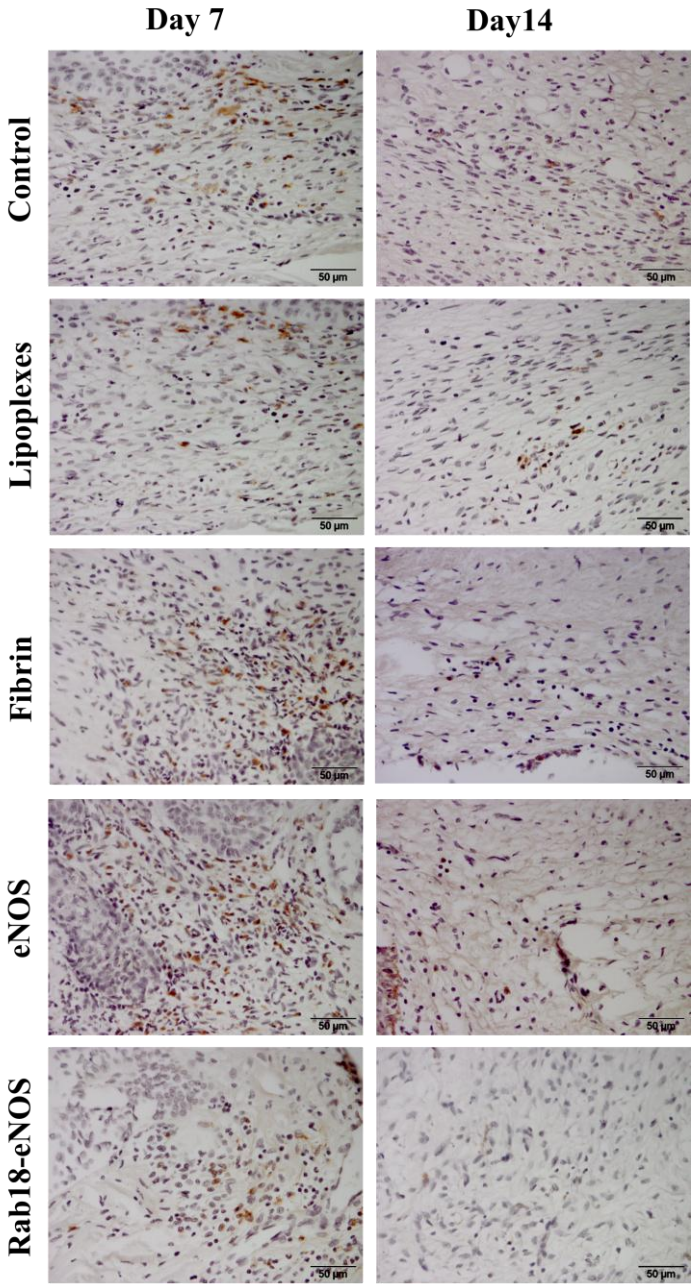

Figure 5.6: Ram11 immunostaining for macrophages (stained as brown cells) in various treatments at day 7 and 14. Hematoxylin was used for counterstaining. The scale bars represent 50 µm.

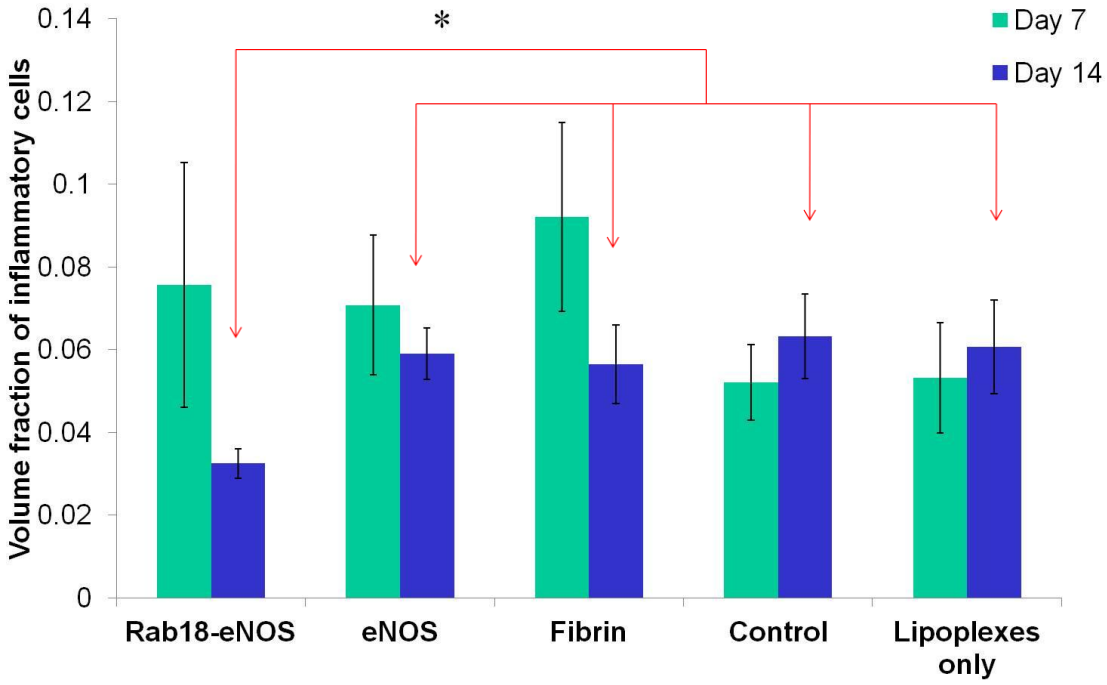

Figure 5.7: Volume fraction of inflammatory cells in the wounds. The addition of Rab18 to eNOS reduces inflammatory reaction significantly compared to all other treatments at day 14 post-surgery. * represents statistical significance by one way ANOVA (n = 8, p < 0.05).

Table 5.2: Pearson's correlations between the wound healing parameters

	Rab18-eNOS					**eNOS**				
	W	***I***	***S***	***L***	***R***	***W***	***I***	***S***	***L***	***R***
I	0.23					-0.34				
S	-0.47	0.05				-0.78	-0.26			
L	0.26	0.68	0.41			-0.47	-0.58	**0.73***		
R	-0.22	**-0.75***	-0.38	**-0.99***		0.48	0.55	-0.67	**-0.98***	
E	0.01	**0.84***	0.08	0.69	**-0.78***	0.20	-0.43	0.21	0.39	-0.36
	Fibrin					**Lipoplexes**				
	W	***I***	***S***	***L***	***R***	***W***	***I***	***S***	***L***	***R***
I	0.03					-0.06				
S	0.50	0.07				-0.22	-0.66			
L	0.17	0.64	0.27			-0.17	-0.83	0.94		
R	-0.12	-0.61	-0.24	**-0.99***		0.34	**0.74***	-0.94	**-0.97***	
E	0.10	0.10	0.60	0.49	-0.53	0.17	-0.41	0.29	0.22	-0.14
	Control									
	W	***I***	***S***	***L***	***R***					
I	-0.44									
S	-0.11	0.22								
L	-0.15	0.08	0.48							
R	0.03	-0.07	-0.38	**-0.97***						
E	0.39	0.09	0.48	-0.30	0.28					

Note: *W* = Wound closure, *I* = volume fraction of inflammatory cells, *S* = Surface density of blood vessels, *L* = Length density of blood vessels, *R* = radial diffusion distance

In the eNOS treated group, the length density of blood vessels was positively correlated to surface density and negatively correlated with the radial diffusion distance. In lipoplexes treated group, increase in inflammation was positively correlated with the increase in radial diffusion distance. In the control treatment and fibrin treated control, apart from the negative correlation between radial diffusion distance and length density, no other significant correlations were found.

5.4 Discussion

Chronic wound healing is a complex pathological phenomenon involving a number of molecular pathways, manifested in gross disruption of all the phases of wound healing. Thus, it can be easily construed that the therapeutic benefit following single gene therapy would be modest at best. Therefore it is logical to appreciate the need for multiple gene therapy promoting normalization of various pathological aspects of diabetic wound healing. To investigate the potential of multiple gene therapy in tissue repair, a number of studies have been performed. A study showed synergistic effect of combination of PDGF and IGF-1 delivery over and above separate individual delivery[53]. Another study found that a combination of PDGF and FGF-2 delivery led to higher DNA content in the wounds than PDGF or FGF-2 delivered individually[54]. Combination, of KGF and IGF-1, also showed beneficial effects resulting in increased re-epithelialization, increased proliferation and decreased apoptosis compared to single gene constructs[55]. Also, simultaneous delivery of VEGF-A and FGF-4 genes led to significantly faster wound closure, increased granulation tissue formation, vascularity and dermal matrix deposition[56]. Beneficial effects of multiple gene therapy have been observed in other repair systems such as bone repair. IGF-1 and IL-6 have been shown independently to stimulate OP-1 action in synergistic fashion in primary cultures of rat osteoblastic cells leading to enhanced alkaline phosphatase activity and bone nodule formation[57 58]. FGF-2 plus BMP-2 combination enhances osteoinductive capacity[59].

Another aspect to consider in multiple gene therapy is the dynamic nature of wound healing with overlapping yet phasic manner of gene regulation orchestrated in the normal progression of wound healing. From this display of gene expression, it can be construed that the simultaneous delivery of multiple genes does not mimic the

physiological process and may not be as rewarding as multiple gene delivery in a controlled manner so as to create a sequential, dynamic, or spatiotemporal pattern of gene delivery and expression thereby. To achieve this goal, tissue engineered scaffolds, are being employed in a number of ways. Current emphasis is on the design of 3D tissue engineered constructs capable of delivering bioactive molecules at different release profiles creating desirable expression patterns. Some of the common strategies are: entrapment of growth factors or gene complexes in 3D constructs by immobilizing them through covalent or electrostatic bonding or through biomolecular interactions; use of crosslinked materials with regions of variable crosslinking; incorporation of particulate systems having different degradation profile within 3D scaffolds; preloading the particles/spheres with different genes and compartmentalizing these particles/spheres within 3D constructs.

In light of these considerations, this study was designed for a treatment with multiple genes in a dynamically controlled manner. Steps towards development of treatment involved choice of genes to target the reduced angiogenesis and increased inflammation and proteolysis and utilization of fibrin-in-fibrin temporal release system, capable of delivering genes in a dynamically controlled manner. In this study, proangiogenic gene eNOS was used. Previously, therapeutic benefit of eNOS delivery to increase functional angiogenesis has been shown in the same animal model as used in this study[32]. While the previous study used adenoviral carrier, the non-viral carrier employed in this study can be considered as an advantage in terms of its superior safety profile. It is interesting to note that the results at day 7 post-surgery show significantly higher surface density in eNOS treated group compared to groups treated with fibrin, lipoplexes alone and control, suggesting that the therapeutic effect of eNOS is not compromised by the use of a non-viral carrier.

The Rab18 gene was employed as secretory control molecule to reduce inflammation and proteolysis. Rab18 gene complexes were encapsulated in fibrin microspheres which were embedded in fibrin gel that carried eNOS gene complexes. This fibrin-in-fibrin system was employed for dynamic release of two genes (Figure 5.8).

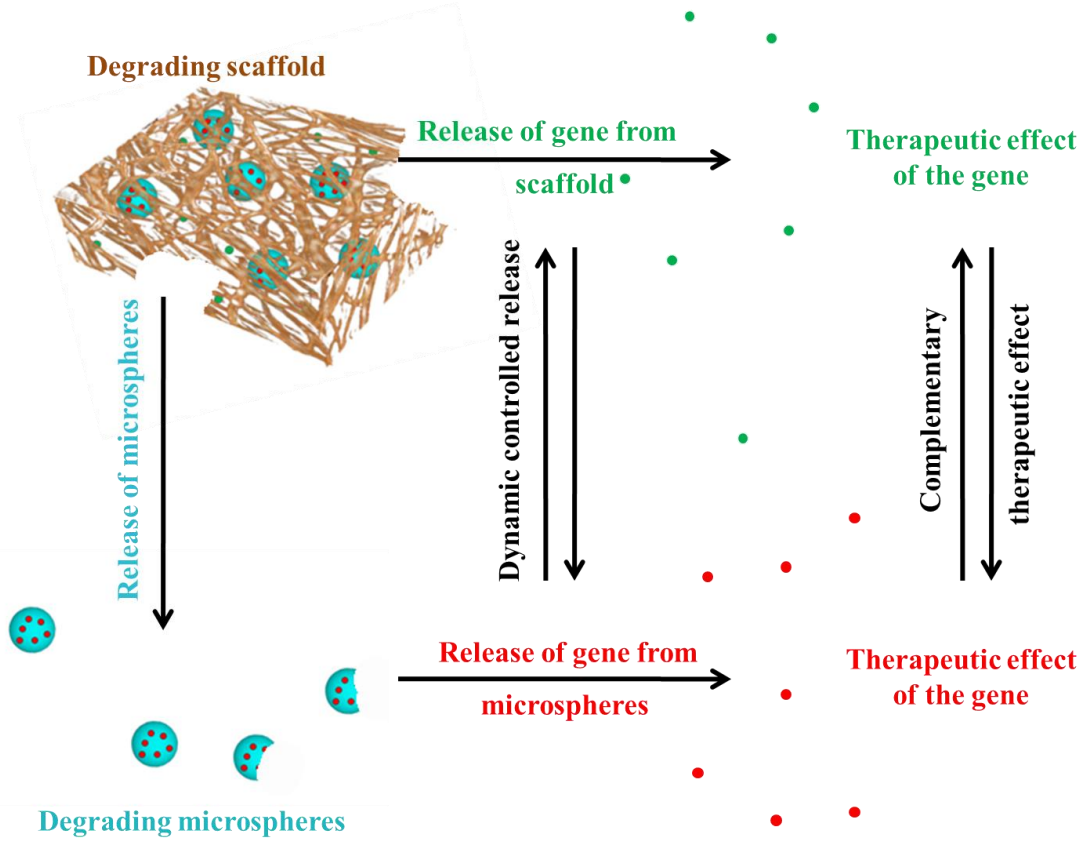

Figure 5.8: Schematic showing differentially degrading fibrin-in-fibrin system for dynamic controlled delivery of two therapeutic genes, eNOS in fibrin scaffold and Rab18 in fibrin microspheres embedded in fibrin scaffold. This system can be adjusted to the need by varying the degradation profile of the components to suit particular therapeutic need. The use of non-viral gene carriers within this system complements the therapeutic effect.

Previously, the fibrin microspheres have been shown to degrade with a release profile different to that of fibrin gel[50]. Although, the delivery system was not designed for purely sequential delivery, the peaks of eNOS and Rab18 release will be dynamically separated in space and time. Considering the secretory control function of Rab18, there was apprehension that the delivery of two genes can result in detrimental effects on the paracrine functions of eNOS or NO. Comparable results of surface density of blood vessels in eNOS treated and Rab18-eNOS treated group suggests that addition of Rab18 to eNOS gene therapy, by employing fibrin-in-fibrin system, did not have a negative effect on the angiogenic function of eNOS. Rather, Rab18-eNOS resulted in more functional angiogenesis, evident from higher length density and reduced radial diffusion distance in Rab18-eNOS treated group compared eNOS treated at day 14 post-surgery.

Pearson's coefficient of correlations between healing parameters in Rab18-eNOS treated group revealed many complex interactions. A decrease in radial diffusion distance correlated with increase in percent epithelialization. This negative correlation between radial diffusion distance and percent epithelialization was significant. Yet, even when radial diffusion distance in the Rab18-eNOS treated group was significantly reduced compared to all other treatments; the percent epithelialization did not show any significant differences. There are few possible explanations based on the observations in the study. For the power of study to be close to 80%, high "n" number is required for percent epithelialization calculations. In addition, there was positive correlation of percent epithelialization with inflammation in the Rab18-eNOS treated group where the inflammation was significantly lower compared to all other groups. Although, ideally all correlations are expected to be significant from the treatment, considering no significant correlations in control group suggests that the Rab18-eNOS treatment leads to more correlated parameters, a step towards normalization of wound healing.

While the mechanism of the beneficial effect of Rab18-eNOS is not completely understood, the concomitant reduction of inflammation, manifested as significantly lower volume of inflammatory cells, is likely to have an effect. Although all the fibrin containing treatments showed some trend towards increase in the volume fraction of inflammatory cells at day 7, the Rab18-eNOS treatment showed significantly lower

inflammatory cell infiltration at day 14 compared to all other treatments. As a direct result of reduced inflammation and increased functional angiogenesis following Rab18-eNOS treatment, the percent wound closure was significantly increased at day 14. Thus, proposed secretory control function of Rab18 can be thought to have played a beneficial effect. One of the limitations of the current study is the difficulty in corroborating this notion with molecular studies at mRNA level. In order to identify molecular interactions, given the dynamic nature of the delivery system, more than two time points are required. The current study was designed for feasibility assessment and for assessment at molecular a more mechanistic study needs to be designed.

In summary, addition of Rab18 to eNOS treatment, via fibrin-in-fibrin system, enhances wound closure, increases functional angiogenesis and reduces inflammation. This action of Rab18 can be attributed to its negative regulation of secretion of pro-inflammatory cytokines as hypothesized. Thus, the beneficial effect of combined Rab18-eNOS treatment, using the dynamically controlled fibrin-in-fibrin gene delivery system, on wound healing can thus be exploited for treatment of diabetic wounds.

5.5 References

1. Brem H, Jacobs T, Vileikyte L, Weinberger S, Gibber M, Gill K, Tarnovskaya A, Entero H, Boulton AJ. Wound-healing protocols for diabetic foot and pressure ulcers. *Surg Technol Int* 2003;11:85-92.

2. Martin A, Komada MR, Sane DC. Abnormal angiogenesis in diabetes mellitus. *Med Res Rev* 2003;23(2):117-45.

3. Schaffer MR, Tantry U, Efron PA, Ahrendt GM, Thornton FJ, Barbul A. Diabetes-impaired healing and reduced wound nitric oxide synthesis: a possible pathophysiologic correlation. *Surgery* 1997;121(5):513-9.

4. Amadeu TP, Costa AM. Nitric oxide synthesis inhibition alters rat cutaneous wound healing. *J Cutan Pathol* 2006;33(7):465-73.

5. Schulz G, Stechmiller J. Wound healing and nitric oxide production: too little or too much may impair healing and cause chronic wounds. *Int J Low Extrem Wounds* 2006;5(1):6-8.

6. Nakai K, Fujii S, Yamamoto A, Igarashi J, Kubota Y, Kosaka H. Effects of high glucose on NO synthesis in human keratinocyte cell line (HaCaT). *J Dermatol Sci* 2003;31(3):211-8.

7. Liu ZJ, Velazquez OC. Hyperoxia, endothelial progenitor cell mobilization, and diabetic wound healing. *Antioxid Redox Signal* 2008;10(11):1869-82.

8. Childress BB, Stechmiller JK. Role of nitric oxide in wound healing. *Biol Res Nurs* 2002;4(1):5-15.

9. Witte MB, Barbul A. Role of nitric oxide in wound repair. *Am J Surg* 2002;183(4):406-12.

10. Efron DT, Most D, Barbul A. Role of nitric oxide in wound healing. *Curr Opin Clin Nutr Metab Care* 2000;3(3):197-204.

11. Frank S, Kampfer H, Wetzler C, Pfeilschifter J. Nitric oxide drives skin repair: novel functions of an established mediator. *Kidney Int* 2002;61(3):882-8.

12. Stallmeyer B, Anhold M, Wetzler C, Kahlina K, Pfeilschifter J, Frank S. Regulation of eNOS in normal and diabetes-impaired skin repair: implications for tissue regeneration. *Nitric Oxide* 2002;6(2):168-77.

13. Witte MB, Kiyama T, Barbul A. Nitric oxide enhances experimental wound healing in diabetes. *Br J Surg* 2002;89(12):1594-601.

14. Dhaunsi GS, Ozand PT. Nitric oxide promotes mitogen-induced dna synthesis in human dermal fibroblasts through cGMP. *Clin Exp Pharmacol Physiol* 2004;31(1-2):46-9.

15. Silva SY, Rueda LC, Marquez GA, Lopez M, Smith DJ, Calderon CA, Castillo JC, Matute J, Rueda-Clausen CF, Orduz A, Silva FA, Kampeerapappun P, Bhide M, Lopez-Jaramillo P. Double blind, randomized, placebo controlled clinical trial for the treatment of diabetic foot ulcers, using a nitric oxide releasing patch: PATHON. *Trials* 2007;8:26.

16. Schaffer M, Bongartz M, Fischer S, Proksch B, Viebahn R. Nitric oxide restores impaired healing in normoglycaemic diabetic rats. *J Wound Care* 2007;16(7):311-6.

17. Li Y, Lee PI. Controlled nitric oxide delivery platform based on S-nitrosothiol conjugated interpolymer complexes for diabetic wound healing. *Mol Pharm* 2010;7(1):254-66.

18. Weller RB. Nitric oxide-containing nanoparticles as an antimicrobial agent and enhancer of wound healing. *J Invest Dermatol* 2009;129(10):2335-7.

19. Masters KS, Leibovich SJ, Belem P, West JL, Poole-Warren LA. Effects of nitric oxide releasing poly(vinyl alcohol) hydrogel dressings on dermal wound healing in diabetic mice. *Wound Repair Regen* 2002;10(5):286-94.

20. Bove PF, Wesley UV, Greul AK, Hristova M, Dostmann WR, van der Vliet A. Nitric oxide promotes airway epithelial wound repair through enhanced activation of MMP-9. *Am J Respir Cell Mol Biol* 2007;36(2):138-46.

21. Burrow JW, Koch JA, Chuang HH, Zhong W, Dean DD, Sylvia VL. Nitric oxide donors selectively reduce the expression of matrix metalloproteinases-8 and -9 by human diabetic skin fibroblasts. *J Surg Res* 2007;140(1):90-8.

22. Lizarbe TR, Garcia-Rama C, Tarin C, Saura M, Calvo E, Lopez JA, Lopez-Otin C, Folgueras AR, Lamas S, Zaragoza C. Nitric oxide elicits functional MMP-13 protein-tyrosine nitration during wound repair. *FASEB J* 2008;22(9):3207-15.

23. Schaffer MR, Efron PA, Thornton FJ, Klingel K, Gross SS, Barbul A. Nitric oxide, an autocrine regulator of wound fibroblast synthetic function. *J Immunol* 1997;158(5):2375-81.

24. Lopez-Rivera E, Lizarbe TR, Martinez-Moreno M, Lopez-Novoa JM, Rodriguez-Barbero A, Rodrigo J, Fernandez AP, Alvarez-Barrientos A, Lamas S, Zaragoza C. Matrix metalloproteinase 13 mediates nitric oxide activation of endothelial cell migration. *Proc Natl Acad Sci U S A* 2005;102(10):3685-90.

25. Romana-Souza B, Nascimento AP, Monte-Alto-Costa A. Propranolol improves cutaneous wound healing in streptozotocin-induced diabetic rats. *Eur J Pharmacol* 2009;611(1-3):77-84.

26. Luo JD, Hu TP, Wang L, Chen MS, Liu SM, Chen AF. Sonic hedgehog improves delayed wound healing via enhancing cutaneous nitric oxide function in diabetes. *Am J Physiol Endocrinol Metab* 2009;297(2):E525-31.

27. Houreld NN, Sekhejane PR, Abrahamse H. Irradiation at 830 nm stimulates nitric oxide production and inhibits pro-inflammatory cytokines in diabetic wounded fibroblast cells. *Lasers Surg Med* 2010;42(6):494-502.

28. Bizzarro MJ, Bhandari V. Nitric Oxide. In: Bowlin GL, Wnek G, editors. *Encyclopaedia of Biomaterials and Biomedical Engineering*. New York: Marcel Dekker, Inc, 2004:1075-83.

29. Schwentker A, Billiar TR. Nitric oxide and wound repair. *Surg Clin North Am* 2003;83(3):521-30.

30. Knowles RG, Moncada S. Nitric oxide synthases in mammals. *Biochem J* 1994;298 (Pt 2):249-58.

31. Hagensen MK, Shim J, Falk E, Bentzon JF. Flanking recipient vasculature, not circulating progenitor cells, contributes to endothelium and smooth muscle in murine allograft vasculopathy. *Arterioscler Thromb Vasc Biol* 2011;31(4):808-13.

32. Breen A, Dockery P, O'Brien T, Pandit A. The use of therapeutic gene eNOS delivered via a fibrin scaffold enhances wound healing in a compromised wound model. *Biomaterials* 2008;29(21):3143-51.

33. Pradhan L, Nabzdyk C, Andersen ND, LoGerfo FW, Veves A. Inflammation and neuropeptides: the connection in diabetic wound healing. *Expert Rev Mol Med* 2009;11:e2.

34. Mishima Y, Kuyama A, Tada A, Takahashi K, Ishioka T, Kibata M. Relationship between serum tumor necrosis factor-alpha and insulin resistance in obese men with Type 2 diabetes mellitus. *Diabetes Res Clin Pract* 2001;52(2):119-23.

35. Jude EB, Blakytny R, Bulmer J, Boulton AJ, Ferguson MW. Transforming growth factor-beta 1, 2, 3 and receptor type I and II in diabetic foot ulcers. *Diabet Med* 2002;19(6):440-7.

36. Tsunawaki S, Sporn M, Ding A, Nathan C. Deactivation of macrophages by transforming growth factor-beta. *Nature* 1988;334(6179):260-2.

37. Lobmann R, Ambrosch A, Schultz G, Waldmann K, Schiweck S, Lehnert H. Expression of matrix-metalloproteinases and their inhibitors in the wounds of diabetic and non-diabetic patients. *Diabetologia* 2002;45(7):1011-6.

38. Mast BA, Schultz GS. Interactions of cytokines, growth factors, and proteases in acute and chronic wounds. *Wound Repair Regen* 1996;4(4):411-20.

39. Bullen EC, Longaker MT, Updike DL, Benton R, Ladin D, Hou Z, Howard EW. Tissue inhibitor of metalloproteinases-1 is decreased and activated gelatinases are increased in chronic wounds. *J Invest Dermatol* 1995;104(2):236-40.

40. Liu Y, Min D, Bolton T, Nube V, Twigg SM, Yue DK, McLennan SV. Increased matrix metalloproteinase-9 predicts poor wound healing in diabetic foot ulcers. *Diabetes Care* 2009;32(1):117-9.

41. Ladwig GP, Robson MC, Liu R, Kuhn MA, Muir DF, Schultz GS. Ratios of activated matrix metalloproteinase-9 to tissue inhibitor of matrix metalloproteinase-1 in wound fluids are inversely correlated with healing of pressure ulcers. *Wound Repair Regen* 2002;10(1):26-37.

42. Lobmann R, Zemlin C, Motzkau M, Reschke K, Lehnert H. Expression of matrix metalloproteinases and growth factors in diabetic foot wounds treated with a protease absorbent dressing. *J Diabetes Complications* 2006;20(5):329-35.

43. Muller M, Trocme C, Lardy B, Morel F, Halimi S, Benhamou PY. Matrix metalloproteinases and diabetic foot ulcers: the ratio of MMP-1 to TIMP-1 is a predictor of wound healing. *Diabet Med* 2008;25(4):419-26.

44. Lobmann R, Schultz G, Lehnert H. Proteases and the diabetic foot syndrome: mechanisms and therapeutic implications. *Diabetes Care* 2005;28(2):461-71.

45. Wall SJ, Sampson MJ, Levell N, Murphy G. Elevated matrix metalloproteinase-2 and -3 production from human diabetic dermal fibroblasts. *Br J Dermatol* 2003;149(1):13-6.

46. Nwomeh BC, Liang HX, Cohen IK, Yager DR. MMP-8 is the predominant collagenase in healing wounds and nonhealing ulcers. *J Surg Res* 1999;81(2):189-95.

47. Pirila E, Korpi JT, Korkiamaki T, Jahkola T, Gutierrez-Fernandez A, Lopez-Otin C, Saarialho-Kere U, Salo T, Sorsa T. Collagenase-2 (MMP-8) and matrilysin-2 (MMP-26) expression in human wounds of different etiologies. *Wound Repair Regen* 2007;15(1):47-57.

48. Terasaki K, Kanzaki T, Aoki T, Iwata K, Saiki I. Effects of recombinant human tissue inhibitor of metalloproteinases-2 (rh-TIMP-2) on migration of epidermal keratinocytes in vitro and wound healing in vivo. *J Dermatol* 2003;30(3):165-72.

49. Wall SJ, Bevan D, Thomas DW, Harding KG, Edwards DR, Murphy G. Differential expression of matrix metalloproteinases during impaired wound healing of the diabetes mouse. *J Invest Dermatol* 2002;119(1):91-8.

50. Kulkarni MM, Greiser U, O'Brien T, Pandit A. A temporal gene delivery system based on fibrin microspheres. *Mol Pharm* 2011;8(2):439-46.

51. Lenzen S, Panten U. Alloxan: history and mechanism of action. *Diabetologia* 1988;31(6):337-42.

52. Garcia Y, Breen A, Burugapalli K, Dockery P, Pandit A. Stereological methods to assess tissue response for tissue-engineered scaffolds. *Biomaterials* 2007;28(2):175-86.

53. Lynch SE, Nixon JC, Colvin RB, Antoniades HN. Role of platelet-derived growth factor in wound healing: synergistic effects with other growth factors. *Proc Natl Acad Sci U S A* 1987;84(21):7696-700.

54. Sprugel KH, McPherson JM, Clowes AW, Ross R. Effects of growth factors in vivo. I. Cell ingrowth into porous subcutaneous chambers. *Am J Pathol* 1987;129(3):601-13.

55. Jeschke MG, Klein D. Liposomal gene transfer of multiple genes is more effective than gene transfer of a single gene. *Gene Ther* 2004;11(10):847-55.

56. Jazwa A, Kucharzewska P, Leja J, Zagorska A, Sierpniowska A, Stepniewski J, Kozakowska M, Taha H, Ochiya T, Derlacz R, Vahakangas E, Yla-Herttuala S, Jozkowicz A, Dulak J. Combined vascular endothelial growth factor-A and fibroblast growth factor 4 gene transfer improves wound healing in diabetic mice. *Genet Vaccines Ther* 2010;8:6.

57. Yeh LC, Zavala MC, Lee JC. Osteogenic protein-1 and interleukin-6 with its soluble receptor synergistically stimulate rat osteoblastic cell differentiation. *J Cell Physiol* 2002;190(3):322-31.

58. Yeh LC, Adamo ML, Olson MS, Lee JC. Osteogenic protein-1 and insulin-like growth factor I synergistically stimulate rat osteoblastic cell differentiation and proliferation. *Endocrinology* 1997;138(10):4181-90.

59. Takita H, Tsuruga E, Ono I, Kuboki Y. Enhancement by bFGF of osteogenesis induced by rhBMP-2 in rats. *Eur J Oral Sci* 1997;105(6):588-92.

Chapter Six

Summary and Future Directions

Contents of this chapter have previously been published:

Kulkarni M., Greiser U., O'Brien T. and Pandit A. 'Liposomal Gene Delivery Mediated by Tissue-engineered Scaffolds.' *Trends Biotechnol* 2010;28(1):28-36.

6.1 Introduction

With almost epidemic growth in incidence of diabetes worldwide in recent years, the chronic non-healing leg and foot ulcers have emerged as a major challenge medically, economically and socially. The current rigorous medical and surgical regimens aiming to aid healing process have met with only modest success to lower the amputation rate. Since the chronic nature of diabetic wound healing is multifactorial, development of a gene delivery system capable of delivering multiple therapeutic genes in a spatiotemporally controlled manner addressing the pathological disarray is required. However, the gene regulation in chronic wound healing is not completely understood. Hence, a molecular approach should be taken to unwind the effects of hyperglycemia at genetic level. The overall goal in this project was normalization of chronic wound healing by developing a fibrin based gene delivery system with controlled release.

6.2 Summary

6.2.1 Phase I – Fibrin-lipoplex System

The objective of phase I (Chapter 2) was to assess the feasibility of a fibrin gel to deliver lipoplexes that encode multiple genes. This was achieved by assessing the *in vitro* release profile of lipoplexes from the fibrin gel, qualitative study of biomolecular interaction between components of fibrin gel and lipofectin to discern the mechanism for the controlled release and finally assessing the functional viability of released lipoplexes by investigating the *in vitro* and *in vivo* transfection efficiency of the lipoplexes released from fibrin gel. Fibrin-lipoplex system was successfully fabricated for simultaneous delivery of multiple genes in phase I of this project. The combinatorial approach taken was based on the complementary improvement provided through embedding the lipoplexes in highly concentrated fibrin gel (at fibrinogen concentration of 60 mg/ml and thrombin concentration of 4 IU). Although, by adjusting fibrinogen and thrombin concentrations, the release profile of the bioactive molecules embedded within fibrin gel can be altered, in this study the choice of fibrin component concentration was dictated by the fact that the intended *in vivo* use and future clinical use of the combined fibrin-lipoplex system treatment require almost immediate gelling on the wound.

The results of release study suggest that there is some biomolecular interaction between components of fibrin-lipoplex system which accounts for encapsulating the lipoplexes within the system and allowing release only after enzymatic dissolution. The surface plasmon resonance study confirmed at least qualitatively that this biomolecular interaction exists between fibrinogen and lipofectin. Further to this, the concern of functional viability of lipoplexes embedded in the fibrin was addressed through *in vitro* transfection study and *in vivo* study with simultaneous delivery of two reporter genes. The delivery at day 7 post-surgery of both the reporter genes in the *in vivo* study suggested that the fibrin-lipoplex system, at the concentrations used for instant gelling, is functionally suitable.

6.2.2 Phase II – Fibrin Microspheres

In order to emulate the dynamic control in the delivery system and to extend the loading capacity of the system, the phase II (Chapter 3) of this project was focused on development of a more compact scaffold in the form of fibrin microspheres. Since these microspheres were fabricated using fibrin, the delivery system remained similar to fibrin-lipoplex system. Additionally, the lipoplexes can be embedded in the gel and microspheres. It was for the first time that fibrin microspheres were being used for gene delivery.

Some modifications were made to the routine preheated-oil in water emulsion method in order to fabricate fibrin microspheres embedding lipoplexes. In order to protect DNA from being exposed to the high temperature at which fibrin microspheres were fabricated, the biomolecular interaction between in the fibrinogen and lipofectin was exploited. The lipoplexes were first mixed with fibrinogen before addition of thrombin. This gave extra protection to the lipoplexes. Addition of two surfactants, one for oil phase and other for water phase of the emulsion ensured formation of emulsion rapidly again aiding the stability of lipoplexes and DNA. This addition of two surfactants along with overnight stirring also aided fabrication of the desired micron sized spheres.

After confirming the encapsulation through fluorescence studies, the fibrin microspheres were subjected to *in vivo* evaluation for functional stability of encapsulated lipoplexes. eNOS used as model therapeutic molecule was also a relevant

molecule for future use in compromised wound healing. There was a significant increase in the mRNA levels of eNOS and subsequent increase in angiogenesis 7 days after the delivery of fibrin microspheres. Then the release profiles of fibrin gel and fibrin microspheres were compared and significant differences were observed in the degradation rates. Based on this differential degradation, a fibrin in fibrin system was designed which will embed fibrin microspheres carrying one therapeutic gene complexes in fibrin gel which also carried another therapeutic gene complexes. Thus, dynamic controlled delivery of therapeutic genes was envisioned through fibrin-in-fibrin system.

6.2.3 Phase III – Gene Expression Analysis

Having developed the fibrin-in-fibrin system, phase III (Chapter 4) was focused on molecular expression analysis during *in vitro* scratch wound healing in primary human keratinocytes under the hyperglycemia. This analysis was done to identify a suitable therapeutic gene which will complement another therapeutic gene eNOS. eNOS was chosen because reduced angiogenesis is well established pathology in diabetic wound healing[1] [2] and eNOS delivery has been shown to be therapeutically beneficial[3]. A detailed rationale for use of eNOS is described in chapter 5. To fathom the other therapeutic gene, the differential regulation of gene expression was investigated in wounded primary human keratinocytes grown in normal and high glucose conditions. Gene regulation was studied by microarray analysis following a meticulously designed *in vitro* wound healing experiment. The *in vitro* wound model comprised of multiple predetermined scratch wounds designed to ensure that more than 50% cells take part in wound healing was thus suitable for molecular studies. The migration of cells was significantly affected in high glucose in confirmation with previous findings and hence the gene expression pattern that microarray analysis revealed was more reliable. As detailed in chapter, thousands of genes were found to be dysregulated in wound healing under high glucose conditions. Rab18 was chosen as potential target (Chapter 4, section 4.4.1) in the light of its secretory control function and hypersecretory profile diabetic wound healing which includes proinflammatory cytokines like TNF-α, IL-1β and proteolytic enzymes like MMP-2 and MMP-9.

6.2.4 Phase IV – Fibrin-in-fibrin System

In phase IV (Chapter 5), an *in vivo* feasibility study was performed to investigate the beneficial effect of Rab18 gene complexes delivered with eNOS gene complexes through the dynamically controlled fibrin-in-fibrin system in an alloxan induced rabbit ear ulcer model of compromised wound healing. The effect of the treatment on wound healing was investigated stereologically by quantification of parameters such as percent wound closure, volume fraction of inflammatory cells, surface and length density of blood vessels and radial diffusion distance. Comparisons were made between Rab18-eNOS treatment and eNOS alone and also control treatments such as lipoplexes alone, fibrin alone and no treatment control. Rab18-eNOS treatment showed highest wound closure at day 14 post-surgery with reduction in inflammation and increased functional angiogenesis. These beneficial effects of Rab18-eNOS treatment may be considered to be due to the combination of proangiogenic effect of eNOS and secretion control by Rab18. The possible role of Rab18 in secretion control is depicted in Figure 6.1. The most salient findings of the project are depicted in the Figure 6.2. This list is not comprehensive however is "at a glance" schematic.

6.3 Limitations

6.3.1 Phase I

The fibrin lipoplex system developed in phase I has at least two major limitations which need to be dealt with for its further investigation for delivery therapeutic genes leading to normalization of compromised wound healing. One limitation is the loading capacity of the system. Since the practical application of the system is dependent on gelling time, the amount of lipoplexes the system can carry are intuitively limited as adding more will result in dilution and thereby longer gelling time. Another limitation is more mechanistic in nature. The simultaneous delivery of multiple genes is not always beneficial as in normal physiological repair/regeneration following an injury the key genes are not simultaneously overexpressed; rather there appears to be innate dynamic control over the gene expression patterns. In view of this fact, a number of scaffold based non-viral gene delivery systems have employed various strategies to create spatiotemporal pattern[4].

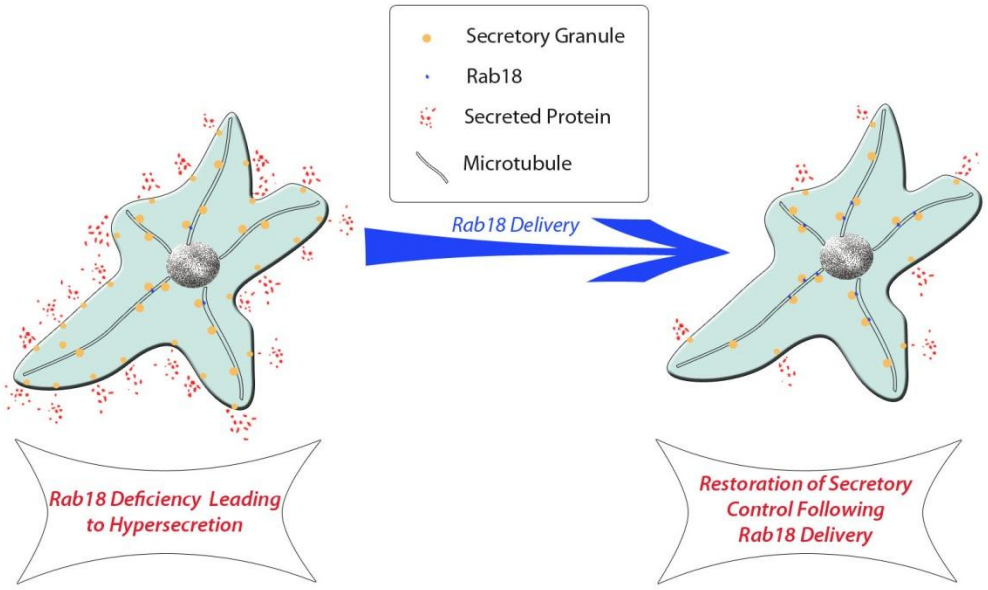

Figure 6.1: Schematic showing the proposed effect of Rab18 delivery on secretion control

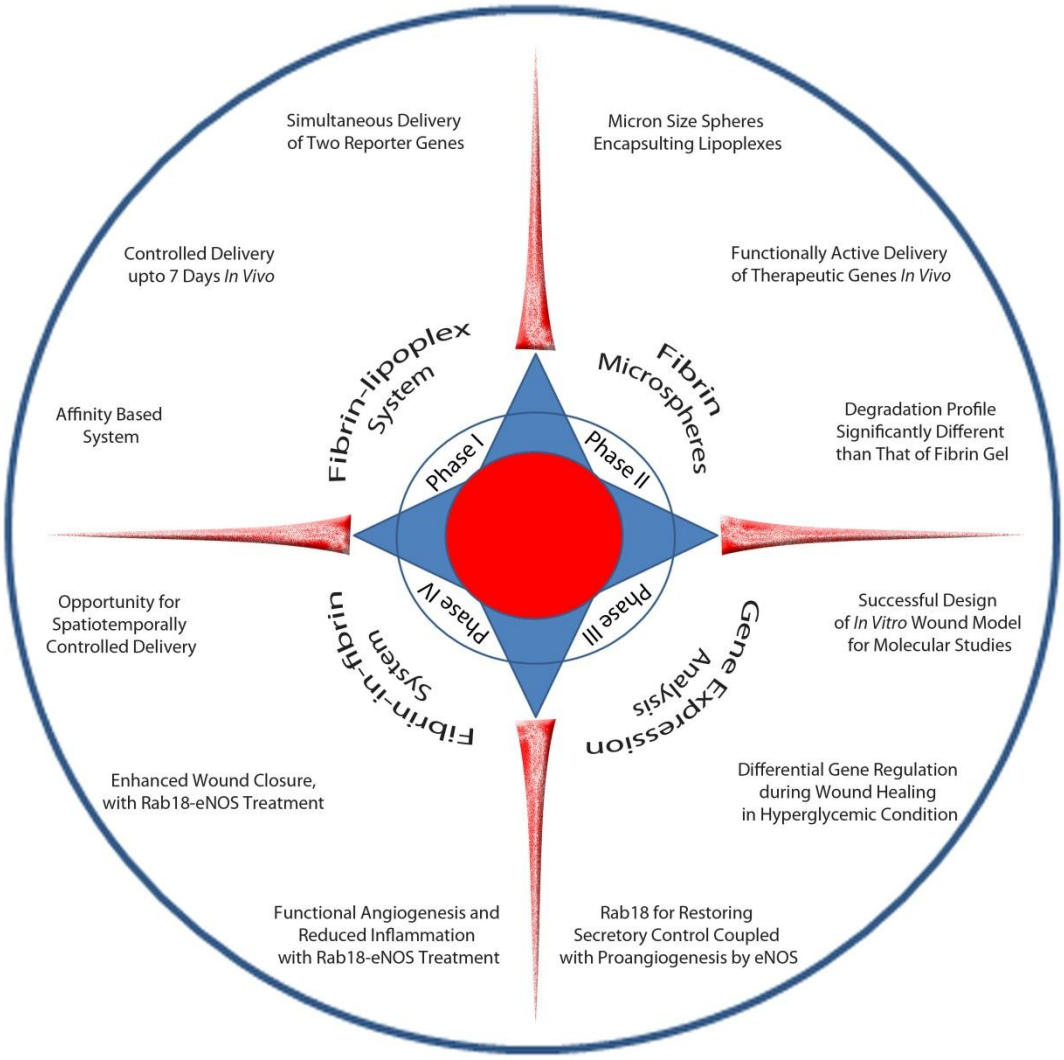

Figure 6.2: Schematic showing salient milestones achieved during the project. The each of the four phases resulted in a number of important findings. Only the most important ones are listed in this schematic.

The fibrin-lipoplex system is affinity based but the biomolecular studies in this research have only been done qualitatively and with the particular liposomes used in the study. A thorough understanding of interactions between liposomes and the scaffold with quantification and investigating exact binding sites might pave the way towards fathoming the release mechanisms and adding additional levels of control.

6.3.2 Phase II

In order to increase the loading capacity of fibrin-lipoplex system and to give an opportunity for dynamic control, phase II was focused on fibrin microspheres. Although, fibrin microspheres, encapsulating lipoplexes, fabricated by the method developed in phase II were successful to maintain the functional integrity of the DNA, probably due to affinity between the fibrinogen and lipofectin; the high temperature used in the fabrication protocol may limit its use in a non-affinity based systems and further research in alternative methods using lower temperature may be performed.

6.3.3 Phase III

The target discovery route taken in the phase III resulted in many interesting findings with a number of up- and down-regulated genes. For practical reasons, one best candidate from amongst the downregulated genes (i.e. Rab18) was chosen. One limitation of the experimental design can be the fact that wounding was performed under only hyperglycemia as the salient defining feature of diabetes. It can be argued that since hyperglycemia does not represent the complete complexity of the diabetic pathology, it is oversimplification. However, hyperglycemia has been reported to cause significant compromisation in wound healing by hampering proliferation and migration of keratinocytes[5-11]. In phase III experiments (Chapter 4, section 4.3.2), similar compromisation was observed in the wounded keratinocytes grown in hyperglycemic conditions. Thus, the relevance of the model is established. Moreover, beneficial effect on the wound healing observed following the gene delivery of Rab18-eNOS (Chapter 5) reinforces the validity of the *in vitro* model. Nevertheless, it is admitted that assessment of gene regulation in samples from diabetic patients matched for confounding factors or *in vitro* experimental design using different cells affected by diabetes in an environment

simulating more closely the complex biochemical pathology of diabetes (discussed in section 6.5.1) can be rewarding.

6.3.4 Phase IV

In phase IV, an alloxan induced rabbit ear ulcer of compromised wound healing was utilized. This model has been validated previously for compromised wound healing[12]. However, since it is chemically induced hyperglycemia for one week, an animal model representing chronicity of diabetes and including other aspects of diabetes such as ischemia will be more appropriate. Efforts have been made to create a long term diabetic rabbit model by maintaining hyperglycemia for one year[13]. Induction of ischemia by ligating the artery supplying rabbit ear along with induction of hyperglycemia makes the model more close to the diabetic scenario. This can create a new animal model better suited for wound healing experiments. However, stability of the model and validation for compromised healing will be required. Also, to recreate the pathology of diabetes at molecular level, research is needed for development of a genetic model of rabbit. Although there are genetic models available in other species such as db/db mice, rabbit ear ulcer model is ideal for quantification of various parameters by stereological analysis while all the back ulcer models suffer from major disadvantage of wound contraction. The back ulcer models also lack a reference plane which is required for quantification purpose whereas the ear ulcer model provides the cartilage as a perfect reference plane. Hence, it will be worth performing research on development of genetic model of diabetes in rabbit.

Another challenge was the evaluation of effects of gene therapy at molecular level. Although the fibrin microspheres and the fibrin gel have been shown to degrade at different rates (Chapter 3, section 3.3.4), the peaks in their release profiles were not expected to be distinctly sequential; rather presence of multiple peaks with dynamic spatiotemporal distribution is more likely. The current study, however, was designed for investigating the feasibility of Rab18-eNOS gene therapy via fibrin in fibrin study for normalization of or at least improvement in the compromised wound healing. Therefore, the time points chosen for this study were suitable to evaluate and quantify the wound healing parameters. However, in order to investigate the effects of Rab18-

eNOS gene therapy at molecular level, a more mechanistic study with more time points will be required and probably in an animal model is validated for the molecular changes consistent with diabetes.

6.4 Conclusions

The conclusions derived from the research performed in the current project can be summarized as follows:

6.4.1 Phase I

The objective of this phase was to assess the feasibility of a fibrin gel to deliver lipoplexes that encode multiple genes.

Conclusions:

- *In vitro* release study showed that lipoplexes were held within the fibrin gel with very minimal release up to 144 hours and upon plasmin dilution of the fibrin gel, the DNA plasmid in the complexes was intact.
- There exists a biomolecular interaction between fibrinogen and lipofectin (the commercially available liposomes used in the study).
- The lipoplexes released from the fibrin gel remained viable and showed successful *in vitro* transfection of mouse fibroblast cells.
- The fibrin lipoplex system successfully delivered two reporter genes *in vivo* in a rabbit ear ulcer model with significant transfection evident at 7 days post-surgery.
- This study, for the first time, showed the feasibility of fibrin-lipoplex system to deliver multiple genes up to 7 days.

6.4.2 Phase II

The objective of this phase was to develop fibrin-in-fibrin (fibrin microspheres in fibrin gel) gene delivery system for increased DNA carrying capacity with respect to gelation time and temporal control.

Conclusions:

- Fibrin microspheres encapsulating lipoplexes were successfully fabricated without any degradation of DNA.
- The lipoplexes, carrying model therapeutic gene eNOS, encapsulated within the fibrin microspheres remained functionally integral *in vivo* as shown by induction of angiogenesis at 7 days post-surgery in a pilot study performed using an alloxan induced ear ulcer model of compromised wound healing.
- Fibrin microspheres degraded at a significantly slower rate than fibrin gel enabling the design of fibrin in fibrin (fibrin microspheres in fibrin gel) release system.
- This study, for the first time, showed the feasibility of fibrin microspheres for gene delivery.

6.4.3 Phase III

The objective of this phase was to assess the differential gene regulation in human keratinocytes grown in high and normal glucose conditions during an *in vitro* assay of multiple scratch wounds.

Conclusions:

- Primary cultures of human keratinocytes were established under normal (6 mM) and high glucose (25 mM) conditions.
- An *in vitro* wound model of multiple scratch wounds was developed which allowed almost 40-50% of cells to take part in the healing of scratch wounds.
- The migration of keratinocytes was significantly slower in high glucose compared to that in normal glucose conditions.
- Microarray performed on the RNA isolated from wounded human keratinocytes grown under normal and high glucose conditions with non-wounded keratinocytes as controls revealed differential gene regulation during wound healing under hyperglycemia with a number of genes up- and down- regulated.
- Of the number of downregulated genes, Rab18 was chosen for further investigation for its proposed secretory control action which is complementary to proangiogenic effect of eNOS.

- This was the first study showing the differential regulation of gene expression in wounded keratinocytes under hyperglycemic conditions.

6.4.4 Phase IV

The objective of this phase was to evaluate the efficiency of fibrin-in-fibrin system encoding eNOS and Rab18 genes to promote wound healing in an alloxan induced hyperglycemic rabbit ear ulcer model of compromised wound healing.

Conclusions:

- Fibrin-in-fibrin system encoding Rab18-eNOS resulted in enhanced wound closure, reduced inflammation, increased surface density and length density of blood vessels and decreased radial diffusion distance at day 14 compared to control group.
- Pearson's coefficients of correlation confirmed that percent epithelialization is negatively correlated with radial diffusion distance in the group treated with fibrin-in-fibrin system encoding Rab18-eNOS.
- This study, for the first time, showed therapeutic effect of fibrin based non-viral gene delivery system with proangiogenic and secretory control genes in a preclinical model of compromised wound healing.

6.5 Future Directions

The assessment done in various phases of the study has spanned through efforts to unleash the pathological disarray at molecular level in compromised wound healing and identifying novel gene target/targets, and then developing a flexible gene delivery system capable of delivering multiple genes in a controlled manner and then investigating the system in preclinical model with successful enhancement of wound healing. Each aspect of study can be further investigated by addressing the limitations in the current study and by further analysis of various avenues made available through this work. The major future directions, the current project can take, are summarized schematically in Figure 6.3.

Figure 6.3: Schematic depicting possible future directions of the project. Schematic is arranged in a tree-like format. The roots of the tree represent the basic themes/aspects on which the research in this project was based. The main stem of the tree shows the phases of the project. The text beside the red arrows feeding into the stem shows the plausible lines in which each phase can progress. The center blob of leaves represents the major achievement of the project in the treatment of wounds compromised due to exposure to hyperglycemia. The blobs on the periphery represent the possibility of applying the research in this project to other diseases or carry forward the main theme of the project in different etiopathological set up. This is by no means a comprehensive depiction, rather only the most direct and important aspects are represented. The details are discussed in section 6.5.

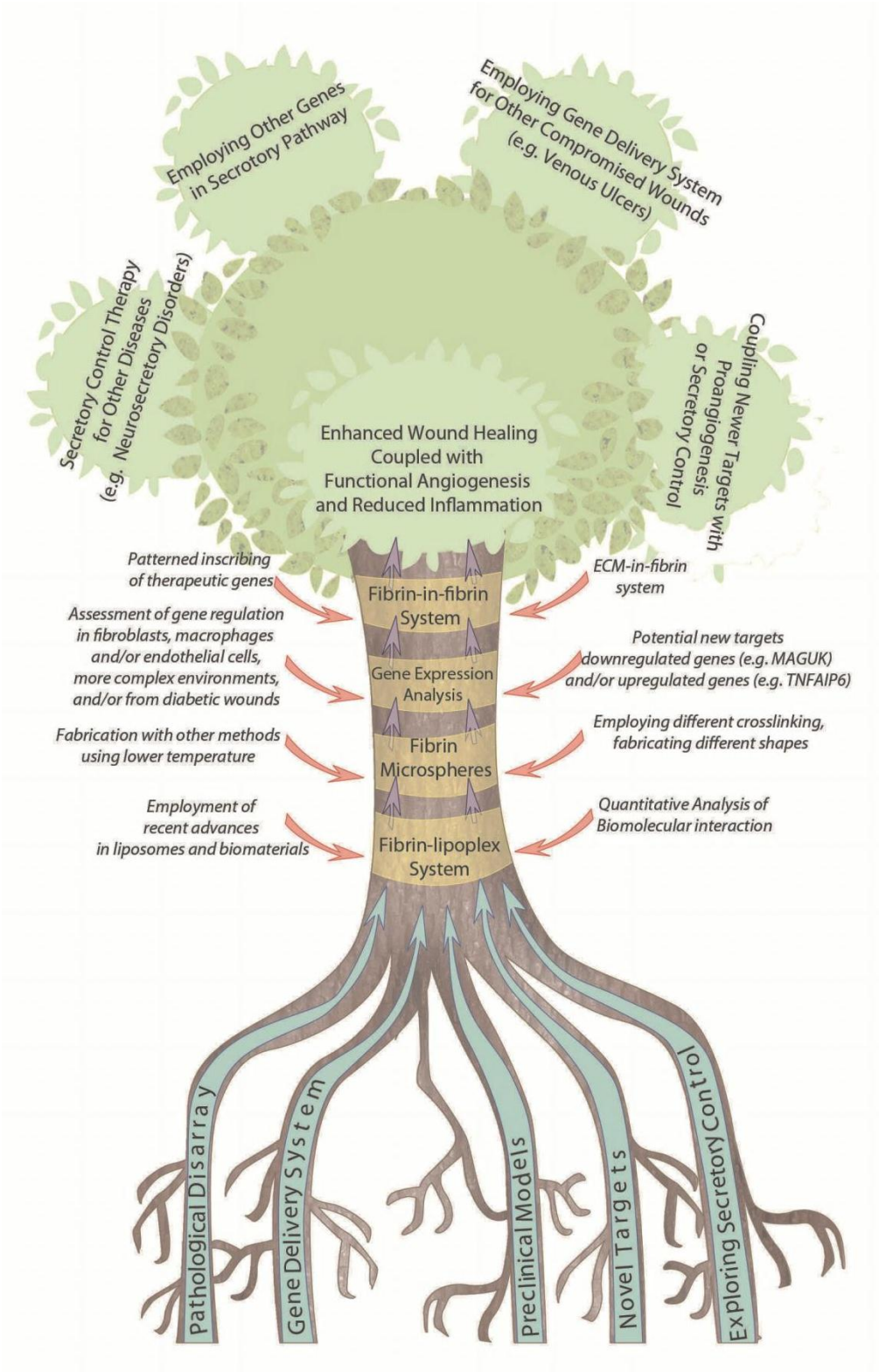
Employing Other Genes in Secrotory Pathway
Employing Gene Delivery System for Other Compromised Wounds (e.g. Venous Ulcers)
Secretory Control Therapy for Other Diseases (e.g. Neurosecretory Disorders)
Coupling Newer Targets with Proangiogenesis or Secretory Control
Enhanced Wound Healing Coupled with Functional Angiogenesis and Reduced Inflammation
Patterned inscribing of therapeutic genes
ECM-in-fibrin system
Fibrin-in-fibrin System
Assessment of gene regulation in fibroblasts, macrophages and/or endothelial cells, more complex environments, and/or from diabetic wounds
Potential new targets downregulated genes (e.g. MAGUK) and/or upregulated genes (e.g. TNFAIP6)
Gene Expression Analysis
Fabrication with other methods using lower temperature
Employing different crosslinking, fabricating different shapes
Fibrin Microspheres
Employment of recent advances in liposomes and biomaterials
Quantitative Analysis of Biomolecular interaction
Fibrin-lipoplex System
Pathological Disarray
Gene Delivery System
Preclinical Models
Novel Targets
Exploring Secretory Control

6.5.1 Unleashing the Pathological Disarray at Molecular Level

In this research, differential regulation of gene expression in primary human keratinocytes during wound healing in hyperglycemic conditions was assessed. The next steps of this aspect of research work are (a) Assessment of gene regulation in complex environment (b) Assessment of gene regulation in fibroblasts, macrophages, and/or endothelial cells (c) Assessment of gene regulation in human diabetic patients.

6.5.1.1 Assessment of Gene Regulation in Complex Environment

Current project looked at the effect of most prominent pathological factor in diabetes, namely hyperglycemia. As a further step, a more complex environment which takes into account other pathological factors such as ischemia can be employed. Thus the differential regulation of gene expression will be assessed in a more complex *in vitro* environment resembling clinical diabetes more closely by use of combination of factors such as hyperglycemia and ischemia. For this purpose, primary human keratinocytes can be grown in high and normal glucose conditions while correspondingly growing them in low oxygen levels. Various combinations of hyperglycemia and ischemia can be investigated to take into account the range of levels seen in clinics.

6.5.1.2 Assessment of Gene Regulation in Fibroblasts, Macrophages, and/or Endothelial Cells

The current project investigated effect of hyperglycemia on keratinocytes. However, other wound healing cells such as fibroblasts, macrophages and/or endothelial cells can be investigated for a similar study at molecular level to unravel the differential gene regulation in these cells, either individually or collectively. All these cells are known to be dysfunctional in diabetic set up. Although research to date has identified dysfunctional aspects of fibroblasts/macrophages/endothelial cells in diabetes, but a comprehensive study investigating the differential gene regulation during wound healing in hyperglycemic or combined hyperglycemic and ischemic environments remains to be done. Also, the crosstalk between dysfunctional cells can be assessed through co-culture systems. Finally, all the molecular effects of diabetes-like conditions on these different cells can be collated and a multiple gene therapy targeting different cells can be envisioned. The current fibrin-in-fibrin system is capable of multiple gene

delivery with controlled release. It also provides opportunity to functionalize the liposomal carriers involved in the fibrin in fibrin system to target the specific cells if deemed necessary. The prospects on that theme of further developing the delivery system are discussed in section 6.5.3.

6.5.1.3 Assessment of Gene Regulation in Human Diabetic Patients

The pathological disarray can be further unraveled by moving the investigation from pure *in vitro* systems to *in vivo* diseased states in human patients with compromised wounds. *In vitro* systems look at the effects of discrete defined factors on different relevant cells, while *in vivo* studies reveal the complexity accounting for various aspects of the diabetic wound healing. Cells can be isolated from chronic wounds of diabetic patients matched for confounding factors such as age, sex, ethnic background, socioeconomic status and other medical conditions including hypertension, obesity and any endocrinal disorders. Due to the complexity involved, very large sample size, in order of few thousands, will be required to derive some conclusion with acceptable level of statistical significance. For this reason and also due to ethical issues in procuring human samples, assessment of gene regulation in human diabetic patients could not done in the current study.

6.5.2 Identification of Novel Gene Targets

The microarray study performed in this research provided an enormous amount of data. This data can be analyzed further to unravel newer molecular targets. In the current project, one of the downregulated genes, Rab18 was used. In fact, there were other downregulated genes independent of eNOS pathway. These downregulated genes can also be investigated. Also, the microarray performed in the current project revealed many upregulated genes as well. These upregulated genes can also be investigated.

6.5.2.1 Investigation of Downregulated Genes

One potential target among the downregulated genes is a gene sequence highly homologous to MAGUK. This was one of the validated genes downregulated in hyperglycemic wounded keratinocytes. The MAGUKs (membrane-associated guanylate kinase homologs) are a family of proteins that act as molecular scaffolds for signaling pathway components at the plasma membrane of animal cells[14]. The MAGUK family

regulates tight junction assembly and cell adhesion by connecting transmembrane proteins with the cytoskeleton[15]. Actually, the presence of a multiple protein-protein interaction domains allows them to perform dual functions of structural organization of junctional complex and signal transduction[16]. A member of MAGUK family has been shown to interact with c-Src in cells to its activity which involves regulation of cell proliferation, migration cell activation[17]. Thus, using the fibrin-in-fibrin system researched in this project could be employed to deliver the MAGUK sequence and eNOS as a controlled release dual gene delivery system.

6.5.2.2 Investigation of Upregulated Genes

Another avenue is to study upregulated genes. These can provide very promising ways to normalize compromised wound healing. The upregulated genes can be knocked down by using RNA interference (RNAi)[18]. One such promising upregulated gene found in microarray analysis is TNFAIP6. This is a gene coding for a secretory protein induced by proinflammatory cytokines such as TNF-α and IL-1. Studies have shown high levels of TNF-α in diabetic wounds and have postulated its role in impairment of wound healing[19 20]. Anti-TNF-α treatment has shown to restore the skin impairment due to diabetes in a mouse model[21]. Thus, it can be hypothesized that diabetic wound healing can be normalized by knocking down TNF-α induced TNFAIP6 found to be upregulated in wounded hyperglycemic keratinocytes. This treatment holds promise of inhibiting the inflammatory actions of TNF-α and address the problem of chronic inflammation in diabetic wound healing.

6.5.3 Gene Delivery System

The fibrin-in-fibrin gene delivery system developed in this research is an interesting and flexible system. Each component of the system can serve as a basis for future development of the system. The full potential of a combined liposome-scaffold approach remains to be investigated as research to date has mainly focused on providing proof of concepts. It is anticipated that the future of a combined liposome-scaffold approach would be centered on two goals: making optimal use of the progress in individual fields and the understanding derived thereof, and utilizing and manipulating interactions between the liposomes and the scaffold material as depicted in Figure 6.4.

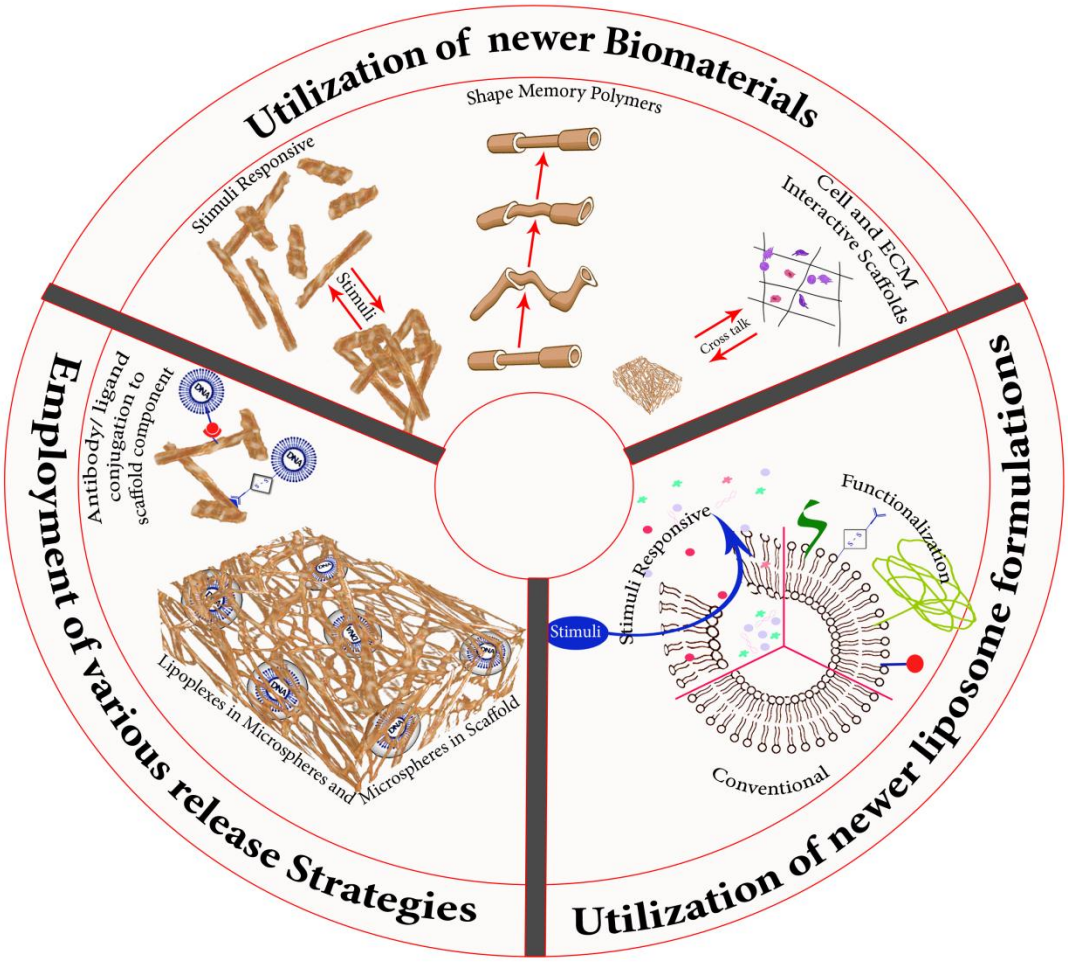

Figure 6.4: Schematic illustration of potential future developments of tissue-engineered scaffold-mediated liposomal delivery. Breakthroughs in the near future will most likely be based on the full utilization and application of recent advances in individual biomaterials, including stimuli-responsive materials, shape memory polymers, and interactive polymers. Advancements in liposome technology, such as the development of stimuli-responsive and functionalized formulations, will also contribute to further progress together with the advent of innovative release strategies.

In particular, the versatility of liposomes has not yet been tested in the context of their inclusion into tissue engineered scaffolds. The recent advances in liposomal gene delivery are yet to be applied in the combined approach. A recent study has already pointed out the need for focusing research on designing lipoplexes with the aim to increase the cellular internalization of DNA for enhancing gene delivery from scaffold surface[22]. It is therefore highly likely that the successful application of combination therapy will depend on advances in liposomal gene delivery with regard to targeted delivery, enhanced intracellular trafficking and nuclear localization. The combined strategy can also be approached from the scaffold using so called "smart" biomaterials, such as stimuli-responsive polymers, or polymers that are cell interactive and based on "click" chemistry. Shape memory polymers can be micropatterned with lipoplexes, then compacted for ease of handling and for reaching the injury site, and upon implantation will return to their original shape containing micropatterned lipoplexes. This approach can be particular useful in areas of nerve regeneration, surgical sutures[23] and vascular stenting[24 25]. *In situ* gelling systems with lower critical solution temperature at body temperature can be employed to carry lipoplexes, which after application to wounds will form a gel and subsequently release lipoplexes in a sustained manner. Also, research in the field of whole tissue organ regeneration can be geared up through micropatterned lipoplexes in 3-D scaffolds for the creation of a highly controlled spatio-temporal gene expression, mimicking the natural embryonic development. Also, newer more effective polymeric carriers with better safety profiles can replace the liposomes in the system. Also, the successful gene delivery by fibrin in fibrin system can be employed in other diseases such as other forms of chronic ulcers like venous ulcers, neuropathic ulcers.

Taking forward the concept of differential degradation and two component scaffold system, a new delivery system – the ECM-in-fibrin system has been conceptualized. This ECM-in-fibrin can be designed in a patterned fashion. Based on similar theme as fibrin in fibrin system, ECM-in-fibrin system can be utilized to deliver multiple genes in a controlled manner. ECM in this system will be produced from wound healing cells like fibroblasts or stem cells like MSCs grown in specific culture conditions and specific geometrical constraints. It is hypothesized that such conditions and constraints

will allow cells to produce large amounts of ECM while cells themselves will eventually die, forming material which will be a cell-derived ECM without living cells. This material will be used as raw material for developing ECM spheres (or particles of different shapes and sizes), carrying therapeutic gene/genes of interest complexed with non-viral gene carriers. These ECM spheres/particles will be embedded in fibrin gel (which will also contain gene complexes), in a predesigned patterned fashion so as to create expression patterns for optimal therapeutic benefit. For example, it can potentially be investigated in the same disease set up and with same set of therapeutic genes, as has the fibrin in fibrin system been in current project. The ECM microspheres/particles can incorporate Rab18 gene complexes and these ECM spheres/particles can then be embedded in fibrin gel that carries a complementary therapeutic gene, namely eNOS. The combined effect of two genes and the ECM in fibrin system itself can be exploited for chronic/compromised wound healing.

6.5.4 Exploring the Secretory Control Approach

The journey of secretory vesicles to plasma membrane and subsequent exocytosis is essential for normal cellular function in various cell types. Using pancreatic exocrine cells, George Palade portrayed the pathway of secretory proteins through the cells in his classical experiments[26]. Thereafter, the secretory pathway has been studied in a number of cell types including pancreatic β cells[27-31], due to involvement in diabetes mellitus, and platelets[32-35] and neutrophils[36-39] which play a pivotal role in physiological and pathological immune responses. A wide variety of other cells such as neuroendocrine and endocrine cells such as neurons[40-42] (secreting neurotransmitters), pituitary cells[43] and adrenal medullary cells[44] (or their tumor counterpart PC12 cells[45]) and specialized exocrine cells such as G cells in gastric mucosa[46], goblet cells[47 48] in intestines and lungs, juxtaglomerular cells[49] in kidney, type II alveolar cells[50] in lungs and also some very specialized cells like sperms and eggs have very intricately regulated secretory functions. Even cells such as endothelial cells[51], fibroblasts[52] and keratinocytes[53] exhibit significant secretory functions.

Thus, regulated secretion of bioactive molecules is an important physiological phenomenon and hence it is not very surprising that a number of diseases have a

secretory dysfunction at the root of their pathology. This is why understanding the secretory pathway and exploiting the knowledge to rectify the pathology can be rewarding. The current project explored an outlook of diabetic wound healing as hypersecretory pathology and developed a gene therapy addressing this problem based on the finding of downregulated secretory control molecule from Rab family, the Rab18. Now, this approach can be further explored potentially in numerous ways. Quite logically, the same fibrin-in-fibrin delivery system used here can be explored to link secretory control therapy with appropriate gene/genes in a controlled way in many other diseases which pose hypersecretory pathology such as neurosecretory disorders.

Other Rab proteins (60 known in humans[54]) can also be explored for potential use in secretory control therapy. Rab proteins localized to distinct characteristic organelles[55] and along with their effectors regulate intracellular vesicle dynamics, from vesicle formation, tethering, docking and fusion with the correct target membrane[56-59]. Rab proteins function as molecular switches with gaunosine triphosphate (GTP) bound "on" state and "off" state upon GTP hydrolysis[60]. Rab3 isoforms, Rab4 and Rab27 isoforms are the most studied ones[61-66] and recently Rab18[67], Rab43[68], Rab34[69] and others are being attributed with very important and specific functions. On account of these core organizational and transport functions, dysfunction or reduced synthesis of Rab proteins insinuate severe pathological conditions[70] and thus gene therapy of Rabs offer unique therapeutic potential. Other very important molecules involved in secretory pathway are SNAREs, NSFs and α-SNAP, Sec1 proteins and Ca^{2+} binding proteins. These molecules can also be explored for therapeutic purposes.

6.6 References

1. Brem H, Jacobs T, Vileikyte L, Weinberger S, Gibber M, Gill K, Tarnovskaya A, Entero H, Boulton AJ. Wound-healing protocols for diabetic foot and pressure ulcers. *Surg Technol Int* 2003;11:85-92.

2. Martin A, Komada MR, Sane DC. Abnormal angiogenesis in diabetes mellitus. *Med Res Rev* 2003;23(2):117-45.

3. Breen A, Dockery P, O'Brien T, Pandit A. The use of therapeutic gene eNOS delivered via a fibrin scaffold enhances wound healing in a compromised wound model. *Biomaterials* 2008;29(21):3143-51.

4. Houchin-Ray T, Huang A, West ER, Zelivyanskaya M, Shea LD. Spatially patterned gene expression for guided neurite extension. *J Neurosci Res* 2009;87(4):844-56.

5. Spravchikov N, Sizyakov G, Gartsbein M, Accili D, Tennenbaum T, Wertheimer E. Glucose effects on skin keratinocytes: implications for diabetes skin complications. *Diabetes* 2001;50(7):1627-35.

6. Lu SL, Qiao L, Xie T, Yang YM, Jin SW, Qing C. [Effects of the cutaneous and blood contents of glucose on wound healing in diabetic rats with superficial partial thickness scalding]. *Zhonghua Yi Xue Za Zhi* 2005;85(27):1899-902.

7. Deveci M, Gilmont RR, Dunham WR, Mudge BP, Smith DJ, Marcelo CL. Glutathione enhances fibroblast collagen contraction and protects keratinocytes from apoptosis in hyperglycaemic culture. *Br J Dermatol* 2005;152(2):217-24.

8. Terashi H, Izumi K, Deveci M, Rhodes LM, Marcelo CL. High glucose inhibits human epidermal keratinocyte proliferation for cellular studies on diabetes mellitus. *Int Wound J* 2005;2(4):298-304.

9. Lan CC, Liu IH, Fang AH, Wen CH, Wu CS. Hyperglycaemic conditions decrease cultured keratinocyte mobility: implications for impaired wound healing in patients with diabetes. *Br J Dermatol* 2008;159(5):1103-15.

10. Portugal-Cohen M, Kohen R. Exposure of human keratinocytes to ischemia, hyperglycemia and their combination induces oxidative stress via the enzymes inducible nitric oxide synthase and xanthine oxidase. *J Dermatol Sci* 2009;55(2):82-90.

11. Lan CC, Wu CS, Kuo HY, Huang SM, Chen GS. Hyperglycaemic conditions hamper keratinocyte locomotion via sequential inhibition of distinct pathways: new insights on poor wound closure in patients with diabetes. *Br J Dermatol* 2009;160(6):1206-14.
12. Breen A, Mc Redmond G, Dockery P, O'Brien T, Pandit A. Assessment of wound healing in the alloxan-induced diabetic rabbit ear model. *J Invest Surg* 2008;21(5):261-9.
13. Wang J, Wan R, Mo Y, Zhang Q, Sherwood LC, Chien S. Creating a long-term diabetic rabbit model. *Exp Diabetes Res* 2010;2010:289614.
14. Dimitratos SD, Woods DF, Stathakis DG, Bryant PJ. Signaling pathways are focused at specialized regions of the plasma membrane by scaffolding proteins of the MAGUK family. *Bioessays* 1999;21(11):912-21.
15. Kimura R, Ishida T, Kuriyama M, Hirata K, Hayashi Y. Interaction of endothelial cell-selective adhesion molecule and MAGI-1 promotes mature cell-cell adhesion via activation of RhoA. *Genes Cells* 2010;15(4):385-96.
16. Gonzalez-Mariscal L, Betanzos A, Avila-Flores A. MAGUK proteins: structure and role in the tight junction. *Semin Cell Dev Biol* 2000;11(4):315-24.
17. Baumgartner M, Weiss A, Fritzius T, Heinrich J, Moelling K. The PDZ protein MPP2 interacts with c-Src in epithelial cells. *Exp Cell Res* 2009;315(17):2888-98.
18. Fire A, Xu S, Montgomery MK, Kostas SA, Driver SE, Mello CC. Potent and specific genetic interference by double-stranded RNA in Caenorhabditis elegans. *Nature* 1998;391(6669):806-11.
19. Siqueira MF, Li J, Chehab L, Desta T, Chino T, Krothpali N, Behl Y, Alikhani M, Yang J, Braasch C, Graves DT. Impaired wound healing in mouse models of diabetes is mediated by TNF-alpha dysregulation and associated with enhanced activation of forkhead box O1 (FOXO1). *Diabetologia* 2010;53(2):378-88.
20. Liu R, Bal HS, Desta T, Behl Y, Graves DT. Tumor necrosis factor-alpha mediates diabetes-enhanced apoptosis of matrix-producing cells and impairs diabetic healing. *Am J Pathol* 2006;168(3):757-64.

21. Goren I, Muller E, Schiefelbein D, Christen U, Pfeilschifter J, Muhl H, Frank S. Systemic anti-TNFalpha treatment restores diabetes-impaired skin repair in ob/ob mice by inactivation of macrophages. *J Invest Dermatol* 2007;127(9):2259-67.

22. Bengali Z, Rea JC, Gibly RF, Shea LD. Efficacy of immobilized polyplexes and lipoplexes for substrate-mediated gene delivery. *Biotechnol Bioeng* 2009;102(6):1679-91.

23. Lamprakis AA, Fortis AP, Kostopoulos V, Vlasis K. Biomechanical testing of a shape memory alloy suture in a meniscal suture model. *Arthroscopy* 2009;25(6):632-8.

24. Ajili SH, Ebrahimi NG, Soleimani M. Polyurethane/polycaprolactane blend with shape memory effect as a proposed material for cardiovascular implants. *Acta Biomater* 2009;5(5):1519-30.

25. Baer GM, Wilson TS, Small Wt, Hartman J, Benett WJ, Matthews DL, Maitland DJ. Thermomechanical properties, collapse pressure, and expansion of shape memory polymer neurovascular stent prototypes. *J Biomed Mater Res B Appl Biomater* 2009;90(1):421-9.

26. Palade G. Intracellular aspects of the process of protein synthesis. *Science* 1975;189(4200):347-58.

27. Lang J. Molecular mechanisms and regulation of insulin exocytosis as a paradigm of endocrine secretion. *Eur J Biochem* 1999;259(1-2):3-17.

28. Easom RA. Beta-granule transport and exocytosis. *Semin Cell Dev Biol* 2000;11(4):253-66.

29. Kasai H, Hatakeyama H, Ohno M, Takahashi N. Exocytosis in islet beta-cells. *Adv Exp Med Biol* 2010;654:305-38.

30. Takahashi N, Kasai H. Exocytic process analyzed with two-photon excitation imaging in endocrine pancreas. *Endocr J* 2007;54(3):337-46.

31. Takahashi N, Kishimoto T, Nemoto T, Kadowaki T, Kasai H. Fusion pore dynamics and insulin granule exocytosis in the pancreatic islet. *Science* 2002;297(5585):1349-52.

32. Battinelli EM, Markens BA, Italiano JE, Jr. Release of angiogenesis regulatory proteins from platelet alpha granules: modulation of physiologic and pathologic angiogenesis. *Blood* 2011;118(5):1359-69.

33. Morrell CN, Matsushita K, Chiles K, Scharpf RB, Yamakuchi M, Mason RJ, Bergmeier W, Mankowski JL, Baldwin WM, 3rd, Faraday N, Lowenstein CJ. Regulation of platelet granule exocytosis by S-nitrosylation. *Proc Natl Acad Sci U S A* 2005;102(10):3782-7.

34. Robertson C, Booth SA, Beniac DR, Coulthart MB, Booth TF, McNicol A. Cellular prion protein is released on exosomes from activated platelets. *Blood* 2006;107(10):3907-11.

35. Shirakawa R, Higashi T, Tabuchi A, Yoshioka A, Nishioka H, Fukuda M, Kita T, Horiuchi H. Munc13-4 is a GTP-Rab27-binding protein regulating dense core granule secretion in platelets. *J Biol Chem* 2004;279(11):10730-7.

36. Johnson JL, Hong H, Monfregola J, Kiosses WB, Catz SD. Munc13-4 restricts motility of Rab27a-expressing vesicles to facilitate lipopolysaccharide-induced priming of exocytosis in neutrophils. *J Biol Chem* 2011;286(7):5647-56.

37. Neeli I, Dwivedi N, Khan S, Radic M. Regulation of extracellular chromatin release from neutrophils. *J Innate Immun* 2009;1(3):194-201.

38. Borregaard N. Development of neutrophil granule diversity. *Ann N Y Acad Sci* 1997;832:62-8.

39. Ligeti E, Mocsai A. Exocytosis of neutrophil granulocytes. *Biochem Pharmacol* 1999;57(11):1209-14.

40. Thureson-Klein AK, Klein RL. Exocytosis from neuronal large dense-cored vesicles. *Int Rev Cytol* 1990;121:67-126.

41. Zhu PC, Thureson-Klein A, Klein RL. Exocytosis from large dense cored vesicles outside the active synaptic zones of terminals within the trigeminal subnucleus caudalis: a possible mechanism for neuropeptide release. *Neuroscience* 1986;19(1):43-54.

42. Thureson-Klein A. Exocytosis from large and small dense cored vesicles in noradrenergic nerve terminals. *Neuroscience* 1983;10(2):245-59.

43. Saermark T, Andersen NM, Atke A, Jones PM, Vilhardt H. Processing and secretion in the neurohypophysis. Stability of isolated secretory vesicles and role of internal pH. *Biochem J* 1986;236(1):77-84.

44. Crivellato E, Belloni A, Nico B, Nussdorfer GG, Ribatti D. Chromaffin granules in the rat adrenal medulla release their secretory content in a particulate fashion. *Anat Rec A Discov Mol Cell Evol Biol* 2004;277(1):204-8.

45. Taupenot L. Analysis of regulated secretion using PC12 cells. *Curr Protoc Cell Biol* 2007;Chapter 15:Unit 15 12.

46. Sato A. Quantitative electron miscroscopic studies on the kinetics of secretory granules in G-cells. *Cell Tissue Res* 1978;187(1):45-59.

47. Davis CW, Dickey BF. Regulated airway goblet cell mucin secretion. *Annu Rev Physiol* 2008;70:487-512.

48. Valentijn JA, van Weeren L, Ultee A, Koster AJ. Novel localization of Rab3D in rat intestinal goblet cells and Brunner's gland acinar cells suggests a role in early Golgi trafficking. *Am J Physiol Gastrointest Liver Physiol* 2007;293(1):G165-77.

49. Friis UG, Jensen BL, Hansen PB, Andreasen D, Skott O. Exocytosis and endocytosis in juxtaglomerular cells. *Acta Physiol Scand* 2000;168(1):95-9.

50. Garcia-Verdugo I, Ravasio A, de Paco EG, Synguelakis M, Ivanova N, Kanellopoulos J, Haller T. Long-term exposure to LPS enhances the rate of stimulated exocytosis and surfactant secretion in alveolar type II cells and upregulates P2Y2 receptor expression. *Am J Physiol Lung Cell Mol Physiol* 2008;295(4):L708-17.

51. Valentijn KM, van Driel LF, Mourik MJ, Hendriks GJ, Arends TJ, Koster AJ, Valentijn JA. Multigranular exocytosis of Weibel-Palade bodies in vascular endothelial cells. *Blood* 2010;116(10):1807-16.

52. Rodriguez A, Webster P, Ortego J, Andrews NW. Lysosomes behave as Ca2+-regulated exocytic vesicles in fibroblasts and epithelial cells. *J Cell Biol* 1997;137(1):93-104.

53. Chavez-Munoz C, Morse J, Kilani R, Ghahary A. Primary human keratinocytes externalize stratifin protein via exosomes. *J Cell Biochem* 2008;104(6):2165-73.

54. Bock JB, Matern HT, Peden AA, Scheller RH. A genomic perspective on membrane compartment organization. *Nature* 2001;409(6822):839-41.

55. Burgoyne RD, Morgan A. Secretory granule exocytosis. *Physiol Rev* 2003;83(2):581-632.

56. Angers CG, Merz AJ. New links between vesicle coats and Rab-mediated vesicle targeting. *Semin Cell Dev Biol* 2011;22(1):18-26.

57. Jordens I, Marsman M, Kuijl C, Neefjes J. Rab proteins, connecting transport and vesicle fusion. *Traffic* 2005;6(12):1070-7.

58. Hammer JA, 3rd, Wu XS. Rabs grab motors: defining the connections between Rab GTPases and motor proteins. *Curr Opin Cell Biol* 2002;14(1):69-75.

59. Fukuda M. Regulation of secretory vesicle traffic by Rab small GTPases. *Cell Mol Life Sci* 2008;65(18):2801-13.

60. Rybin V, Ullrich O, Rubino M, Alexandrov K, Simon I, Seabra MC, Goody R, Zerial M. GTPase activity of Rab5 acts as a timer for endocytic membrane fusion. *Nature* 1996;383(6597):266-9.

61. Huang CC, Yang DM, Lin CC, Kao LS. Involvement of Rab3A in vesicle priming during exocytosis: interaction with Munc13-1 and Munc18-1. *Traffic* 2011;12(10):1356-70.

62. Yu E, Kanno E, Choi S, Sugimori M, Moreira JE, Llinas RR, Fukuda M. Role of Rab27 in synaptic transmission at the squid giant synapse. *Proc Natl Acad Sci U S A* 2008;105(41):16003-8.

63. Merrins MJ, Stuenkel EL. Kinetics of Rab27a-dependent actions on vesicle docking and priming in pancreatic beta-cells. *J Physiol* 2008;586(Pt 22):5367-81.

64. Saxena SK, Kaur S. Rab27a negatively regulates CFTR chloride channel function in colonic epithelia: involvement of the effector proteins in the regulatory mechanism. *Biochem Biophys Res Commun* 2006;346(1):259-67.

65. Tsuboi T, Fukuda M. Rab3A and Rab27A cooperatively regulate the docking step of dense-core vesicle exocytosis in PC12 cells. *J Cell Sci* 2006;119(Pt 11):2196-203.

66. Shirakawa R, Yoshioka A, Horiuchi H, Nishioka H, Tabuchi A, Kita T. Small GTPase Rab4 regulates Ca2+-induced alpha-granule secretion in platelets. *J Biol Chem* 2000;275(43):33844-9.

67. Vazquez-Martinez R, Cruz-Garcia D, Duran-Prado M, Peinado JR, Castano JP, Malagon MM. Rab18 inhibits secretory activity in neuroendocrine cells by interacting with secretory granules. *Traffic* 2007;8(7):867-82.

68. Dejgaard SY, Murshid A, Erman A, Kizilay O, Verbich D, Lodge R, Dejgaard K, Ly-Hartig TB, Pepperkok R, Simpson JC, Presley JF. Rab18 and Rab43 have key roles in ER-Golgi trafficking. *J Cell Sci* 2008;121(Pt 16):2768-81.

69. Goldenberg NM, Silverman M. Rab34 and its effector munc13-2 constitute a new pathway modulating protein secretion in the cellular response to hyperglycemia. *Am J Physiol Cell Physiol* 2009;297(4):C1053-8.

70. Zerial M, McBride H. Rab proteins as membrane organizers. *Nat Rev Mol Cell Biol* 2001;2(2):107-17.

APPENDICES

A. List of Reagents / Compounds Used

Table A.1: List of compounds and reagents used in this study

Material	Supplier
Agarose	Sigma-Aldrich Ireland Ltd., Dublin, Ireland
Ampicillin	
Bovine serum albumin	
DMEM	
DMSO	
Eosin	
Ethanol	
Fetal bovine serum	
Fish gelatin	
Formaldehyde	
Glutaraldehyde	
Glycerol	
Goat serum	
Hank's balanced salt solution	
Hematoxylin	
Kanamycin	
LB agar	
LB broth	
L-Glutamine	
Masson's trichrome reagents	
Penicillin-streptomycin	
Phosphate buffered saline	
Potassium ferrocyanide / ferricyanide	
RNAse away	
Sodium carbonate / bicarbonate	
Spam80	
TBE buffer	
Tris hydrochloride	
Triton® X-100	
Trypsin	
Tween 20	
Xylene	
Anti-CD31	Dako Diagnostics Ltd, Dublin, Ireland
Anti-mouse IgG Biotin	
Anti-rabbit IgG HRP	

Anti-rabbit Ram11	
Amine coupling kit	BiaCore Life Sciences, GE Healthcare Ltd., UK
Getting starter kit	
HBS-EP buffer	
Sensor chip CM3	
Sodium acetate pH4.5	
Giga prep plasmid kit	Qiagen, West Sussex, United Kingdom
RNeasy® kit	
dNTP mix: (200µl, 10mM)	Promega, Dublin, Ireland
ImProm-II™ reverse transcriptase	
Luciferase assay system	
Nuclease-free water	
Oligo (dT) primers	
PCR core system I	
Random primer (20µg)	
Tissue Ruptor™	
Label IT® Cy™5 labeling kit	Mirus Bio, Madison, WI, USA
6000 Nano LabChip® kit	Agilent Technologies, Dublin, Ireland
XL1-Blue supercompetent cells	
Anti-endothelial nitric oxide synthase antibody	BD Biosciences, UK
Primers	MWG Biotech, UK
Anti-βGal	Abcam plc., UK
Fast SYBR® green master mix mini-pack	Applied Biosciences, Warrington, United Kingdom
MicroAmp® fast optical 96-well reaction plate	
MicroAmp® optical adhesive film	
Biotinylated anti-mouse horse radish peroxidase conjugated antibody	Calbiochem, UK

B. Fibrin-lipoplex System Fabrication

1. Fibrinogen protein solution and thrombin concentrate are kindly gifted by Baxter Healthcare Corporation, Vienna (Tisseel®).
2. Prepare the product according to product insert instructions.
3. Provided in the 2ml kit is:
    - Fibrinogen protein concentrate – approximately 120 mg/ml

- Thrombin concentrate – 4 IU (500 IU also provided but not needed)
- Aprotinin – 3000 KIU
- Calcium chloride – 40mM
- 2ml syringe (x4)
- Y-shaped syringe applicator

4. Baxter Ireland kindly donated a specifically designed incubator, which incorporated a magnetic stirrer.
5. Switch on the device. It will heat up to 37^0C.
6. Immediately prior to use, pre-heat fibrinogen solution and aprotinin solution provided to 37°C for ten minutes.
7. Place the mixture on the magnetic stirrer at 37°C for a further eight minutes, until the solution becomes clear.
8. Dilute the fibrinogen solution with fibrinogen dilution solution (kindly donated by Baxter Healthcare, Vienna) to a concentration of 60mg/ml.
9. Draw up the calcium chloride solution with a 2ml syringe and add to the thrombin solution. This will make the thrombin solution (4IU).
10. Keep this solution at 37°C until it is needed.
11. Perform large scale plasmid preparations utilizing the Gigaprep kits (Qiagen) as explained in section E.
12. Prior to scaffold fabrication, prepare the lipoplexes using lipofectin (Invitrogen) and plasmid DNA, encoding either green fluorescent protein for the *in vitro* transfection study or β-galactosidase and firefly luciferase for the *in vivo* study.
13. To prepare lipoplexes, gently mix the DNA solution and lipofectin solution in 1: 10 w/w ratio. Incubate the mix at room temperature for 20 min before use.
14. Gently mix the lipoplexes with 100 µl thrombin solution by inversion. Do not vortex.
15. For *in vitro* study, this thrombin solution containing lipoplexes is mixed with 100 µl fibrinogen solution in wells of 24 well plate.
16. For *in vivo* study, deliver 100 µl of thrombin solution containing lipoplexes and 100 µl of fibrinogen solution simultaneously to the wound and allow polymerizing on the wound.

C. Fibrin-in-fibrin System Fabrication

This system essentially has fibrin microspheres embedded in fibrin gel-lipoplex system. There are two major steps involved in fabrication of this system: fibrin microspheres fabrication and then embedding them in the fibrin gel-lipoplex system.

Fabrication of Fibrin Microspheres by Modified 'Water in Preheated Oil' Emulsion

1. Mix fibrinogen solution (20 mg/ml) and thrombin solution (4 IU) containing lipoplexes (carrying 10 µg of Rab18 plasmid DNA).
2. Prior to formation of the gel, while it was still in liquid phase, pour the solution drop wise into a pre-heated mineral oil at 75^0C and stir over night at 250 rpm to evaporate the water phase.
3. Use two surfactants. Tween20 in the water phase (just before mixing fibrinogen and thrombin) and spam80 in the oil phase (before preheating).
4. After overnight stirring, decant the oil.
5. First centrifuge at low speed (1000 rpm) and then at high speed (4500 rpm).
6. Wash fibrin microspheres by ethanol, hexane and acetone and then air dry.

Embedding Fibrin Microspheres in Fibrin Gel – Lipoplex System

1. Disperse fibrin microspheres containing RAB18 complexes in fibrinogen solution (60 mg/ml) and disperse the eNOS lipoplexes in thrombin solution (4 IU).
2. Apply the two solutions to the wound where the gel is formed. Thus, fibrin in fibrin system is formed.

D. Cell Culture

Thawing Cells

1. Wear protective gloves and face shield and remove tube containing cells from liquid nitrogen cylinder.
2. Thaw the contents of tube by rubbing in palm or in waterbath at 37^0C.
3. Transfer the contents of the tube in 15 ml falcon tube containing 10ml of appropriate media.
4. Centrifuge the tube at 1500rpm for five minutes.
5. Remove the supernatant and discard.

6. Add 1ml of pre-warmed media with gentle aspiration to homogeneously distribute cells.
7. Count cells using hemocytometer.
8. Transfer 1ml of cells (of known cell density) to a new T75 flask or as appropriate.
9. Add 9ml or appropriate amount of culture media.
10. Label the flask with name, date and cell type.
11. Place the flask in an incubator set at 37^0C and 5% CO_2.
12. Refresh media every 2-3 days or as per requirement.

Culturing Cells

1. Monitor cells using bright light microscope.
2. If cells are starting to float or media changes color, take off old media and rinse the cells using DPBS.
3. Add fresh appropriate culture media.
4. Monitor cells for confluence.
5. When they are ready to split (70-80 % confluent), take off the media.
6. Rinse cells using 10ml DPBS, and pour off DPBS.
7. Add 5 ml of trypsin/EDTA and either incubate at 37°C or room temperature (for primary keratinocytes) for five minutes.
8. When trypsin starts to lift cells from the flask, tap the bottom of flask and bring cells to the corner.
9. Use cell scraper if needed (for primary keratinocytes).
10. Add 5 ml of serum containing media to halt the action of trypsin.
11. Rinse the bottom of the flask with this solution several times.
12. Transfer the contents in 15 ml tube and centrifuge the tube at 1500rpm for five minutes.
13. Discard the supernatant and resuspend the cell pellet in 3ml or appropriate amount of fresh culture media.
14. Count the cells using hemocytometer.
15. Plate the cells (with known density) in three new flasks (or two flasks for primary keratinocytes) with sufficient appropriate culture media.

Counting Cells

1. Trypsinize cells as above.
2. Add equal amount of serum containing media, aspirate several times and transfer the cell suspension to a new tube.
3. Ensure the hemocytometer is clean using 70% ethanol.
4. Take 10µl of cell suspension and add 10µl of trypan blue.
5. Take 20µl of this solution and add 10µl to each side of the hemocytometer under the cover slip.
6. Allow the sample to be drawn out of the pipette by capillary action, the fluid should run to the edges of the grooves only.
7. Focus on the grid lines of the hemocytometer using the 10X objective of the microscope.
8. Focus on one set of 16 corner square as indicated by the circle in Figure D.1.
9. Count the number of cells in this area of 16 squares.
10. Count only healthy cells unstained by trypan blue.
11. Count cells that are within the square and any positioned on the right hand or bottom boundary line.
12. Dead cells stained blue with trypan blue can be counted separately for a viability count.
13. Move the hemocytometer to another set of 16 corner squares and carry on counting until all 4 sets of 16 corner squares are counted.
14. Get the average count and then multiply by two to adjust for the 1:2 dilution in trypan blue.
15. This is equivalent to number of cells x 10^4 /ml.
16. Finally total number of cells can be obtained by multiplying the above number by the volume of cell suspension.

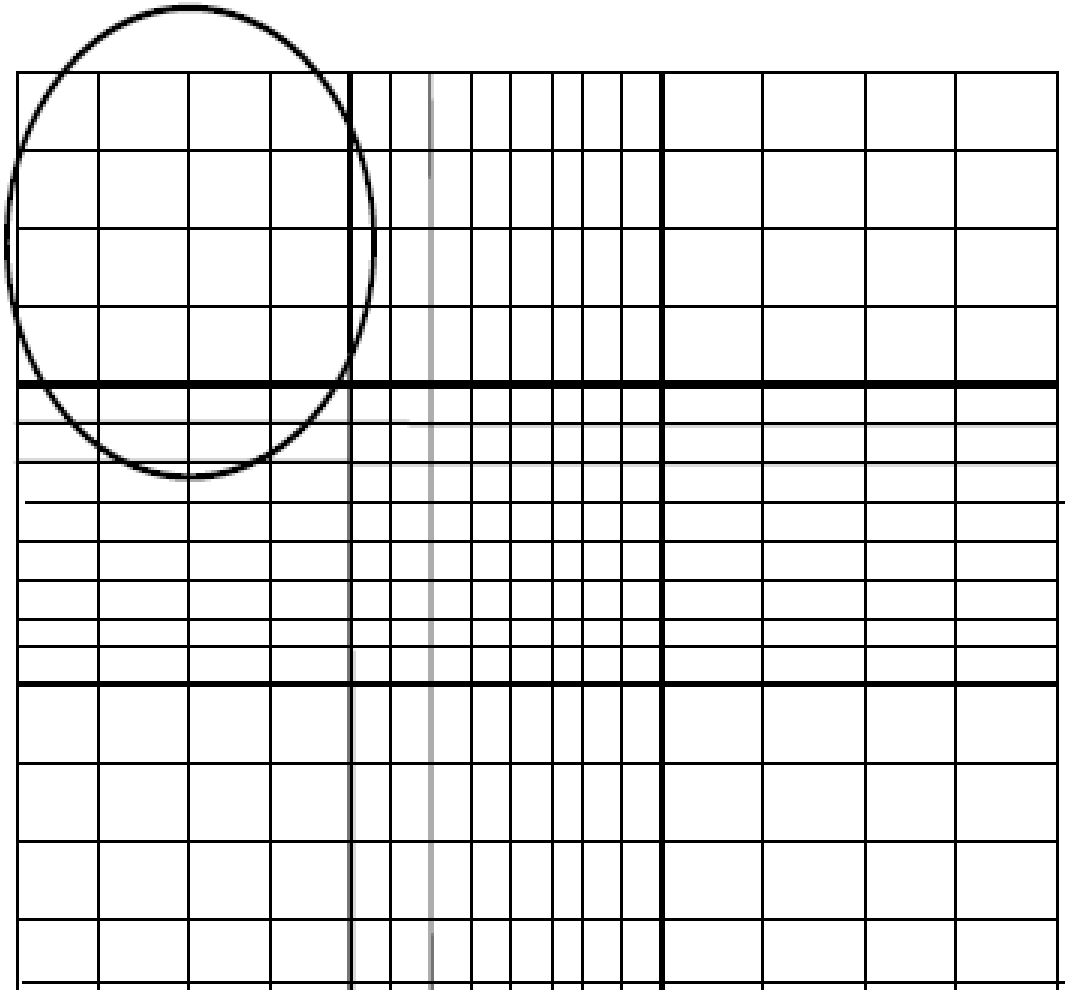

Figure D.1: Gridlines on hemocytometer.

Plating Cells for In Vitro Transfection Study

1. Pre-heat culture media for 30 minutes in a 37°C water bath.
2. One confluent T75 flask is needed for each 24 well plate.
3. Place one 22mm diameter cover slip in each well.
4. Trypsinize cells as above.
5. Add 3ml of media and aspirate several times as above.
6. Transfer 500µl of cells suspension to each of the six wells across the plate.
7. Overlay every well with 1ml of media, and incubate 37°C overnight.
8. After 24 hours, cells should be 70-80% confluent and ready for transfection.

Transfecting Cells

1. Defrost samples of collected elution samples from the fibrin-lipoplex system and samples from digested fibrin lipoplex system at different time points.
2. Prepare lipoplexes freshly with 1ug plasmid DNA as positive control.
3. Take 24 well plate cultured cells from incubator and remove media.
4. Rinse cells with DPBS, and add 1ml of media.
5. Add the contents of one collected sample vial to each well, ensuring to label lid of plate adequately.
6. Incubate plates at 37°C for 48 hours.
7. Cells are ready for analysis by fluorescent microscopy.

Freezing Cells

1. Trypsinize cells as above and centrifuge to form cell pellet.
2. Resuspend the pellet in adequate amount of freezing medium (40% FBS + 10% DMSO + 50% media for 3T3 and serum free freezing medium, Cryo-SFM, bought from Promocell for primary keratinocytes) so as to make a cell suspension of $1x10^6$ cells per ml.
3. Pipette up and down several times gently to ensure homogenous suspension.
4. Transfer 1 ml of cell suspension to each freezing vial, giving the $1x10^6$ cells per vial.
5. Label each tube with date, cell line, passage number and initials.
6. Transfer the vials to -80^0C freezer overnight and then to liquid nitrogen.

7. Ensure that sufficient amount of liquid nitrogen is maintained in the tank.

E. Plasmid DNA Expansion

LB Agar Plates

1. Add 7.5 g agar per 500 ml media in a 1 L flask.
2. Cover the flask with foil and sterilize by autoclaving.
3. When removed allow it to cool until it can be handled comfortably. Obviously, do not cool down too much or else it will start to solidify.
4. Prepare Bunsen burner and plates.
5. Remove the foil covering the flask with the LB agar.
6. Run the top across the Bunsen flame.
7. Add antibiotics. Mix well by swirling. Typical antibiotic final concentrations:
    - Kanamycin 30-50 μg/ml or
    - Ampicillin 100 μg/ml
8. Pour into the plates in close vicinity to the flame.
9. Let plates set at room temperature.
10. Label the plates with date and antibiotic used and username, seal each plate with paraffin film and store in cold room ($4 – 8^0$C).

Transformation

1. Turn on the water bath and set the temperature to 42^0C.
2. Take out the plates for transformation and place at room temperature to warm up.
3. Fill ice in the ice box.
4. Take 1 μg of plasmid DNA which is needs to be expanded in a tube. Label the tube.
5. Label another tube as control.
6. Take one tube of XL1Blue (bacteria) from box in -800C freezer and thaw on ice.
7. When thawed add 50 μl bacteria to each tube.
8. Mix by flicking.
9. Leave on ice for 2 min.
10. Place the tubes in waterbath initially set to 42^0C for 45 sec.
11. Place the tubes on ice again for 2 min.

12. Repeat the process of heat shock for couple times more.
13. Add 1 ml autoclaved LB broth (without antibiotic) to each tube.
14. Tape up-right on shaker (200 rpm, 37^0C) for 1 hour.
15. Prepare plates, Bunsen burner, spreader, 70% ethanol.
16. The optical density of the LB broth will change indicating bacterial growth.
17. Add 100 µl of inoculum in previously prepared LB agar plates containing appropriate antibiotics depending on the plasmid DNA.
18. Take out the spreader from 70% ethanol and burn off quickly in flame. Let it cool off. Touch off edge of LB agar before spreading.
19. Spread the inoculum over the plate.
20. Finish spreading all the plates and let them sit at room temperature for 10 min.
21. Put in incubator at 37^0C with upside down.
22. Take out of the incubator in 8 -10 hr when colonies of bacteria are obvious but still separate and not merged. These plates can be stored up to 4 weeks for further use.

Plasmid Expansion by Giga Prep

P1, P2, P3, Buffer FWB2, Buffer ER, Buffer QN, and Buffer TE are all supplied in Giga Prep Kit (Qiagen). Things to do before starting:

- Add the provided RNase A solution to Buffer P1 before use. Use one vial of RNase A per bottle of Buffer P1.
- Check Buffer P2 for SDS precipitation due to low storage temperatures. If necessary, dissolve the SDS by warming to 37°C.
- Pre-chill Buffer P3 at 4°C.

Giga Prep (as per Instructions Given in Qiagen Plasmid Purification Handbook)

1. Prepare LB media (2L; 25g/L) and sterilize by autoclaving. Add appropriate antibiotic.
2. Pick up a single colony from a freshly streaked plate selected on appropriate antibiotic.
3. Inoculate a started culture. Use 50 ml tubes for this purpose. Incubate 8 hr in upright position at 37^0C with vigorous shaking at 200 rpm.

4. Pour 5-10 ml of started culture in 2L of LB media (autoclaved and containing appropriate antibiotic).
5. Incubate at 37^0C with continuous shaking at 200 rpm for 12-16 hrs.
6. Harvest the bacterial cells by centrifugation at 6000 x *g* for 15 min at 4°C. If needed, freeze the cell pellets at this stage for continuing protocol later.
7. Resuspend the bacterial pellet in 125 ml of Buffer P1 (RNase A added to it). Use a 1L bottle to allow proper mixing of the lysis buffer.
8. Add 125 ml of Buffer P2, mix thoroughly by vigorous inversion for 4–6 times, and incubate at room temperature for 5 min. Do not vortex.
9. Add 125 ml of chilled Buffer P3, mix immediately and thoroughly by vigorous inversion for 4–6 times, and incubate on ice for 30 min. A fluffy white material should be formed and the lysate should become less viscous.
10. Centrifuge at 20,000 x *g* for 30 min at 4°C and promptly remove supernatant containing plasmid DNA.
11. Centrifuge the supernatant again at 20,000 x *g* for 15 min at 4°C and promptly remove supernatant containing plasmid DNA. At this stage, 75 µl of cleared lysate supernatant can be removed and saved for analysis.
12. Equilibrate a QIAGEN-tip 10000 by applying 75 ml Buffer QBT, and allow the column to empty by gravity flow.
13. Apply the supernatant from step 11 to the QIAGEN-tip and allow it to enter the resin by gravity flow.
14. Wash the QIAGEN-tip with 2 x 30 ml Buffer QC. Allow Buffer QC to move through the QIAGEN-tip by gravity flow.
15. Elute DNA with 15 ml Buffer QF. Collect the eluate in a 50 ml tube.
16. Precipitate DNA by adding 10.5 ml room-temperature isopropanol to the eluted DNA. Mix and centrifuge immediately at 15,000 x *g* for 30 min at 4°C. Carefully decant the supernatant.
17. Wash DNA pellet with 5 ml of room-temperature 70% ethanol, and centrifuge at 15,000 x *g* for 10 min. Carefully decant the supernatant without disturbing the pellet.

18. Air-dry the pellet for 5–10 min, and redissolve the DNA in a suitable volume of TE buffer. While redissolving, rinse the walls of the tube to collect all DNA.
19. Determine the yield by UV spectrophotometry at 260 nm.

F. Picogreen Assay

The assay was performed according to the instructions supplied with the kit (Quant-iT™ PicoGreen® dsDNA kit, Invitrogen). The standard curve and experimental protocol are described below.

Preparing the Assay Buffer

1. Prepare a 1X TE working solution by diluting the concentrated buffer (supplied with the kit) 20-fold with sterile, distilled, DNase-free water.

Preparing the Assay Reagent

1. Prepare an aqueous working solution of the Quant-iT™ PicoGreen® reagent by making a 200-fold dilution of the concentrated solution in 1X TE buffer.
2. For best results, use this solution within a few hours of its preparation and protect from light by covering with tin foil.
3. Handle with care as this reagent binds with DNA. Although there is no data available, still it should be considered as mutagen and hence appropriate care should be taken.

DNA Standard Curve

Following points must be considered while preparing standard curves

- For making standard curve, use same or similar dsDNA as in the experimental samples.
- Treat the dsDNA solution for standard curve in same way as the experimental samples are treated.
- Prepare the dsDNA solution for standard curve with same level of compounds present in the experimental samples as these samples may have confounding effects on the fluorescence reading.

- To minimize photo bleaching effects, keep the time for fluorescence measurement constant for all samples.

Depending on the anticipated levels in the samples, either high range (1 ng/ml to 1 µg/ml) or low range (25 pg/ml to 25 ng/ml) standard curves or both must be prepared.

1. Follow the protocol in Table F1 for high range standard curve.
2. After making these dilutions, mix well and incubate for 2 to 5 min at room temperature. Make sure that the solutions are protected from light.
3. For microplate reader, use 200 µl from each dilution.
4. Measure the sample fluorescence using a fluorescence microplate reader and standard fluorescein wavelengths (excitation ~480 nm, emission ~520 nm).
5. Adjust the gain in the reader to accommodate highest fluorescence signals.
6. Subtract the fluorescence value of the reagent blank from that of each of the samples.
7. Use corrected data to generate a standard curve of fluorescence versus DNA concentration.
8. For low range standard curve from 25 pg/ml to 25 ng/ml, prepare a 40-fold dilution of the 2 µg/ml DNA solution to yield a 50 ng/ml DNA stock solution.
9. Follow protocol in Table F2 for the making the low range standard curve.
10. Continue as in steps 2 to 4.
11. Adjust the gain in the reader to accommodate the lowest fluorescence signals
12. Continue with steps 6 and 7.

Sample Analysis

1. Dilute the experimental samples with known suitable dilution factor to a final volume of 100 µl.
2. Add 100 µl of the aqueous working solution of the Quant-iT™ PicoGreen® reagent to each sample.
3. Incubate for 2 to 5 minutes at room temperature, protected from light.

Table F1: Protocol for preparing high range standard curve

Volume of TE/buffer in experimental samples (µl)	**Volume of 2 µg/ml DNA Stock (µl)**	**Volume of Diluted Reagent (µl)**	**Final DNA Concentration**
0	1000	1000	1 µg/ml
900	100	1000	100 ng/ml
990	10	1000	10 ng/ml
999	1	1000	1 ng/mL
1000	0	1000	blank

Table F2: Protocol for preparing low range standard curve

Volume of TE/buffer in experimental samples (µl)	**Volume of 50 ng/ml DNA Stock (µl)**	**Volume of Diluted Reagent (µl)**	**Final DNA Concentration**
0	1000	1000	1 µg/ml
900	100	1000	100 ng/ml
990	10	1000	10 ng/ml
999	1	1000	1 ng/mL
1000	0	1000	blank

4. Measure the fluorescence of the sample using instrument parameters that correspond to those used when generating standard curve.
5. Subtract the fluorescence value of the reagent blank from that of each of the samples.
6. Determine the DNA concentration of the sample from the standard curve generated in DNA standard curve. The assay may be repeated using a different dilution of the sample to confirm the quantitation results.

G. Gel Electrophoresis

Materials Needed

- Agarose
- TAE buffer
- 6X sample loading buffer
- DNA ladder standard
- Electrophoresis chamber
- Power supply
- Gel casting tray and combs
- SYBR® Safe DNA gel stain
- Staining tray
- Gloves
- Pipette and tips

Recipes

TAE Buffer

4.84 g Tris Base

1.14 ml Glacial Acetic Acid

2 ml 0.5M EDTA (pH 8.0)

Bring the total volume up to 1L with water

Preparing Agarose Gel

1. Measure 0.7g of agarose powder and add it to 500 ml conical flask.

2. Add 100 ml of TAE buffer to the flask (depending on the number of samples and size of casting tray available, total volume of the gel may vary).
3. Melt the agarose in microwave until the solution becomes clear. Generally it takes around 1 min. Care should be taken not to over boil the solution as it may boil out of the flask.
4. Let the solution cool to about 50-55°C by swirling occasionally for even cooling.
5. Add 10 µl of SYBR® Safe DNA gel stain to the solution and mix by swirling.
6. Place appropriate combs in the casting tray at appropriate position.
7. Pour the solution in the gel casting tray. Make sure that the ends of the tray are sealed properly.
8. Allow the gel to cast in the tray until it is solid. It should generally take around 30 min.
9. Pull out the comb carefully.
10. Place the gel in the electrophoresis chamber and add enough TAE buffer so that the level of buffer is at least 2-3 mm over the gel.

Loading Gel

11. Note down the order in which samples will be loaded in the gel.
12. On a paraffin film, add 8 µl of each DNA sample one beside the other in the sequence the samples will be loaded. Use separate pipette tip each time. Add 2 µl of loading dye to each sample.
13. Using a fresh loading tip, mix each sample with the loading dye and load the sample in the appropriate well.
14. Pipette 10 µl of the DNA ladder standard in at least one of the wells.
15. If there are empty wells load them with loading dye appropriately diluted in TE.

Running Gel

16. Place the lid on the gel box and connect the electrodes correctly (Red to positive and black to negative).
17. Turn on the power supply and set voltage to 100 volts.

18. Check to make sure that current is running through the buffer. This can be confirmed by presence bubbles forming on each electrode.
19. Check that the direction of the current is correct. This can be checked by observing the direction of movement of the blue loading dye after about couple of minutes of running the gel.
20. Let the gel run until the blue dye reaches the end of the gel. This generally would take 30-45 min.
21. Turn off the power supply and disconnect all the wires.
22. Remove the lid of electrophoresis chamber and using gloves carefully remove the gel with the tray.

Examining the Gel

23. Place the gel onto the transilluminator and ensure that the safety door of the darkroom cabinet is shut securely.
24. Select SYBR safe filter. The transilluminator should turn on automatically.
25. Observe the image of gel on the computer screen. The image may be adjusted by opening or closing the aperture, or by increasing or decreasing the exposure time.
26. Once satisfied with the adjustments, click "capture" to capture image. At this stage, changes can be made such as cropping the image for new area of interest or enhance by adjusting brightness/contrast etc. Save the image/s.
27. Switch off the darkroom.
28. Remove the gel from the transilluminator, wrap in a tissue paper, discard in appropriate waste bin and wipe dry the transilluminator.

H. Fluorescent Microscopy

Fluorescent microscopy was used for *in vitro* transfection study. The cells were grown on glass coverslips (Thermanox™) in 24-well plate. This makes it easier to place the coverslip on glass slide for viewing under microscope.

1. At appropriate time point, remove the media from the cells.
2. Gently wash the coverslips with hank's balanced salt solution.

3. Add 500 µl of 4% paraformaldehyde. Note that it takes time for paraformaldehyde to dissolve in PBS so stirring on magnetic hot plate is required. It is wise to prepare the solution a night before the actual experiment
4. Incubate at room temperature for 15 min to allow fixation.
5. After fixation, remove paraformaldehyde solution and gently wash 2-3 times with PBS.
6. Place the coverslip on the glass slide with cell surface facing the slide. Place a drop of glycerol or DPX (A mixture of distyrene, a plasticizer, and xylene) in the center of glass slide before placing the coverslip.
7. Seal the edges of the glass coverslip with nail polish to prevent the samples from drying out.
8. Focus the cells under microscope with bright field and take snaps.
9. With the same field of view, now change the filter to FITC (green) filter to see green fluorescence from GFP. The bright light should be turned off at this stage.
10. Presence of green fluorescence confirms transfection and comparison with the bright field images confirm that fluorescence is from cells.

I. Surface Plasmon Resonance

The surface plasmon resonance studies were performed to qualitatively assess biomolecular interaction between fibrinogen and lipofectin. Please note that quantification of the interaction remains to be done.

Preparation of Instrument (Biacore 2000)

1. Set the instrument temperature to 25°C.
2. Dock a clean maintenance chip.
3. Place distilled water bottle into BiaCore 2000 unit, and insert tube into lid and prime.
4. Then run DESORB.
5. Prime 2X with water.
6. Undock existing maintenance chip, and dock new CM3 chip.
7. Place HBS-EP bottle into BiaCore 2000 unit, and insert tube into lid
8. Prime the system with HBS-EP buffer.

Immobilization

1. Solutions required
    - EDC 0.1 M 1-ethyl-3-(3-dimethylaminopropyl)-carbodiimide in water
    - NHS 0.1 M N-hydroxysuccinimide in water
    - Ethanolamine 1 M ethanolamine-HCl pH 8.5
    - Fibrinogen 60 mg/ml
2. Mix 35µl of 0.1M NHS with 35µl of 0.1M EDC, and add mixture to a tube and place in tube rack.
3. Dilute fibrinogen in sodium acetate pH 4.0 to 60 mg/ml.
4. Place a tube containing 70µl of 1M ethanolamine-HCl, pH 8.5 in tube rack.
5. Set up the commands to carry out the following injections
    - EDC/NHS – Over all four flow cells (Fc), inject at a rate of 5µl/min for 7 min.
    - Fibrinogen – Immobilize on Fc 2 and 4 only: Inject at a rate 5µl/min for 7 min.
    - Ethanolamine – Over all Fc, inject at a rate of 5µl/min for 7 min.

Binding Study

1. Prepare lipofectin solution of high (0.5 mg/ml) and low (0.05 mg/ml) concentrations in 10 mM HEPES pH 7.4.
2. Inject high concentration solution over Fc 2 and 4 at a rate of 30 µl/min for 7 min.
3. Repeat the injection to ensure saturation.
4. Regenerate the surface using 10 mM glycine, pH 2.5.
5. Inject low concentration solution of lipofectin over regenerated surface of Fc 2 and 4 at a rate of 30 µl/min for 7 min.
6. Regenerate the surface using 10 mM glycine, pH 2.5.
7. Make sure non-specific binding is got rid of by subtracting response units (RU) readings of Fc 1 and 3 (reference) from those of Fc 2 and 4 respectively.
8. Measure RU due to binding, by subtracting RU before injection from RU after injection.

J. Luciferase Assay

This assay was performed using luciferase assay system (Promega, UK) and measured by Wallac Multi-label Counter, PerkinElmer. Before starting the procedure, following care should be taken.

- Store the tissue to be assayed immediately after extraction in liquid nitrogen until assay is done.
- Perform the steps in the assay in a walk in cold room. Key is always keeping the samples chilled.

The assay is performed as follows:

1. Homogenize the tissue sample using Tissue Ruptor^{TM} (Promega, UK) in 500 µl of cell culture lysis buffer.
2. Subject the tissues extracts to three cycles of freeze thaw (3 min in liquid nitrogen and 3 min at 37^0C).
3. Centrifuge at 10,000 rpm and 4^0C in a bench-top microfuge for 10 min.
4. Pipette out 50 µl of the supernatant and mix with 100 µl of luciferase assay buffer (Promega, UK).
5. Measure the light units immediately using Wallac multi-label counter (PerkinElmer).

K. Scratch Assay

1. Plate normal human epidermal keratinocytes (NHEK) on 60 mm cell culture dishes at density of 10^5 cells/dish.
2. Grow to confluence in keratinocyte growth medium 2 (Promocell) either with high glucose (25mM) or normal glucose (6.5mM) for 7 days.
3. Create multiple scratch wounds (4 scratch wounds per dish each passing through the centre of dish and at an angle of 45 degrees) using 200 µl pipette tips on the confluent monolayer of cells, as shown in Figure K1.
4. Allow the cells to heal the scratch wounds for 36 hours.
5. Conduct all the experiments in triplicate.
6. Take photographs at five predetermined fields of vision using a digital camera.

7. Calculate the average distance between the edges of the scratch wound using image analysis software (Image Pro Plus 7.0, Media Cybernetics).
8. Quantify the percentage recovery of scratch wounds.

L. Alloxan Treatment (SOP AF/AP/023)

Alloxan treatment and care of rabbits is carried out according to SOP AF/AP/023/02 and SOP AF/AP/024/02

SOP NO: AF/AP/023

TITLE: Induction of diabetes mellitus in the rabbit

Written by: Dr. Ariella Magee, Clinical Technician

Date: 04-10-2006

1. Introduction

This SOP details the procedure to be followed when creating a rabbit model of diabetes mellitus by the National center for biomedical engineering science (NCBES) and Regenerative medicine institute (REMEDI), NUI Galway.

2. Health and Safety

- Wherever there are animals present there exists the potential for animal allergy to develop.
- Always wear gloves and overcoat/ lab coat when working with alloxan as it is a harmful chemical. Always weigh alloxan in a fume hood.

3. Procedure

3.1. Preoperative Preparation

- The rabbit is restricted from food for 12 hrs prior to the procedure.
- The rabbit is weighed.
- The rabbit is sedated using Acepromazine 1mg/kg SC and the posterior surface of his ear shaved using a shaver. Emla® cream is applied and gently massaged into the skin and left in situ for 20 minutes.
- The rabbit is placed in a 'bunny snuggle'. The Emla® cream is removed using a tissue and the skin is then sterilized over the area of the marginal ear vein using betadine.

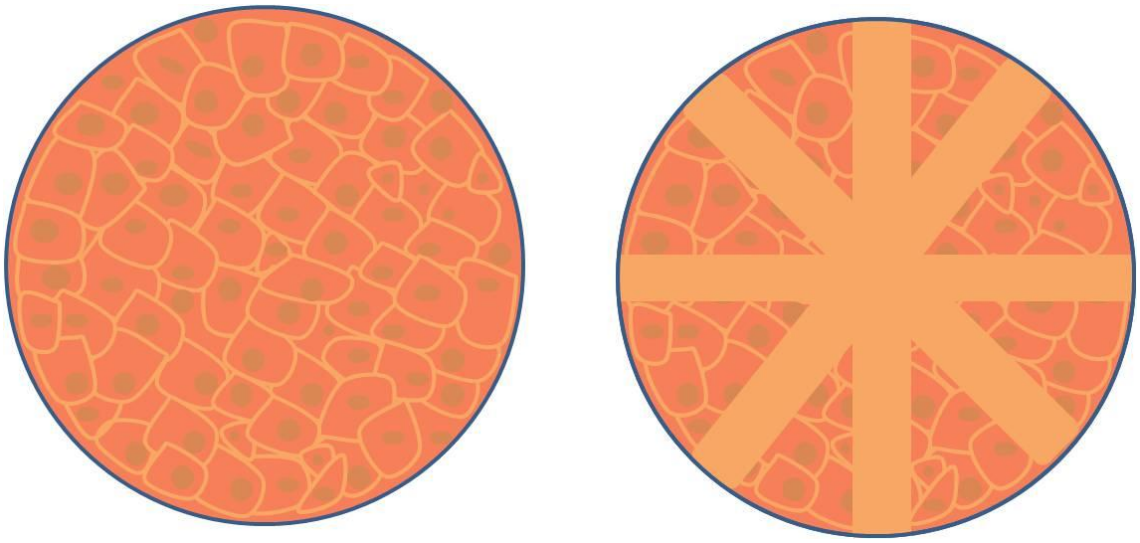

Figure K.1: Schematic showing confluent monolayer of primary human keratinocytes on the left and scratch wounds created on the monolayer shown on the right. The schematic is not drawn to scale.

3.2. Alloxan Infusion Preparation

- Alloxan is kept in the fridge @ 4°C.
- 150mg/kg of Alloxan is carefully weighed into a sterile container using a weigh boat in an appropriate vacuum hood in the NCBES.
- The alloxan is dissolved in 3 ml of sterile 0.9% normal saline in a sterile container and drawn up into syringe through a syringe filter. Keep the solution on ice until used. The solution is then transferred into 50 ml sterile syringe in which 27 ml of sterile 0.9% normal saline has already been drawn up to make 30 ml.

3.3. Alloxan Infusion

- A 24 gauge butterfly IV cannula is flushed with saline and the syringe containing the alloxan is attached to the butterfly needle. Make sure there are no air bubbles in the tube before inserting butterfly needle into vein. The butterfly needle is inserted into the marginal ear vein and secured in place using tape.
- The solution is infused at a rate of 2 ml/minute over 30 minutes.
- Once the infusion is completed the butterfly needle is removed and pressure is applied over the puncture site using cotton wool.
- The rabbit is then placed back into his cage and given free access to food.
- A bottle containing 500 ml of water with two spoons of sugar is placed daily on the cage for 48 hours as alloxan can initially cause hypoglycemia in the initial 48 hours post infusion.

M. Management of Diabetes Mellitus in Rabbit (SOP AF/AP/024)

SOP NO: AF/AP/024

TITLE: Management of diabetes mellitus in the rabbit

Written by: Dr. Ariella Magee, Clinical Technician

Date: 04-10-2006

1. Introduction

This SOP details the procedure to be implemented following induction of diabetes mellitus in the rabbit model by the Department of Medicine in NUI Galway.

2. Health and Safety

Wherever there are animals present there exists the potential for animal allergy to develop.

3. Assessment of the Rabbit:

- Glucose:

  Daily for 9 days

  Weekly thereafter until the rabbit is euthanized

  Spot glucose assessment if the rabbit appears:

  - In distress
  - Withdrawn
  - Ears flattened
  - Not eating
  - Reduced fluid intake

- Weight: Weigh the rabbit twice / week.
- Dietary Intake: Weigh food daily, i.e. check if rabbit ate.
- Apply molasses to front paw of the rabbit if he is not eating well and treat hyperglycemia.
- Fluid Intake: Measure fluid intake daily.
- Give 30mls 0.9% normal saline SC (in the scruff) if the rabbit has reduced fluid intake.
- Treat hyperglycemia if reduced fluid intake.

4. Blood Glucose Evaluation

- The rabbit is allowed free access to food and water post induction of diabetes mellitus. Note that diabetic rabbits will dehydrate easily if not given free access to water.

- The skin on the posterior surface of the ear is cleansed using betadine.
- The glucometer is turned on and a test strip with corresponding number as displayed on the screen is placed into it.
- A needle stick injury is applied to the marginal ear vein and the resultant blood is collected onto the test strip and a read-out of the serum glucose level will be given on the screen.

5. **Insulin Dosing Regimen:**
    - Give insulin if the rabbit appears to be withdrawn with flattened ears, has a reduced oral (diet/fluid) intake or has an infection.
    - The following doses of insulin can be given SC if required
        - Blood glucose > 24 mmol/L - 2 units of Mixtard
        - Blood glucose > 30 mmol/L - 4 units of Mixtard
        - Blood glucose Hi mmol/L - 6 units of Mixtard
    - Only give insulin if rabbit is:
        - Not eating
        - Not drinking
        - Drinking > 500mls/day
        - Has infection
        - Appear very withdrawn; flattened ears
    - The following doses of insulin should be given SC when rabbit is about to receive anesthesia:
        - Blood glucose > 18 mmol/L - 2 units of Mixtard
        - Blood glucose > 26 mmol/L - 4 units of Mixtard

N. Surgical Procedure

1. After 7 days of hyperglycemia, Anesthetize the rabbit using 0.1ml/kg xylazine and 0.12 ml/kg ketamine (this **is half dose**, non-diabetic rabbits receive full dose) (Figure N.1)
2. Shave hair is from the rabbit ear (Figure N.2).

Figure N.1: Induction of Anesthesia.

Figure N.2: Shaving the ventral surface of the ear.

Figure N.3: Oxygen and sedation.

3. Maintain the anesthesia using 2% isofluorane for the duration of surgery (Figure N.3).
4. Prior to surgery, clean surgical bed with 70% alcohol and lay out surgical drape.
5. Prepare the treatments in hood with all aseptic precautions.
6. Sterilize the following instruments
    - Scalpel handle
    - Forceps (fine point and thick point)
    - Small and large scissors
    - Other instruments: 6mm diameter punch biopsies (Panvet) are disposable sterilized. Scalpel blades (no. 15) are disposable sterilized.
7. Lay out sterile swabs and surgical drape.
8. Prepare a container of betadine.
9. Scrub up according to GMP, having an assistant open sterile glove packet.
10. Have an assistant open the surgical drape, take it and place over the rabbit (Figure N.4).
11. Place another drape in the instrument tray.
12. Have the assistant open the sterilized instrument package, punch biopsy and swab package and drop them into tray, along with scalpel blade.
13. Take the blade and attach it to the handle.
14. Dip swab in betadine and using the wet side, rub the inside of the rabbit ear from distal to proximal, and turn swab over to dry the ear in the same direction (Figure N.5).
15. Take the 6mm punch biopsy and depress it gently into ear, taking care that the underlying cartilage is not cut (Figure N.6).
16. When the dermis has been punctured, use a fine point forceps to pull skin from punch area (Figure N.7-1 and N.7-2).
17. Use a scalpel blade to aid in removal of dermis from underlying cartilage, until the 6mm diameter wound has been created (Figure N.8).
18. Repeat to create four wounds on each ear.

Figure N.4: Draping.

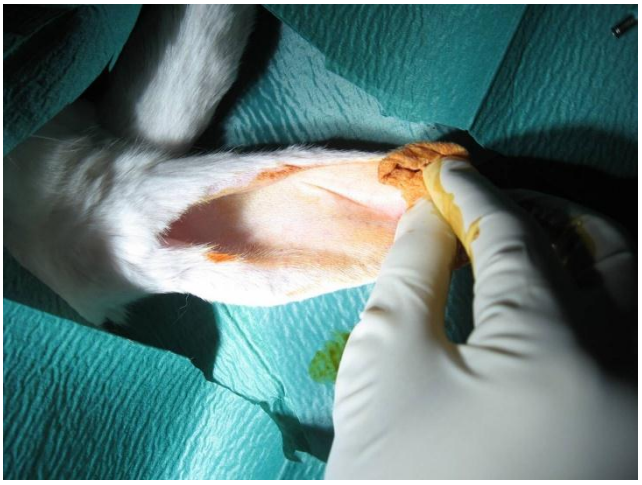

Figure N.5: Cleaning.

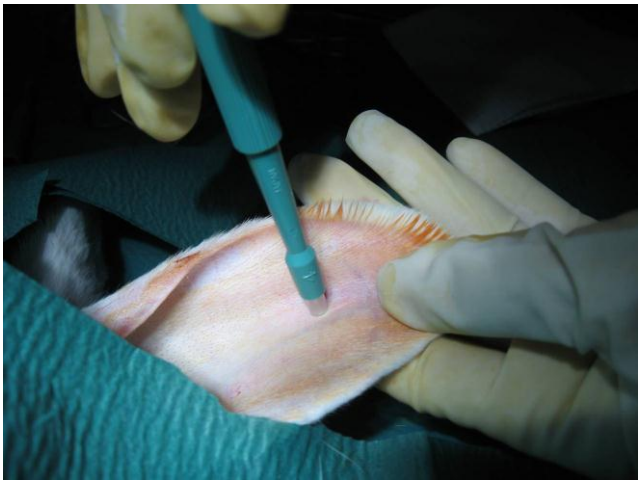

Figure N.6: Punch biopsy.

19. Place wound site avoiding blood vessels with adequate spacing between wounds for tissue harvesting and to avoid mixing of treatments.
20. Take high quality digital images, with a ruler placed next to the ear with same settings in the camera each time and keeping the distance from the ear the same
21. Administer treatments as per the predesigned random treatment allotment sheet (Figure N.9).
22. Protect the treatments from scratching by either suturing the edges of ear together as shown (Figure N.10 and N.11) or taping together using operfix.
23. Place a collar around the rabbit neck.
24. Place rabbit back in cage, and monitor appearance, food and water intake and dressings.

O. Necropsy

Euthanisation

1. At day of sacrifice, measure blood glucose level.
2. Anesthetize the rabbit using full dose ketamine (0.3mg/ml) and xylazine (0.35mg/ml).
3. Once asleep, give 2ml of sodium pentobarbital (Dolethal) to euthanize.
4. When heart beat has stopped, remove rabbit to necropsy room.

Tissue Harvesting

1. Remove rabbit ear.
2. Take high quality digital images, with a ruler placed next to the ear with same. settings in the camera each time and keeping the distance from the ear the same
3. Cut each wound in two (in LR plane).
4. Formalin fix one half.
5. Place the second half in the RNAlater for RNA isolation and store at -80^{0}C.
6. After one hour of formalin fixation, the tissue can be processed by using overnight processing technique.

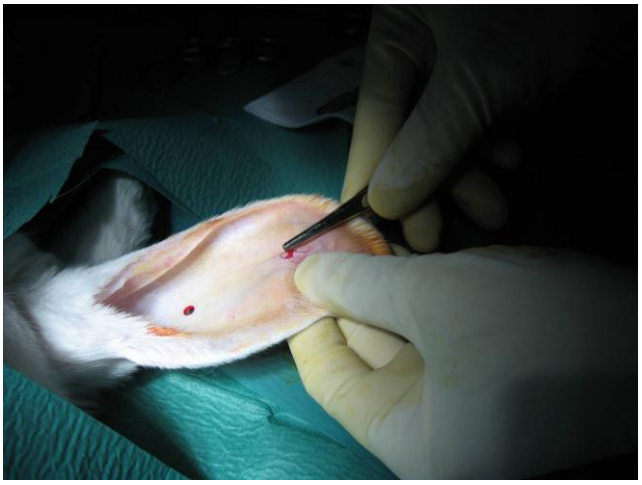

Figure N.7-1: Removal of skin and subcutaneous tissue to expose cartilage.

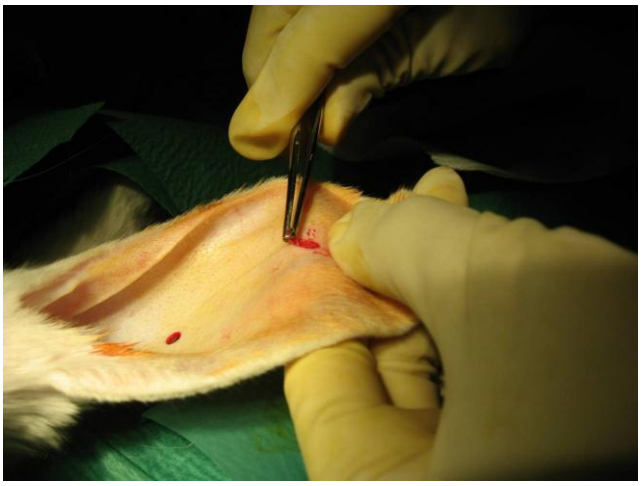

Figure N.7-2: Removal of skin and subcutaneous tissue to expose cartilage.

Figure N.8: Cartilage exposed.

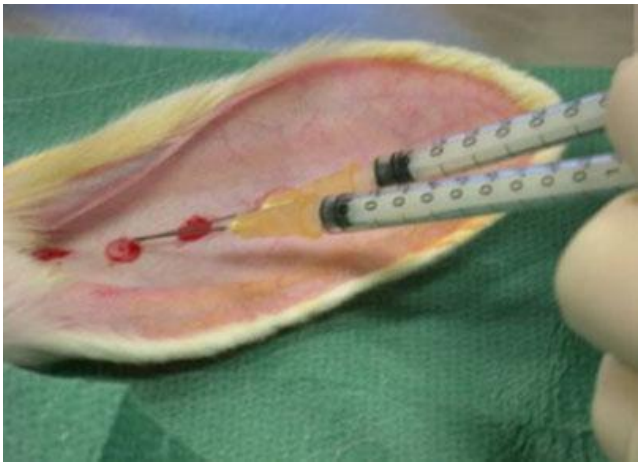

Figure N.9: Application of treatments.

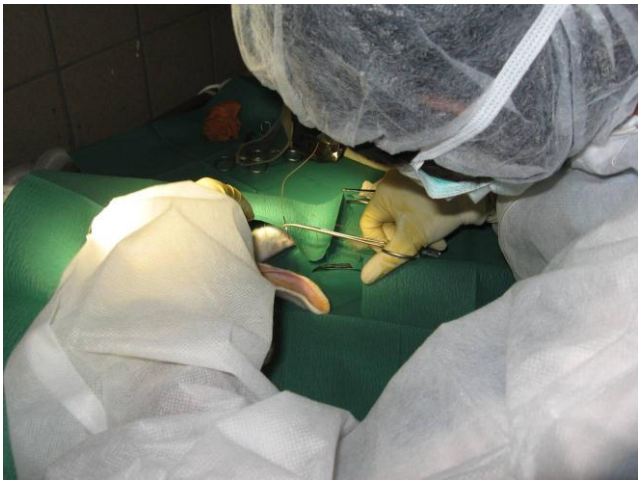

Figure N.10: Stitching the edges of ear together to avoid scratching.

Figure N.11: Ear after stitching.

Tissue Processing

1. Transfer tissue to labeled cassettes and place cassettes in slide tray.
2. Place the slide tray in the processing machine (Leica).
3. Choose routine overnight (16 hours) program for the processing.

Embedding

1. After processing, switch on wax unit and cold plate.
2. Fill a plastic mould (Lennox) with melted wax, and transfer tissue to mould, making sure to orientate wound properly (edge facing down).
3. As wax starts to solidify, ensure tissue is uptight, place labeled cassette (without lid) on wide base of mould, and cover with wax
4. Transfer to cold plate, until ready to keep in fridge.
5. Keep at 4°C at least overnight, to ensure adequate embedding.

Sectioning

1. Preheat water bath for 10 min.
2. Mount block on microtome.
3. Make sure to put on safety lock.
4. Set trim to 20 microns and cut to 5 microns.
5. Bring blade unit back behind block (approx. 4 mm), and line up block.
6. Advance blade until it meets block, and set function to trim.
7. Turn off safety lock and start to move block.
8. Trim block until it reaches tissue, and start to collect sections.
9. Change setting to cut (5 microns), and slowly raise and lower block.
10. Try to get six consecutive sections, and transfer to water bath.
11. Lift end of sections with a forceps and remove from blade with a pencil tip.
12. Gently place on top of cold water, and separate each section with tweezers.
13. Have slides labeled, and collect six sections.
14. Trim for 200 um and repeat sectioning.
15. Trim for 200 um once again and repeat sectioning.

P. Staining

Following are the protocols for the staining with formalin fixed, paraffin embedded (FFPE) samples. The fresh frozen samples do not need rehydration and dehydration steps. All the steps involving xylene and DPX must be done under chemical hood with protective equipments.

Haematoxylin and Eosin

1. Place slides in oven for 60^0C for 2 hours.
2. Bring slides to water.
3. Xylene for 10 minutes, then 5 min
    - 100% Alcohol – 3 min
    - 95% Alcohol – 3 min
    - 70% Alcohol – 3 min
4. Stain slides in Mayer's hematoxylin for 10 min.
5. Dip slides in tap water for 5 min.
6. Dip slides in acid alcohol for 10-15 seconds (here precaution must be taken not to remove too much of hematoxylin. If in doubt, check in microscope at this stage and if repeat the step 3 and reduce time in step 5).
7. Soak slides in tap water for 3 min (it is in this step the slides develop violet color of hematoxylin, so don't be impatient at stage 3).
8. Stain slides in eosin for 5 min.
9. Soak slides in tap water for 3 min.
10. Dehydrate slides in the following series of solutions:
    - 70% alcohol 5 min
    - 90% alcohol 5 min
    - 100% alcohol 5 min
11. Clear in xylene and mount slides using DPX and coverslips.

Q. Immunohistochemistry

β-Galactosidase

1. Bring slides to water:
    - Xylene for 10 minutes, then 5 min

- 100% Alcohol – 3 min
- 95% Alcohol – 3 min
- 70% Alcohol – 3 min

2. Rinse in distilled water.
3. Draw a circle around tissue with PAP tissue blocker pen (Sigma Aldrich).
4. Add 100µl of Proteinase-K 1X solution to each section. Leave for 20 min at 37°C.
5. Take out of incubator and cool for 10 min.
6. Rinse twice in PBST for three minutes each.
7. Block with 100µl of normal blocking buffer for 30 min (in humidity chamber)
8. Tap off blocking buffer.
9. Add 50µl primary mouse anti βGal (AbCam Ab116) 1:100 in primary dilution buffer. Leave for two hours at room temperature (or overnight at 4^0C).
10. Rinse 2 to 3 min in PBST.
11. Block with 3% H_2O_2 (2ml 30% H_2O_2 + 18ml water) for 10 min.
12. Rinse 2 to 3 min in PBST.
13. Add 50µl of secondary biotin conjugated anti-mouse IgG (Dako) 1:100 in secondary dilution buffer for 1 hour at room temperature.
14. Rinse 2 to 3 min in PBST.
15. Add 50µl of streptavidin AB Complex HRP (Dako) for 30 min. Make freshly just 30 min prior for mixing reaction to occur: In 5ml of PBS (0.01M), add 1 drop of solution A and 1 drop of solution B).
16. Rinse 2 to 3 min in PBST and add DAB Chromagen (1mg/ml in PBS, Sigma) for 4 - 8 min. Activate the DAB prior to use with 3µl of H_2O_2. Rinse twice in PBST.
17. Counterstain in Mayer's hematoxylin for 30 sec and wash under running water for 3 min.
18. Dehydrate:
    - 70% Alcohol – 3 min
    - 95% Alcohol – 3min
    - 100% Alcohol – 3min

- Clear in xylene and mount with DPX

CD31

1. Bring slides to water (frozen sections do not need this step):
    - Xylene for 10 minutes, then 5 min
    - 100% Alcohol – 3 min
    - 95% Alcohol – 3 min
    - 70% Alcohol – 3 min
2. Rinse in distilled water.
3. Draw around tissue with PAP tissue blocker pen (Lennox).
4. Add 100µl of Proteinase-K 1X solution to each section. Leave for 20 min at 37°C. Take out of incubator and cool for 10 min.
5. Rinse twice in PBST for three minutes each.
6. Block with 100µl of normal blocking buffer for 30 min (in humidity chamber).
7. Tap off blocking buffer.
8. Add 50µl primary mouse anti CD31 (DakoCytomation) 1:30 in primary dilution buffer. Leave for one hour at room temperature (or overnight at 4ºC).
9. Rinse 2x3 min in PBST. Block with 3% H2O2 (2ml 30% H2O2 + 18ml water) for 10 min.
10. Rinse 2x3 min in PBST and add 50µl of secondary biotin conjugated anti-mouse IgG (Dako) 1:100 in secondary dilution buffer for 1 hour at room temperature.
11. Rinse 2x3mins in PBST, and add 50µl of streptavidin AB Complex HRP (Dako) for 20 min. **(**Make **30 min prior** for mixing reaction to occur: In 5ml of PBS, add 1 drop of solution A and 1 drop of solution B).
12. Rinse 2x3 min in PBST and add DAB Chromagen (1mg/ml in PBS, Sigma) for 3 min. Activate the DAB prior to use with 3µl of H2O2. Rinse twice in PBS.
13. Counterstain in hematoxylin for 30 sec, and wash under running water for 5 min.
14. Dehydrate (frozen sections do not need this step):
    - 70% Alcohol – 3 min
    - 95% Alcohol – 3 min
    - 100% Alcohol – 3 min

- Clear in xylene and mount with DPX

Ram11

1. Bring slides to water (frozen sections do not need this step):
    - Xylene for 10 minutes, then 5 min
    - 100% Alcohol – 3 min
    - 95% Alcohol – 3 min
    - 70% Alcohol – 3 min
2. Rinse in distilled water.
3. Draw around tissue with PAP tissue blocker pen (Lennox).
4. Add 100µl of Proteinase-K 1X solution to each section. Leave for 20 min at 37°C. Take out of incubator and cool for 10 min.
5. Rinse twice in PBST for three minutes each.
6. Block with 100µl of normal blocking buffer for 30 min (in humidity chamber).
7. Tap off blocking buffer.
8. Add 50µl primary mouse monoclonal anti-rabbit macrophage clone Ram11 (Dako, Dublin, Ireland) 1:100 in primary dilution buffer. Leave for overnight at 4ºC.
9. Rinse 2x3 min in PBST. Block with 3% H2O2 (2ml 30% H2O2 + 18ml water) for ten minutes.
10. Rinse 2x3 min in PBST and add 50µl of secondary biotinylated anti-mouse horse radish peroxidase conjugated antibody (Calbiochem) for 40 min at room temperature in secondary dilution buffer.
11. Rinse 2x3 min in PBST and add DAB Chromagen (1mg/ml in PBS, Sigma) for 3 min. Activate the DAB prior to use with 3µl of H2O2. Rinse twice in PBS.
12. Counterstain in hematoxylin for 30 sec, and wash under running water for 5 min.
13. Dehydrate (frozen sections do not need this step):
    - 70% Alcohol – 3 min
    - 95% Alcohol – 3 min
    - 100% Alcohol – 3 min

- Clear in xylene and mount with DPX

Reagents for Histology and Immunohistochemistry

1. **1% Acid Alcohol**

   2ml HCL

   198ml IMS

2. **Phosphotungstic / Phosphomolybdic acid (make fresh every use)**

   50ml of 5% Phosphotungstic acid

   50ml of 5% Phosphomolybdic acid

   100ml of distilled water

3. **1X PBS (0.01M) – 500ml**

   0.54g Na2HPO4

   0.16g NaH2PO4

   4.5g NaCl

   in 500 ml distilled water, bring to pH 7.2

4. **1X PBST (0.01M, 0.05% Tween) – 500ml**

   0.54g Na2HPO4

   0.16g NaH2PO4

   4.5g NaCl

   in 500 ml distilled water, bring to pH 7.2

   Add 250µl of Tween 20

5. **Proteinase K 1x Working Solution (20µg/ml) – 20ml**

   Proteinase K 20x stock solution - 1ml

   TE Buffer, pH 8.0 - 19ml

   Aliquot and store at -20°C

6. **Proteinase K 20x Stock Solution (400µg/ml) - 10ml**

   Proteinase K - 4mg

   TE buffer, pH8.0 - 10ml

   Aliquot and store at -20°C

7. **TE Buffer (50mM Tris Base, 1mM EDTA, pH8.0) – 100ml**

   Tris Base 0.61g

EDTA 0.037g

Distilled Water 100ml

Store at room temperature

8. **Normal Blocking Serum – 10ml**

   2% goat serum (blocking) - 0.2ml

   1%BSA (stabilizer) - 0.1ml

   0.1% cold fish skin gelatin (blocking) - 0.01ml

   0.1% Triton X-100 (penetration enhancer) - 0.01ml

   0.05% Tween 20 (detergent and surface tension reducer) - 5µl

   0.05% sodium azide (preservative) - 5mg

   0.01M PBS, pH 7.2 – 10ml

   Mix well and store at 4 ºC.

9. **Primary Antibody Dilution Buffer – 10ml**

   1%BSA (stabilizer) - 0.1ml

   0.1% cold fish skin gelatin (blocking) - 0.01ml

   0.05% sodium azide (preservative) - 5mg

   0.01M PBS, pH 7.2

10. **Secondary Antibody Dilution Buffer –**

    0.05% sodium azide (preservative) 5mg

    0.01M PBS, pH 7.2

R. Stereology

1. Place stained slide under bright field light.
2. Capture an image at 1.25X objective.
3. Align the slide using 10X objective, so that the cartilage is parallel to the viewing frame.
4. Identify one of the wounds edges, by the change in thickness of epithelium, the change in collagen (blue) density), the change in cellularity, and the lack of skin appendages.
5. Capture an image using the 40X objective.
6. Move the stage, so that each section of the wounded area is viewed.

7. Capture a further 5 images at random within the wounded area.

Wound Volume and Closure

1. Using image analysis software (Image Pro®), calibrate each image at 1.25X magnification.
2. Using the line command, trace the base of the wound from edge to edge along the cartilage. This is the diameter of the wound at day of sacrifice (D_i).
3. Repeat the procedure for the day zero wound. This is D_0 and will be used for all further calculations regarding wound closure.
4. Using image analysis, measure the thickness of the wound, by drawing lines perpendicular to the cartilage layer.
5. Create six measurements across the width of the wound, and get the average value for thickness (t).

    - The volume of the wound is calculated by: $V = A_i \text{ X } t$
    - Percent closure (%C) is measured by: $(D_0 – D_i / D_0) \text{ X } 100$

Epithelialisation

1. Calibrate each image at 1.25X magnification.
2. Using image analysis, measure the distance between two encroaching sections of epithelium. This value is E_i.
3. The epithelial gap at day zero (E_0) is equal to the same value as measured for the wound diameter at day zero.

    - Percent epithelialization (%E) is measured by: $(E_0 – E_i / E_0) \text{ X } 100$

Volume Fraction of Inflammatory Cells

1. Open each image separately in Image Pro®.
2. For each image, choose the ‘grid mask’ command.
3. In the pop-up window, set the type of grid, grid size and margins to be used.
4. To determine volume fraction, choose a line grid with 40X40 pixel spacing, and margins of 20 pixels.

5. Make sure that the cell type or object of interest is not bigger than the area enclosed by four grid points.
6. Click ‘apply’ and the grid will overlay the image.
7. Use the ‘measurements’ command to count intersections between the cell type of interest (inflammatory cells) and the grid intersections.
8. In an excel sheet, type in the number of intersections for each field of view.
9. Also record the number of grid points which hit the tissue of interest.
10. When the number of intersections and grid points has been counted for the six fields of view from one section, calculate the cumulative volume fraction, using the following equation:

$$Vv = \frac{\sum P_P}{\sum P_T}$$

Where $\sum P_P$ is the total number of cell/ grid point intersections, and $\sum P_T$ is the total number of grid points in the reference space for the six fields of view.

Surface Density of Blood Vessels

1. Choose a ‘cycloid’ grid in the command box.
2. Calibrate all images for this measurement. A microscope slide with markings of known dimensions has been captured in Image Pro® previously, with images at every objective and saved on the computer.
3. Open the calibration folder.
4. Select the appropriate objective lens folder, and open an image.
5. Scroll down ‘measurements’ toolbar, and select ‘calibration wizard’.
6. In the pop-up menu, select ‘set calibration’.
7. Choose the objective lens, and measure the size of the circle on the open image.
8. In the next command, enter the actual measurement of the circle (given in the name of the image).
9. Save this calibration, in your working folder.

10. When Image Pro® is re-opened, it is important to open this calibration file every time.
11. Go to ‘measurements,’ and ‘open.’ Open the calibration file.
12. Next, go to ‘measurements’ and ‘set system’.
13. To measure surface density, place a cycloid grid on the field of view of interest.
14. Choose a radius of 20µm and a spacing of 40µm.
15. Set margins at 20µm.
16. Overlay the grid, as described for volume fraction.
17. Ensure that the image is aligned, so that the cartilage layer is parallel to the major (x-axis) of the grid.
18. As the length of a cycloid arc is twice the height, each arc is 40µm.
19. Count the number of arcs on the reference space, and multiply by 40, to give the total length of test line.
20. Count the number of intersections between blood vessels and the test line, and calculate surface density according to the following equation.

$$S_V = 2 \times \frac{I}{L_T}$$

Where I is the number of intersections and L_T is the total length of test line. Again, a cumulative surface area for the six fields of view must be calculated.

Length Density of Blood Vessels

1. Rotate each image by 90 degrees, so that the cartilage lies along a y-axis.
2. Apply the same grid as in surface density.
3. The cartilage is now perpendicular to the major axis of the grid.
4. Count the intersections between blood vessels and cycloid arcs and use the following equation to calculate length density.

$$Lv = \frac{(2 \times I_L)}{T_S}$$

Where I_L is the number of intersections per unit of test line and Ts is the thickness of the section.

S. RNA Isolation

1. Homogenize cells with 1 ml Trizol/Tri-reagent by incubating at room temperature for 1min and then pipetting.
2. For wound tissue, cut the wound tissue using sterile scalpel, add 1 ml Trizol/Tri-reagent and then homogenize using Tissue Ruptor™ probes (Qiagen, United Kingdom).
3. Use fresh probe for each sample. The probes can be sterilized by autoclaving and can be reused later.
4. Incubate the homogenate at room temperature for 5 min to complete dissociation.
5. At this stage, samples can be stored at -80^{0}C and the protocol can be proceeded at a later stage.
6. Thaw the frozen samples.
7. Add 200 µl of chloroform to 1 ml of Trizol.
8. Shake vigorously by inversion several times.
9. Incubate at room temperature for 15 min.
10. Centrifuge at 12 000 g for 15 min at 4^{0}C.
11. Following centrifugation, phase separation takes place creating three distinct layers: Lower phenol chloroform layer, middle interphase, upper translucent aqueous phase.
12. Remove translucent aqueous phase (~650 µl) and add in a fresh tube.
13. Add one volume (~700 µl) of 70% ethanol slowly and carefully mix by inversion.
14. Apply the sample (700 µl at a time) to RNeasy® mini spin column (Qiagen), centrifuge for 15s at 8000 g and discard follow through.
15. Add 350 µl of RW1 buffer to center of column, centrifuge for 15s at 8 000g, discard follow through.
16. Add 10µl DNase stock solution to 70 µl Buffer RDD and add the DNase incubation mix directly onto the RNeasy column. Incubate at RT for 15 min.

17. Add 350 µl of RW1 buffer to center of column, centrifuge for 15s at 8 000g, discard flow-through.
18. Transfer column to new 2ml collection tube.
19. Add 500 µl RPE to the centre of column, centrifuge for 15s at 8 000 g, discard flow-through.
20. Add 500 µl of RPE buffer to the centre of column, centrifuge for 15s at 8 000g, discard flow-through, centrifuge for a further 2 minutes at 8 000g.
21. Transfer column to new 1.5 ml tube , add 10 µl RNase-free water onto the column, incubate at RT for 1 min, centrifuge for 1 minute at 8 000g.
22. Add a further 10 µl RNase-free water onto the column, incubate at RT for 1 min, centrifuge for 1 minute at 8000 g.
23. Take back the 10 µl of eluate and add again onto the column, incubate at RT for 1 min, centrifuge for 1 minute at 8000 g.
24. Determine the concentration at the NanoDrop and freeze at -80°C.

T. RNA Integrity

The integrity of RNA is checked using Agilent 2100 Bioanalyzer and Agilent RNA 6000 Nano kit according to the protocol given in Agilent RNA 6000 Nano Kit Guide.

Equipment Needed

1. Chip priming station (supplied with the Agilent 2100 Bioanalyzer)
2. IKA vortex mixer (supplied with the Agilent 2100 Bioanalyzer)
3. 16-pin bayonet electrode cartridge (supplied with the Agilent 2100 Bioanalyzer)
4. RNase AWAY® (Sigma) for electrode decontamination
5. RNase-free water
6. Pipettes (10 µl and 1000 µl) with compatible tips (RNase-free, no filter tips, no autoclaved tips)
7. 1.5 ml microcentrifuge tubes (RNase-free)
8. Microcentrifuge (≥1300 g)
9. Heating block or water bath for ladder/sample denaturation

Before Beginning

1. Replace the syringe at the chip priming station with each new DNA kit.
2. Adjust the base plate of the chip priming station.
3. Adjust the syringe clip at the chip priming station.
4. Decontaminate the electrodes using RNase decontamination protocol with RNase AWAY in electrode cleaner.
5. Adjust the bioanalyzer's chip selector.
6. Set up the vortex mixer.
7. Bring all reagents, except RNA and ladder to room temperature for 30 min before use. Protect the dye concentrate from light while bringing it to room temperature.
8. Finally, make sure that the software is started before loading the chip.

Preparing Gel

1. Place 550 µl of Agilent RNA 6000 Nano gel matrix into the top receptacle of a spin filter.
2. Centrifuge for 10 min at 4000 rpm.
3. Aliquot 65 µl filtered gel into 0.5 ml RNase-free microfuge tubes that are included in the kit. Store the aliquots at 4 °C and use them within one month of preparation.

Preparing Gel-dye Mix

1. Vortex RNA 6000 Nano dye concentrate for 10 seconds and spin down.
2. Add 1 µl of RNA 6000 Nano dye concentrate to a 65 µl aliquot of filtered gel.
3. Cap the tube, vortex thoroughly and visually inspect proper mixing of gel and dye. Store the dye concentrate at 4 °C in the dark again.
4. Spin tube for 10 minutes at room temperature at 14000 rpm. Use prepared gel-dye mix within one day.

Loading Gel-dye Mix, Marker, Samples and Ladder

1. Place a new RNA nano chip on the chip priming station.

2. Pipette 9 µl of the gel-dye mix at the bottom of the well marked "G" for the gel dye mix.
3. Pressurize using the plunger exactly for 30 sec.
4. Pipette 9 µl of the gel-dye mix in each of the marked wells.
5. Pipette 5 µl of the RNA 6000 Nano marker into the well marked with the ladder symbol and each of the 12 sample wells. Do not leave any well empty, even if samples are less than 12.
6. To minimize secondary structure, heat denature (70°C, 2 minutes) the samples before loading on the chip. The ladder is heat denatured and aliquoted upon arrival.
7. Pipette 1 µl of the RNA ladder into the well marked with the ladder symbol
8. Pipette 1 µl of each sample into each of the 12 sample wells. Pipette 1 µl of buffer in which samples are diluted in each of the unused wells if any.
9. Place the chip horizontally in the adapter of the IKA vortex mixer and vortex at 2000 rpm for 60 sec, taking to avoid liquid spills.

Inserting Chip, Starting Run and Cleaning Up After Run

1. Open the lid of Agilent 2100 Bioanalyser and Check that the electrode cartridge is inserted properly and the chip selector is in position.
2. Clean electrodes on the Agilent 2100 Bioanalyser using RNAzap for 1min and RNAse free water for 1 min.
3. Place the chip carefully into the receptacle.
4. Carefully close the lid. The electrodes in the cartridge fit into the wells of the chip. At this stage the software should indicate that chip is inserted and lid is closed.
5. Select proper assay (eukaryotic RNA program), give name and start the run.
6. After the run is finished, remove the chip and discard according to good laboratory practice. Data is saved automatically. Check the RNA integrity number (RIN).
7. To clean the electrode, place the electrode cleaner in the Bioanalyser, close the lid and keep it closed for 10 sec, open the lid, wait another 10 sec for water to evaporate.

U. Microarray

1. For isolation of RNA, homogenize cells by Trizol and then phase separate in chloroform and isolate RNA using RNeasy® Micro Kit (Qiagen), following the manufacturer's protocol.
2. Check the quantity of RNA isolated spectrophotometrically using a NanoDrop.
3. Check the quality using Agilent RNA 6000 Nano Chips and Agilent 2100 Bioanalyser.
4. Perform microarrays on three biological replicates using GeneChip Human Genome U133 Plus 2.0 Array (Affymetrix) (this was done at Karolinska Biomic Center, Stockholm). Following protocol was followed.
5. Convert 2 µg of total RNA to cDNA and clean up.
6. Synthesize the Biotin labeled cRNA.
7. Remove unincorporated NTPs and assess the quality using Agilent 2100 bioanalyzer.
8. For generating unlabeled cRNA, use 100ng of total RNA for cDNA synthesis. This cRNA was then cleaned up and reverse transcribed in the second cycle first strand cDNA synthesis, double-stranded cDNA cleaned up, amplified and labeled. The newly synthesized biotin labeled cRNA was cleaned removing unincorporated NTPs and quality assessed.
9. Fragment 25µg of cRNA generated in the *in vitro* transcription (IVT) reaction using 5X fragmentation buffer and RNase-free water. The fragmentation reaction was carried out at 94°C for 35 min to generate 35-200 base fragments for hybridization. Quality was assessed at this stage.
10. Prior to hybridization, calculate the adjusted cRNA yield for total RNA carryover in the IVT reaction.
11. Add 15µg of fragmented cRNA made up into a hybridization cocktail to HG-U133 Plus 2.0 array, then hybridize for 16hrs at 45°C, wash and stain on fluidics station.
12. Once completed, scan the samples using GeneChip® Scanner 3000. The results were obtained as CEL files.

13. Pre-process the CEL files, which store the results of the intensity calculations on the pixel values of probes as the first order data analysis for the background correction using Robust Multichip Averaging (RMA) algorithm using Affymetrix GeneChip® Operating Software (GCOS).
14. Create a virtual replicate as a mean for further normalization, aiming at estimation of overall average of the gene expression and estimation of fold change later in the analysis, by non-linear polynomial curve fitting, using convergence of the replicates (OriginPro 8 SRO computer software v8.0724, OriginLab Corporation, One Roundhouse Plaza, Northampton MA 01060).
15. Scale the data points of replicates to the polynomial curve fitted value for each treatment separately.
16. Normalize the background corrected data by per-chip, per-gene and the global median polishing normalization method using GeneSpring bioinformatics software (GeneSpring GX 7.3.1, Silicon Genetics, Redwood City, CA). Statistical analysis was based on significance analysis of microarrays algorithm implementing multiple t-test, considering false discovery rate (FDR) estimate using R-Bioconductor integrated module.
17. Convert the estimated Q-values, as a measure of significance to P-Values for the ease of reading.
18. Generate list of genes for expression profiles by using gene filtering on normalized intensity followed by fold changes >2-fold and P-Value of < 0.05. Annotation provided by Affymetrix was extended using DAVID.
19. Generate functional clustering of lists of differentially expressed genes by comparing them against the ontology terms for molecular function, cellular composition and biological processes using Gene Ontology databases (GO), the Medical Subject Heading Terms Database) (MeSH) and KEGG PATHWAY Database. The examples of pathways dysregulated in the hyperglycemic wounded keratinocytes are depicted in Figure U1.
20. For validating the microarray data, perform real time PCR. The isolated RNA was first reverse transcribed using ImProm-II™ Reverse Transcription System (Promega). The cDNA thus obtained was then used for real time

PCR reaction (ABI *StepOnePlus*™ Real-Time PCR System, software v2.1) with specific designed primers and Fast SYBR® Green Master Mix (Applied Biosystems), under standard conditions.

V. cDNA Synthesis

This is reverse transcription of RNA to cDNA. This cDNA is then used for real time PCR.

Preparation before Reverse Transcription

- Clean the work surface and spray RNAse away.
- Wipe dry all the pipettes and gloves with RNAse away.
- Use sterile nuclease free tubes which are pre-chilled on ice.
- Use 1µg of RNA template and 0.5 µg of oligo dT primers and random primers.
- Denature the target RNA and primers by incubation at 70°C for 5 min.
- Quick-chill on ice for 5 min.

Recipe for Reverse Transcription Reaction Mix

1. Begin with highest volume.
2. Add the reverse transcriptase enzyme at the last.
3. Prepare the reaction mix on ice and keep on ice until incubation.
4. Follow Table V.1 for volumes.
5. After combining all components, vortex gently to mix.
6. After mixing, place the tube with reaction mix into the reverse transcription machine and run the program as detailed in Table V.2.
7. After reaction is complete proceed with polymerase chain reaction (PCR) or store cDNA at -20°C for future use.

W. PCR

1. Dilute cDNA template so as to obtain a final concentration of 20ng per well.
2. Make sure that the cDNA concentration must not exceed 100ng/reaction and 10% of the final volume.

(A)

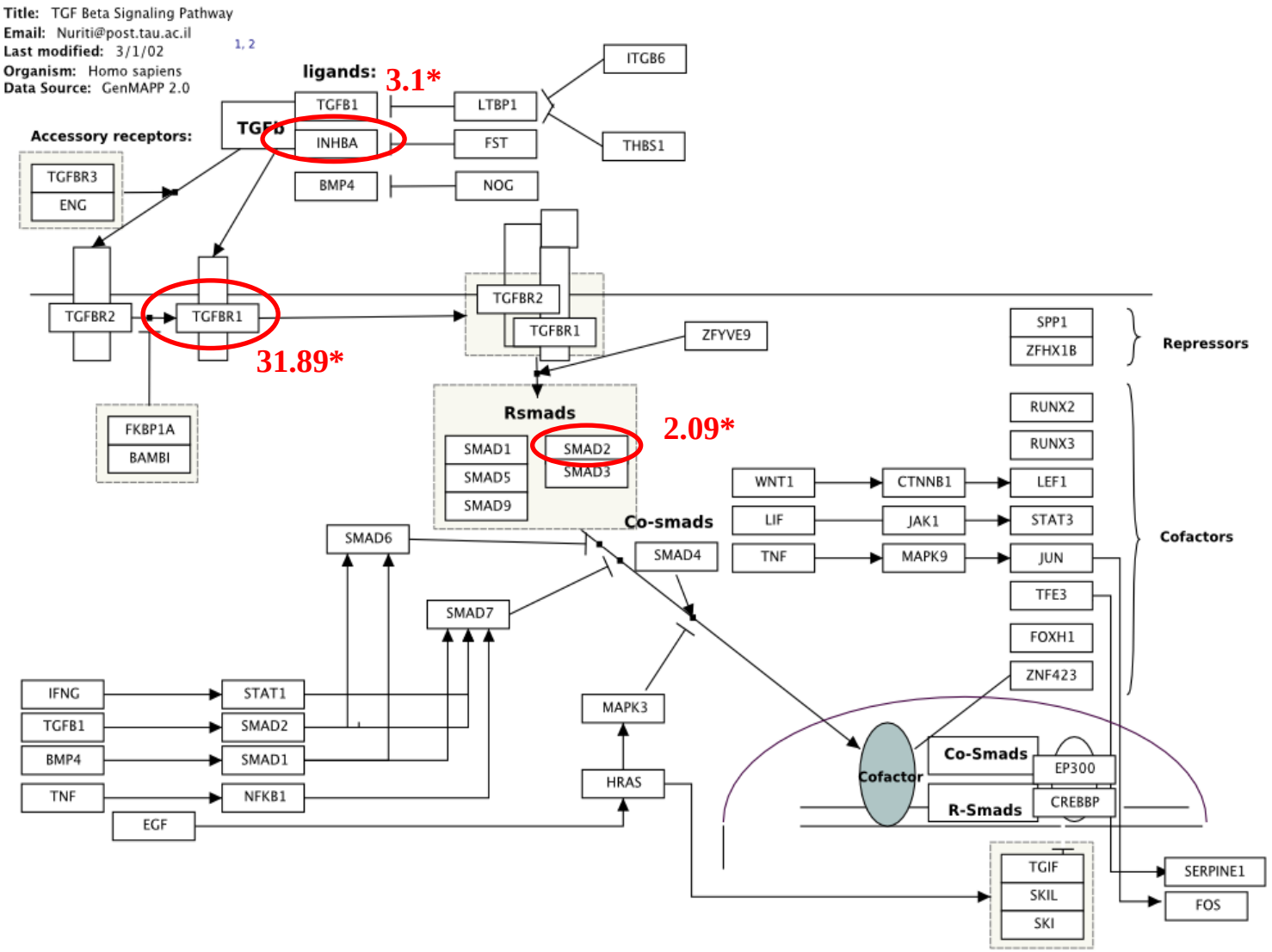
Title: TGF Beta Signaling Pathway
Email: Nuriti@post.tau.ac.il
Last modified: 3/1/02
Organism: Homo sapiens
Data Source: GenMAPP 2.0
1, 2
ligands:
3.1*
TGFB1
INHBA
BMP4
TGFB
LTBP1
FST
NOG
ITGB6
THBS1
Accessory receptors:
TGFBR3
ENG
TGFBR2
TGFBR1
31.89*
TGFBR2
TGFBR1
ZFYVE9
FKBP1A
BAMBI
Rsmads
SMAD1
SMAD5
SMAD9
SMAD2
SMAD3
2.09*
Co-smads
SMAD4
SMAD6
SMAD7
WNT1
LIF
TNF
CTNNB1
JAK1
MAPK9
LEF1
STAT3
JUN
TFE3
FOXH1
ZNF423
SPP1
ZFHX1B
Repressors
RUNX2
RUNX3
Cofactors
IFNG
TGFB1
BMP4
TNF
EGF
STAT1
SMAD2
SMAD1
NFKB1
MAPK3
HRAS
Cofactor
Co-Smads
R-Smads
EP300
CREBBP
TGIF
SKIL
SKI
SERPINE1
FOS

(B)

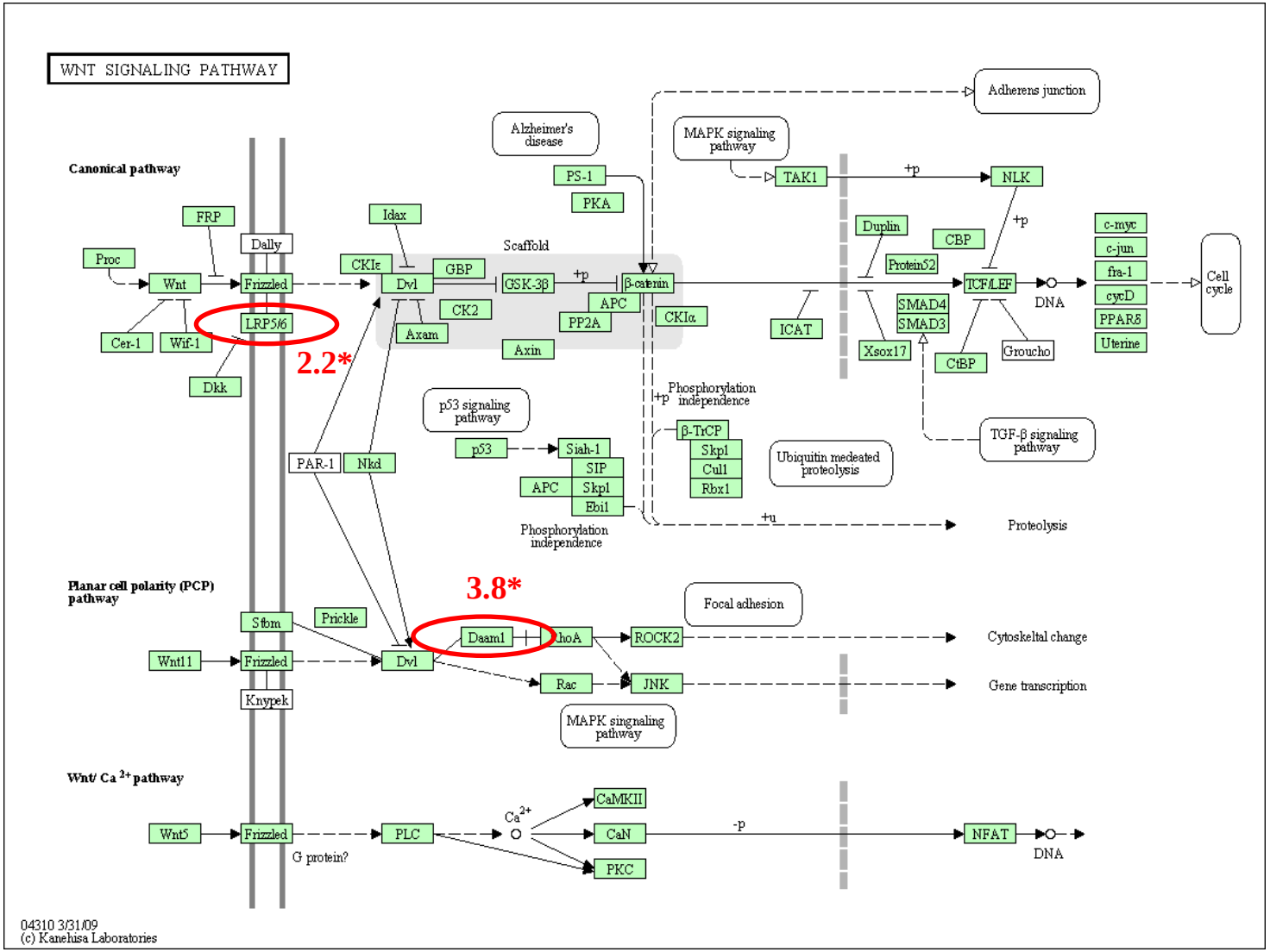
WNT SIGNALING PATHWAY
Canonical pathway
Planar cell polarity (PCP) pathway
Wnt/ Ca 2+ pathway
Adherens junction
Alzheimer's disease
MAPK signaling pathway
PS-1
PKA
TAK1
NLK
+p
Duplin
CBP
Protein52
c-myc
c-jun
fra-1
cycD
PPARδ
Uterine
Cell cycle
FRP
Dally
Idax
Scaffold
Proc
Wnt
Frizzled
CKIε
Dvl
GBP
GSK-3β
β-catenin
APC
CK2
PP2A
CKIα
Axam
Axin
LRP5/6
Cer-1
Wif-1
Dkk
2.2*
ICAT
SMAD4
SMAD3
Xsox17
CtBP
Groucho
TCF/LEF
DNA
p53 signaling pathway
Phosphorylation independence
β-TrCP
Skp1
Cul1
Rbx1
Ubiquitin medeated proteolysis
TGF-β signaling pathway
p53
Siah-1
SIP
APC
Skp1
Ebi1
PAR-1
Nkd
Proteolysis
3.8*
Focal adhesion
Sfrm
Prickle
Daam1
RhoA
ROCK2
Cytoskeltal change
Wnt11
Frizzled
Dvl
Rac
JNK
Gene transcription
Knypek
MAPK singnaling pathway
Wnt5
Frizzled
G protein?
PLC
Ca2+
CaMKII
CaN
PKC
-p
NFAT
DNA
04310 3/31/09
(c) Kanehisa Laboratories

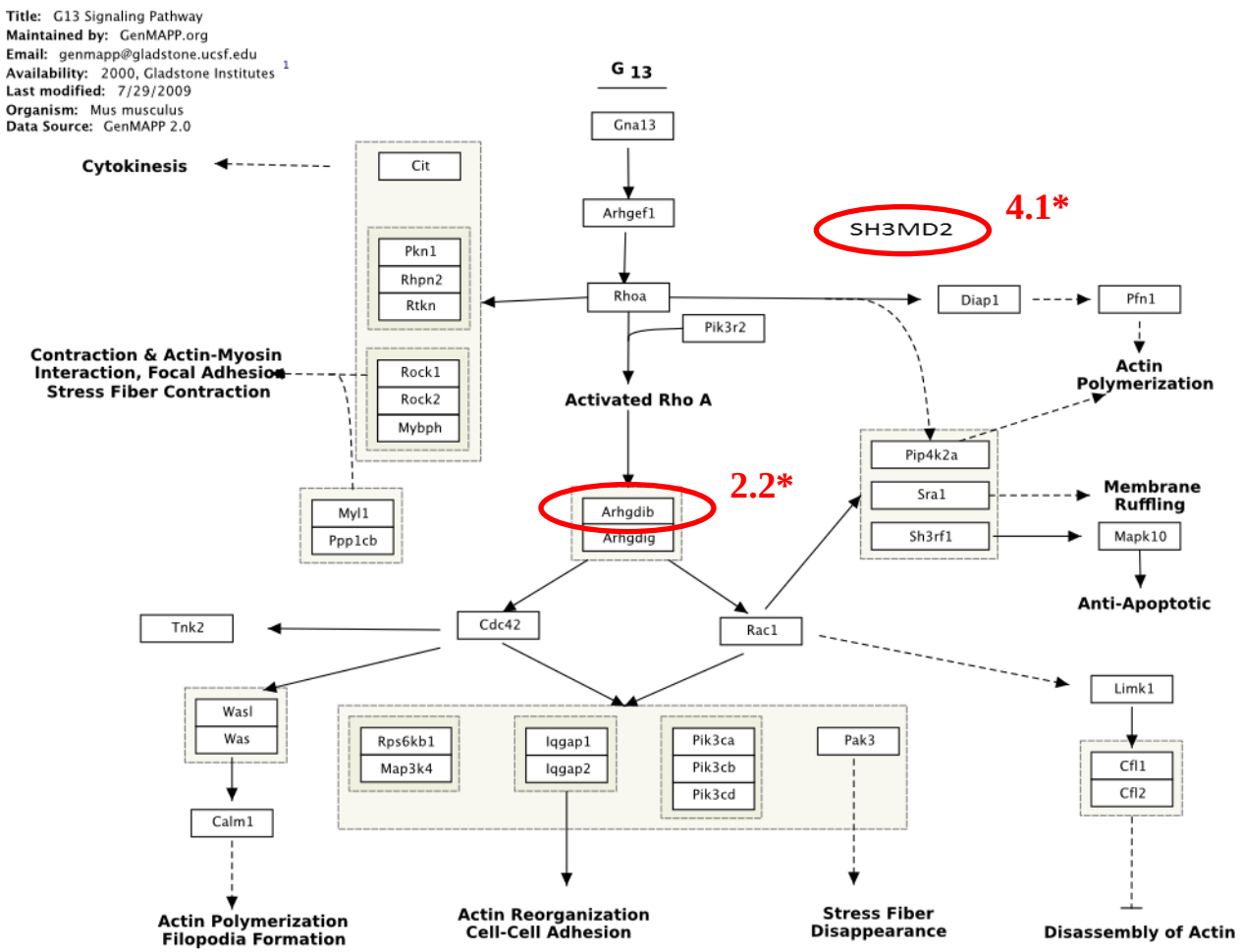

Figure U1. Examples of pathways dysregulated in hyperglycemic wounded keratinocytes. (A) TGF-β pathway, (B) Wnt Signaling pathway and (C) G13 signaling pathway. The sources are mentioned in the images. * denotes significance (n=3, $p < 0.05$).

Table V.1: Reaction components and quantities required for a single reverse transcriptase reaction

Component	**Volume per Reaction (in µl)**	**Final Concentration**
Nuclease free water	5.6	
ImProm-II™ 5X reaction buffer	4	1X
MgCl2, 25mM	2.4	3mM
dNTP mix (10mMeach dNTP)	1	0.5mM
Recombinant Rnasin ribonuclease inhibitor	1	1U/µl
ImProm-II™ reverse transcriptase	1	
Final volume reaction mix	15	

Table V.2: Program

Step	**Temperature**	**Time**
Annealing	25°C	5 min
Extension	42°C	60 min
Heat inactivation reverse transcriptase	70°C	15 min
End	4°C	Forever

3. Add the components listed in Table W.1 to prepare master mix.
4. For a triplicate reaction, add cDNA template in triplicate and also add a negative control by replacing cDNA with nuclease free water.
5. Mix well the master mix by pipetting and add to each well to obtain final volume of 25µl.
6. Add the plastic cover provided by supplier on the PCR plate.
7. Centrifuge 1 minute at 1400 rpm.
8. Place the plate in the machine.
9. Open the step one software and enter the details to map the plate on the software.
10. Choose Sybr Green filter for each well.
11. Choose the endogenous control from the plate and enter in the software.
12. Set up the steps in accordance to the gene and melting temperature (Tm) of the primers. A general program is detailed in Table W.2.

X. Scanning Electron Microscopy

1. Spray the fibrin microspheres samples (before and after degradation with 0.1 N NaOH) on to the black carbon tab on the metal stub.
2. Let them air dry for 24 hr.
3. Gold coat the dried samples at 25mA.
4. Insert the gold coated samples in the vacuum chamber of the microscope at appropriate height of the stub and start imaging.

Y. Transmission Electron Microscopy

1. Resuspend fibrin microspheres in water and film a formvar carbon coated grid with this fibrin microspheres suspension.
2. Make sure to film on shiny surface of the grid.
3. Leave the filmed grid on a bloating paper to absorb extra moisture.
4. Let the filmed grid sit for 5 min.
5. Load the filmed grid, with shiny surface up, in the vacuum chamber.
6. Image with standard settings.

Table W.1: Polymerase chain reaction components

Component	**Volume per Reaction (in µl)**	**Final Concentration**
2X Quantifast SYBR Green PCR master mix	12.5	1.5mM
Forward, pmol	0.25	1 µM
Reverse, pmol	0.25	1 µM
Template DNA	1.49	≤100ng/reaction
Nuclease water (to bring volume to 25 µl)	10.51	1U/µl
Final volume	25	

Table W.2: Typical real time PCR program

Step	**Temperature**	**Time**	**Ramp Rate**	**No. of Cycles**
Initial step	50°C	2 min	Maximal/fast mode	1
PCR initial activation step	95°C	5 min		1
Two step cycling				
Denaturation	95°C	10 sec	Maximal/fast mode	35
Annealing/Extension	60°C	30 sec		
Final step				
Denaturation	95°C	15 sec	Maximal/fast mode	1
Annealing/Extension	60°C	20 sec		
Final denaturation	95°C	15 sec		

Z. List of Publications

Z1. *Journal Article Publications*

1. **Kulkarni M.**, Greiser U, O'Brien T, Pandit A. 'A Temporal Gene Delivery System Based on Fibrin Microspheres'. Mol Pharm. 2011: 8: 439-46
2. **Kulkarni M.**, Greiser, U., O'Brien, T. and Pandit, A. 'Liposomal Gene Delivery Mediated by Tissue-engineered Scaffolds.' Trends Biotechnol. 2010: 28(1): 28-36.
3. **Kulkarni M.**, Breen, A. Greiser, U., O'Brien, T. and Pandit, A. **'**Fibrin-lipoplex System for Controlled Topical Delivery of Multiple Genes.' Biomacromolecules. 2009: 10(6): 1650-1654.
4. Falco E., Wang M., Thompson J., Chetta J., Yoon D., Li E., **Kulkarni M.**, Shah S., Pandit A., Roth J. and Fisher, J. 'Porous EH and EH-PEG scaffolds as gene delivery vehicles to skeletal muscle.' Pharm Res, 2011: 28: 1306-16

Z2. *Manuscripts Submitted*

1. O'Loughlin A., **Kulkarni M.,** Vaughan E., Creane M., Liew A., Dockery P., Pandit A., O'Brien T. 'Autologous Circulating Angiogenic Cells Treated with Osteopontin and Delivered via a Collagen Scaffold Enhances Wound Healing in the Alloxan-induced Diabetic Rabbit Ear Ulcer Model.' submitted to Biomaterials.

Z3. *Manuscripts in Preparation*

1. **Kulkarni M.,** O'Loughlin A., Vazquez R., Mashayekhi K., Greiser U., O'Toole E., O'Brien T., Malagon M. and Pandit A. 'Spatiotemporally Controlled Proangiogenic and Secretory Control Therapy for Compromised Wound Healing'

Z4. Conference Proceedings – Podium Presentations

1. **Kulkarni M.,** O'Loughlin A., Vazquez R., Mashayekhi K., Greiser U., O'Toole E. A., O'Brien T., Malagon M. and Pandit. A. 'Spatiotemporally Controlled Proangiogenic and Secretory Control Therapy for Compromised

Wound Healing.' Podium presentation at the 24th European Conference on Biomaterials, September 4 – 8, 2011, Dublin, Ireland

2. **Kulkarni M.** and Pandit A. 'Design of Appropriate *In Vitro* and *in Vivo* Models for BioDiscovery of Novel Targets for Proangiogenic and Secretory Control Therapy for Compromised Wound Healing.' Keynote presentation at the 38th Annual Meeting & Exposition of the Controlled Release Society (CRS), July 30 – August 3, 2011, Maryland, USA
3. **Kulkarni M.,** Minor W., Carroll O., Mashayekhi K., Greiser U., O'Toole E., O'Brien T. and Pandit A. Hyperglycemia Leads to Differential Gene Expression in Wounded Keratinocytes, Podium presentation at the Tissue Engineering and Regenerative Medicine – EU Meeting, June 7 – 10, 2011, Granada, Spain
4. **Kulkarni M.**, Greiser U., O'Brien T. and Pandit A. 'Fibrin Microspheres Extend the Gene Delivery Capacity in a Fibrin Scaffold.' Podium presentation at the 23rd European Conference on Biomaterials, September 11 – 15, 2010, Tampere, Finland
5. **Kulkarni M.,** Greiser U., O'Brien T. and Pandit A. 'Fibrin Microspheres Extend the Gene Delivery Capacity in a Fibrin Scaffold.' Podium presentation at the Tissue Engineering Regenerative Medicine International Society – EU Meeting, June 13 – 17, 2010, Galway, Ireland.
6. O'Loughlin A., **Kulkarni M.**, Ward J., Dockery P., Pandit A. and O'Brien T. 'Mediating Cell Delivery to a Diabetic Wound with the use of a Collagen Scaffold.' Podium presentation at the Tissue Engineering Regenerative Medicine International Society – EU Meeting, June 13 – 17, 2010, Galway, Ireland.
7. **Kulkarni M.,** Breen A., Greiser U., O'Brien T. and Pandit A. 'Towards Development of Safe and Efficient Fibrin Based Topical Gene Delivery Systems for Angiogenesis in Compromised Wound Healing.' Podium presentation at the 5th Joint Meeting of The European Tissue Repair Society and The Wound Healing Society, Limoges, France, 2009.

8. **Kulkarni M.**, Breen A., Greiser U., O'Brien T. and Pandit A. 'Fibrin-lipoplex System for Controlled Delivery of Multiple Genes.' Podium presentation at the 36th Annual Meeting and Exposition of the Controlled Release Society, Copenhagen, Denmark, 2009.
9. Griallais R., Breen A., **Kulkarni M.**, Dockery P., O'Brien T. and Pandit A. 'Stereological Methods in the Assessment of Functionalized Scaffolds in Vivo.' Podium presentation at the Tissue Engineering and Regenerative Medicine International Society, Porto, Portugal, 2008.

Z5. Conference Proceedings – Poster Presentations

1. **Kulkarni M.**, Breen A., Greiser U., O'Brien T., Pandit A. 'Bio-molecular Interaction between Fibrin and Lipoplexes Results in Extended Release of Plasmid DNA.' Poster presentation at the Tissue Engineering and Regenerative Medicine International Society, Porto, Portugal, 2008. **– Best Poster Prize**
2. **Kulkarni M.**, Breen, A., Greiser, U. and Pandit, A. 'Investigation of the Effect of Binding of Fibrinogen with Lipofectin.' Poster presentation at the 8th World Biomaterials Congress, Amsterdam, Holland, 2008.
3. Falco E., **Kulkarni M.**, Roth S., Fisher J. and Pandit A. 'Use of EH Networks as a Delivery System for GFP Encoded Lipoplexes.' Poster presentation at the 21st European Conference on Biomaterials, Brighton, UK, 2007.
4. **Kulkarni M.**, Greiser U. and Pandit A. 'Towards Development of Antibody Targeted Liposomes for Gene Delivery.' Poster presentation at the Tissue Engineering and Regenerative Medicine International Society, London, U.K., 2007.